

Table of Contents

4.0 THERMAL EVALUATION 4.1-1

4.1 Discussion 4.1-1

 4.1.1 Standard Configuration (24 PWR, 56 BWR)..... 4.1-2

 4.1.2 Advanced Configuration (32 PWR)..... 4.1-3

4.2 Summary of Thermal Properties of Materials 4.2-1

4.3 Technical Specifications for Components..... 4.3-1

4.4 Thermal Evaluation for Normal Conditions of Storage 4.4-1

 4.4.1 Thermal Models 4.4.1-1

 4.4.1.1 Thermal Models for Standard Configuration 4.4.1-1

 4.4.1.2 Thermal Models for Advanced Configuration 4.4.1-54

 4.4.2 Test Model..... 4.4.2-1

 4.4.3 Maximum Temperatures for PWR and BWR Fuel 4.4.3-1

 4.4.3.1 Maximum Temperatures for the Standard Configuration 4.4.3-1

 4.4.3.2 Maximum Temperatures for the Advanced Configuration 4.4.3-17

 4.4.4 Minimum Temperatures..... 4.4.4-1

 4.4.5 Maximum Internal Pressures..... 4.4.5-1

 4.4.5.1 Maximum Internal Pressure for PWR Fuel in the Standard
 Canister..... 4.4.5-1

 4.4.5.2 Maximum Internal Pressure for BWR Fuel in the Standard
 Canister..... 4.4.5-3

 4.4.5.3 Maximum Internal Pressure for PWR Fuel in the Advanced
 Canister..... 4.4.5-3

 4.4.6 Maximum Thermal Stresses..... 4.4.6-1

 4.4.7 Maximum Allowable Cladding Temperature and Canister Heat Load..... 4.4.7-1

 4.4.7.1 Maximum Allowable Cladding Temperature and Canister Heat
 Load for the Standard Configuration..... 4.4.7-1

Table of Contents (Continued)

4.4.7.2	Maximum Allowable Cladding Temperature and Canister Heat Load for the Advanced Configuration.....	4.4.7-12
4.4.8	Evaluation of System Performance for Normal Conditions of Storage.....	4.4.8-1
4.5	Thermal Evaluation for Site Specific Spent Fuel.....	4.5-1
4.5.1	Maine Yankee Site Specific Spent Fuel.....	4.5-1
4.5.1.1	Thermal Evaluation for Maine Yankee Site Specific Spent Fuel	4.5-3
4.5.1.2	Maximum Allowable Heat Loads for Maine Yankee Site Specific Spent Fuel	4.5-17
4.6	References.....	4.6-1

List of Figures

Figure 4.4.1.1.1-1 Two-Dimensional Axisymmetric Air Flow and Concrete Cask Model: PWR – Standard Configuration	4.4.1-9
Figure 4.4.1.1.1-2 Two-Dimensional Axisymmetric Air Flow and Concrete Cask Finite Element Model: PWR – Standard Configuration.....	4.4.1-10
Figure 4.4.1.1.1-3 Axial Power Distribution for PWR Fuel.....	4.4.1-11
Figure 4.4.1.1.1-4 Axial Power Distribution for BWR Fuel	4.4.1-12
Figure 4.4.1.1.2-1 Three-Dimensional Standard Canister Model for PWR Fuel	4.4.1-18
Figure 4.4.1.1.2-2 Three-Dimensional Standard Canister Model for PWR Fuel – Cross-Section	4.4.1-19
Figure 4.4.1.1.2-3 Three-Dimensional Standard Canister Model for BWR Fuel	4.4.1-20
Figure 4.4.1.1.2-4 Three-Dimensional Standard Canister Model for BWR Fuel – Cross-Section	4.4.1-21
Figure 4.4.1.1.3-1 Two-Dimensional Axisymmetric Standard and Advanced Transfer Cask and Canister Model - PWR	4.4.1-28
Figure 4.4.1.1.4-1 Three-Dimensional Periodic Standard Canister Internal Model – PWR.....	4.4.1-35
Figure 4.4.1.1.4-2 Three-Dimensional Periodic Standard Canister Internal Model – BWR	4.4.1-36
Figure 4.4.1.1.5-1 Two-Dimensional PWR (17×17) Fuel Model	4.4.1-39
Figure 4.4.1.1.6-1 Two-Dimensional Fuel Tube Model: PWR Fuel.....	4.4.1-43
Figure 4.4.1.1.6-2 Two-Dimensional Fuel Tube Model: BWR Fuel Tube With BORAL	4.4.1-44
Figure 4.4.1.1.6-3 Two-Dimensional Fuel Tube Model: BWR Fuel Tube Without BORAL.....	4.4.1-45
Figure 4.4.1.1.7-1 Two-Dimensional Axisymmetric Finite Element Model for Transfer Cask Forced Air Cooling.....	4.4.1-47
Figure 4.4.1.1.7-2 Two-Dimensional Axisymmetric Outlet Air Flow Model for Transfer Cask Cooling	4.4.1-48
Figure 4.4.1.1.7-3 Two-Dimensional Axisymmetric Inlet Air Flow Model for Transfer Cask Cooling	4.4.1-49
Figure 4.4.1.1.7-4 Non-Uniform Heat Load from Canister Contents.....	4.4.1-50







List of Figures (Continued)

Figure 4.4.1.1.7-5	Maximum Standard Canister Temperature Versus Air Volume Flow Rate	4.4.1-51
Figure 4.4.1.1.8-1	Three-Dimensional Standard Transfer Cask and Canister Model	4.4.1-53
Figure 4.4.1.2-1	Two-Dimensional Axisymmetric Air Flow and Concrete Cask Model for Advanced Configuration	4.4.1-60
Figure 4.4.1.2-2	Two-Dimensional Axisymmetric Air Flow and Concrete Cask CFD Mesh – Advanced Configuration	4.4.1-61
Figure 4.4.1.2.2-1	Three-Dimensional Canister Model for PWR Fuel – Advanced Configuration	4.4.1-65
Figure 4.4.1.2.2-2	Three-Dimensional Canister Model for PWR Fuel – Cross-Section – Advanced Configuration	4.4.1-66
Figure 4.4.1.2.2-3	PWR Basket – Advanced Configuration – Design Heat Load (29.2 kW) Preferential Loading Pattern	4.4.1-67
Figure 4.4.1.2.3-1	Three-Dimensional Transfer Cask Canister Model for PWR Fuel – Advanced Configuration	4.4.1-70
Figure 4.4.1.2.4-1	Three-Dimensional Periodic Canister Internal Model – PWR – Advanced Configuration	4.4.1-73
Figure 4.4.1.2.5-1	Two-Dimensional PWR (14×14) Fuel Model – PWR Fuel – Advanced Configuration	4.4.1-77
Figure 4.4.1.2.6-1	Two-Dimensional Fuel Basket Neutron Absorber Plate Model – PWR Fuel – Advanced Configuration	4.4.1-81
Figure 4.4.1.2.7-1	Two-Dimensional Advanced PWR Basket Cooling Insert Model	4.4.1-85
Figure 4.4.3.1-1	Temperature Distribution (°F) for the Normal Storage Condition: PWR Fuel – Standard Configuration	4.4.3-5
Figure 4.4.3.1-2	Air Flow Pattern in the Concrete Cask in the Normal Storage Condition: PWR Fuel – Standard Configuration	4.4.3-6
Figure 4.4.3.1-3	Air Temperature (°F) Distribution in the Concrete Cask During the Normal Storage Condition: PWR Fuel – Standard Configuration....	4.4.3-7

List of Figures (Continued)

Figure 4.4.3.1-4	Concrete Temperature (°F) Distribution During the Normal Storage Condition: PWR Fuel – Standard Configuration.....	4.4.3-8
Figure 4.4.3.1-5	History of Maximum Component Temperature (°F) for Transfer Conditions for BWR Fuel with Design Basis 23 kW Uniformly Distributed Heat Load – Standard Configuration.....	4.4.3-9
Figure 4.4.3.1-6	History of Maximum Component Temperature (°F) for Transfer Conditions for BWR Fuel with Design Basis 23 kW Uniformly Distributed Heat Load – Standard Configuration.....	4.4.3-10
Figure 4.4.3.1-7	Basket Location for the Thermal Analysis for Reduced Heat Load Cases – Standard Configuration	4.4.3-11
Figure 4.4.3.2-1	Temperature Distribution (°F) for the Normal Storage Condition: PWR Fuel for the Advanced Configuration.....	4.4.3-22
Figure 4.4.3.2-2	Contours of Velocity Magnitude (m/s) in the Lower Portion of the Model for the Normal Storage Condition (PWR Fuel) for the Advanced Configuration	4.4.3-23
Figure 4.4.3.2-3	Contours of Velocity Magnitude (m/s) in the Upper Portion of the Model for the Normal Storage Condition (PWR Fuel) for the Advanced Configuration	4.4.3-24
Figure 4.4.3.2-4	Temperature (°F) Distribution, in the Range of 76°F – 200°F, in the Concrete Cask During the Normal Storage Condition: PWR Fuel for the Advanced Configuration	4.4.3-25
Figure 4.4.3.2-5	Component Temperature History for the Normal Condition with the Design Heat Load (29.2 kW) – PWR Fuel – Advanced Configuration	4.4.3-26
Figure 4.4.3.2-6	PWR Fuel Basket Preferential Loading Zones for Reduced Heat Loads During Transfer Conditions for the Advanced Configuration.....	4.4.3-27
Figure 4.4.7.1-1	PWR Fuel Dry Storage Temperature versus Cladding Stress – Standard Configuration.....	4.4.7-6
Figure 4.4.7.1-2	WR Fuel Dry Storage Temperature versus Cladding Stress – Standard Configuration.....	4.4.7-6

List of Figures (Continued)

Figure 4.4.7.1-3	PWR and BWR Fuel Cladding Dry Storage Temperature versus Basket Heat Load – Standard Configuration	4.4.7-7
Figure 4.4.7.2-1	Maximum Allowable Assembly Heat Load by PWR Canister Zone – Advanced Configuration	4.4.7-21
Figure 4.4.7.2-2		4.4.7-22
Figure 4.4.7.2-3		4.4.7-23
Figure 4.4.7.2-4		4.4.7-24
Figure 4.4.7.2-5		4.4.7-25
Figure 4.4.7.2-6		4.4.7-26
Figure 4.4.7.2-7		4.4.7-27
Figure 4.5.1.1-1	Quarter Symmetry Model for Maine Yankee Consolidated Fuel	4.5-12
Figure 4.5.1.1-2	Maine Yankee Three-Dimensional Periodic Canister Internal Model	4.5-13
Figure 4.5.1.1-3	Evaluated Locations for the Maine Yankee Consolidated Fuel Lattice in the PWR Fuel Basket	4.5-14
Figure 4.5.1.1-4	Active Fuel Region in the Three-Dimensional Canister Model	4.5-15
Figure 4.5.1.1-5	Fuel Debris and Damaged Fuel Regions in the Three-Dimensional Canister Model	4.5-16
Figure 4.5.1.2-1	Canister Basket Preferential Loading Plan	4.5-22
Figure 4.5.1.2-2	Maximum Allowable Cladding Temperature at Initial Storage versus Cladding Stress (50,000 MWD/MTU)	4.5-23

List of Tables

Table 4.1-1	Summary of Thermal Design Conditions for Storage.....	4.1-5
Table 4.1-2	Summary of Thermal Design Conditions for Transfer.....	4.1-6
Table 4.1-3	Maximum Allowable Material Temperatures	4.1-7
Table 4.1-4	Summary of Thermal Evaluation Results for the Universal Storage System: PWR Fuel – Standard Configuration	4.1-8
Table 4.1-5	Summary of Thermal Evaluation Results for the Universal Storage System: BWR Fuel – Standard Configuration	4.1-9
Table 4.1-6	Summary of Thermal Evaluation Results for the Universal Storage System: PWR Fuel – Advanced Configuration	4.1-10
Table 4.2-1	Thermal Properties of Solid Neutron Shield (NS-4-FR and NS-3).....	4.2-2
Table 4.2-2	Thermal Properties of Stainless Steel.....	4.2-2
Table 4.2-3	Thermal Properties of Carbon Steel	4.2-3
Table 4.2-4	Thermal Properties of Chemical Copper Lead.....	4.2-3
Table 4.2-5	Thermal Properties of Type 6061-T651 and Type 6061-T6 Aluminum Alloy.....	4.2-3
Table 4.2-6	Thermal Properties of Helium.....	4.2-4
Table 4.2-7	Thermal Properties of Dry Air	4.2-4
Table 4.2-8	Thermal Properties of Zircaloy and Zircaloy-4 Cladding	4.2-5
Table 4.2-9	Thermal Properties of Fuel (UO ₂).....	4.2-5
Table 4.2-10	Thermal Properties of BORAL Composite Sheet	4.2-6
Table 4.2-11	Thermal Properties of Concrete	4.2-6
Table 4.2-12	Thermal Properties of Water	4.2-7
Table 4.2-13	Thermal Properties of METAMIC	4.2-7
Table 4.2-14	Thermal Properties of 1100 Aluminum Alloy	4.2-7
Table 4.4.1.1.2-1	Effective Thermal Conductivities for PWR Fuel Assemblies	4.4.1-22
Table 4.4.1.1.2-2	Effective Thermal Conductivities for BWR Fuel Assemblies	4.4.1-23
Table 4.4.1.1.2-3	Effective Thermal Conductivities for PWR Fuel Tubes	4.4.1-24
Table 4.4.1.1.2-4	Effective Thermal Conductivities for BWR Fuel Tubes.....	4.4.1-25
Table 4.4.1.1.3-1	Effective Thermal Properties for the Active Fuel Region for the Two- Dimensional Axisymmetric Standard Transfer Cask and Canister Model: PWR.....	4.4.1-29

List of Tables (Continued)

Table 4.4.1.1.3-2	Effective Thermal Properties for the Region Below the Active Fuel for the Two-Dimensional Axisymmetric Standard Transfer Cask and Canister Model: PWR.....	4.4.1-30
Table 4.4.1.1.3-3	Effective Thermal Properties for the Active Fuel Region for the Two-Dimensional Axisymmetric Standard Transfer Cask and Canister Model: BWR.....	4.4.1-31
Table 4.4.1.1.3-4	Effective Thermal Properties for the Region Below the Active Fuel for the Two-Dimensional Axisymmetric Standard Transfer Cask and Canister Model: BWR	4.4.1-32
Table 4.4.1.2.4-1	Effective Thermal Conductivity for the Advanced Canister Internal Components.....	4.4.1-74
Table 4.4.1.2.5-1	Effective Thermal Conductivities for PWR 14 × 14 Fuel Assembly – Advanced Configuration.....	4.4.1-78
Table 4.4.1.2.6-1	Effective Thermal Properties for the Fuel Basket Neutron Absorber Plate Region – Advanced Configuration – PWR	4.4.1-82
Table 4.4.1.2.7-1	Effective Thermal Properties for the Advanced PWR Basket Cooling Inserts Region.....	4.4.1-86
Table 4.4.3.1-1	Maximum Component Temperatures for the Normal Storage Condition – Standard Configuration – PWR.....	4.4.3-12
Table 4.4.3.1-2	Maximum Component Temperatures for the Normal Storage Condition – Standard Configuration – BWR.....	4.4.3-13
Table 4.4.3.1-3	Maximum Component Temperatures for the Transfer Condition – PWR Fuel with Design Basis 23 kW Uniformly Distributed Heat Load – Standard Configuration.....	4.4.3-14
Table 4.4.3.1-4	Maximum Component Temperatures for the Transfer Condition – BWR Fuel with Design Basis 23 kW Uniformly Distributed Heat Load – Standard Configuration.....	4.4.3-14
Table 4.4.3.1-5	Maximum Limiting Component Temperatures in Transient Operations for the Reduced Heat Load Cases for PWR Fuel – Standard Configuration.....	4.4.3-15
Table 4.4.3.1-6	Maximum Limiting Component Temperatures in Transient Operations for the Reduced Heat Load Cases for PWR Fuel after In-Pool Cooling – Standard Configuration.....	4.4.3-16

List of Tables (Continued)

Table 4.4.3.2-1	Maximum Component Temperatures for the Normal Storage Condition – PWR – Advanced Configuration.....	4.4.3-28
Table 4.4.3.2-2	Maximum Component Temperatures for the Normal Transfer Condition with the Design Heat Load (29.2 kW) – PWR – Advanced Configuration.....	4.4.3-29
Table 4.4.3.2-3	Time Limits for Transfer Operations with In-Pool Remedial Action – PWR – Advanced Configuration	4.4.3-29
Table 4.4.3.2-4	Maximum Component Temperatures for In-Pool Cooling Following the Vacuum and Drying Operations for the Design Heat Load of 29.2 kW – PWR – Advanced Configuration.....	4.4.3-29
Table 4.4.3.2-5	Time Limits for Transfer Operations with Forced Air Cooling Remedial Action – PWR – Advanced Configuration.....	4.4.3-30
Table 4.4.3.2-6	Maximum Component Temperatures for Forced Air Cooling Following the Vacuum and Drying Operations for the Design Heat Load of 29.2 kW – PWR – Advanced Configuration.....	4.4.3-30
Table 4.4.3.2-7	Time Limits for Transfer Operations with In-Pool Cooling Following Helium Backfill for the Design Heat Load of 29.2 kW – Advanced Configuration (PWR)	4.4.3-31
Table 4.4.3.2-8	Maximum Component Temperatures for In-Pool Cooling Following Helium Backfill for the Design Heat Load of 29.2 kW – Advanced Configuration (PWR).....	4.4.3-31
Table 4.4.3.2-9	Time Limits for Transfer Operations with Forced Air Cooling Following Helium Backfill for the Design Heat Load of 29.2 kW – Advanced Configuration (PWR).....	4.4.3-32
Table 4.4.3.2-10	Maximum Component Temperatures for Forced Air Cooling Following Helium Backfill for the Design Heat Load of 29.2 kW – Advanced Configuration (PWR).....	4.4.3-32
Table 4.4.3.2-11	Reduced Heat Loads Preferential Loading Patterns – PWR – Advanced Configuration.....	4.4.3-33
Table 4.4.3.2-12	Time Limits for Normal Transfer Conditions for Reduced Heat Loads – PWR – Advanced Configuration	4.4.3-33
Table 4.4.3.2-13	Time Limits for Normal Transfer Conditions for Reduced Heat Loads – PWR – Advanced Configuration	4.4.3-34

List of Tables (Continued)

Table 4.4.3.2-14	Time Limits for Transfer Operations with In-Pool Cooling Remedial Action for Reduced Heat Loads – PWR – Advanced Configuration	4.4.3-35
Table 4.4.3.2-15	Maximum Component Temperatures for In-Pool Cooling Following the Vacuum and Drying Operations – PWR – Advanced Configuration	4.4.3-35
Table 4.4.3.2-16	Time Limits for Transfer Operations with Forced Air Cooling Remedial Action for Reduced Heat Loads – PWR – Advanced Configuration	4.4.3-36
Table 4.4.3.2-17	Maximum Component Temperatures for Forced Air Cooling Following the Vacuum and Drying Operations – PWR – Advanced Configuration	4.4.3-36
Table 4.4.3.2-18	Time Limits for Transfer Operations with In-Pool Cooling Following Helium Backfill for Reduced Heat Loads - Advanced Configuration (PWR)	4.4.3-37
Table 4.4.3.2-19	Maximum Component Temperatures for In-Pool Cooling Following Helium Backfill for Reduced Heat Loads – Advanced Configuration (PWR)	4.4.3-37
Table 4.4.3.2-20	Time Limits for Transfer Operations with Forced Air Cooling Following Helium Backfill for Reduced Heat Loads – Advanced Configuration (PWR)	4.4.3-38
Table 4.4.3.2-21	Maximum Component Temperatures for Forced Air Cooling Following Helium Backfill for Reduced Heat Loads – Advanced Configuration (PWR)	4.4.3-38
Table 4.4.5-1	UMS® PWR Per Assembly Fuel Generated Gas Inventory (Standard and Advanced)	4.4.5-5
Table 4.4.5-2	Standard PWR Canister Free Volume	4.4.5-5
Table 4.4.5-3	Standard PWR Maximum Normal Condition Pressure by Canister Class	4.4.5-5
Table 4.4.5-4	Fuel Generated Gas Inventory for BWR Fuel in the Standard Canister	4.4.5-5
Table 4.4.5-5	Standard BWR Canister Free Volume (No Fuel or Inserts)	4.4.5-6

List of Tables (Continued)

Table 4.4.5-6	Standard BWR Maximum Normal Condition Pressure by Canister Class.....	4.4.5-6
Table 4.4.5-7	Advanced PWR Canister Free Volume (No Fuel or Inserts).....	4.4.5-6
Table 4.4.5-8	Advanced PWR Maximum Normal Condition Pressure by Canister Class.....	4.4.5-6
Table 4.4.7.1-1	PWR Cladding Stress Level Comparison Chart – Standard Configuration.....	4.4.7-8
Table 4.4.7.1-2	BWR Cladding Stress Level Comparison Chart– Standard Configuration.....	4.4.7-8
Table 4.4.7.1-3	Cladding Stress as a Function of Fuel Assembly Average Burnup and Temperature – Standard Configuration.....	4.4.7-9
Table 4.4.7.1-4	Maximum Allowable Initial Storage Temperature (°C) As a Function of Initial Cladding Stress and Initial Cool Time – Standard Configuration.....	4.4.7-9
Table 4.4.7.1-5	Maximum Allowable Cladding Temperature for PWR and BWR Fuel Assemblies – Standard Configuration.....	4.4.7-10
Table 4.4.7.1-6	Cladding Maximum Temperature as a Function of Basket Heat Load (PWR) – Standard Configuration.....	4.4.7-10
Table 4.4.7.1-7	Cladding Maximum Temperature as a Function of Basket Heat Load (BWR) – Standard Configuration.....	4.4.7-10
Table 4.4.7.1-8	Maximum Allowable Decay Heat for Standard Configuration PWR and BWR Universal Storage Systems.....	4.4.7-11
Table 4.4.7.1-9	Temperature Bias Applied to Maximum Allowable Decay Heats.....	4.4.7-11
Table 4.4.7.2-1	
	
	4.4.7-28
Table 4.4.7.2-2	
	
	4.4.7-28
Table 4.4.7.2-3	
	4.4.7-29

List of Tables (Continued)

Table 4.4.7.2-4	[REDACTED]	
	[REDACTED]	4.4.7-29
Table 4.4.7.2-5	[REDACTED]	
	[REDACTED]	4.4.7-29
Table 4.5.1.2-1	Cladding Stress for 50,000 MWD/MTU Burnup Fuel – Standard Configuration.....	4.5-24
Table 4.5.1.2-2	Maximum Allowable Cladding Temperature for 50,000 MWD/MTU Burnup Fuel – Standard Configuration.....	4.5-24
Table 4.5.1.2-3	Maximum Allowable Canister Heat Load for 50,000 MWD/MTU Burnup Fuel – Standard Configuration.....	4.5-24
Table 4.5.1.2-4	Heat Load for Interior Assemblies for the Configuration with 0.958 kW Assemblies in Peripheral Locations	4.5-25
Table 4.5.1.2-5	Heat Load Limit for Interior Assemblies for the Configuration with 1.05 kW Assemblies in Peripheral Locations	4.5-25

4.0 THERMAL EVALUATION

This section presents the thermal design and analyses of the Universal Storage System for normal conditions of storage of spent nuclear fuel. The system is provided in two configurations: the Standard and the Advanced configuration. The analyses for the Standard configuration include consideration of design basis PWR and BWR fuel. The analyses for the Advanced configuration include the PWR fuel only. Results of the analyses demonstrate that with the design basis contents, the Universal Storage System meets the thermal performance requirements of 10 CFR 72 [1].

4.1 Discussion

The Universal Storage System consists of a Transportable Storage Canister, Vertical Concrete Cask, and a transfer cask. The Standard and Advanced configurations have similar thermal design for heat rejection of the system in storage. In long-term storage, the canister is placed in the concrete cask, which provides passive radiation shielding and natural convection cooling. The fuel is loaded in a basket structure positioned within the canister. The transfer cask is used for the handling of the canister. The thermal performance of the concrete cask containing the design basis fuel (during storage) and the performance of the transfer cask containing design basis fuel (during handling) are evaluated herein.

The significant thermal design feature of the Vertical Concrete Cask is the passive convective air flow up along the side of the canister. Cool (ambient) air enters at the bottom of the concrete cask through four inlets. Heated air exits through the four outlets at the top of the cask. Radiant heat transfer occurs from the canister shell to the concrete cask liner, which also transmits heat to the adjoining air flow. Conduction does not play a substantial role in heat removal from the canister surface. Natural circulation of air inside the Vertical Concrete Cask, in conjunction with radiation from the canister surface, maintains the fuel cladding temperature and all of the concrete cask component temperatures below their design limits.

4.1.1 Standard Configurations (24 PWR, 56 BWR)

The Universal Storage System design basis heat load for the Standard configuration is 23.0 kW for up to 24 PWR or up to 56 BWR fuel assemblies. As shown in Section 4.4.7.1, the thermal analysis considers a range of fuel assembly burnup and cooling times for both fuel types to establish the allowable cladding temperatures. These limits are used to establish the UMS[®] Storage System allowable decay heat loads for fuel having cooling times of 5 years, or longer.

The thermal evaluation considers normal, off-normal, and accident conditions of storage. Each of these conditions can be described in terms of the environmental temperature, use of solar insolation, and the condition of the air inlets and outlets, as shown in Table 4.1-1. The design conditions for transfer are defined in Table 4.1-2. The transfer conditions consider the transient effect for a total of 43 hours for PWR fuel and 51 hours for BWR fuel, starting from the removal of the transfer cask/canister from the spent fuel pool. The canister is considered under normal operation to be inside the transfer cask and filled with water for 17 hours, in vacuum condition for 10 hours, back-filled with helium for 16 hours for PWR fuel and 24 hours for BWR fuel, and then transferred into the Vertical Concrete Cask.

This evaluation applies different component temperature limits and different material stress limits for long-term conditions and short-term conditions. Normal storage is considered to be a long-term condition. Off-normal and accident events, as well as the transfer condition that temporarily occurs during the preparation of the canister while it is in the transfer cask, are considered as short-term conditions. Thermal evaluations are performed for the design basis PWR and BWR fuels for all design conditions. The maximum allowable material temperatures for long-term and short-term conditions are provided in Table 4.1-3.

During normal conditions of storage and hypothetical accident conditions, the concrete cask must reject the fuel decay heat to the environment without exceeding the operational temperature ranges of the components important to safety. In addition, to maintain fuel rod integrity for normal conditions of storage the fuel must be maintained at a sufficiently low temperature in an inert atmosphere to preclude thermally induced fuel rod cladding deterioration. To preclude fuel degradation, the maximum allowable cladding temperatures under normal conditions of storage for 5-year cooled PWR fuel and BWR fuel are determined to be 716°F (380°C). For either of these fuel types, the maximum cladding temperature under off-normal, transfer and accident conditions must remain below 1,058°F (570°C). Finally, for the structural components of the

storage system, the thermally induced stresses, in combination with pressure and mechanical load stresses, must be below material allowable stress levels.

Thermal evaluations for normal conditions of storage and transfer (canister handling) condition operations are presented in Section 4.4. The finite element method is used to calculate the temperatures for the various components of the concrete cask, canister, basket, fuel cladding and transfer cask. Thermal models used in evaluation of normal and transfer conditions for the Standard configuration are described in Section 4.4.1.1.

A summary of the thermal evaluation results for the Standard Universal Storage System configuration is provided in Tables 4.1-4 and 4.1-5 for the PWR and BWR Standard configuration cases, respectively. Evaluation results for accident conditions of "All air inlets and outlets blocked" and "Fire" are presented in Chapter 11. The results demonstrate that the calculated temperatures are below the allowable component temperatures for all normal (long-term) storage conditions and for short-term events. The thermally induced stresses, combined with pressure and mechanical load stresses, are also within the allowable levels, as demonstrated in Chapter 3.

4.1.2 Advanced Configuration (32 PWR)

The Universal Storage System design basis heat load for the Advanced configuration is 29.2 kW for up to 32 PWR fuel assemblies. As shown in Section 4.4.7.2, the thermal analysis considers a range of fuel assembly burnup and cooling times for the fuel type to establish the allowable cladding temperatures.

The thermal evaluation considers normal, off-normal, and accident conditions of storage. Each of these conditions can be described in terms of the environmental temperature, use of solar insolation, and the condition of the air inlets and outlets, as shown in Table 4.1-1. The design conditions for transfer are defined in Table 4.1-2. The transfer conditions consider the transient effect for a total of 91 hours for the fuel, starting from the removal of the transfer cask/canister from the spent fuel pool. The canister is considered under normal operation to be inside the transfer cask and filled with water for 17 hours, in vacuum condition for 44 hours, back-filled with helium for 30 hours for PWR fuel, and then transferred into the Vertical Concrete Cask.

This evaluation applies different component temperature limits and different material stress limits for long-term conditions and short-term conditions. Normal storage is considered to be a long-term condition. Off-normal and accident events, as well as the transfer condition that temporarily occurs during the preparation of the canister while it is in the transfer cask, are considered as short-term conditions. Thermal evaluations are performed for the design basis PWR fuels for all design conditions. The maximum allowable material temperatures for long-term and short-term conditions are provided in Table 4.1-3.

During normal conditions of storage and hypothetical accident conditions, the concrete cask must reject the fuel decay heat to the environment without exceeding the operational temperature ranges of the components important to safety. Using the methodology of the NAC High Burnup Topical Report 790-TR-001 [39], a peak clad temperature (PCT) limit of 390°C (734°F) is defined based on saturated cladding creep for long-term storage conditions. The maximum cladding temperature under off-normal, transfer and accident conditions must remain below 1,058°F (570°C). Finally, for the structural components of the storage system, the thermally induced stresses, in combination with pressure and mechanical load stresses, must be below material allowable stress levels.

Thermal evaluations for normal conditions of storage and transfer (canister handling) condition operations are presented in Section 4.4. The finite element and finite volume method is used to calculate the temperatures for the various components of the concrete cask, canister, basket, fuel cladding and transfer cask. Thermal models used in the evaluation of normal and transfer conditions for the Advanced configuration are described in Section 4.4.1.2.

A summary of the thermal evaluation results for the Universal Storage System Advanced configuration is provided in Table 4.1-6 for the PWR fuels. Evaluation results for accident conditions of "All air inlets and outlets blocked" and "Fire" are presented in Chapter 11. The results demonstrate that the calculated temperatures are below the allowable component temperatures for all normal (long-term) storage conditions and for short-term events. The thermally induced stresses, combined with pressure and mechanical load stresses, are also within the allowable levels, as demonstrated in Chapter 3.

Table 4.1-1 Summary of Thermal Design Conditions for Storage

Condition ¹		Environmental Temperature (°F)	Solar Insolation ²	Condition of Concrete Cask Inlets and Outlets
Normal		76	Yes	All inlets and outlets open
Off-Normal - Half Air Inlets Blocked		76	Yes	Half inlets blocked and all outlets open
Off-Normal - Severe Heat		106	Yes	All inlets and outlets open
Off-Normal - Severe Cold		-40	No	All inlets and outlets open
Accident - Extreme Heat		133	Yes	All inlets and outlets open
Accident - All Air Inlets and Outlets Blocked ³		76	Yes	All inlets and outlets blocked
Accident - Fire ⁴	During Fire	1475	Yes	All inlets and outlets open
	Before and After Fire	76	Yes	All inlets and outlets open

1. Off-normal and accident condition analyses are presented in Chapter 11.
2. Solar Insolation per 10 CFR 71:
Curved Surface: 400 g cal/cm² (1475 Btu/ft²) for a 12-hour period.
Flat Horizontal Surface: 800 g cal/cm² (2950 Btu/ft²) for a 12-hour period.
3. This condition bounds the case in which all inlets are blocked, with all outlets open.
4. The evaluated fire accident is the described in Section 11.2.6.

Table 4.1-2 Summary of Thermal Design Conditions for Transfer

Condition ^{1,3}	Maximum Duration (Hours)		
	Standard Configuration		Advanced Configuration
	PWR	BWR	PWR
Canister Filled with Water ²	17	17	17
Vacuum Drying	10	10	44
Canister Filled with Helium	16	24	30

- (1) The canister is inside the transfer cask, with an ambient temperature of 76°F. The design conditions for the Standard configuration consider the transient effect for a total of 43 hours (PWR) or 51 hours (BWR) starting from the removal of the transfer cask/canister from the spent fuel pool. The design conditions for the Advanced configuration consider the transient effect for a total of 91 hours, starting from the removal of the transfer cask/canister from the spent fuel pool.
- (2) The initial water temperature is considered to be 100°F.
- (3) See Chapter 12, Appendix 12A, for Technical Specifications for specific limiting conditions.

Table 4.1-3 Maximum Allowable Material Temperatures

Material	Temperature Limits (°F)		Reference
	Long Term	Short Term	
Concrete	150(B)/ 300(L) ⁽¹⁾	350	ACI-349 [4] NUREG 1536 [43]
Fuel Clad (Standard Configuration)			
PWR Fuel (5-year cooled)	716 ⁽²⁾	1,058	PNL-6189 [5] and PNL-4835 [2]
BWR Fuel (5-year cooled)	716 ⁽²⁾	1,058	
Fuel Clad (Advanced Configuration)			
PWR Fuel	734 ⁽³⁾	1,058	PNL-6189 [5]
Aluminum 6061-T651	650	700	MIL-HDBK-5G [7]
NS-4-FR	300	300	GESC [8]
Chemical Copper Lead	600	600	Baumeister [9]
SA693 17-4PH Type 630 Stainless Steel	650	800	ASME Code [13] ARMCO [11]
SA240 Type 304 Stainless Steel	800	800	ASME Code [13]
SA240 Type 304L Stainless Steel	800	800	ASME Code [13]
ASTM A533 Type B Carbon Steel	700	700	ASME Code [13]
ASME SA588 Carbon Steel	700	700	ASME Code Case N-71-17 [12]
ASTM A36 Carbon Steel	700	700	ASME Code Case N-71-17 [12]
ASTM SA537 Class 2 Carbon Steel	700	850	ASME Code Case N-71-17 [12] and ASME Code Case N-650 [44]

- (1) B and L refer to bulk temperatures and local temperatures, respectively. The local temperature allowable applies to a restricted region where the bulk temperature allowable may be exceeded.
- (2) In accordance with PNL-6189, the temperature limit of 380°C (716°F) is used for the evaluation of fuel considered in the design basis heat load (23 kW). For temperature limits corresponding to different burnup and cooling times, refer to Table 4.4.7-5.
- (3) The fuel cladding temperature limit of 734°F (390°C) for the Advanced configuration is established based on the methodology of the NAC High Burnup Topical Report, 790-TR-001. See Section 4.4.7.2 for details.

Table 4.1-4 Summary of Thermal Evaluation Results for the Universal Storage System:
PWR Fuel – Standard Configuration

Long-Term Condition:						
Maximum Temperatures (°F)						
Design Condition	Concrete		Heat Transfer Disks	Support Disks ⁽¹⁾	Canister ⁽²⁾	Fuel Clad
Normal (76°F Ambient)	Bulk	Local				
	135	186	612	615	351	670
Allowable	150	300	650	650	800	716
Short-Term Condition:						
Maximum Temperatures (°F)						
Design Condition	Concrete		Heat Transfer Disks	Support Disks ⁽¹⁾	Canister ⁽²⁾	Fuel Clad
Off-Normal - Half Inlets Blocked (76°F Ambient)	191		613	617	350	671
Off-Normal - Severe Heat (106°F Ambient)	228		638	642	381	694
Off-Normal - Severe Cold (-40°F Ambient)	17		516	521	226	584
Accident - Extreme Heat (133°F Ambient)	262		661	664	408	715
Accident - Fire	244		652	655	459	710
Transfer - Vacuum Drying	N/A		538 ⁽³⁾	538 ⁽³⁾	244	538
Transfer - Backfilled with Helium	N/A		686 ⁽³⁾	686 ⁽³⁾	416	686
Allowable	350		700	800	800	1058

1. SA 693, 17-4PH Type 630 SS.
2. SA240, Type 304L SS (including canister shell, lid and bottom plate).
3. The maximum fuel cladding temperature is conservatively used.

Table 4.1-5 Summary of Thermal Evaluation Results for the Universal Storage System:
BWR Fuel – Standard Configuration

Long-Term Condition:						
Maximum Temperatures (°F)						
Design Condition	Concrete		Heat Transfer Disks	Support Disks ⁽¹⁾	Canister ⁽²⁾	Fuel Clad
	Bulk	Local				
Normal (76°F Ambient)	136	192	622	624	376	651
Allowable	150	300	650	700	800	716
Short-Term Condition:						
Maximum Temperatures (°F)						
Design Condition	Concrete		Heat Transfer Disks	Support Disks ⁽¹⁾	Canister ⁽²⁾	Fuel Clad
Off-Normal - Half Inlets Blocked (76°F Ambient)	195		622	625	374	652
Off-Normal - Severe Heat (106°F Ambient)	231		648	651	405	677
Off-Normal - Severe Cold (-40°F Ambient)	20		513	515	252	548
Accident - Extreme Heat (133°F Ambient)	266		675	677	432	702
Accident - Fire	244		662	664	416	691
Transfer - Vacuum Drying	N/A		447 ⁽³⁾	447 ⁽³⁾	235	447
Transfer - Backfilled with Helium	N/A		654 ⁽³⁾	654 ⁽³⁾	432	654
Allowable	350		700	700	800	1058

1. SA 533, Type B, CS.
2. SA240, Type 304L SS (including canister shell, lid and bottom plate).
3. The maximum fuel cladding temperature is conservatively used.

Table 4.1-6 Summary of Thermal Evaluation Results for the Universal Storage System: PWR
Fuel – Advanced Configuration

Long-Term Condition:					
Maximum Temperatures (°F)					
Design Condition	Concrete		Basket Plates ⁽¹⁾	Canister ⁽²⁾	Fuel Clad
Normal (76°F Ambient)	Bulk	Local			
	138	199	693	368	707
Allowable	150	300	700	800	734
Short-Term Condition:					
Maximum Temperatures (°F)					
Design Condition	Concrete		Basket Plates ⁽¹⁾	Canister ⁽²⁾	Fuel Clad
Off-Normal - Half Inlets Blocked (76°F Ambient)	202		694	369	709
Off-Normal - Severe Heat (106°F Ambient)	240		720	399	733
Off-Normal - Severe Cold (-40°F Ambient)	39		586	248	605
Accident - Extreme Heat (133°F Ambient)	276		745	426	757
Accident - Fire	267		749	424	763
Transfer - Vacuum Drying	N/A		819	452	853
Transfer - Backfilled with Helium	N/A		831	553	853
Allowable	350		850	800	1058

(1) SA 537 Carbon Steel.

(2) SA 240, Type 304L (including canister shell, lids and bottom plate).

4.2 Summary of Thermal Properties of Materials

The material thermal properties used in the thermal analyses are shown in Tables 4.2-1 through 4.2-14. Derivation of effective conductivities is described in Section 4.4.1. Tables 4.2-1 through 4.2-14 include only the materials that form the heat transfer pathways employed in the thermal analysis models. Materials for small components, which are not directly modeled are not included in the property tabulation.

Table 4.2-1 Thermal Properties of Solid Neutron Shield (NS-4-FR and NS-3)

Property (units) [8]	NS-4-FR	NS-3
Conductivity (Btu/hr-in-°F)	0.0311	0.0407
Density (borated) (lbm/in ³)	0.06	0.0621
Density (nonborated) (lbm/in ³)	0.0607	0.0640
Specific Heat (Btu/lbm-°F)	0.319	0.149

Table 4.2-2 Thermal Properties of Stainless Steel

Type 304 and 304L

Property (units)	Value at Temperature				
	100°F	200°F	400°F	550°F	750°F
Conductivity (Btu/hr-in-°F) [13]	0.7250	0.7750	0.8667	0.9250	1.0000
Density (lb/in ³) [14]	0.2896	0.2888	0.2872	0.2857	0.2839
Specific Heat (Btu/lbm-°F) [14]	0.1156	0.1202	0.1274	0.1314	0.1355
Emissivity [14]	← 0.36 →				

17-4PH, Type 630

Property (units)	Value at Temperature			
	70°F	200°F	400°F	650°F
Conductivity (Btu/hr-in-°F) [13]	0.824	0.883	0.975	1.083
Density (lb/in ³) [13]	← 0.291 →			
Specific Heat (Btu/lbm-°F) [11]	← 0.11 →			
Emissivity [15]	← 0.58 →			

Table 4.2-3 Thermal Properties of Carbon Steel

Material ¹ Property (units)	Value at Temperature					
	100°F	200°F	400°F	500°F	700°F	850°F
Conductivity (Btu/hr-in-°F) [13]	1.992	2.033	2.017	1.975	1.867	1.767
Density (lb/in ³) [16]	←————— 0.284 —————→					
Specific Heat (Btu/lbm-°F) [17]	←————— 0.113 —————→					
Emissivity [9]	←————— 0.80 —————→					

1. A-36, SA-533, A-588, SA-350 and SA-537.

Table 4.2-4 Thermal Properties of Chemical Copper Lead

Property (units)	Value at Temperature			
	209°F	400°F	581°F	630°F
Conductivity (Btu/hr-in-°F) [18]	1.6308	1.5260	1.2095	1.0079
Density (lb/in ³) [18]	←————— 0.411 —————→			
Specific Heat (Btu/lbm-°F) [18]	←————— 0.03 —————→			
Emissivity [9]	←————— 0.28 (75°F) —————→			

Table 4.2-5 Thermal Properties of Type 6061-T651 and Type 6061-T6 Aluminum Alloy

Property (units)	Value at Temperature					
	200°F	300°F	400°F	500°F	600°F	700°F
Conductivity (Btu/hr-in-°F) [7,13]	8.25	8.38	8.49	8.49	8.49	8.49
Specific Heat (Btu/hr-in-°F) [13]	←————— 0.23 —————→					
Emissivity [15]	←————— 0.22 —————→					

Table 4.2-6 Thermal Properties of Helium

Property (units)	Value at Temperature			
	80°F	260°F	440°F	800°F
Conductivity (Btu/hr-in-°F) [20]	0.00751	0.00915	0.01068	0.01355

Property (units)	Value at Temperature			
	200°F	400°F	600°F	800°F
Density (lb/in ³) [19]	4.83E-06	3.70E-06	3.01E-06	2.52E-06
Specific Heat (Btu/lbm-°F) [19]	←————— 1.24 —————→			

Table 4.2-7 Thermal Properties of Dry Air

Property (units)	Value at Temperature			
	100°F	300°F	500°F	700°F
Conductivity (Btu/hr-in-°F) [19]	0.00128	0.00161	0.00193	0.00223
Density (lb/in ³) [19]	4.11E-05	3.01E-05	2.38E-05	1.97E-05
Specific Heat (Btu/lbm-°F) [19]	0.240	0.244	0.247	0.253

Table 4.2-8 Thermal Properties of Zircaloy and Zircaloy-4 Cladding

Property (units)	Value at Temperature			
	392°F	572°F	752°F	932°F
Conductivity (Btu/hr-in-°F) [22]	0.69	0.73	0.80	0.87
Density (lb/in ³) [23]	←————— 0.237 —————→			
Specific Heat (Btu/lbm-°F) [22]	0.072	0.074	0.076	0.079
Emissivity [22]	←————— 0.75 —————→			

Table 4.2-9 Thermal Properties of Fuel (UO₂)

Property (units)	Value at Temperature				
	100°F	257°F	482°F	707°F	932°F
Conductivity (Btu/hr-in-°F) [22]	0.38	0.347	0.277	0.236	0.212
Specific Heat (Btu/lbm-°F) [22]	0.057	0.062	0.067	0.071	0.073
Density (lbm/in ³) [23]	←————— 0.396 —————→				
Emissivity [22]	←————— 0.85 —————→				

Table 4.2-10 Thermal Properties of BORAL Composite Sheet

Property (units)	Value at Temperature	
	100°F	500°F
Conductivity (Btu/hr-in-°F)		
Aluminum Clad [24]	7.805	8.976
Core Matrix		
PWR (calculated)	3.45	3.05
BWR (calculated)	6.60	7.23
Emissivity ⁽¹⁾ [25]	← 0.15 →	

⁽¹⁾ The emissivity of the aluminum clad of the BORAL sheet ranges from 0.10 to 0.19. An averaged value of 0.15 is used.

Table 4.2-11 Thermal Properties of Concrete

Property (units)	Value at Temperature		
	100°F	200°F	300°F
Conductivity (Btu/hr-in-°F) [26]	0.091	0.089	0.086
Density (lbm/in ³) [27]	← 140 →		
Specific Heat (Btu/lbm-°F) [17]	← 0.20 →		
Emissivity ⁽¹⁾ [17,28]	← 0.90 →		
Absorptivity [29]	← 0.60 →		

⁽¹⁾ Emissivity = 0.93 for masonry, 0.94 for rough concrete; 0.9 is used.

Table 4.2-12 Thermal Properties of Water

Property (units)	Value at Temperature		
	70°F	200°F	300°F
Conductivity (Btu/hr-in-°F) [32]	0.029	0.033	0.033
Specific Heat (Btu/lbm-°F) [32]	0.998	1.00	1.03
Density (lbm/in ³) [32]	0.036	0.035	0.033

Table 4.2-13 Thermal Properties of METAMIC

Property (units)	Value at Temperature		
	77°F	212°F	482°F
Conductivity (Btu/hr-in-°F) [37]	4.54	4.42	4.64
Specific Heat (Btu/lbm-°F) [37]	0.2207	0.2412	0.2938
Density (lbm/in ³) [37]	← 0.094 →		
Emissivity [37]	200	500	800
	0.85	0.81	0.76

Table 4.2-14 Thermal Properties of 1100 Aluminum Alloy

Property (units)	Value at Temperature				
	70°F	100°F	200°F	300°F	400°F
Conductivity (Btu/hr-in-°F) [38]	11.1	11.0	10.7	10.5	10.4
Specific Heat (Btu/lbm-°F) [38]	← 0.23 →				
Density (lbm/in ³) [38]	← 0.098 →				
Emissivity [45]	← 0.40 →				

THIS PAGE INTENTIONALLY LEFT BLANK

4.3 Technical Specifications for Components

Five major components of the Universal Storage System must be maintained within their safe operating temperature ranges: the concrete, the lead gamma shield, the NS-4-FR solid neutron shield in the transfer cask, the aluminum heat transfer components, and the steel basket and canister structural components. The safe operating ranges for these components are from a minimum temperature of -40°F to the maximum temperatures as shown in Table 4.1-3.

The criterion for the safe operating range of the lead gamma shield is the prevention of the lead from reaching its melting point of 620°F [9]. The maximum operating temperature limit of the NS-4-FR solid neutron shield material, determined by the manufacturer, is to ensure sufficient neutron shielding capacity. The primary consideration in establishing the safe operating range of the aluminum heat transfer disks and steel support disks is maintaining the integrity of the aluminum and steel.

THIS PAGE INTENTIONALLY LEFT BLANK

4.4 Thermal Evaluation for Normal Conditions of Storage

The finite element and finite volume methods are used to evaluate the thermal performance of the Universal Storage System for normal conditions of storage. The general-purpose finite element analysis program ANSYS [6] [40] and the finite volume analysis program FLUENT [41] are used to perform the thermal evaluations.

THIS PAGE INTENTIONALLY LEFT BLANK

4.4.1 Thermal Models

4.4.1.1 Thermal Models for Standard Configuration

Finite element models are utilized for the thermal evaluation of the Universal Storage System, as shown below. These models are used separately to evaluate the system for the storage of PWR or BWR fuel.

1. Two-Dimensional Axisymmetric Air Flow and Concrete Cask Models
2. Three-Dimensional Canister Models
3. Two-Dimensional Axisymmetric Transfer Cask and Canister Models
4. Three-Dimensional Periodic Canister Internal Models
5. Two-Dimensional Fuel Models
6. Two-Dimensional Fuel Tube Models
7. Two-Dimensional Forced Air Flow Model for Transfer Cask Cooling
8. Three-Dimensional Transfer Cask and Canister Model

The two-dimensional axisymmetric air flow and concrete cask model includes the concrete cask, air in the air inlets, annulus and the air outlets, the canister and the canister internals, which are modeled as homogeneous regions with effective thermal conductivities. The effective thermal conductivities for the canister internals in the radial direction are determined using the three-dimensional periodic canister internal models. The effective conductivities in the canister axial direction are calculated using classical methods. The two-dimensional axisymmetric air flow and concrete cask model is used to perform computational fluid dynamic analyses to determine the mass flow rate, velocity and temperature of the air flow, as well as the temperature distribution of the concrete, concrete cask steel liner and the canister. Two models are generated for the evaluations of the PWR and the BWR systems, respectively. These models are essentially identical, but have slight differences in dimensions and the effective properties of the canister internals.

The three-dimensional canister model comprises the fuel assemblies, fuel tubes, stainless steel or carbon steel support disks, aluminum heat transfer disks, top and bottom weldments, the canister shell, lids and bottom plate. The canister model is employed to evaluate the temperature distribution of the fuel cladding and basket components. The fuel assemblies and the fuel tubes in the three-dimensional canister model are modeled using effective conductivities. The effective conductivities for the fuel assemblies are determined using the two-dimensional fuel

models. The effective conductivities for the fuel tubes are determined using the two-dimensional fuel tube models. Two three-dimensional canister models are generated for the PWR and BWR canisters, respectively.

The two-dimensional axisymmetric transfer cask model includes the transfer cask and the canister with its internals modeled as homogeneous regions with effective thermal properties. This model is used to perform transient analyses for the transfer condition, starting from removing the transfer cask/canister from the spent fuel pool, vacuum drying and finally back-filling the canister with helium. Separate transfer cask models are required for PWR and BWR systems.

The three-dimensional canister internal model consists of a periodic section of the canister internals. For the PWR canister, the model contains one support disk with two heat transfer disks (half thickness) on its top and bottom, fuel assemblies, fuel tubes and the media in the canister. For the BWR canister, two models are required. The first model, for the central region of the BWR canister, contains one heat transfer disk with two support disks (half thickness) on its top and bottom, fuel assemblies, fuel tubes and the media in the canister. The other model, for the region without heat transfer disks, contains two support disks (half thickness), fuel assemblies, fuel tubes and the media in the canister. The purpose of the three-dimensional periodic canister internal model is to determine the effective thermal conductivity of the canister internals in the canister radial direction. The effective conductivities are used in the two-dimensional axisymmetric air flow and concrete cask models and two-dimensional axisymmetric transfer cask and canister models. Three types of media are considered: helium, water and a vacuum. The fuel assemblies and fuel tubes in this model are modeled as homogeneous regions with effective thermal properties, which are determined by the two-dimensional fuel models and the two-dimensional fuel tube models.

The two-dimensional fuel model includes the fuel pellets, cladding and the media occupying the space between fuel rods. The media is considered to be helium for storage conditions and water, vacuum or helium for transfer conditions. The model is used to determine the effective thermal conductivities of the fuel assembly. In order to account for various types of fuel assemblies, a total of seven fuel models are generated: Four models for the 14×14, 15×15, 16×16 and 17×17 PWR fuel assemblies and three models for the 7×7, 8×8 and 9×9 BWR fuel assemblies. The effective properties are used in the three-dimensional canister models and the three-dimensional periodic canister internal models.

The two-dimensional fuel tube model is used to determine the effective conductivities of the fuel tube wall and BORAL plate. The effective properties are used in the three-dimensional canister models and the three-dimensional periodic canister internal models.

The two-dimensional axisymmetric air flow model is used to determine the air flow rate needed for the forced air cooling of the canister inside the transfer cask.

The three-dimensional transfer cask and canister model is used to evaluate the transfer operation for PWR fuel heat load cases with less than the design basis heat load of 23 kW.

Detailed description of the finite element models are presented in Sections 4.4.1.1.1 through 4.4.1.1.8.

4.4.1.1.1 Two-Dimensional Axisymmetric Air Flow and Concrete Cask Models

This section describes the finite element models used to evaluate the thermal performance of the vertical concrete cask for the PWR and BWR configurations. The model includes the concrete cask, the air in the air inlets, the annulus and the air outlets, the canister and the canister internals, which are modeled as homogeneous regions with effective thermal conductivities. Two separate two-dimensional axisymmetric models are used for the PWR and BWR configurations, respectively. The PWR model is shown in Figures 4.4.1.1.1-1 and 4.4.1.1.1-2. The BWR model is essentially identical to the PWR model, but it incorporates different effective thermal properties of the canister internals, and slight differences in dimensions.

The fuel canister is cooled by (1) natural/free convection of air through the lower vents (the air inlets), the vertical air annulus, and the upper vents (the air outlets); and (2) radiation heat transfer between the surfaces of the canister shell and the steel liner. The heat transferred to the liner is rejected by air convection in the annulus and by conduction through the concrete. The heat flow through the concrete is dissipated to the surroundings by natural convection and radiation heat transfer. The temperature in the concrete region is controlled by radiation heat transfer between the vertical annulus surfaces (the canister shell outer surface and the steel liner inner surface), natural convection of air in the annulus, and boundary conditions applicable to the concrete cask outer surfaces—e.g., natural convection and radiation heat transfer between the

outer surfaces and the environment, including consideration of incident solar energy. These heat transfer modes are combined in the air flow and concrete cask model. The entire thermal system, including mass, momentum, and energy, is analyzed using the two-dimensional axisymmetric air flow and concrete cask models. The temperature distributions of the concrete cask, the air region and the canister are determined by these models. Detailed thermal evaluations for the canister internals (fuel cladding, basket, etc.) are performed using the three-dimensional canister models as described in Section 4.4.1.1.2.

The concrete cask has four air inlets at the bottom and four air outlets at the top that extend through the concrete. Since the configuration is symmetrical, it can be simplified into a two-dimensional axisymmetric model by using equivalent dimensions for the air inlets and outlets, which are assumed to extend around the concrete cask periphery. The canister internals are modeled as three homogeneous regions using effective thermal conductivities - the active fuel region and the regions above and below the active fuel region. The two-dimensional axisymmetric model is shown schematically in Figure 4.4.1.1.1-1. Determination of the effective properties is described in Section 4.4.1.1.4.

ANSYS FLOTTRAN FLUID141 fluid thermal elements are used to construct the two-dimensional axisymmetric finite element models, as shown in Figure 4.4.1.1.1-2. In the air region (including the air inlet, outlet and annulus regions), only quadrilateral elements are used and the element sizes are nonuniform with much smaller element sizes close to the walls. In other regions, to simulate conduction, a mix of quadrilateral elements and triangular elements are used. Radiation heat transfer that occurs in the following regions is included in the model:

1. From the concrete outer surfaces to the ambient
2. Across the vertical air annulus (from the canister shell to the concrete cask liner)
3. From the top of the active fuel region to the bottom of the canister shield lid
4. From the bottom of the active fuel region to the top of the canister bottom plate
5. From the canister structural lid to the shield plug
6. From the shield plug to the concrete cask lid

Loads and Boundary Conditions

1. Heat generation in the active fuel region.

The distribution of the heat generation is based on the axial power distribution shown in Figures 4.4.1.1.1-3 and 4.4.1.1.1-4 for PWR and BWR fuels, respectively (see description in Chapter 5, Section 5.2.4, for the design-basis fuel).

2. Solar insolation to the outer surfaces of the concrete cask.

The solar insolation to the concrete cask outer surfaces is considered in the model. The incident solar energy is applied based on 24-hour averages as shown below.

$$\text{Side surface: } \frac{1475\text{Btu} / \text{ft}^2}{24\text{hrs}} = 61.46\text{Btu} / \text{hr} \cdot \text{ft}^2$$

$$\text{Top surface: } \frac{2950\text{Btu} / \text{ft}^2}{24\text{hrs}} = 122.92\text{Btu} / \text{hr} \cdot \text{ft}^2$$

3. Natural convection heat transfer at the outer surfaces of the concrete cask.

Natural convection heat transfer at the outer surfaces of the concrete cask is evaluated by using the heat transfer correlation for vertical and horizontal plates [17, 29]. This method assumes a surface temperature and then estimates Grashof (Gr) or Rayleigh (Ra) numbers to determine whether a heat transfer correlation for a laminar flow model or for a turbulent flow model should be used. Since Grashof or Rayleigh numbers are much higher than the critical values, correlation for the turbulent flow model is used as shown in the following.

Side surface [17]:

$$\begin{aligned} \text{Nu} &= 0.13(\text{Gr} \cdot \text{Pr})^{1/3} && \text{for } \text{Gr} > 10^9 \\ h_c &= \text{Nu} \cdot k_f / H_{\text{VCC}} \end{aligned}$$

Top surface [29]:

$$\begin{aligned} \text{Nu} &= 0.15\text{Ra}^{1/3} && \text{for } \text{Ra} > 10^7 \\ h_c &= \text{Nu} \cdot k_f / L \end{aligned}$$

where:

Gr	Grashof number
h_c	Average natural convection heat transfer coefficient
H_{vcc}	Height of the vertical concrete cask
k_f	Conductivity
L	Top surface characteristic length, $L = \text{area} / \text{perimeter}$
Nu	Average Nusselt number
Pr	Prandtl number
Ra	Rayleigh number

All material properties required in the above equations are evaluated based on the film temperature, that is, the average value of the surface temperature and the ambient temperature.

4. Radiation heat transfer at the concrete cask outer surfaces.

The radiation heat transfer between the outer surfaces and the ambient is evaluated in the model by calculating an equivalent radiation heat transfer coefficient.

$$h_{\text{rad}} = \frac{\sigma(T_1^2 + T_2^2)(T_1 + T_2)}{\frac{1}{\varepsilon_1} + \frac{1}{\varepsilon_2} + \frac{1}{F_{12}} - 2}$$

where:

h_{rad}	Equivalent radiation heat transfer coefficient
F_{12}	View factor
T_1 & T_2	Surface (T_1) and ambient (T_2) temperatures
ε_1 & ε_2	Surface (ε_1) and ambient ($\varepsilon_2=1$) emissivities
σ	Stefan-Boltzmann Constant

At the concrete cask side, an emissivity for a concrete surface of $\varepsilon_1 = 0.9$ is used and a calculated view factor (F_{12}) = 0.182 [29] is applied. The view factor is determined by conservatively assuming that the cask is surrounded by eight casks.

At the cask top, an emissivity, ϵ_1 , of 0.8 is conservatively used (emissivity for concrete is 0.9), and a view factor, F_{12} , of 1 is applied.

Accuracy Check of the Numerical Simulation

To ensure the accuracy of the numerical simulation of the air flow in the concrete cask, and to ensure reliable numerical results, the following checks and confirmations are performed.

1. Global convergence of the iteration process for the nonlinear system.

The system controlling air flow through the cask and, therefore, the temperature field is nonlinear and is solved iteratively.

The global iteration process is monitored by checking the variation of parameters with the global iteration—e.g., the maximum air temperature, the mass flow rate, and the net heat carried out of the concrete cask by air convection. All of the results presented are at the converged state.

2. Overall energy balance and mass balance.

This step validates the overall energy balance and mass balance. At the converged state, the mass flow rate at the air inlets matches the mass flow rate at the air outlets, showing that an excellent mass balance has been obtained.

The overall energy balance is checked by computing the total heat input (Q_{in}) and total heat output (Q_{out}). The total heat input includes the total heat from the fuel (Q_{fuel}) and the total absorbed solar energy (Q_{sun}) incident on the concrete cask outer surfaces. The total heat output is the sum of the net heat carried out of the cask by air (Q_{air}) and by convection and radiation heat loss at the concrete cask outer surfaces (Q_{con}).

For the normal storage condition with the PWR design heat load of 23.0 kW:

$$\begin{aligned}Q_{in} &= Q_{fuel} + Q_{sun} = 23.0 \text{ kW} + 9.18 \text{ kW} = 32.18 \text{ kW} \\Q_{out} &= Q_{air} + Q_{con} = 20.97 \text{ kW} + 11.72 \text{ kW} = 32.69 \text{ kW} \\Q_{out}/Q_{in} &= 1.016\end{aligned}$$

For the normal storage condition with the BWR design heat load of 23.0 kW:

$$Q_{in} = Q_{fuel} + Q_{sun} = 23.0 \text{ kW} + 9.52 \text{ kW} = 32.52 \text{ kW}$$

$$Q_{out} = Q_{air} + Q_{con} = 20.70 \text{ kW} + 12.12 \text{ kW} = 32.82 \text{ kW}$$

$$Q_{out}/Q_{in} = 1.009$$

The overall energy balance is demonstrated to be within 2 percent for all design conditions.

3. Finite Element Mesh Adequacy Study.

A sensitivity evaluation is performed to assess the effect of the number of elements used in the Two-dimensional Axisymmetric Air Flow and Concrete Cask Models. The sensitivity evaluation is performed with a reduced element model based on the model for the PWR fuel configuration. The total number of elements in the reduced-element model (13,371 elements) is 21% less than the number of elements used in the axisymmetric air flow and concrete cask model described above. The reduction in the number of elements occurs in the air flow region in the radial direction, which has the largest gradients in velocity and temperature. As shown below, the temperatures calculated by the reduced element model (Case ES1) are essentially the same as the temperatures calculated by the axisymmetric air flow and concrete cask model (Case ES2).

Case	Number of Elements in Model	Max. Air Temp. in Annular Region (Canister Surface)	Maximum Concrete Temp.	Average Air Temp. at the Outlet	Maximum Canister Shell Temp.
ES1	13,371	451 K	360 K	335 K	452 K
ES2	16,835	448 K	359 K	339 K	449 K
ES1/ES2	0.79	1.01	1.00	0.99	1.01

A comparison of the two models (Case ES1/ES2) shows that the maximum difference is 1%. Therefore, the number of elements used in the Two-dimensional Axisymmetric Air Flow and Concrete Cask Model (16,835) is adequate.

Supplemental Shielding Fixture Evaluation

The effect of the installation of an optional supplemental shielding fixture, shown in Drawing 790-613, installed in the air inlet is evaluated based on one-half of the air inlets blocked. The analysis results show that the maximum temperature increase is 5°F, which remains well below normal condition allowables. The pipes in the shielding fixture are offset to block (gamma) radiation, but allow air flow.

Figure 4.4.1.1.1-1 Two-Dimensional Axisymmetric Air Flow and Concrete Cask Model:
PWR – Standard Configuration

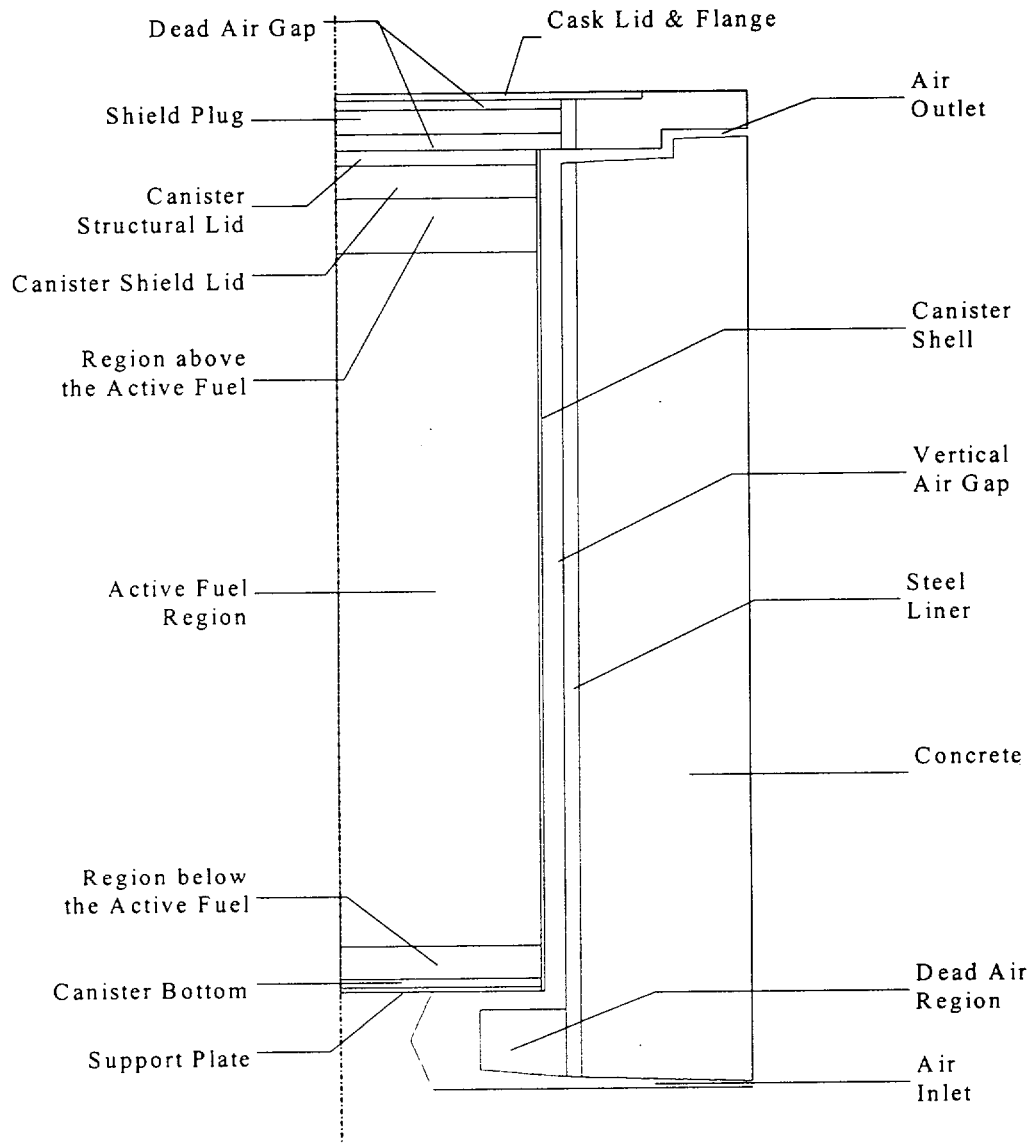


Figure 4.4.1.1.1-2 Two-Dimensional Axisymmetric Air Flow and Concrete Cask Finite Element Model: PWR – Standard Configuration

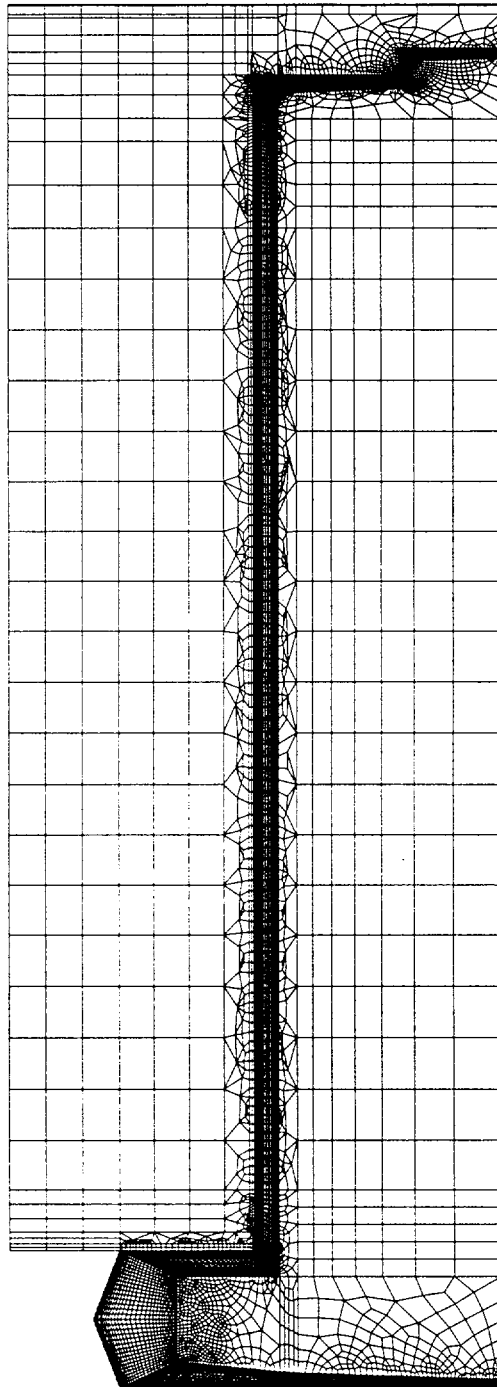


Figure 4.4.1.1.1-3 Axial Power Distribution for PWR Fuel

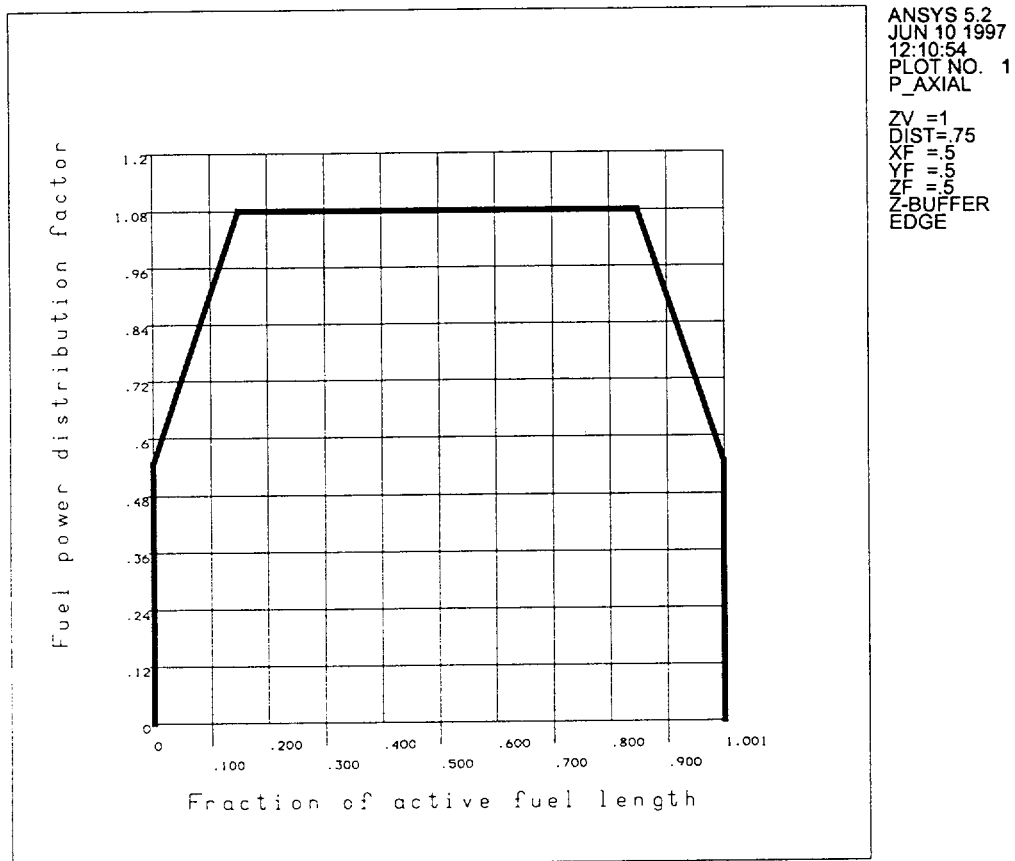
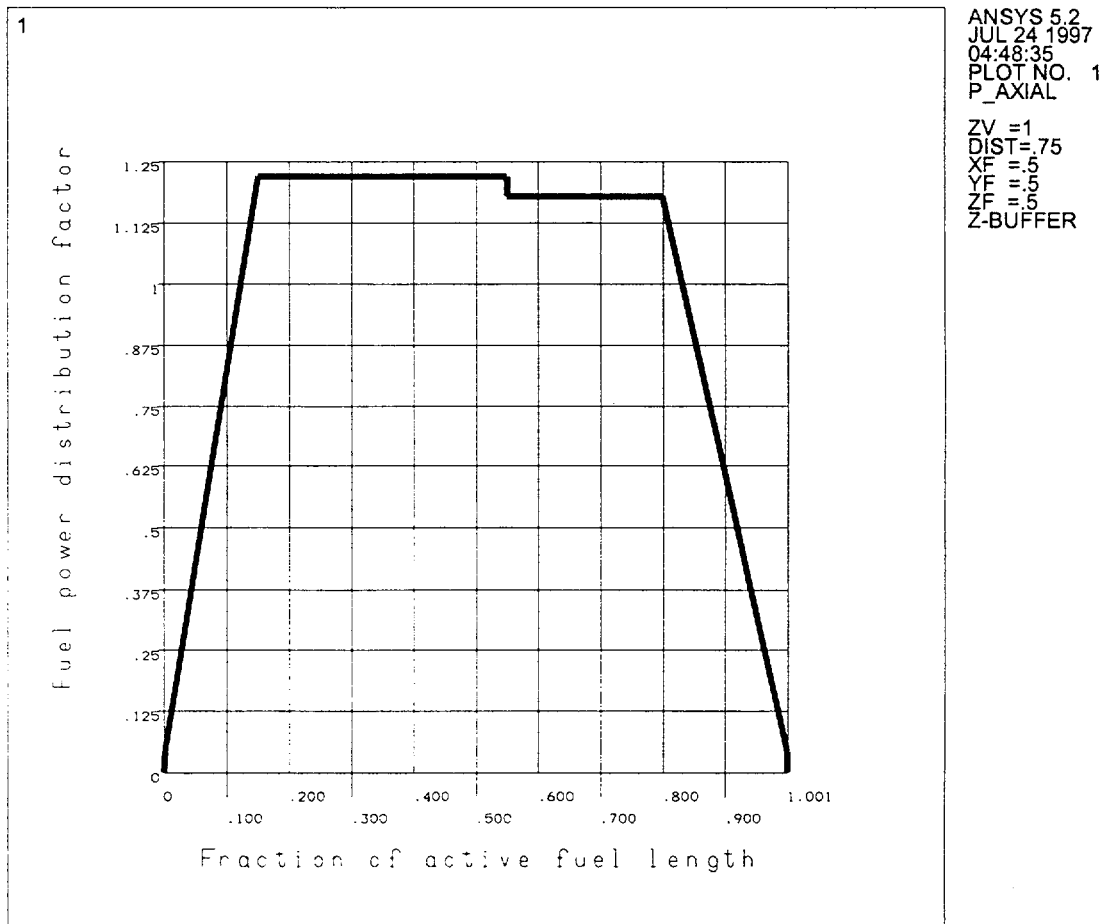


Figure 4.4.1.1.1-4 Axial Power Distribution for BWR Fuel



4.4.1.1.2 Three-Dimensional Standard Canister Models

Two three-dimensional canister models are used to evaluate the temperature distribution of the fuel cladding and basket components inside the Standard canister for the PWR and BWR configurations, respectively. The model for PWR fuel is shown in Figures 4.4.1.1.2-1 and 4.4.1.1.2-2. The model for BWR fuel is shown in Figures 4.4.1.1.2-3 and 4.4.1.1.2-4.

ANSYS SOLID70 three-dimensional conduction elements and LINK31 radiation elements are used to construct the model. The model includes the fuel assemblies, fuel tubes, support disks, heat transfer disks, top and bottom weldments, canister shell, lids, bottom plate and gas inside the canister (helium). Based on symmetry, only half of the canister is modeled. The plane of symmetry is considered to be adiabatic.

The canister outer surface temperatures obtained from the two-dimensional axisymmetric air flow and concrete cask model (Section 4.4.1.1.1) are applied at the canister surfaces in the model as boundary conditions. In the model, the fuel assemblies are considered to be centered in the fuel tubes. The fuel tubes are centered in the slots of the support disks and heat transfer disks. The basket is centered in the canister. These assumptions are conservative since any contact between components will provide a more efficient path to reject the heat.

The gaps used in the three-dimensional canister model between the support disks and canister shell, as well as between the heat transfer disk and the canister shell are:

		Nominal Gap At Room Temperature (inch)	Gap Used in the 3-D Thermal Model (inch)	
			At Room Temperature	At Elevated Temperature
PWR	Gap between Support Disk and Canister Shell	0.120	0.155	0.165
	Gap between Heat Transfer Disk and Canister Shell	0.245	0.280	0.190
BWR	Gap between Support Disk and Canister Shell	0.120	0.155	0.165
	Gap between Heat Transfer Disk and Canister Shell	0.280	0.315	0.227

The gaps at room temperature are first used in the model to calculate preliminary temperature distribution and to determine the differential thermal expansion of the disks and canister shell at the elevated temperatures. The gaps at elevated temperature are then established, based on the differential thermal expansions between components, and used in the model for final solution. As shown above, the room temperature gaps used in the thermal model bound the actual nominal gaps at room temperature.

These gap sizes are adjusted in the model to account for differential thermal expansion of the disks and canister shell based on thermal conditions. The gaps used in the model are shown to be larger than the actual gap size based on thermal expansion calculation using the thermal analysis results; therefore, the model is conservative.

A sensitivity study was performed to assess the effect of gap sizes on temperature results, with consideration of fabrication tolerance of the canister and basket. The ANSYS three-dimensional canister model for the PWR fuel is used for the study. The gaps between the disks and canister shell are increased to account for the worst case fabrication tolerance of the canister and basket. The gaps are also adjusted based on the differential thermal expansion of the canister and basket at elevated temperature. Compared to the gaps used in the original three-dimensional thermal model, the gap between the support disk and the canister shell is increased by 27% and the gap between the heat transfer disk and the canister shell is increased by 24%. The results of the sensitivity study indicate that the increase in the maximum fuel cladding and basket temperatures is less than 9°F, which is less than 3% of the temperature difference between the maximum temperature of the fuel cladding/basket and the canister shell. Therefore, the effect of the thermal model gap size on the maximum temperature of the basket and fuel cladding is not significant.

The structural lid and the shield lid are expected to be in full contact due to the weight of the structural lid. The thermal resistance across the contact surface is considered to be negligible and, therefore, no gap is modeled between the lids.

All material properties used in the model, except the effective properties discussed below, are shown in Tables 4.2-1 through 4.2-12.

The fuel assemblies and fuel tubes are modeled as homogenous regions with effective conductivities, determined by the two-dimensional fuel models (Section 4.4.1.1.5) and the

two-dimensional fuel tube models (Section 4.4.1.1.6), respectively. The effective properties are listed in Tables 4.4.1.1.2-1 through 4.4.1.1.2-4. The properties corresponding to the PWR 14 × 14 assemblies are used for the PWR model, since the 14 × 14 assemblies have lower conductivities as compared to other PWR assemblies. For the same reason, the properties corresponding to the BWR 9 × 9 assemblies are used in the BWR model.

In the model, radiation heat transfer is taken into account in the following locations:

1. From the top of the fuel region to the bottom surface of the canister shield lid.
2. From the bottom of the fuel region to the top surface of the canister bottom plate.
3. From the exterior surfaces of the fuel tubes (surface between disks) to the inner surface of the canister shell.
4. From the edge of the PWR support disks to the inner surface of the canister shell.
5. From the edge of heat transfer disks to the inner surface of the canister shell.
6. Between disks in the PWR model in the canister axial direction.

The radiation heat transfer from the BWR support disk is conservatively neglected by using an emissivity value of 0.0001 for the BWR support disk in the model.

Radiation elements (LINK31) are used to model the radiation effect for the first three locations. Radiation across the gaps (Locations No. 4 through 6) is accounted for by establishing effective conductivities for the gas in the gap, as shown below. The gaps are small compared to the surfaces separated by the gaps.

Radiation heat transfer between two nodes i (hotter node) and j (colder node) is accounted for by the expression:

$$q_r = \sigma \epsilon A F (T_i^4 - T_j^4)$$

where:

- σ = the Stefan-Boltzman constant
- ϵ = effective emissivity between two surfaces
- A = surface area
- F = the gray body shape factor for the surfaces
- T_i = temperature of the i th node
- T_j = temperature of the j th node

The total heat transfer can be expressed as the sum of the radiation and the conduction processes:

$$Q_t = q_r + q_k$$

where q_r is specified above for the radiation heat transfer and q_k , which is the heat transfer by conduction is expressed as:

$$q_k = \frac{KA}{g}(T_i - T_j)$$

where:

- T_i = temperature of the i th node
- T_j = temperature of the j th node
- g = gap distance (between the two surfaces defined by node i and node j)
- K = conductivity of the gas in the gap
- A = area of gap surface

By combining the two expressions (for q_k and q_r) and factoring out the term $A(T_i - T_j)/g$,

$$Q_t = [g\sigma\epsilon F(T_i^2 + T_j^2)(T_i + T_j) + K][A(T_i - T_j)/g]$$

or

$$Q_t = K_{\text{eff}}A(T_i - T_j)/g$$

where:

$$K_{\text{eff}} = g\sigma\epsilon F(T_i^2 + T_j^2)(T_i + T_j) + K$$

The material conductivity used in the analysis for the elements comprising the gap includes the heat transfer by both conduction and radiation.

Effective emissivities (ϵ) are used for all radiation calculations, based on the formula below [17]. The view factor is taken to be unity.

$$\epsilon = 1 / (1/\epsilon_1 + 1/\epsilon_2 - 1)$$

where ϵ_1 & ϵ_2 are the emissivities of two parallel plates

Radiation between the exterior surfaces of the fuel tubes is conservatively ignored in the model.

Volumetric heat generation (Btu/hr-in³) is applied to the active fuel region based on design heat load, active fuel length of 144 inches and an axial power distribution as shown in Figures 4.4.1.1.1-3 and 4.4.1.1.1-4 for PWR and BWR fuel, respectively.

Figure 4.4.1.1.2-1 Three-Dimensional Standard Canister Model for PWR Fuel

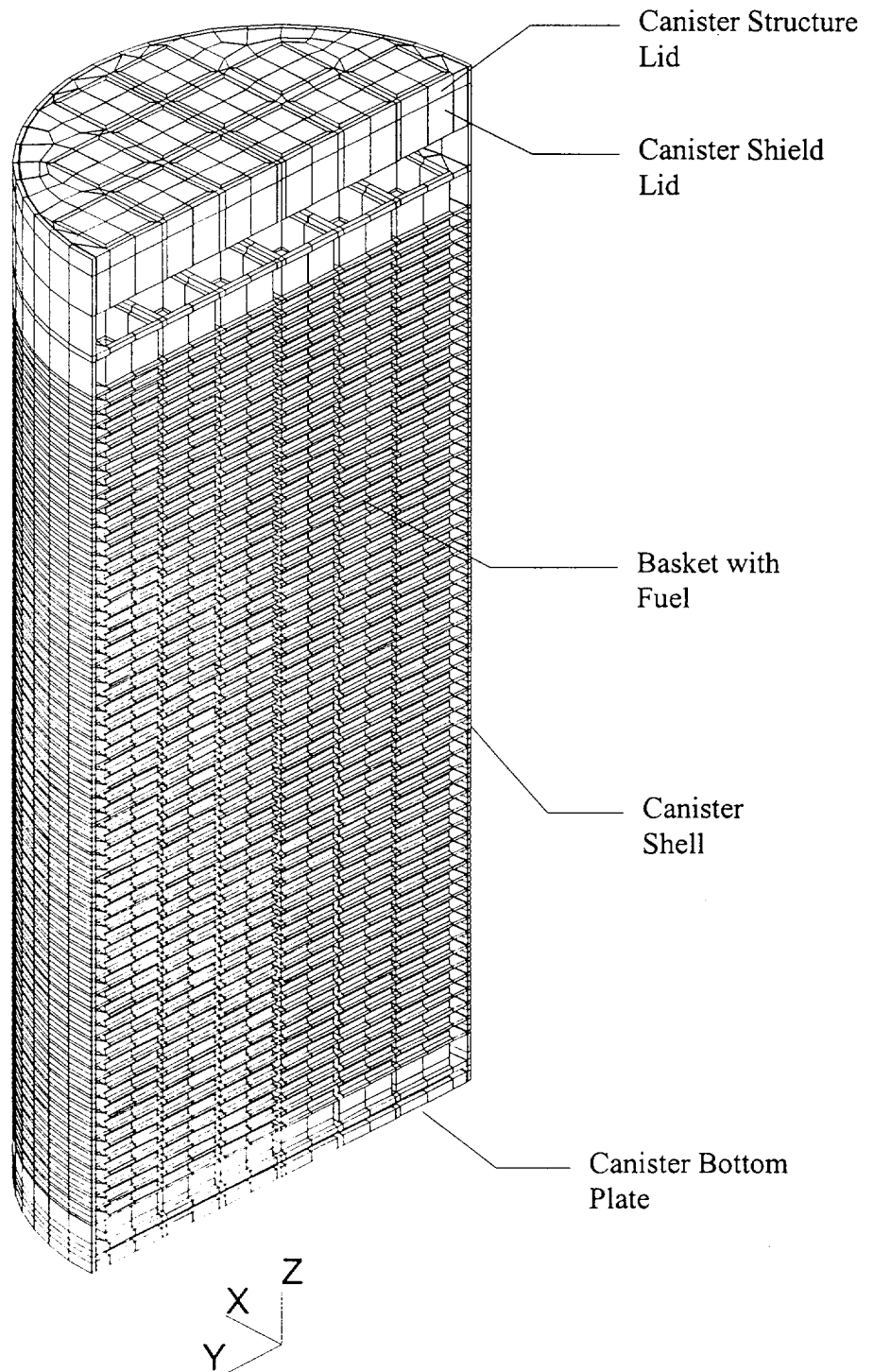


Figure 4.4.1.1.2-2 Three-Dimensional Standard Canister Model for PWR Fuel – Cross-Section

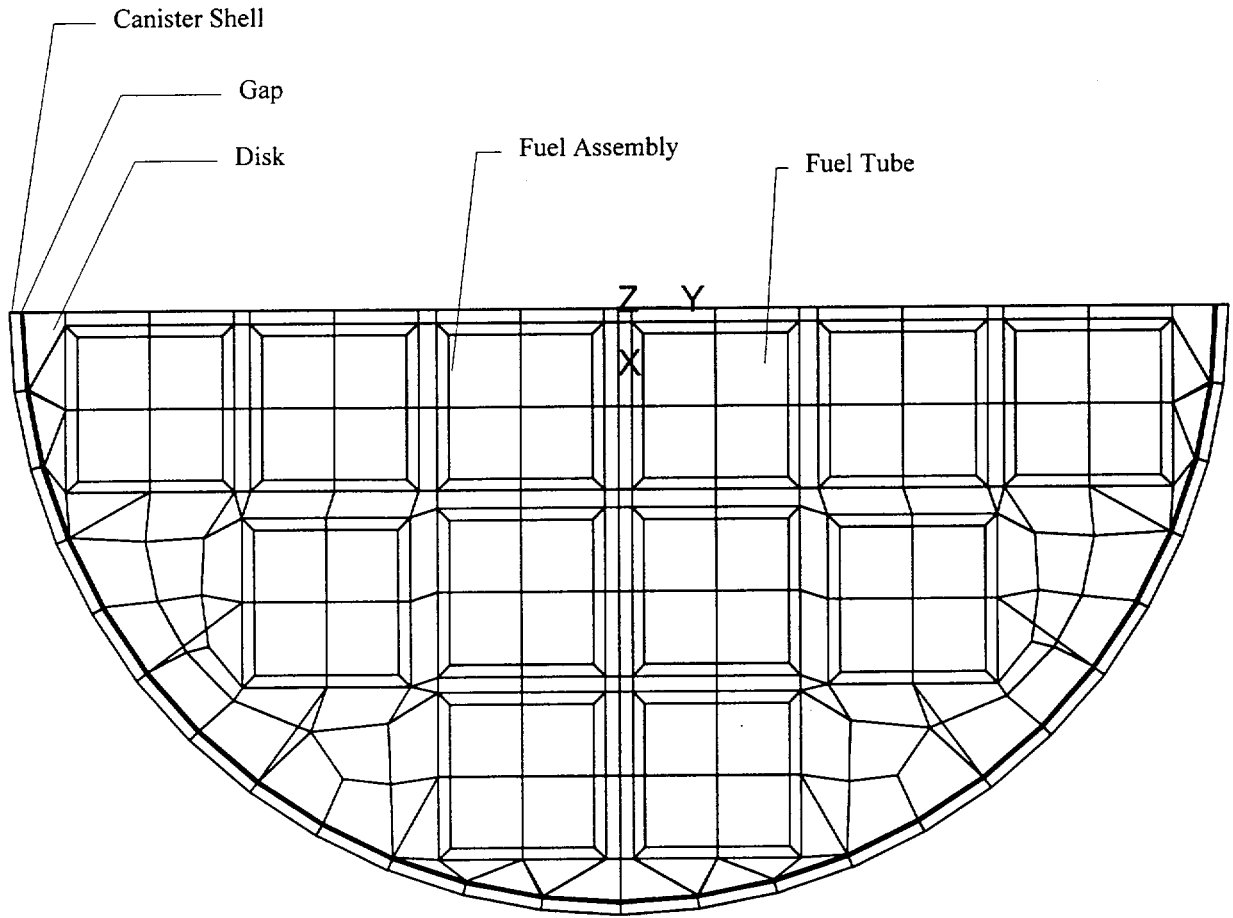


Figure 4.4.1.1.2-3 Three-Dimensional Standard Canister Model for BWR Fuel

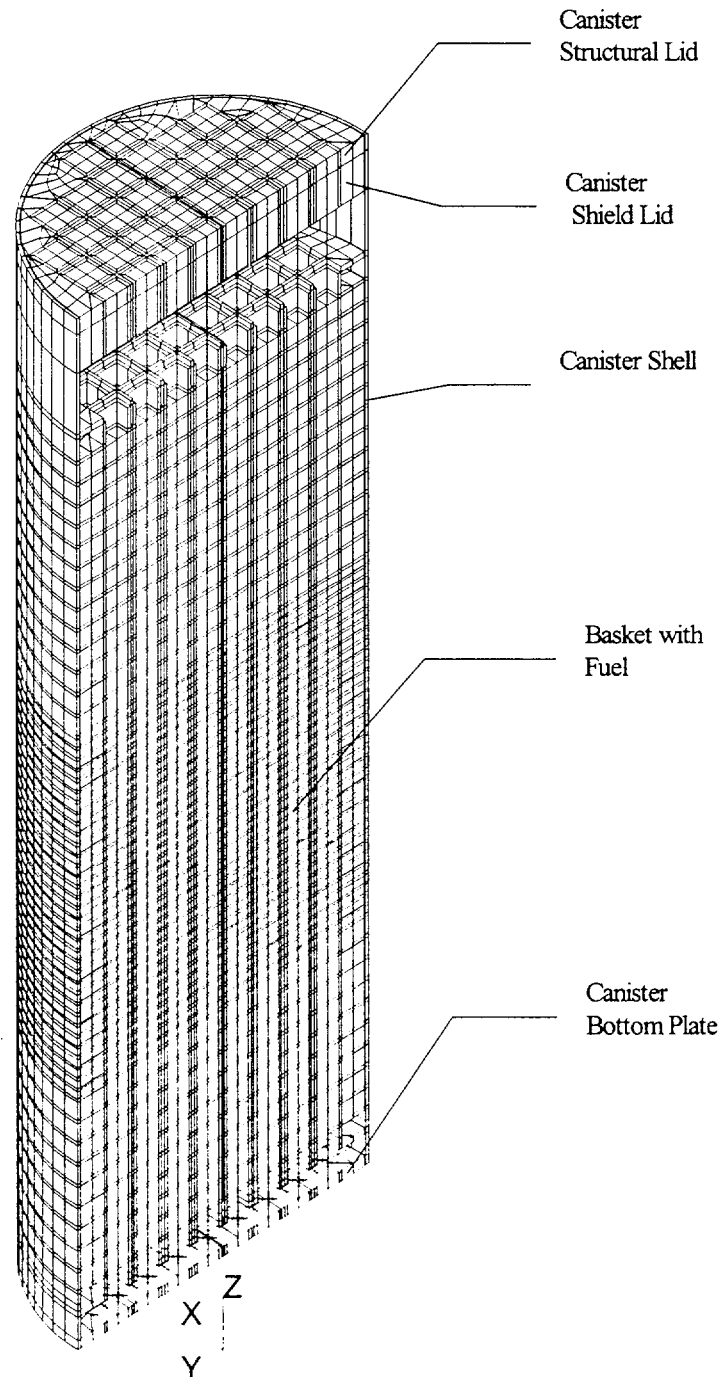


Figure 4.4.1.1.2-4 Three-Dimensional Standard Canister Model for BWR Fuel – Cross-Section

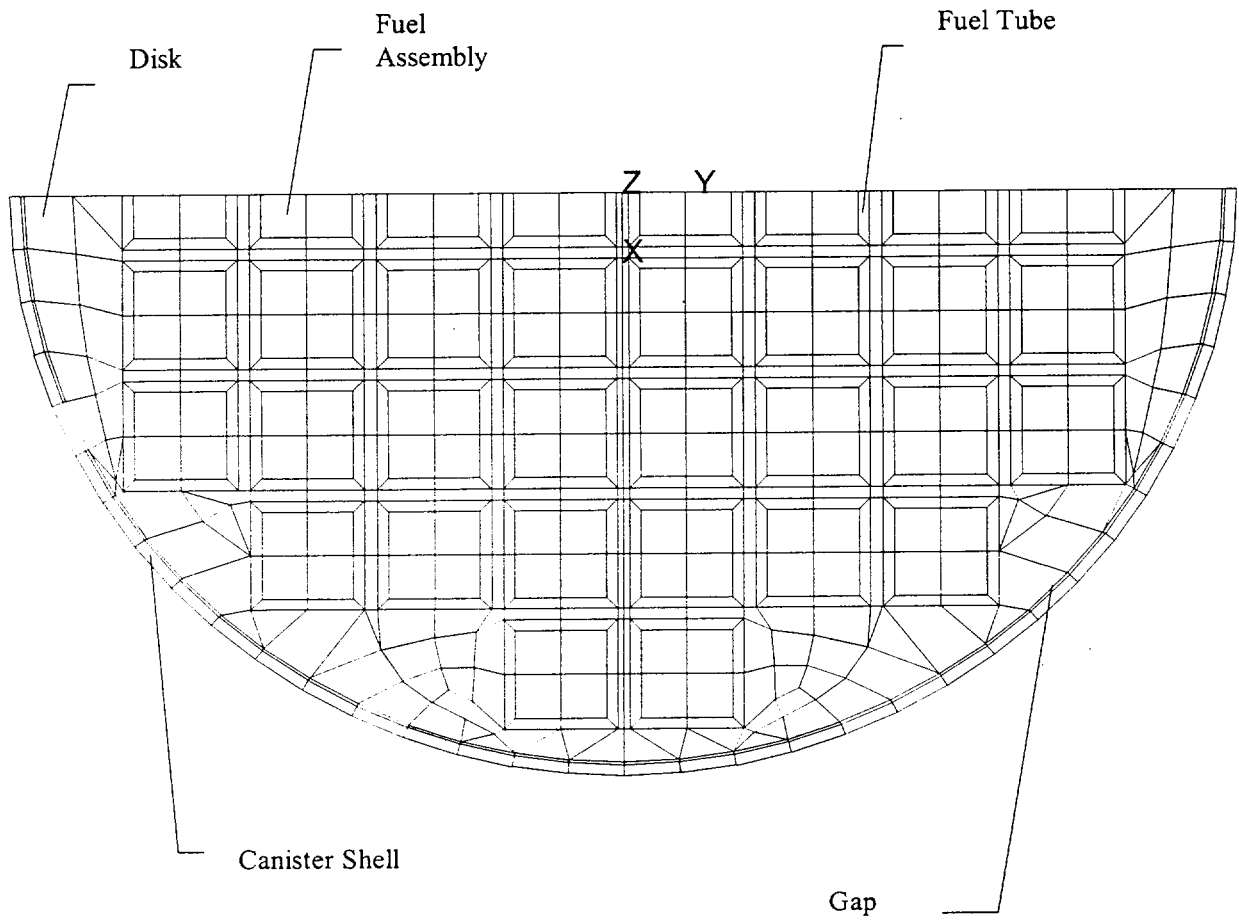


Table 4.4.1.1.2-1 Effective Thermal Conductivities for PWR Fuel Assemblies

Conductivity (Btu/hr-in-°F)	Temperature (°F)			
	200	400	603	807
K _{xx}	0.023	0.030	0.039	0.049
K _{yy}	0.023	0.030	0.039	0.049
K _{zz}	0.150	0.137	0.129	0.129

Note: x, y and z are in the coordinate system shown in Figure 4.4.1.1.2-1.

Table 4.4.1.1.2-2 Effective Thermal Conductivities for BWR Fuel Assemblies

Conductivity (Btu/hr-in-°F)	Temperature (°F)			
	180	386	591	798
Kxx	0.027	0.036	0.046	0.059
Kyy	0.027	0.036	0.046	0.059
Kzz	0.181	0.166	0.157	0.157

Note: x, y and z are in the coordinate system shown in Figure 4.4.1.1.2-3.

Table 4.4.1.1.2-3 Effective Thermal Conductivities for PWR Fuel Tubes

Fuel Assembly Group	Conductivity (Btu/hr-in-°F)	Temperature (°F)			
		200	400	600	800
In SS disk region					
	Kxx	0.013	0.018	0.023	0.030
	Kyy	0.560	0.572	0.581	0.587
	Kzz	0.560	0.572	0.581	0.587
In AL disk region					
	Kxx	0.013	0.018	0.023	0.030
	Kyy	0.560	0.572	0.581	0.587
	Kzz	0.560	0.572	0.581	0.587

Note: Kxx is in the direction across the thickness of the fuel tube wall.
 Kyy is in the direction parallel to the fuel tube wall.
 Kzz is in the canister axial direction.

Table 4.4.1.1.2-4 Effective Thermal Conductivities for BWR Fuel Tubes

Tubes With Neutron Absorber	Conductivity	Temperature (°F)			
	(Btu/hr-in-°F)	200	400	600	800
In CS disk region					
	Kxx	0.015	0.020	0.025	0.031
	Kyy	1.302	1.374	1.417	1.429
	Kzz	1.302	1.374	1.417	1.429
In AL disk region					
	Kxx	0.015	0.020	0.025	0.031
	Kyy	1.302	1.375	1.417	1.429
	Kzz	1.302	1.375	1.417	1.429
Tubes Without Neutron Absorber	Conductivity	Temperature (°F)			
	(Btu/hr-in-°F)	200	400	600	800
In CS disk region					
	Kxx	0.011	0.014	0.018	0.021
	Kyy	0.116	0.123	0.133	0.144
	Kzz	0.116	0.123	0.133	0.144
In AL disk region					
	Kxx	0.012	0.015	0.019	0.024
	Kyy	0.116	0.123	0.133	0.144
	Kzz	0.116	0.123	0.133	0.144

Note: Kxx is in the direction across the thickness of fuel tube wall.
 Kyy is in the direction parallel to fuel tube wall.
 Kzz is in the canister axial direction.

4.4.1.1.3 Two-Dimensional Axisymmetric Standard and Advanced Transfer Cask Models

The two-dimensional axisymmetric Standard and Advanced transfer cask model is an axisymmetric representation of the canister and transfer cask assembly. The model is used to perform a transient thermal analysis to determine the maximum water temperature in the canister for the period beginning immediately after removing the transfer cask and canister from the spent fuel pool. The model is also used to calculate the maximum temperature of the fuel cladding, the transfer cask and canister components during the vacuum drying condition and after the canister is back-filled with helium. The transfer cask is evaluated separately for PWR or BWR fuel using two models. For each fuel type, the class of fuel with the shortest associated canister and transfer cask is modeled in order to maximize the contents heat generation rate per unit volume and minimize the heat rejection from the external surfaces. The model for PWR fuel is shown in Figure 4.4.1.1.3-1. The BWR model is essentially identical to the PWR model with slight differences in canister dimensions and the effective properties for the canister internals.

An initial temperature of 100°F is considered in the model on the basis of typical maximum average water temperature in the spent fuel pool. Under typical operations, the water inside the canister is drained within 17 hours and the canister is back-filled with helium immediately after the vacuum drying and transferred to the concrete cask within 16 hours for the PWR fuel and within 24 hours for BWR fuel, the transient analysis is performed for 17 hours with the water inside the canister, 10 hours (conservative) for the vacuum-dried condition, and 24 hours for the helium condition. ANSYS PLANE55 two-dimensional conduction elements and LINK31 radiation elements are used. The model includes the transfer cask and the canister and its internals. As shown in Figure 4.4.1.1.3-1, the canister contents are modeled as three separate regions. For the condition with water inside the canister, the volume above the active fuel region is modeled as air. The volume above the active fuel region is modeled as a vacuum during the vacuum-dried condition and modeled as helium during the helium back-fill condition. Effective thermal properties are used for the active fuel region and for the region below the active fuel region as listed in Tables 4.4.1.1.3-1 and 4.4.1.1.3-2 for PWR fuel. Tables 4.4.1.1.3-3 and 4.4.1.1.3-4 show the effective properties of canister contents used in the BWR model. Note that the aluminum heat transfer disks exist only at the central region of the BWR basket. Therefore, different effective properties are used for the region with aluminum disks and regions without aluminum disks. The effective conductivities in the canister radial direction for the active fuel region are determined using the three-dimensional periodic canister internal models (Section 4.4.1.1.4). The effective conductivities in the canister radial direction for the region below the active fuel is conservatively considered to be the conductivity of the media (water, vacuum or

helium). While the temperatures for the water properties exceed 212°F (assuming the water remains in liquid form), the analyses are limited to temperatures below 212°F for this phase of the canister in the transfer cask. The effective thermal conductivities in the canister axial direction are calculated based on material cross-sectional area. The conductivities of the support disks and heat transfer disks are conservatively ignored in the calculation of axial conduction. The convection effect is also conservatively excluded in the effective conductivity calculation. The effective specific heat and density are calculated on the basis of material mass and volume ratio, respectively.

Radiation across the gaps was represented by LINK31 elements which used a form factor of one and gray body emissivities for stainless and carbon steels. The combination of radiation and convection at the transfer cask exterior vertical surfaces and canister lid top surface are taken into account in the model using the same method described in Section 4.4.1.1.2 for the three-dimensional canister models. The bottom of the transfer cask is conservatively modeled as being adiabatic during the entire period of the transient analysis. Volumetric heat generation (Btu/hr-in³) is applied to the active fuel region based on a total heat load of 23 kW for both PWR and BWR fuel. The model considers the active fuel length of 144 inches and an axial power distribution, as shown in Figure 4.4.1.1.1-3 and 4.4.1.1.1-4 for PWR and BWR fuel, respectively.

Figure 4.4.1.1.3-1 Two-Dimensional Axisymmetric Standard and Advanced Transfer Cask and Canister Model - PWR

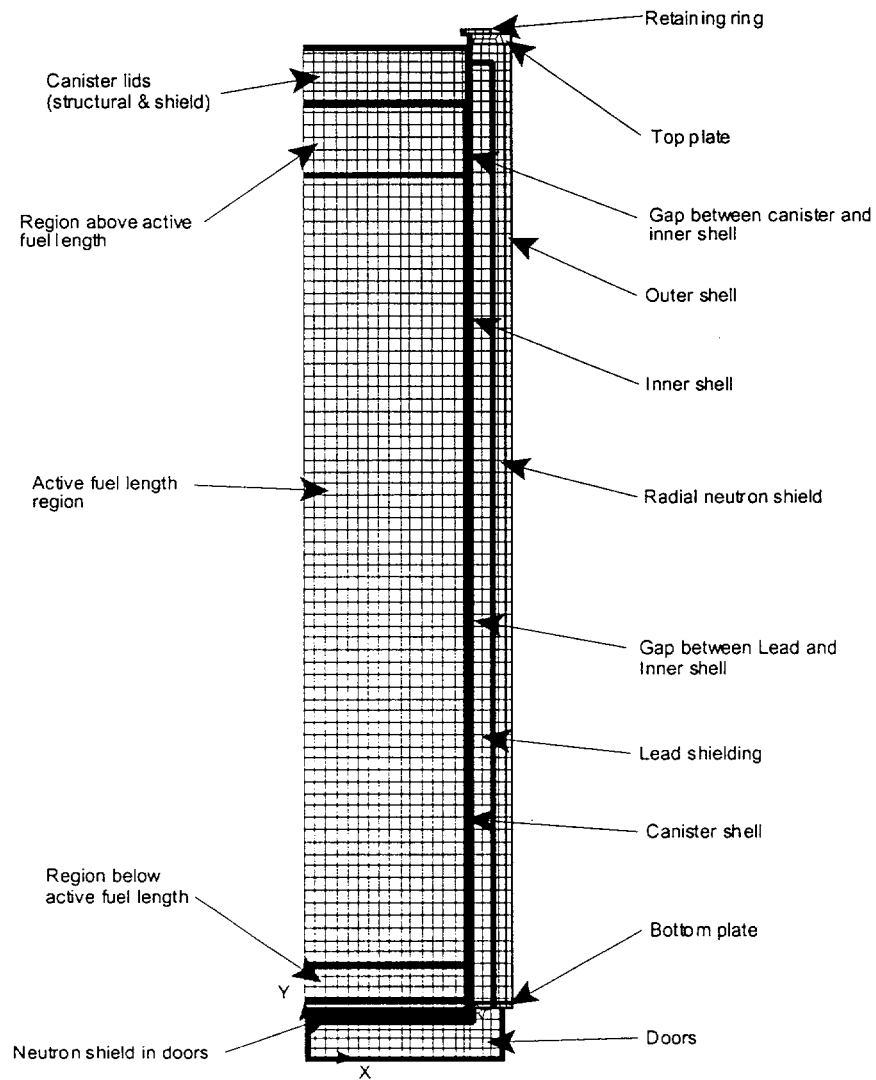


Table 4.4.1.1.3-1 Effective Thermal Properties for the Active Fuel Region for the Two-Dimensional Axisymmetric Standard Transfer Cask and Canister
Model: PWR

Region Fill					
Property (units)					
Water In Canister			Temperature		(°F)
			<u>100</u>	<u>200</u>	<u>300</u>
Conductivity (Btu/hr-in-°F)	Axial	0.178	0.179	0.177	
			Temperature		(°F)
			<u>130</u>	<u>169</u>	<u>208</u> <u>245</u>
Conductivity (Btu/hr-in-°F)	Radial	0.176	0.176	0.177	0.179
Specific Heat (Btu/lbm-°F)		0.303	0.302	0.302	0.302
Density (lbm/in ³)		0.101	0.101	0.101	0.101
Vacuum In Canister			Temperature		(°F)
			<u>100</u>	<u>300</u>	<u>600</u> <u>800</u>
Conductivity (Btu/hr-in-°F)	Axial	0.158	0.153	0.147	0.146
			Temperature		(°F)
			<u>269</u>	<u>375</u>	<u>487</u> <u>601</u>
Conductivity (Btu/hr-in-°F)	Radial	0.027	0.036	0.046	0.057
Specific Heat (Btu/lbm-°F)		0.064	0.065	0.067	0.068
Density (lbm/in ³)		0.075	0.075	0.075	0.075
Helium In Canister			Temperature		(°F)
			<u>100</u>	<u>300</u>	<u>600</u> <u>800</u>
Conductivity (Btu/hr-in-°F)	Axial	0.160	0.158	0.155	0.156
			Temperature		(°F)
			<u>332</u>	<u>427</u>	<u>527</u> <u>630</u>
Conductivity (Btu/hr-in-°F)	Radial	0.117	0.128	0.139	0.150
Specific Heat (Btu/lbm-°F)		0.065	0.067	0.068	0.069
Density (lbm/in ³)		0.075	0.075	0.075	0.075

Table 4.4.1.1.3-2 Effective Thermal Properties for the Region Below the Active Fuel for the Two-Dimensional Axisymmetric Standard Transfer Cask and Canister Model: PWR

Region Fill		Temperature (°F)			
Property (units)					
Water In Canister			<u>100</u>	<u>200</u>	<u>300</u>
Conductivity (Btu/hr-in-°F) ¹	Axial	0.077	0.082	0.084	
Specific Heat (Btu/lbm-°F)		0.587	0.586	0.591	
Density (lbm/in ³)		0.060	0.060	0.058	
Vacuum In Canister			<u>100</u>	<u>300</u>	<u>600</u>
Conductivity (Btu/hr-in-°F) ¹	Axial	0.030	0.033	0.037	0.040
Specific Heat (Btu/lbm-°F)		0.119	0.126	0.134	0.137
Density (lbm/in ³)		0.028	0.028	0.028	0.028
Helium In Canister			<u>100</u>	<u>300</u>	<u>600</u>
Conductivity (Btu/hr-in-°F) ¹	Axial	0.045	0.051	0.059	0.064
Specific Heat (Btu/lbm-°F)		0.119	0.126	0.134	0.134
Density (lbm/in ³)		0.028	0.028	0.028	0.028

Note:

1. Conductivities for the media (water, vacuum or helium) are used in the radial direction. 1.0E-5 Btu/hr-in-°F is used for the vacuum condition.

Table 4.4.1.1.3-3 Effective Thermal Properties for the Active Fuel Region for the Two-Dimensional Axisymmetric Standard Transfer Cask and Canister Model: BWR

Region Fill				
Property (units)				
Water In Canister				
			Temperature	(°F)
		<u>100</u>	<u>200</u>	<u>300</u>
Conductivity (Btu/hr-in-°F) Axial	0.26	0.26	0.26	0.26

Aluminum and Carbon Steel Disk region				
			Temperature	(°F)
		<u>15</u>	<u>95</u>	<u>173</u>
Conductivity (Btu/hr-in-°F) Radial	0.226	0.228	0.231	0.231
Specific Heat (Btu/lbm-°F)	0.277	0.277	0.276	0.276
Density (lbm/in ³)	0.114	0.111	0.110	0.110

Carbon Steel Disk region				
			Temperature	(°F)
		<u>86</u>	<u>164</u>	<u>242</u>
Conductivity (Btu/hr-in-°F) Radial	0.141	0.143	0.144	0.144
Specific Heat (Btu/lbm-°F)	0.290	0.289	0.289	0.289
Density (lbm/in ³)	0.111	0.111	0.110	0.110
Vacuum In Canister				
			Temperature	(°F)
		<u>200</u>	<u>400</u>	<u>600</u>
Conductivity (Btu/hr-in-°F) Axial	0.25	0.25	0.25	0.25

Aluminum and Carbon Steel Disk region				
			Temperature	(°F)
		<u>173</u>	<u>228</u>	<u>323</u>
Conductivity (Btu/hr-in-°F) Radial	0.015	0.022	0.034	0.049
Specific Heat (Btu/lbm-°F)	0.084	0.085	0.086	0.088
Density (lbm/in ³)	0.089	0.089	0.089	0.089

Carbon Steel Disk region				
			Temperature	(°F)
		<u>190</u>	<u>248</u>	<u>344</u>
Conductivity (Btu/hr-in-°F) Radial	0.013	0.019	0.027	0.035
Specific Heat (Btu/lbm-°F)	0.079	0.080	0.081	0.082
Density (lbm/in ³)	0.085	0.085	0.085	0.085
Helium In Canister				
			Temperature	(°F)
		<u>200</u>	<u>400</u>	<u>600</u>
Conductivity (Btu/hr-in-°F) Axial	0.25	0.25	0.25	0.25

Aluminum and Carbon Steel Disk region				
			Temperature	(°F)
		<u>132</u>	<u>265</u>	<u>401</u>
Conductivity (Btu/hr-in-°F) Radial	0.136	0.150	0.165	0.180
Specific Heat (Btu/lbm-°F)	0.084	0.085	0.087	0.089
Density (lbm/in ³)	0.089	0.089	0.089	0.089

Carbon Steel Disk region				
			Temperature	(°F)
		<u>208</u>	<u>340</u>	<u>476</u>
Conductivity (Btu/hr-in-°F) Radial	0.094	0.102	0.110	0.117
Specific Heat (Btu/lbm-°F)	0.080	0.081	0.083	0.085
Density (lbm/in ³)	0.085	0.085	0.085	0.085

Table 4.4.1.1.3-4 Effective Thermal Properties for the Region Below the Active Fuel for the Two-Dimensional Axisymmetric Standard Transfer Cask and Canister Model: BWR

Region	Fill	Property (units)			
Water In Canister		Temperature (°F)			
		<u>100</u>	<u>200</u>	<u>300</u>	
Conductivity (Btu/hr-in-°F) ¹	Axial	0.075	0.081	0.083	
Specific Heat (Btu/lbm-°F)		0.569	0.568	0.572	
Density (lbm/in ³)		0.062	0.061	0.060	
Vacuum In Canister		Temperature (°F)			
		<u>100</u>	<u>300</u>	<u>500</u>	<u>700</u>
Conductivity (Btu/hr-in-°F) ¹	Axial	0.035	0.039	0.043	0.046
Specific Heat (Btu/lbm-°F)		0.112	0.119	0.124	0.127
Density (lbm/in ³)		0.030	0.030	0.030	0.030
Helium In Canister		Temperature (°F)			
		<u>100</u>	<u>300</u>	<u>500</u>	<u>700</u>
Conductivity (Btu/hr-in-°F) ¹	Axial	0.046	0.053	0.059	0.064
Specific Heat (Btu/lbm-°F)		0.113	0.119	0.124	0.127
Density (lbm/in ³)		0.030	0.030	0.030	0.030

Note:

1. Conductivities for the media (water, vacuum or helium) are used in the radial direction.
1.0E-5 Btu/hr-in-°F is used for the vacuum condition.

4.4.1.1.4 Three-Dimensional Periodic Standard Canister Internal Models

The three-dimensional periodic Standard canister internal model consists of a periodic section of the canister internals. A total of three models are used: one for PWR fuel and two for BWR fuel. For the PWR canister, the model contains one support disk with two heat transfer disks (half thickness) on its top and bottom, the fuel assemblies, the fuel tubes and the media in the canister, as shown in Figure 4.4.1.1.4-1. The BWR model, shown in Figure 4.4.1.1.4-2, represents the central region of the BWR canister, which contains one heat transfer disk with two support disks (half thickness) on its top and bottom, the fuel assemblies, the fuel tubes and the media in the canister. The second BWR model (not shown), for the region without heat transfer disks, contains two support disks (half thickness), the fuel assemblies, the fuel tubes and the media in the canister. The difference between the two BWR models is that the second model does not have the heat transfer disk. The purpose of these models is to determine the effective thermal conductivity of the canister internals in the canister radial direction. The effective conductivities are used in the two-dimensional axisymmetric air flow and concrete cask models and the two-dimensional axisymmetric transfer cask and canister models. Three types of media are considered: helium, water and vacuum. The fuel assemblies and fuel tubes in this model are represented by homogeneous regions with effective thermal properties. The effective conductivities for the fuel assemblies and the fuel tubes are determined by the two-dimensional fuel models (Section 4.4.1.1.5) and the two-dimensional fuel tube models (Section 4.4.1.1.6) respectively. The properties corresponding to the PWR 14 × 14 assemblies are used for the PWR model, since the 14 × 14 assemblies have the lowest conductivities as compared to other PWR assemblies. For the same reason, the properties corresponding to the BWR 9 × 9 assemblies are used for the BWR models.

The effective thermal conductivity (k_{eff}) of the fuel region in the radial direction is determined by considering the canister internals as a solid cylinder with heat generation. The temperature distribution in the cylinder may be expressed as [17]:

$$T - T_o = \frac{q''' R^2}{4k_{\text{eff}}} \left[1 - \left(\frac{r}{R} \right)^2 \right]$$

where:

T_o = the surface temperature of the cylinder
 T = temperature at radius "r" of the cylinder
 R = the outer radius of the cylinder,
 r = radius

$$q''' = \text{the heat generation rate} = \frac{Q}{\pi R^2 H}$$

where: Q = total heat generated in the cylinder
 H = length of the cylinder

Considering the temperature at the center of the canister to be T_{\max} , the above equation can be simplified and used to compute the effective thermal conductivity (k_{eff}):

$$k_{\text{eff}} = \frac{Q}{4\pi H(T_{\max} - T_o)} = \frac{Q}{4\pi H\Delta T}$$

where:

Q = total heat generated by the fuel
 H = length of the active fuel region
 T_o = temperature at outer surface internals (inside surface of the canister)
 $\Delta T = T_{\max} - T_o$

The value of ΔT is obtained from thermal analysis using the three-dimensional periodic canister internal model with the boundary temperature constrained to be T_o . The effective conductivity (k_{eff}) is then determined by using the above formula. Analysis is repeated by applying different boundary temperatures so that temperature-dependent conductivities can be determined.

Figure 4.4.1.1.4-1 Three-Dimensional Periodic Standard Canister Internal Model - PWR

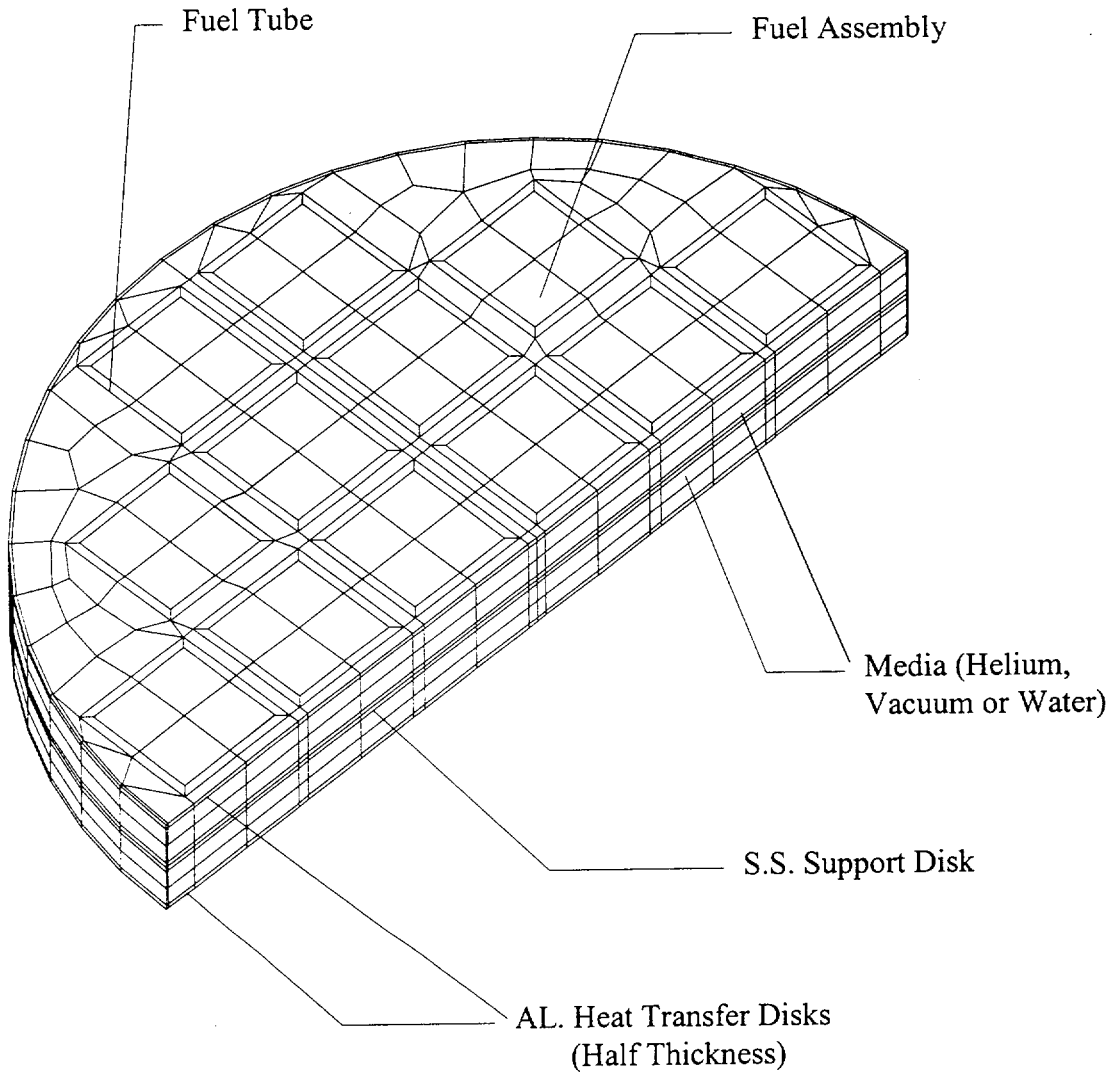
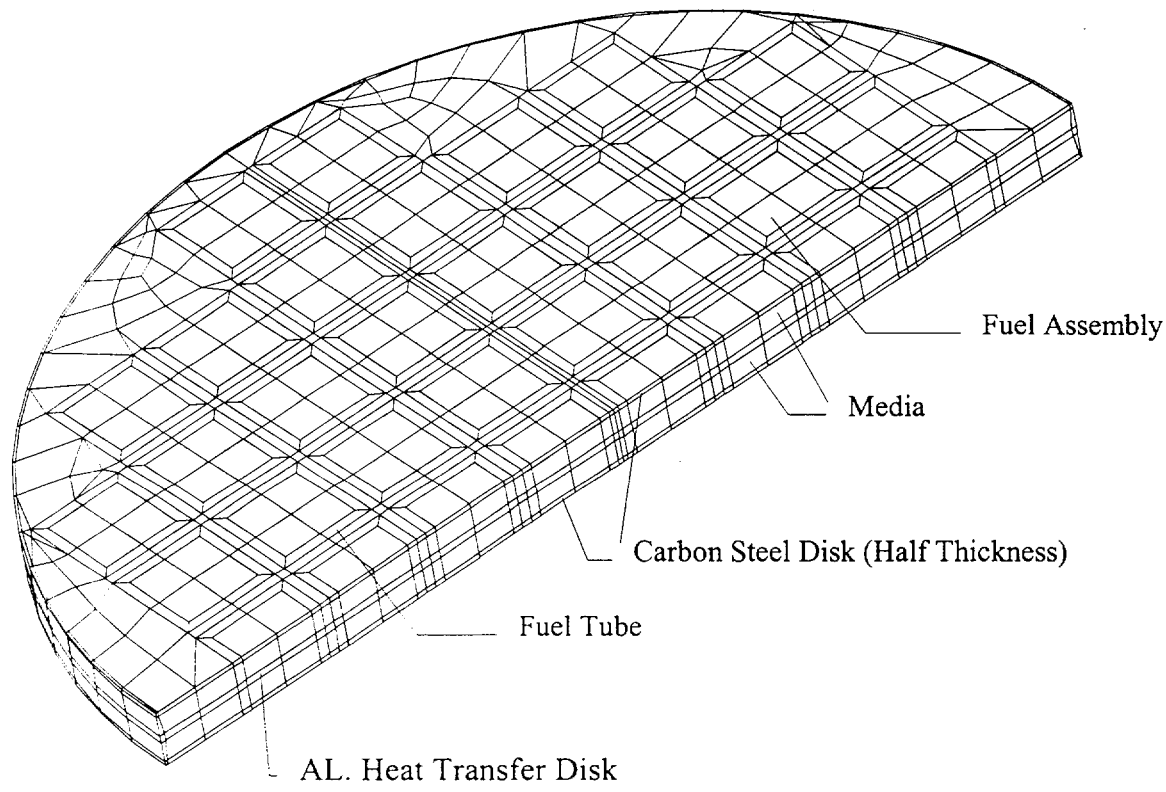


Figure 4.4.1.1.4-2 Three-Dimensional Periodic Standard Canister Internal Model - BWR



4.4.1.1.5 Two-Dimensional Fuel Models

The effective conductivity of the fuel is determined by the two-dimensional finite element model of the fuel assembly. The effective conductivity is used in the three-dimensional canister models (Section 4.4.1.1.2) and the three-dimensional periodic canister internal model (Section 4.4.1.1.4). A total of seven models are required: four models for the 14×14, 15×15, 16×16 and 17×17 PWR fuels and three models for the 7×7, 8×8 and 9×9 BWR fuels. Because of similarity, only the figure for the PWR 17×17 model is shown in this Section (Figure 4.4.1.1.5-1). All models contains only one quarter of the cross-section of a assembly because of symmetry.

The model includes the fuel pellets, cladding, media between fuel rods and helium at the gap between fuel pellet and cladding. Three types of media are considered: helium, water and a vacuum. Modes of heat transfer modeled include conduction and radiation between individual fuel rods for the steady-state condition. ANSYS PLANE55 conduction elements and LINK31 radiation elements are used to model conduction and radiation. Radiation elements are defined between fuel rods. Effective emissivities are determined using the formula shown in Section 4.4.1.1.2. Radiation at the gap between the pellet and the cladding is conservatively ignored.

The effective conductivity for the fuel is determined by using an equation defined in a Sandia National Laboratory Report [30]. The equation is used to determine the maximum temperature of a square cross-section of an isotropic homogeneous fuel with a uniform volumetric heat generation. At the boundary of the square cross-section, the temperature is constrained to be uniform. The expression for the temperature at the center of the fuel is given by:

$$T_c = T_e + 0.29468 (Qa^2 / K_{eff})$$

where: T_c = the temperature at the center of the fuel (°F)

T_e = the temperature applied to the exterior of the fuel (°F)

Q = volumetric heat generation rate (Btu/hr-in³)

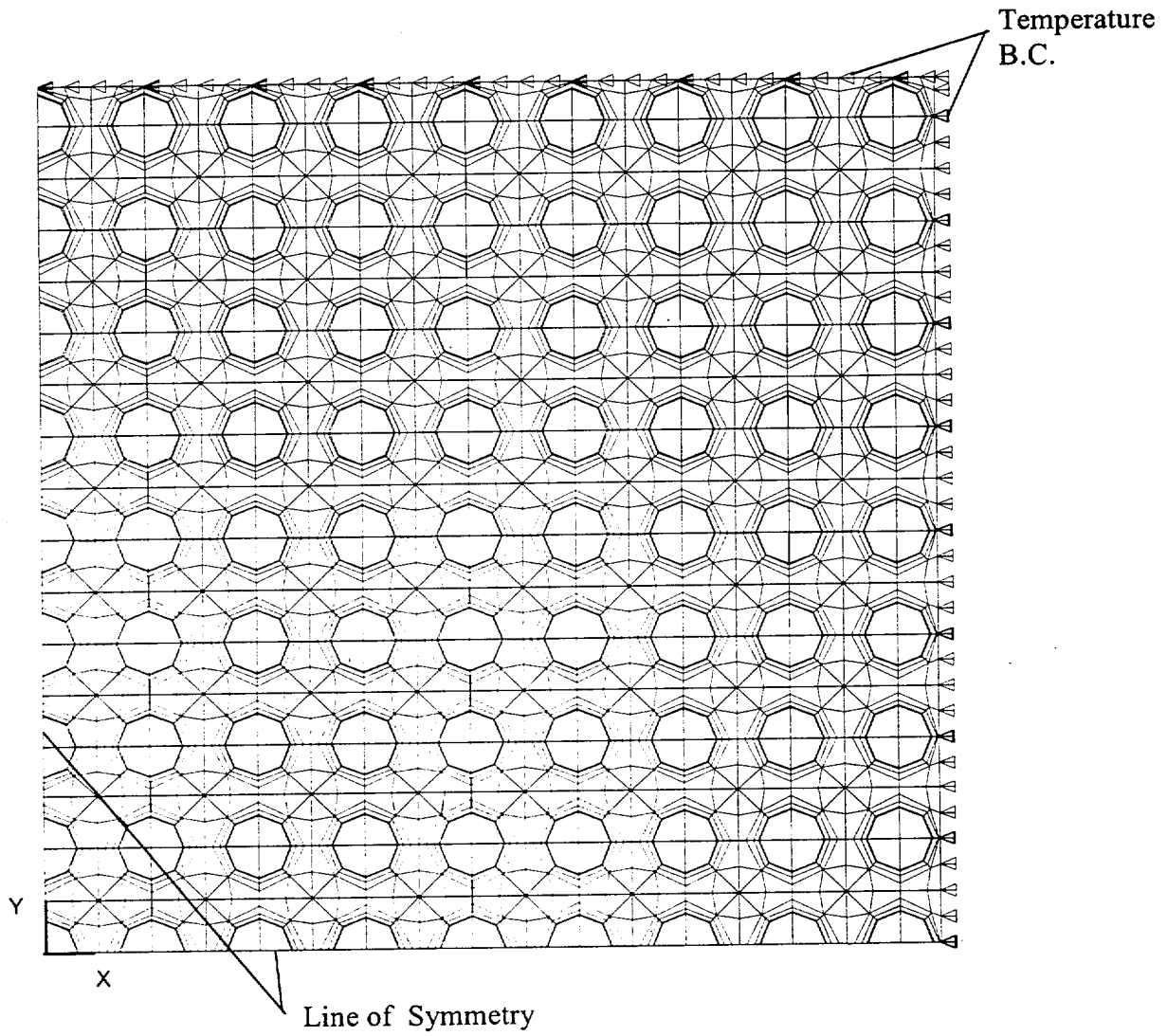
a = half length of the square cross-section of the fuel (inch)

K_{eff} = effective thermal conductivity for the isotropic homogeneous fuel material (Btu/hr-in-°F)

Volumetric heat generation (Btu/hr-in³) based on the design heat load is applied to the pellets. The effective conductivity is determined based on the heat generated and the temperature

difference from the center of the model to the edge of the model. Temperature-dependent effective properties are established by performing multiple analyses using different boundary temperatures. The effective conductivity in the axial direction of the fuel assembly is calculated on the basis of the material area ratio.

Figure 4.4.1.1.5-1 Two-Dimensional PWR (17×17) Fuel Model



4.4.1.1.6 Two-Dimensional Fuel Tube Models

The two-dimensional fuel tube model is used to calculate the effective conductivities of the fuel tube wall and BORAL plate. These effective conductivities are used in the three-dimensional canister models (Section 4.4.1.1.2) and the three-dimensional periodic canister internal model (Section 4.4.1.1.4). A total of six models are required: four PWR models corresponding to the 14×14, 15×15, 16×16 and 17×17 PWR fuels and two BWR models (one with the BORAL plate, one without the BORAL plate), corresponding to the enveloping configurations of the 7×7, 8×8 and 9×9 BWR fuels. Because of similarity, only the PWR model corresponding to the PWR 17×17 fuel is shown Figure 4.4.1.1.6-1. The BWR models are shown in Figures 4.4.1.1.6-2 and 4.4.1.1.6-3.

As shown in Figure 4.4.1.1.6-1, the PWR model includes the gap between the fuel assembly and the fuel tube, the fuel tube, the BORAL plate (including the core matrix sandwiched by aluminum cladding), gaps on both sides of the BORAL plate, and the gap between the stainless steel cladding on the outside of the BORAL plate and the support disk or heat transfer disk. Three conditions of media are considered in the gaps: helium, water and a vacuum.

ANSYS PLANE55 conduction elements and LINK31 radiation elements are used to construct the model. The model consists of nine layers of conduction elements and eight radiation elements (radiation elements are not used for water condition) that are defined at the gaps (two for each gap). The thickness of the model (x-direction) is the distance measured from the outside face of the fuel assembly to the inside face of the slot in the support disk (assuming the fuel tube is centered in the hole in the disk). The tolerance of the BORAL plate thickness, 0.003 inch, is used as the gap size for both sides of the BORAL plate. The height of the model is defined as equal to the width of the model.

The fuel tubes in the BWR fuel basket differ from those in the PWR fuel basket in that not all sides of the fuel tubes contain BORAL. In addition, the BWR fuel assembly is contained in a fuel channel. Therefore, two effective conductivity models are necessary, one fuel tube model with the BORAL plate (a total of 11 layers of materials) and another fuel tube model with a gap replacing the BORAL plate (a total of 5 layers of materials).

As shown in Figure 4.4.1.1.6-2, the BWR fuel tube model with BORAL includes the gap between fuel assembly and the fuel channel, the fuel channel, gap between the fuel channel and

fuel tube, the fuel tube, the BORAL plate (including the core matrix sandwiched by aluminum claddings), gaps on both sides of the BORAL plate, and a gap between the stainless steel cladding for the BORAL plate and the support disk or heat transfer disk. The effective conductivity of the fuel tube without the BORAL plate is determined using the second BWR fuel tube model. As shown in Figure 4.4.1.1.6-3, this model includes the gap between fuel assembly and the fuel channel, the fuel channel, gap between the fuel channel and stainless steel fuel tube, the fuel tube, and a gap between the fuel tube and the support disk or heat transfer disk. An emissivity value of 0.0001 is conservatively used for the BWR support disk in the model.

Heat flux is applied at the left side of the model (fuel tube for PWR models and fuel channel for BWR models), and the temperature at the right boundary of the model is constrained. The heat flux is determined based on the design heat load. The maximum temperature of the model (at the left boundary) and the temperature difference (ΔT) across the model are calculated by the ANSYS model. The effective conductivity (K_{xx}) is determined using the following formula:

$$q = K_{xx} (A/L) \Delta T$$

or

$$K_{xx} = q L / (A \Delta T)$$

where:

K_{xx} = effective conductivity (Btu/hr-in-°F) in X direction in Figure 4.4.1.6-1.

q = heat rate (Btu/hr)

A = area (in²)

L = length (thickness) of model (in)

ΔT = temperature difference across the model (°F)

The temperature-dependent conductivity is determined by varying the temperature constraints at one boundary of the model and resolving for the heat rate (q) and temperature difference. The effective conductivity for the parallel path (the Y direction in Figure 4.4.1.1.6-1) is calculated by:

$$K_{yy} = \frac{\sum K_i t_i}{L}$$

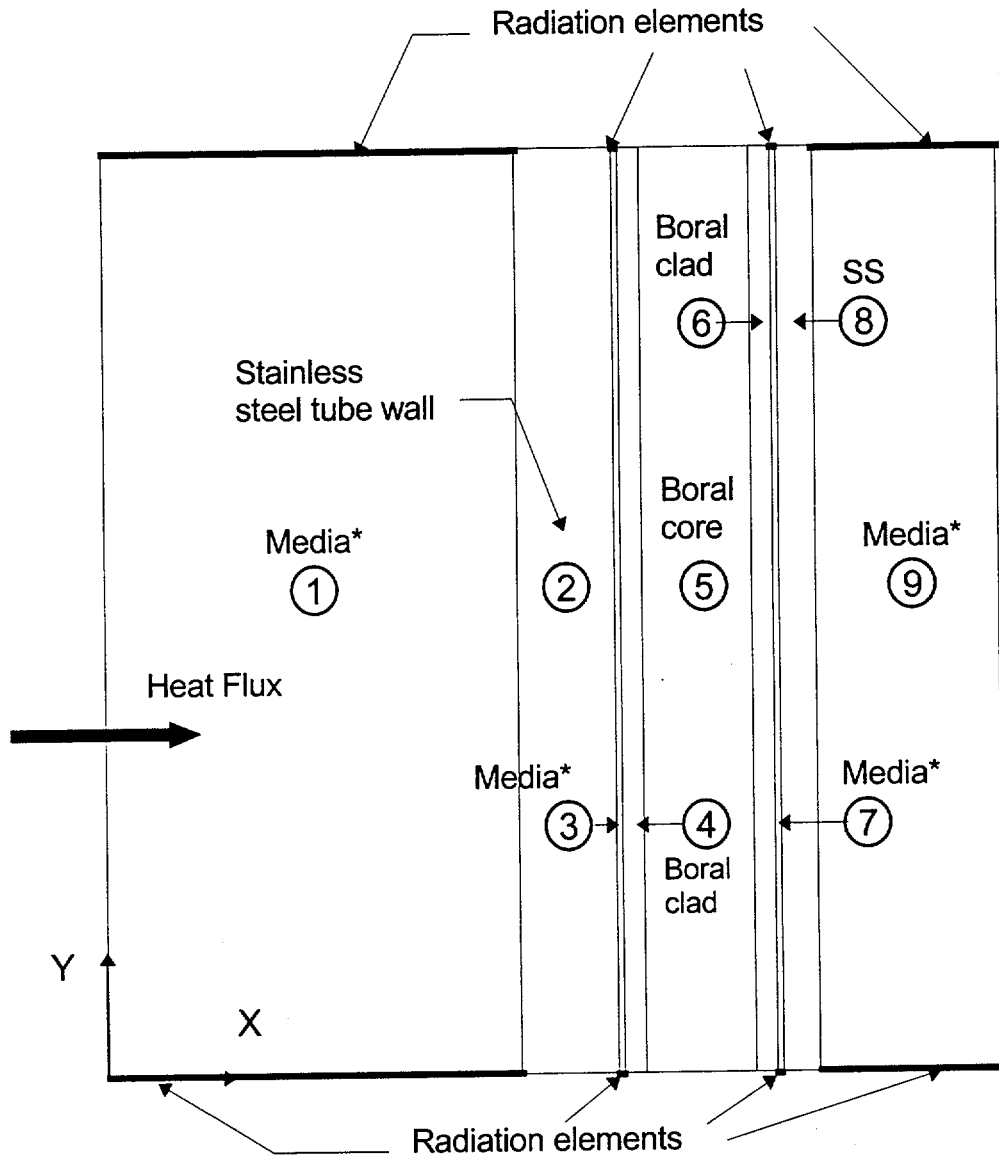
where:

K_i = thermal conductivity of each layer

t_i = thickness of each layer

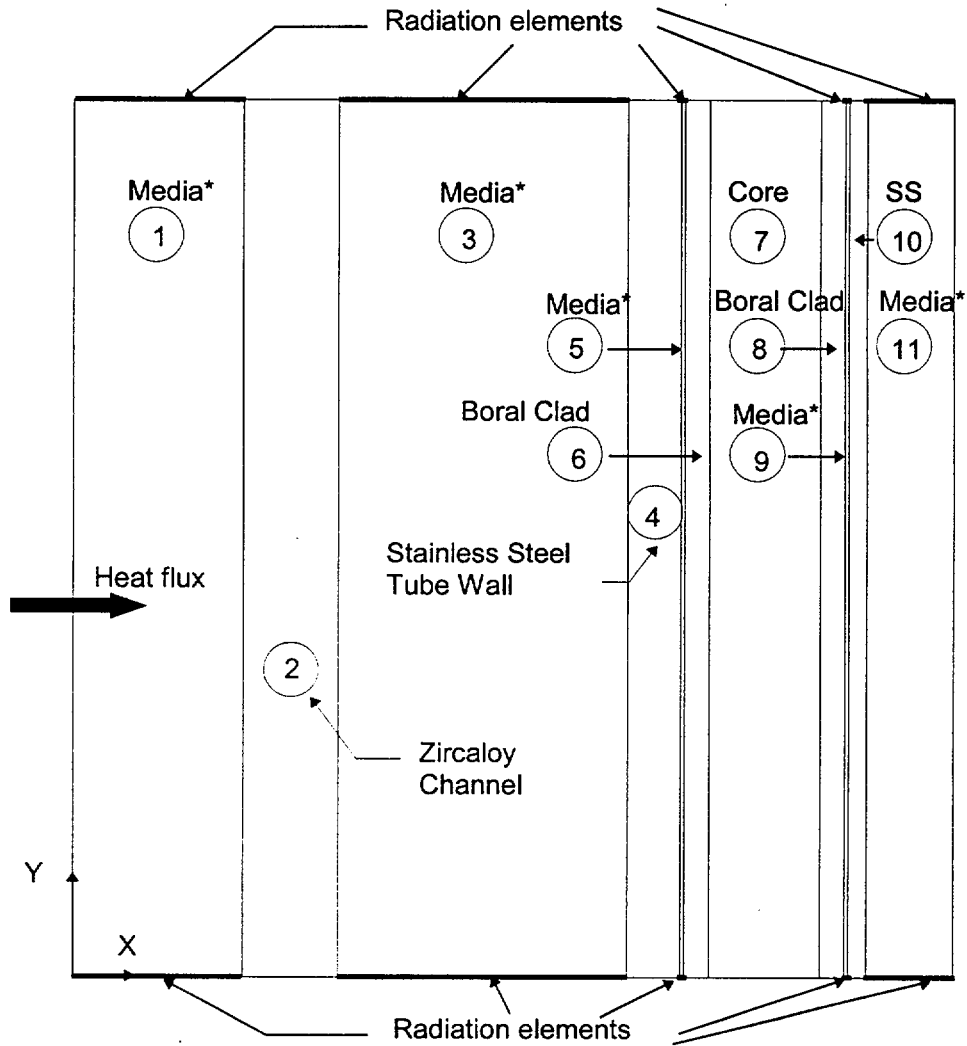
L = total length (thickness) of the model

Figure 4.4.1.1.6-1 Two-Dimensional Fuel Tube Model: PWR Fuel



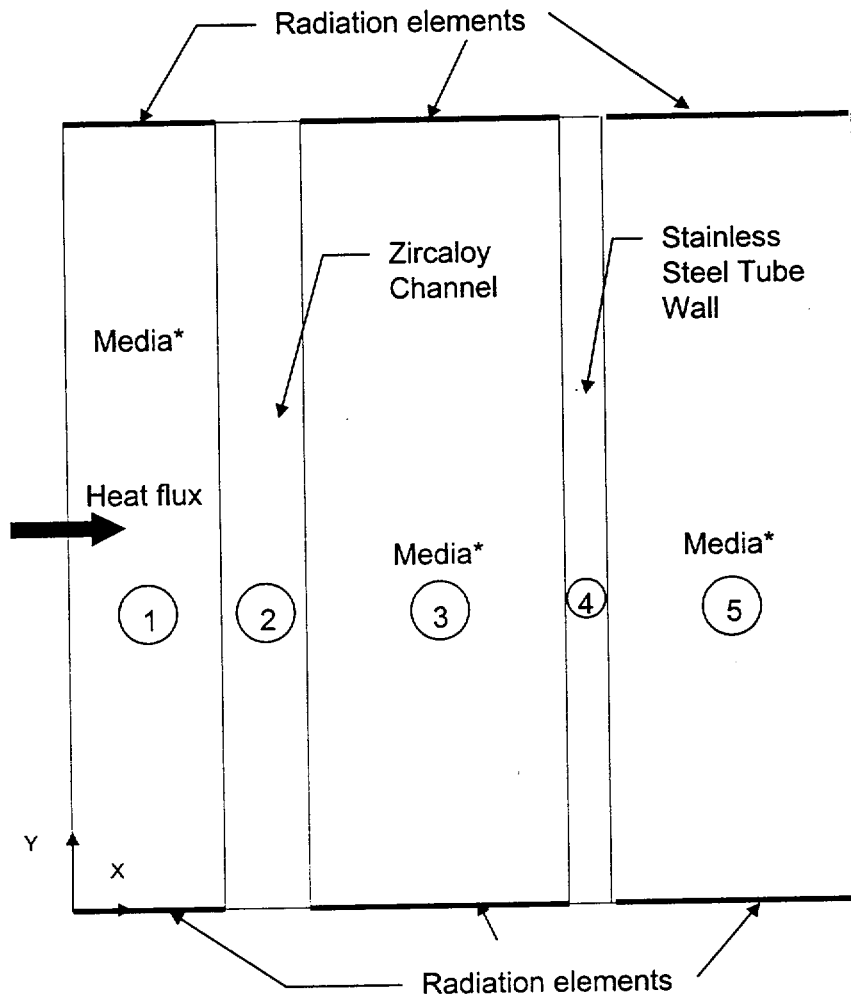
*Media can be water, vacuum, or helium.

Figure 4.4.1.1.6-2 Two-Dimensional Fuel Tube Model: BWR Fuel Tube With BORAL



*Media can be water, vacuum, or helium.

Figure 4.4.1.1.6-3 Two-Dimensional Fuel Tube Model: BWR Fuel Tube Without BORAL



*Media can be water, vacuum, or helium.

4.4.1.1.7 Two-Dimensional Forced Air Flow Model for Standard Transfer Cask Cooling

A two-dimensional axisymmetric air flow model is used to determine the air flow rate needed to ensure that the maximum temperature of the canister shell and canister components inside the transfer cask do not exceed those presented in Tables 4.4.3.1-3 and 4.4.3.1-4 for the helium condition. This air flow model considers a 0.34-inch air annulus between the outer surface of the canister shell and the inner surface of the transfer cask, and has a total length of 191-inches. The fuel canister is cooled by forced convection in the air annulus resulting from air pumped in through fill/drain ports in the body of the transfer cask. The radiation heat transfer between the vertical annulus surfaces (the canister shell outer surface and the transfer cask inner surface) is conservatively neglected. All heat is considered to be removed by the air flow.

ANSYS FLOTTRAN FLUID141 fluid thermal elements are used to construct the two-dimensional axisymmetric air flow finite element model for transfer cask cooling. The model and the boundary conditions applied to the model, are shown in Figures 4.4.1.1.7-1, 4.4.1.1.7-2 and 4.4.1.1.7-3.

As shown in Tables 4.4.3.1-3 and 4.4.3.1-4, the temperature margin of the governing component (the heat transfer disk) for the PWR fuel configuration is lower than the margin for the BWR fuel configuration; therefore, the thermal loading for the PWR configuration is used. The non-uniform heat generation applied in the model, shown in Figure 4.4.1.1.7-4, is based on the axial power distribution shown in Figure 4.4.1.1.1-3 for PWR fuel.

The inlet air velocity is specified based on the volume flow rate. Room temperature (76°F) is applied to the inlet nodes, while zero air velocity, in both the X and Y directions, is defined as the boundary condition for the vertical solid sides.

Results of the analyses of forced air cooling of the canister inside the transfer cask are shown in Figure 4.4.1.1.7-5. As shown in the figure, the maximum canister shell temperature is less than 416°F for a forced air flow rate of 275 ft³/minute, or higher, where 416°F is the calculated maximum canister shell temperature for the typical transfer operation for the PWR configuration (Table 4.4.3.1-3). A forced air volume flow rate of 375 ft³/minute is conservatively specified for cooling the canister in the event that forced air cooling is required. Evaluation of a forced air volume flow rate of 375 ft³/minute, results in a maximum canister shell temperature of 321°F, which is significantly less than the design basis temperature of 416°F.

Figure 4.4.1.1.7-1 Two-Dimensional Axisymmetric Finite Element Model for Transfer Cask
Forced Air Cooling

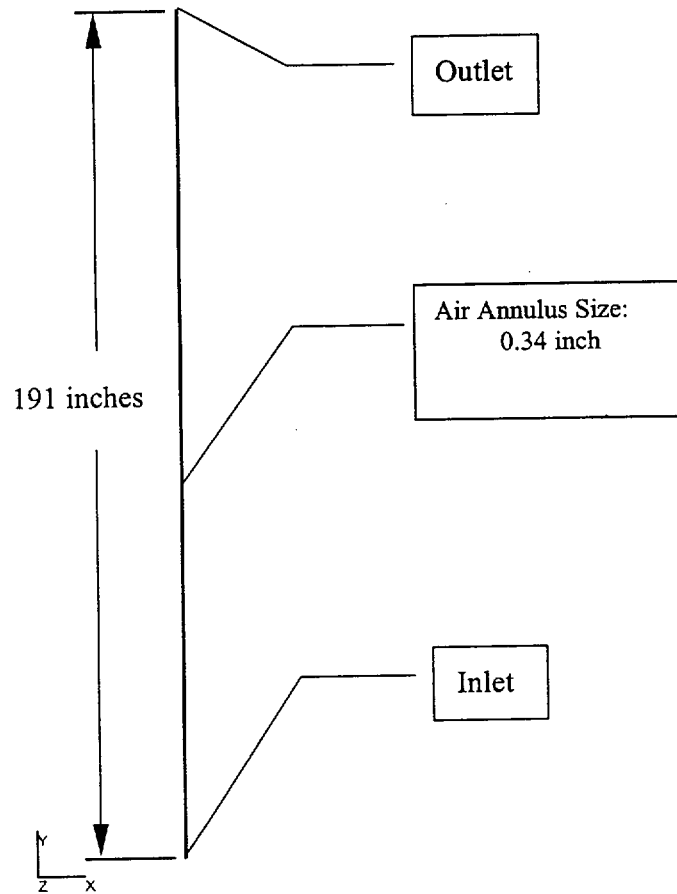


| Figure 4.4.1.1.7-2 Two-Dimensional Axisymmetric Outlet Air Flow Model for Transfer Cask Cooling

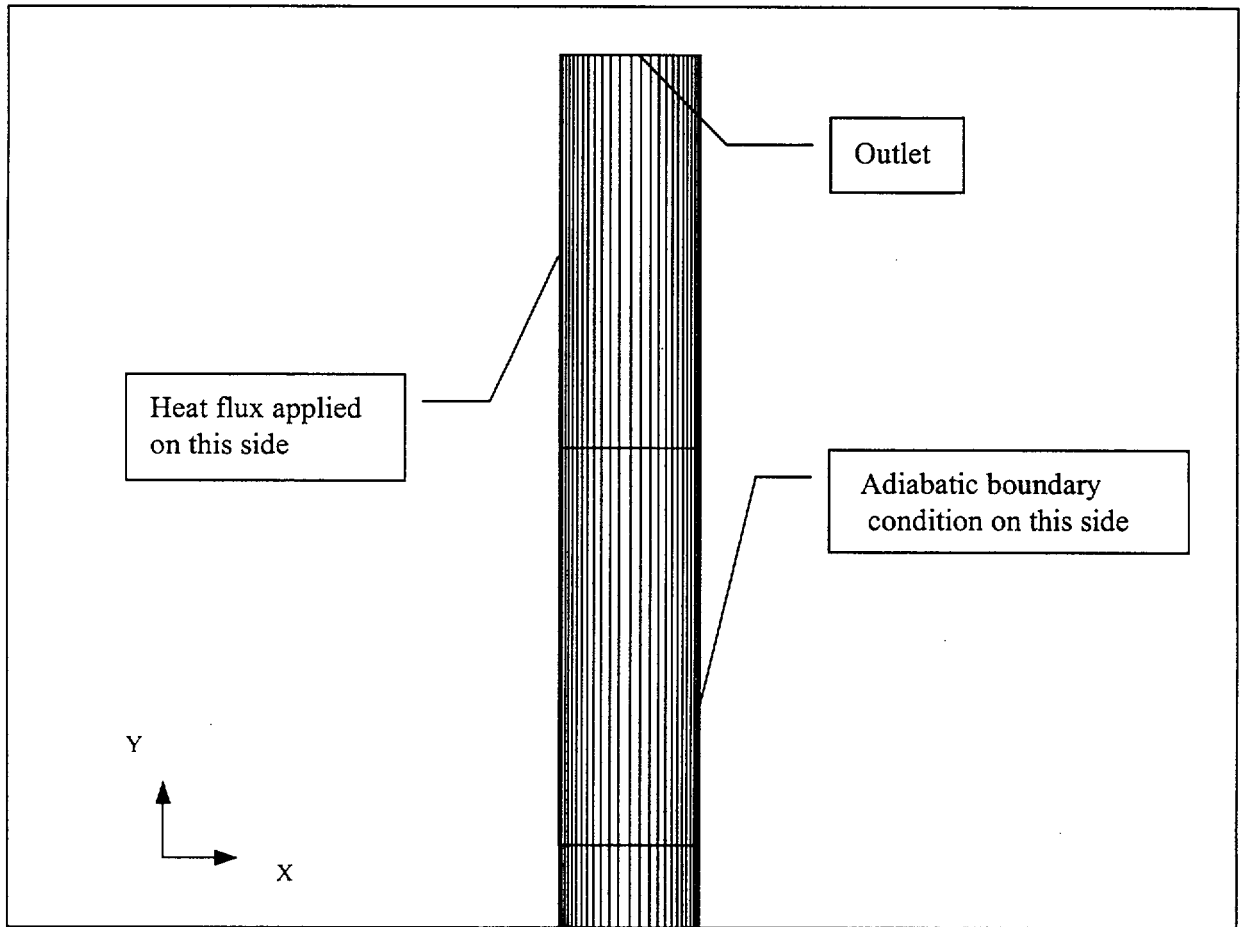
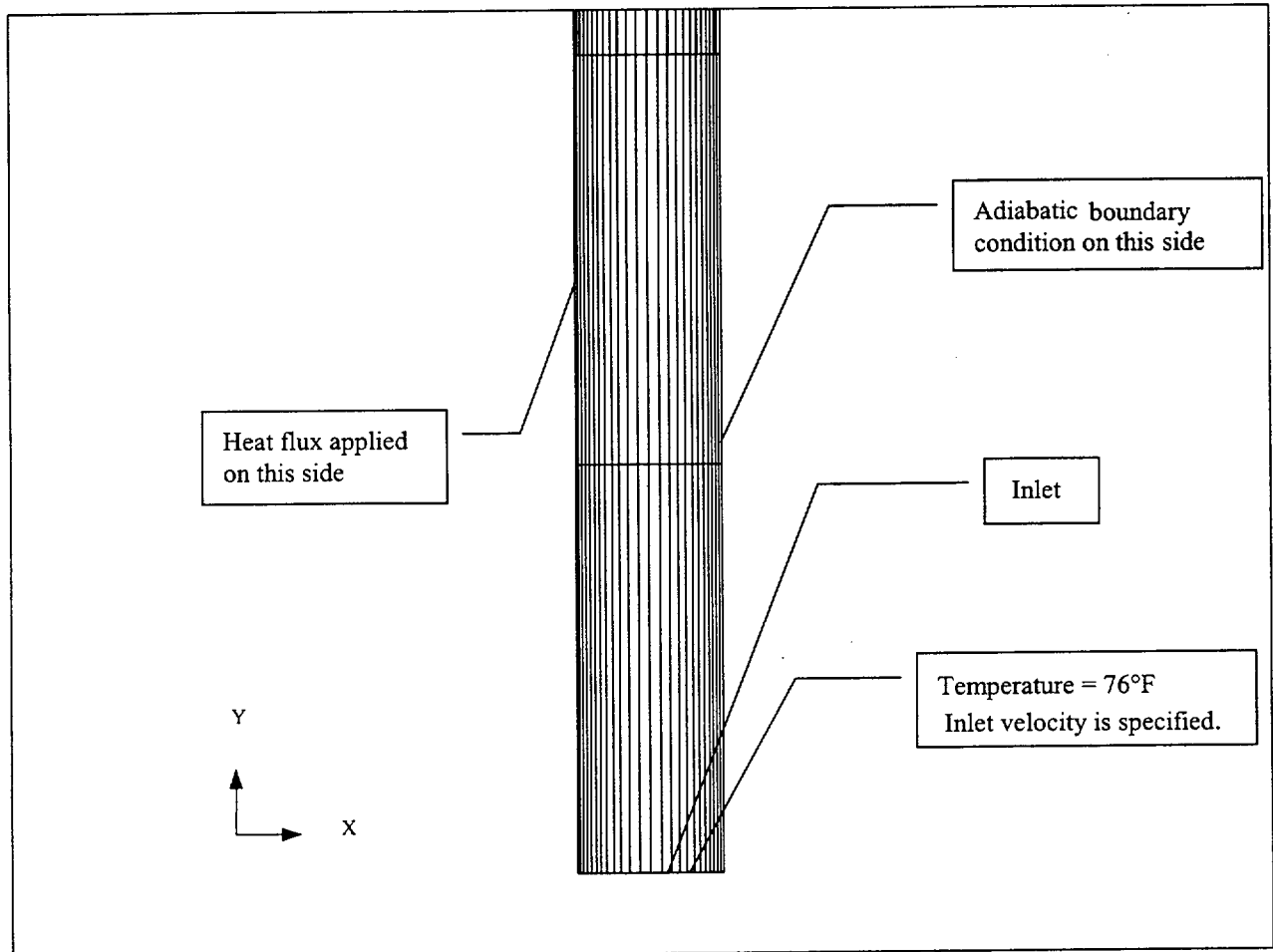


Figure 4.4.1.1.7-3 Two-Dimensional Axisymmetric Inlet Air Flow Model for Transfer Cask Cooling



| Figure 4.4.1.1.7-4 Non-Uniform Heat Load from Canister Contents

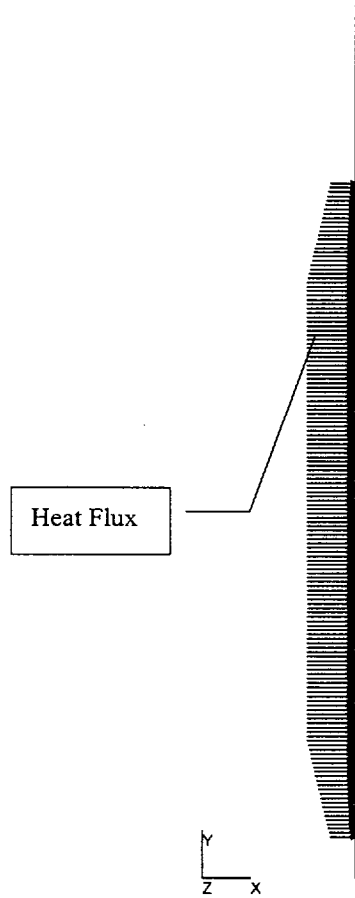
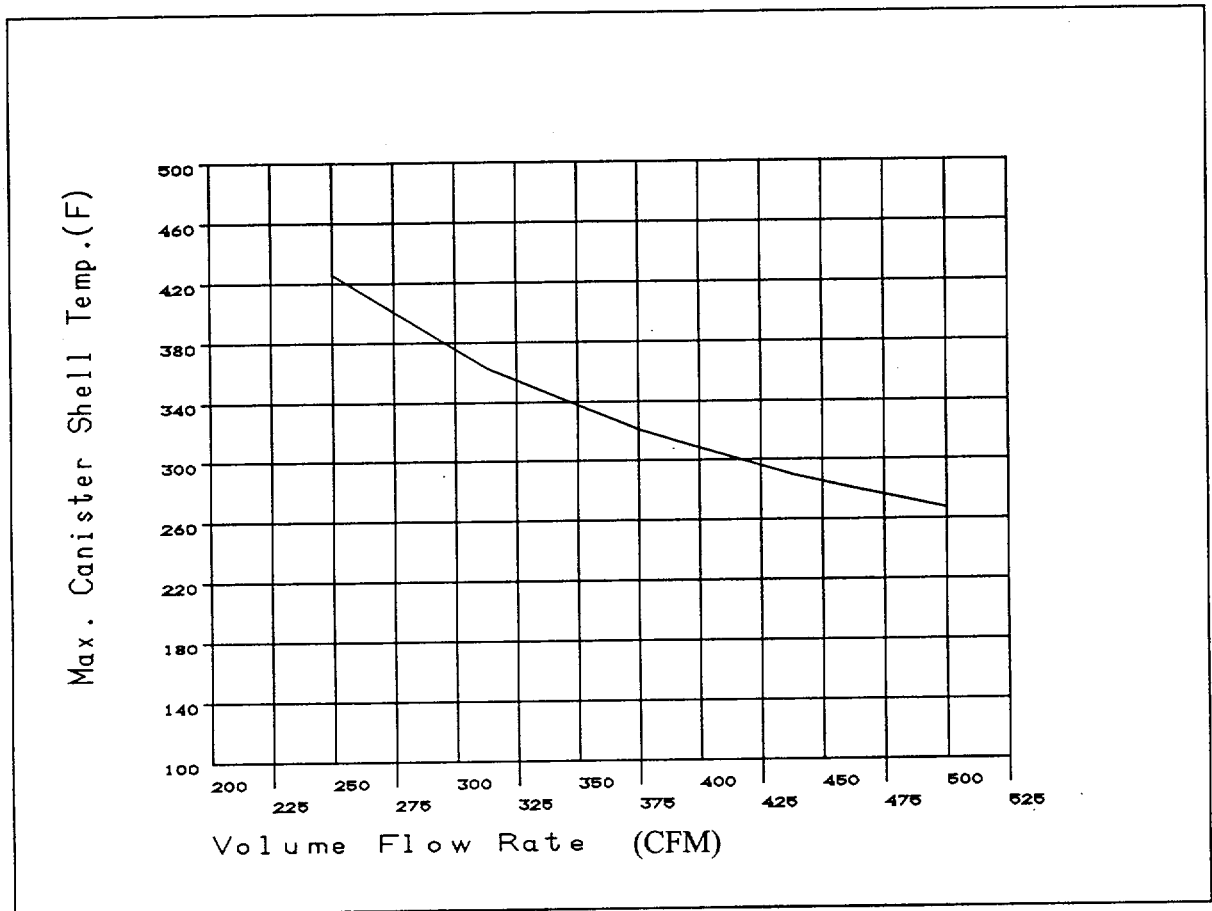


Figure 4.4.1.1.7-5 Maximum Standard Canister Temperature Versus Air Volume Flow Rate



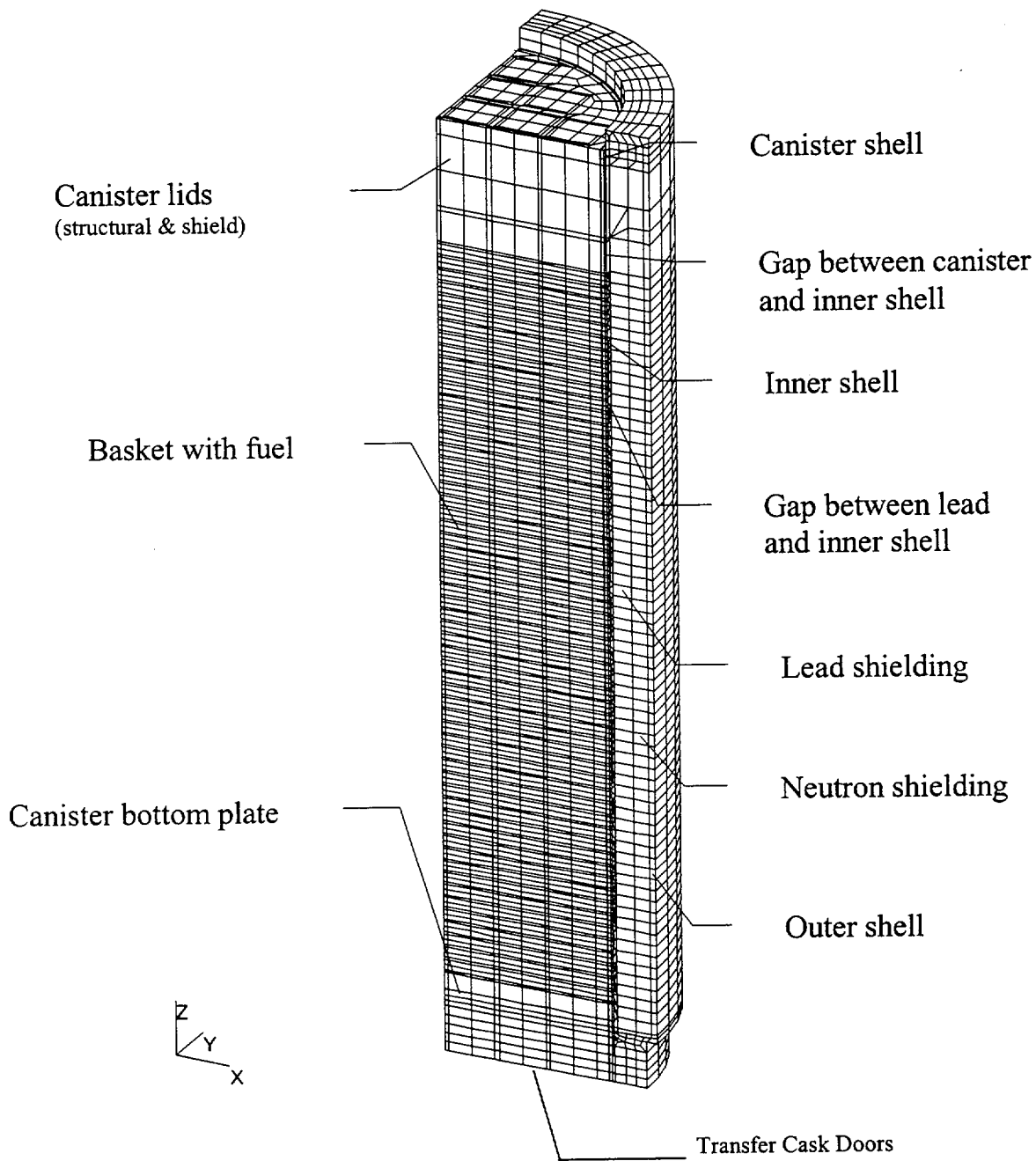
4.4.1.1.8 Three-Dimensional Standard Transfer Cask and Canister Model

A three-dimensional finite element model is generated for the Standard transfer cask with the loaded canister for the PWR fuel configuration, as shown in Figure 4.4.1.1.8-1. The model is used in Section 4.4.3.2 to evaluate the transfer operation for PWR fuel heat load cases with less than the design basis heat load of 23 kW (evaluated in Section 4.4.3.1). A quarter of the transfer cask, basket and canister is modeled due to the symmetry of the components and thermal loads. The planes of symmetry are considered to be adiabatic. The finite element model is comprised of SOLID70 and LINK31 radiation elements. The canister and its contents are modeled using the methodology described for the three-dimensional canister model for PWR fuel in Section 4.4.1.1.2.

The Standard canister contents includes the fuel assemblies, fuel tubes, support and heat transfer disks, top and bottom weldments, the canister shell, lids and bottom plate, and the media (water, vacuum and helium) inside the canister. The effective properties for the fuel assembly region and the fuel tube are determined using the two-dimensional fuel models (Section 4.4.1.1.5) and the two-dimensional fuel tube models (Section 4.4.1.1.6), respectively. The effective properties take into account the different types of media (water, vacuum and helium) in the canister.

The Standard transfer cask in the model consists of the inner shell, lead, neutron shield and outer shell. Convection and radiation are considered at the side and top surfaces of the transfer cask and the top surface of the canister. The ambient temperature is considered to be 76°F. For the transient analysis for transfer operations, an initial temperature of 100°F is considered in the model on the basis of the typical average water temperature in the spent fuel pool. Two air gaps (radial) outside of the canister are considered: a gap of 0.345 inch between the canister and transfer cask inner shell and a gap of 0.03 inch (based on tolerance) between the transfer cask inner shell and lead. Only conduction and radiation are considered across the gaps (no convection). The bottom of the transfer cask is conservatively modeled as adiabatic.

Figure 4.4.1.1.8-1 Three-Dimensional Standard Transfer Cask and Canister Model



4.4.1.2 Thermal Models for Advanced Configuration

Finite element and finite volume models are utilized for the thermal evaluation of the Universal Storage System as shown in the following. These models are used separately to evaluate the system for the storage of PWR fuel in the Advanced configuration.

1. Three-Dimensional Air Flow and Concrete Cask Model
2. Three-Dimensional Canister Model
3. Three-Dimensional Transfer Cask and Canister Model
4. Three-Dimensional Periodic Canister Internal Model
5. Two-Dimensional Fuel Model
6. Two-Dimensional Fuel Basket Neutron Absorber Plate Model

The two-dimensional axisymmetric air flow and concrete cask model includes the concrete cask, air in the air inlets, annulus and the air outlets, the canister and the canister internals, which are modeled as homogeneous regions with effective thermal conductivities. The effective thermal conductivities for the canister internals in the radial direction are determined using the three-dimensional periodic canister internal models. The effective conductivities in the canister axial direction are calculated using classical methods. The two-dimensional axisymmetric air flow and concrete cask model is used to perform computational fluid dynamic analyses to determine the mass flow rate, velocity and temperature of the air flow, as well as the temperature distribution of the concrete, concrete cask steel liner and the canister.

The three-dimensional Advanced canister model is comprised of the fuel assemblies, basket plates, neutron absorber plates, cooling inserts, cooling shunts, top and bottom basket assemblies, the canister shell, lids and bottom plate, and canister media. The canister model is used to evaluate the temperature distribution of the fuel cladding and basket components. The fuel assemblies, neutron absorber plates and the cooling inserts in the three-dimensional canister model are modeled using effective conductivities. The effective conductivities for the fuel assemblies are determined using the two-dimensional fuel model. The effective conductivities for the neutron absorber plates are determined using the two-dimensional fuel basket neutron absorber plate model. The effective conductivities for the cooling inserts are determined using the two-dimensional fuel basket cooling insert model.

The three-dimensional Advanced transfer cask model includes the transfer cask and the canister. This model is used to perform transient analyses for the transfer condition, starting from removing the transfer cask/canister from the spent fuel pool, vacuum drying and finally back-filling the canister with helium.

The three-dimensional periodic Advanced canister internal model consists of a periodic section of the canister internals. This model represents a cut of the three-dimensional canister model. The purpose of the three-dimensional periodic canister internal model is to determine the effective thermal conductivity of the canister internals in the canister radial direction. The effective conductivities are used in the three-dimensional air flow and concrete cask model. The canister media in this model is helium.

The two-dimensional fuel model includes the fuel pellets, cladding and the media occupying the space between fuel rods. The media is considered to be helium for storage conditions and water, vacuum, or helium for transfer conditions. The model is used to determine the effective thermal properties of the fuel assembly. In order to account for various types of fuel assemblies, a total of four fuel models are generated—14×14, 15×15, 16×16 and 17×17 PWR fuel assemblies. The effective properties are used in the three-dimensional canister model, the three-dimensional transfer cask and canister model, and the three-dimensional periodic canister internal model.

The two-dimensional neutron absorber plate model includes the neutron absorber plate and the media separating the neutron absorber plate from the basket plate. The media is considered to be helium for storage conditions and water, vacuum, or helium for transfer conditions. The model is used to determine the effective thermal properties of this region. The effective properties are used in the three-dimensional canister model, the three-dimensional transfer cask and canister model, and the three-dimensional periodic canister internal model.

4.4.1.2.1 Two-Dimensional Axisymmetric Air Flow and Concrete Cask Model-Advanced Configuration

This section describes the computational fluid dynamics model used to evaluate the thermal performance of the vertical concrete cask for the advanced PWR configuration. Similar to the two-dimensional axisymmetric air flow and concrete cask model for the standard configuration (Section 4.4.1.1.1), the model includes the concrete cask, the air in the air inlets, the annulus and the air outlets, the canister and the canister internals, which are modeled as homogeneous regions with effective thermal conductivities. The model is shown in Figures 4.4.1.2-1 and 4.4.1.2-2.

The fuel canister is cooled by (1) natural/free convection of air through the lower vents (the air inlets), the vertical air annulus, and the upper vents (the air outlets); and (2) radiation heat transfer between the surfaces of the canister shell and the steel liner. The heat transferred to the liner is rejected by air convection in the annulus and by conduction through the concrete. The heat flow through the concrete is dissipated to the surroundings by natural convection and radiation heat transfer. The temperature in the concrete region is controlled by radiation heat transfer between the vertical annulus surfaces (the canister shell outer surface and the steel liner inner surface), natural convection of air in the annulus, and boundary conditions applicable to the concrete cask outer surfaces—e.g., natural convection and radiation heat transfer between the outer surfaces and the environment, including consideration of incident solar energy. These heat transfer modes are combined in the air flow and concrete cask model. The entire thermal system, including mass, momentum, and energy, is analyzed using FLUENT 5.5 [41]. The temperature distributions of the concrete cask, the air region and the canister are determined by the model. Detailed thermal evaluations for the canister internals (fuel cladding, basket, etc.) are performed using the three-dimensional canister model as described in Section 4.4.1.2.2.

The concrete cask has four air inlets at the bottom and four air outlets at the top that extend through the concrete. Since the configuration is symmetrical, it can be simplified into a two-dimensional axisymmetric model by using equivalent dimensions for the air inlets and outlets, which are assumed to extend around the concrete cask periphery. The canister internals are modeled as three homogeneous regions using effective thermal conductivities - the active fuel region and the regions above and below the active fuel region. The two-dimensional axisymmetric model is shown schematically in Figure 4.4.1.2-1. The effective properties for the active fuel region in the canister is determined using the three-dimensional periodic model described in Section 4.4.1.2.4. The effective axial conductivities for the region are determined

using classic method based on the results of the three-dimensional canister model (Section 4.4.1.2.2). Conductivity of helium is considered for the radial direction.

GAMBIT version 1.3 [42], a preprocessor for FLUENT, is used to construct the computation mesh (shown in Figure 4.4.1.2-2) for the CFD simulations. The mesh contains quadrilateral cells, with higher mesh density in fluid regions compared with solid regions, to capture sharp velocity and temperature gradients in the flow. The T-shaped channel weldments in the annulus (welded to the steel liner) are not explicitly modeled. The radial dimension of the air annulus between the canister shell and the carbon steel liner of the concrete cask is reduced in the model to account for the slight reduction of the air flow cross-sectional area due to the T-shaped channel weldments. Note that the thickness of the steel liner and the outer diameter of the concrete cask were not changed. Radiation heat transfer that occurs in the following regions is included in the model:

1. From the concrete outer surfaces to the ambient
2. Across the vertical air annulus (from the canister shell to the concrete cask liner)
3. From the canister structural lid to the shield plug
4. From the shield plug to the concrete cask lid

Loads and Boundary Conditions

The loads and boundary conditions in the model are identical to those used in the two-dimensional axisymmetric air flow and concrete cask model for the standard configuration (Section 4.4.1.1.1). The distribution of the heat generation in the active fuel region is based on the axial power distribution for the PWR fuel as shown in Figure 4.4.1.1.1-3. The incident solar heat flux applied to the side surface of concrete, top surface of concrete, and top surface of the cask lid are 120 W/m^2 , 240 W/m^2 , and 320 W/m^2 respectively. The natural convection heat transfer and the radiation heat transfer at the outer surfaces of the concrete cask are considered using the same method described in Section 4.4.1.1.1.

Convergence Check of the Numerical Simulation

To ensure the convergence of the numerical simulation of the air flow in the concrete cask and to ensure reliable numerical results, the following checks and confirmations are performed.

1. Global convergence of the iteration process for the nonlinear system.

The equation system controlling air flow and heat transfer is nonlinear and is solved iteratively. The global iteration process is monitored by checking solution residuals, and the variation of solution parameters with the global iteration—e.g., maximum temperature on various surfaces of the domain, the mass flow rate, and the net heat carried out of the concrete cask by air convection. For all presented results, the solution variables (temperature and velocity) do not change significantly with further iterations and, therefore, the solutions are converged.

2. Overall energy balance and mass balance.

This step validates the overall energy balance and mass balance. At the converged state, the mass flow rate at the air inlets matches the mass flow rate at the air outlets, showing that an excellent mass balance has been obtained. The overall energy balance is checked by computing the net total heat flux, Q_{net} , on surfaces of the model on which boundary conditions are applied, i.e., inlet, outlet, bottom of the steel liner, and all outer solid surfaces, and by comparing this total flux to the heat flux across the boundaries of the active fuel region (which is equal to the applied fuel heat source, Q_{fuel}). For the normal storage condition with the PWR design heat load of 29.2 kW, the difference in Q_{net} and Q_{fuel} is less than 0.2 percent and, therefore, overall heat balance is achieved in the system.

3. CFD Mesh Sensitivity Study.

A sensitivity evaluation is performed based on the model for the PWR fuel configuration to assess the effect of the number of elements used in the two-dimensional axisymmetric air flow and concrete cask model. Since large gradients in velocity and temperature occur in the air annulus, the number of cells along the radial direction in the annulus was increased from 29 to 49, which results in an increase in total number of cells in the air flow domain from 9,158 to 11,658.

Case	Number of Elements in Air Domain	Max. Temp. on Outer Shell Surface	Maximum Concrete Temp.	Average Air Temp. at the Outlet	Maximum Canister Shell Temp.
ES1	9158	458 K	366 K	351 K	487 K
ES2	11,658	454 K	363 K	351 K	484 K
ES1/ES2	0.79	1.01	1.01	1.0	1.01

A comparison of the two models (Case ES1/ES2) shows that the maximum difference is 1%. Therefore, the number of elements used in the two-dimensional axisymmetric air flow and concrete cask model is adequate. The lower density mesh gives a more conservative estimate of maximum temperature values in the canister shell and concrete.

The effect of the installation of the supplemental shielding fixture installed in the air inlet is evaluated based on the off-normal condition of blockage of one-half of the air inlets. The analysis results show that the maximum temperature increase for the fuel cladding and basket is 2°F, which remains well below temperature limits of the normal conditions (Table 4.1-6). The pipes in the shielding fixture are offset to block (gamma) radiation, but allow air flow.

Figure 4.4.1.2-1 Two-Dimensional Axisymmetric Air Flow and Concrete Cask Model for Advanced Configuration

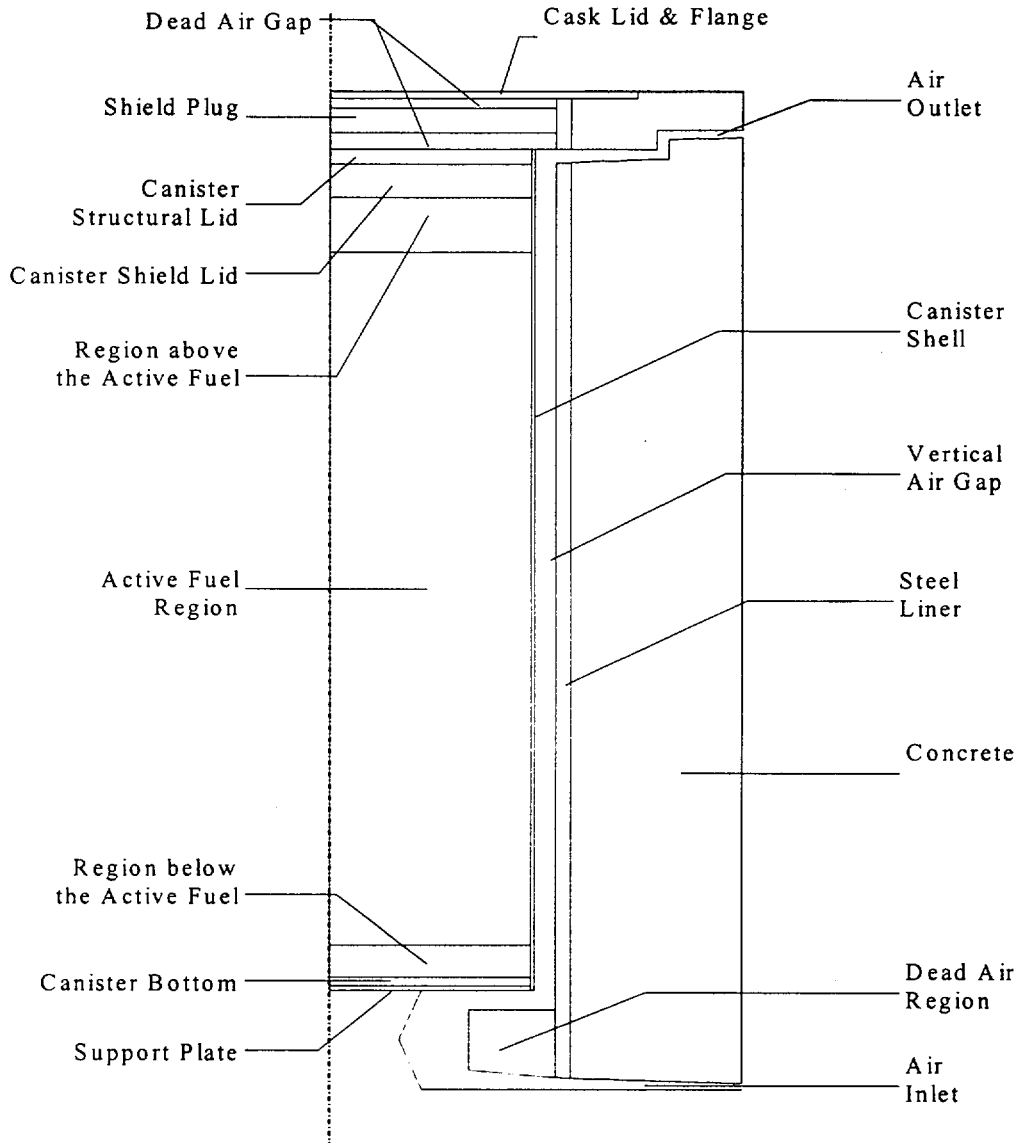
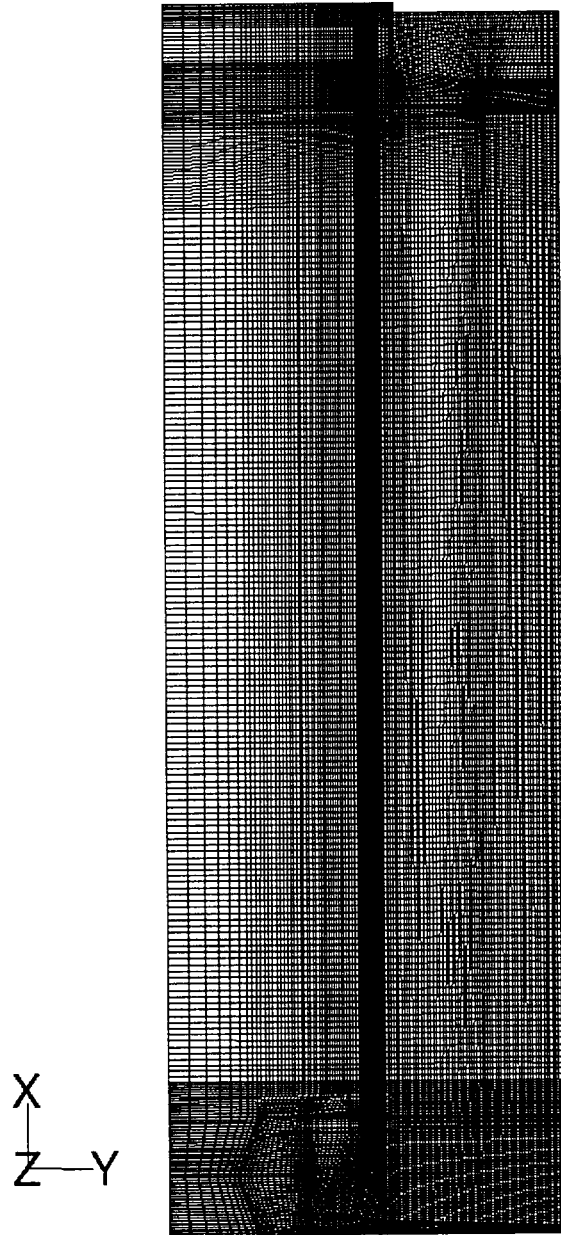


Figure 4.4.1.2-2 Two-Dimensional Axisymmetric Air Flow and Concrete Cask CFD Mesh – Advanced Configuration



4.4.1.2.2 Three-Dimensional Advanced Canister Model

A three-dimensional finite element model of the Advanced configuration PWR basket and canister is used to determine the temperature distribution of the fuel cladding, basket components and canister components. The finite element model is shown in Figures 4.4.1.2.2-1 and 4.4.1.2.2-2.

ANSYS SOLID70 three-dimensional conduction elements, SHELL57 three-dimensional thermal shell conduction elements and MATRIX50 radiation matrix elements are used to construct the model. The model includes the fuel assemblies, neutron absorber plates, basket plates, cooling inserts, cooling shunts, top and bottom basket assemblies, canister shell, lids, and bottom plate, and gas inside the canister (helium). Based on the symmetry of the geometry and loading, only one-quarter of the loaded canister is modeled. The two planes of symmetry are considered to be adiabatic.

The canister outer surface temperatures obtained from the two-dimensional axisymmetric air flow and concrete cask model (Section 4.4.1.2.1) are applied to the canister surfaces in the model as boundary conditions. The decay heat of the fuel assemblies is rejected to the applied canister temperatures via conduction and thermal radiation. The analyses are steady-state.

In the model, the fuel assemblies are centered between the neutron absorber plates and the basket is centered in the canister. This is conservative since any contact between components will provide a more efficient path to reject the heat. Additionally, gaps are modeled between the neutron absorber plates and basket plates. The gaps used in the three-dimensional canister model are based on nominal gap size at room temperature.

Gap Description	Nominal Gap (inch) in the Thermal Model
Gap between neutron absorber plates and basket plates	0.044
Gap between the basket and canister shell	0.155
Gaps between the basket plates at their intersections	0.02

The cooling shunts between the basket and canister are modeled using SHELL57 three-dimensional thermal shell elements. The cooling shunt is designed to be in contact with the basket plate. For conservatism, a gap of 0.005 inch is considered between the cooling insert (all around – 4 sides) and the basket plates.

The structural lid and shield lid are expected to be in full contact due to the weight of the structural lid. The thermal resistance across the contact surface is considered to be negligible and, therefore, no gap is modeled between the lids.

All material properties used in the model, except the effective properties in the following discussion, are shown in Section 4.2.

The fuel assemblies, neutron absorber plate regions and cooling insert regions are modeled as homogenous regions with effective thermal properties. These effective properties are calculated using the two-dimensional fuel model (Section 4.4.1.2.5), the two-dimensional neutron absorber plate region model (Section 4.4.1.2.6), and the two-dimensional cooling insert region model (Section 4.4.1.2.7), respectively. These effective thermal properties account for conduction and thermal radiation exchange in these regions. The effective thermal properties corresponding to the PWR 14×14 assemblies are used since the 14×14 assemblies have lower effective thermal conductivities as compared to fuel sizes of 15×15 , 16×16 , and 17×17 .

Radiation heat transfer exchange, in addition to that modeled in the previously discussed effective thermal properties, is accounted for in the three-dimensional model using MATRIX50 super elements. Radiation exchange is modeled for the following locations:

1. From the top of the fuel region to the bottom surface of the canister shield lid.
2. Between the inner surfaces of the cooling inserts.

Radiation heat transfer between the basket and canister shell is not modeled due to the presence of the cooling shunts.

Volumetric heat generation (Btu/hr-in³) is applied to the active fuel region based on the design heat load of 29.2 kW, an active fuel length of 144 inches, and an axial power distribution as shown in Figure 4.4.1.1.1-3. The design heat load of 29.2 kW is preferentially loaded into the 32 basket slots using the pattern shown in Figure 4.4.1.2.2-3.

Additionally, the three-dimensional canister model is used to determine the effective axial thermal conductivity inside the canister above and below the active fuel region. These effective properties are used in the two-dimensional axisymmetric air flow and concrete cask model (Section 4.4.1.2.1). The axial heat flow, Q, through the regions below and above the active fuel region is described by the following conduction rate equation:

$$Q = k_{\text{eff}} \times A \times \left(\frac{\Delta T}{L} \right)$$

where:

- keff = the effective axial conductivity
- A = the cross-sectional area of the inside of the canister
= $\pi D^2/4 = \pi(65.81 \text{ in.})^2/4 = 3,401.525 \text{ in}^2$,
- D = the inner diameter of the canister, 65.81 in.
- ΔT = the temperature difference for the region
- L = the height of the region—5.0 in. for below the active fuel, and
14.3 in. for above the active fuel.

The heat flow rate to the canister bottom plate is 8,051 Btu/hr, and the heat flow to the canister shield lid is 1,067 Btu/hr based on the design heat load of 29.2 kW as calculated in the three-dimensional canister model. Additionally, the temperature difference between the bottom of the active fuel and the canister bottom plate is 69°F, and the temperature difference between the top of the active fuel and the canister shield lid is 132°F. Rearranging the previous equation and solving for the effective axial conductivity yields:

Below active fuel region: $k_{\text{eff}} = \frac{(8,051 \text{ Btu/hr}) \times (5.0 \text{ in.})}{(3,401.525 \text{ in}^2) \times (69^\circ\text{F})} = 0.172 \text{ Btu/hr-in.} - ^\circ\text{F}$

Above active fuel region: $k_{\text{eff}} = \frac{(1,067 \text{ Btu/hr}) \times (14.3 \text{ in.})}{(3,401.525 \text{ in}^2) \times (132^\circ\text{F})} = 0.034 \text{ Btu/hr-in.} - ^\circ\text{F}$

Figure 4.4.1.2.2-1 Three-Dimensional Canister Model for PWR Fuel – Advanced Configuration

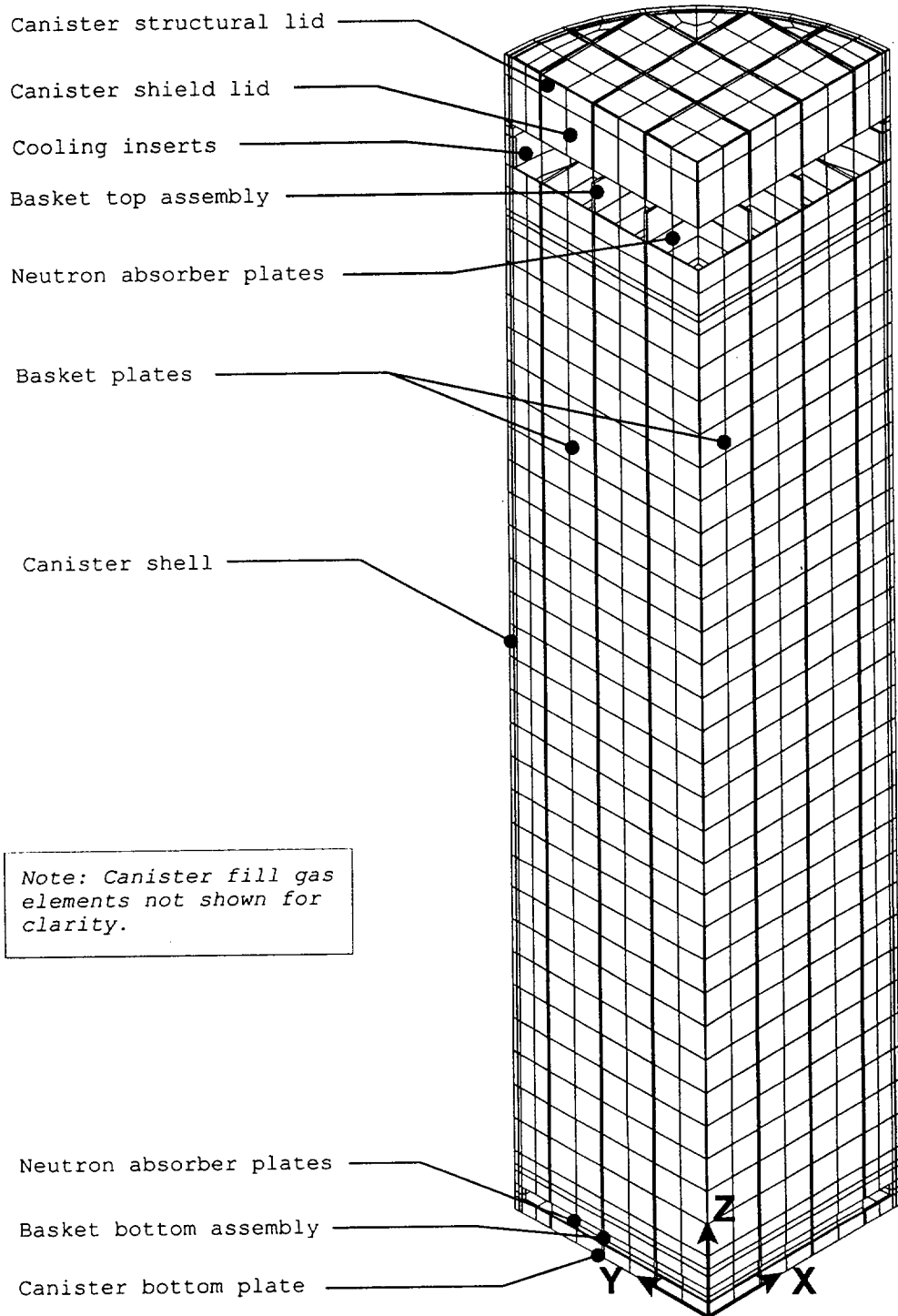


Figure 4.4.1.2.2-2 Three-Dimensional Canister Model for PWR Fuel – Cross-Section –
Advanced Configuration

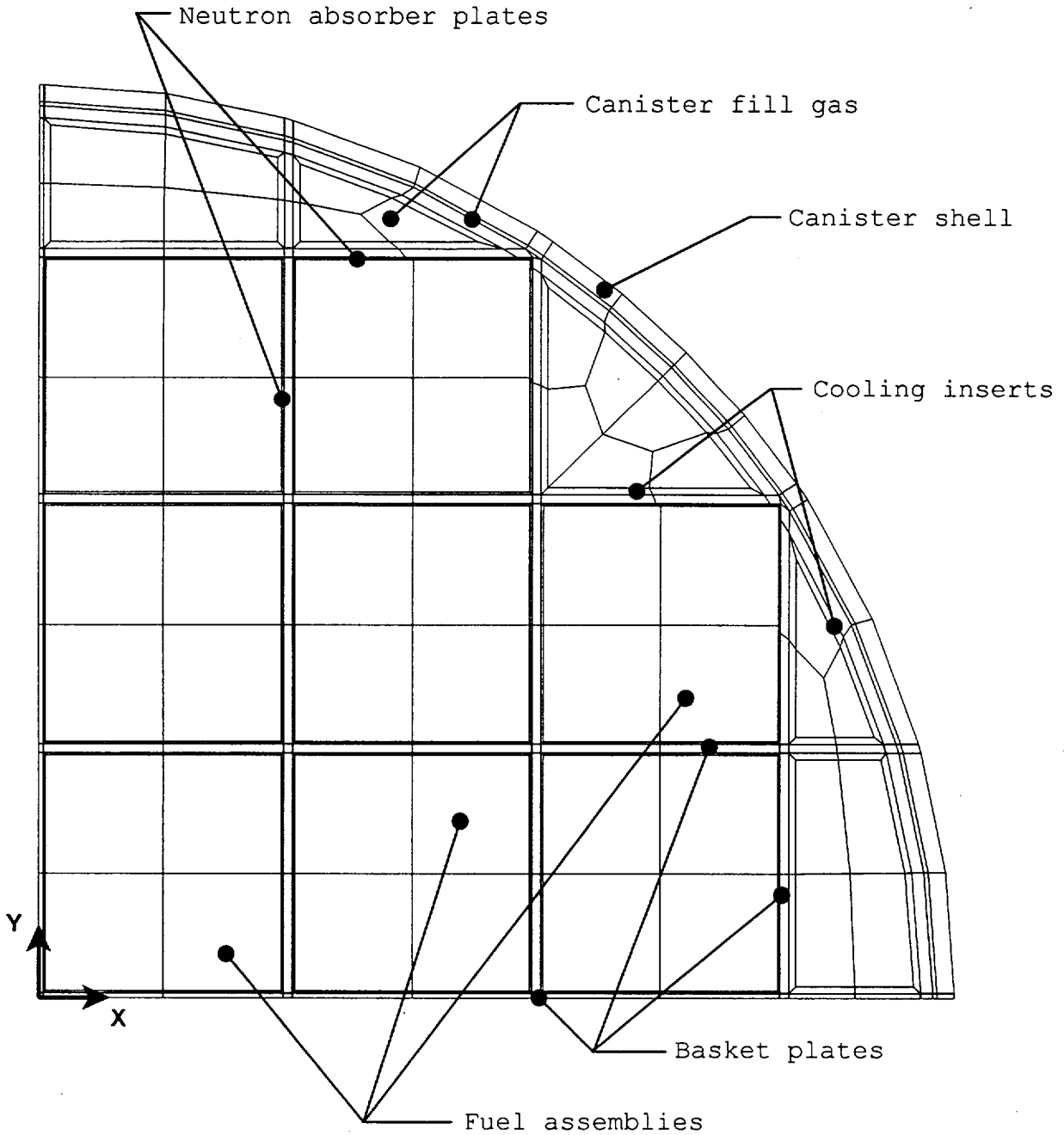
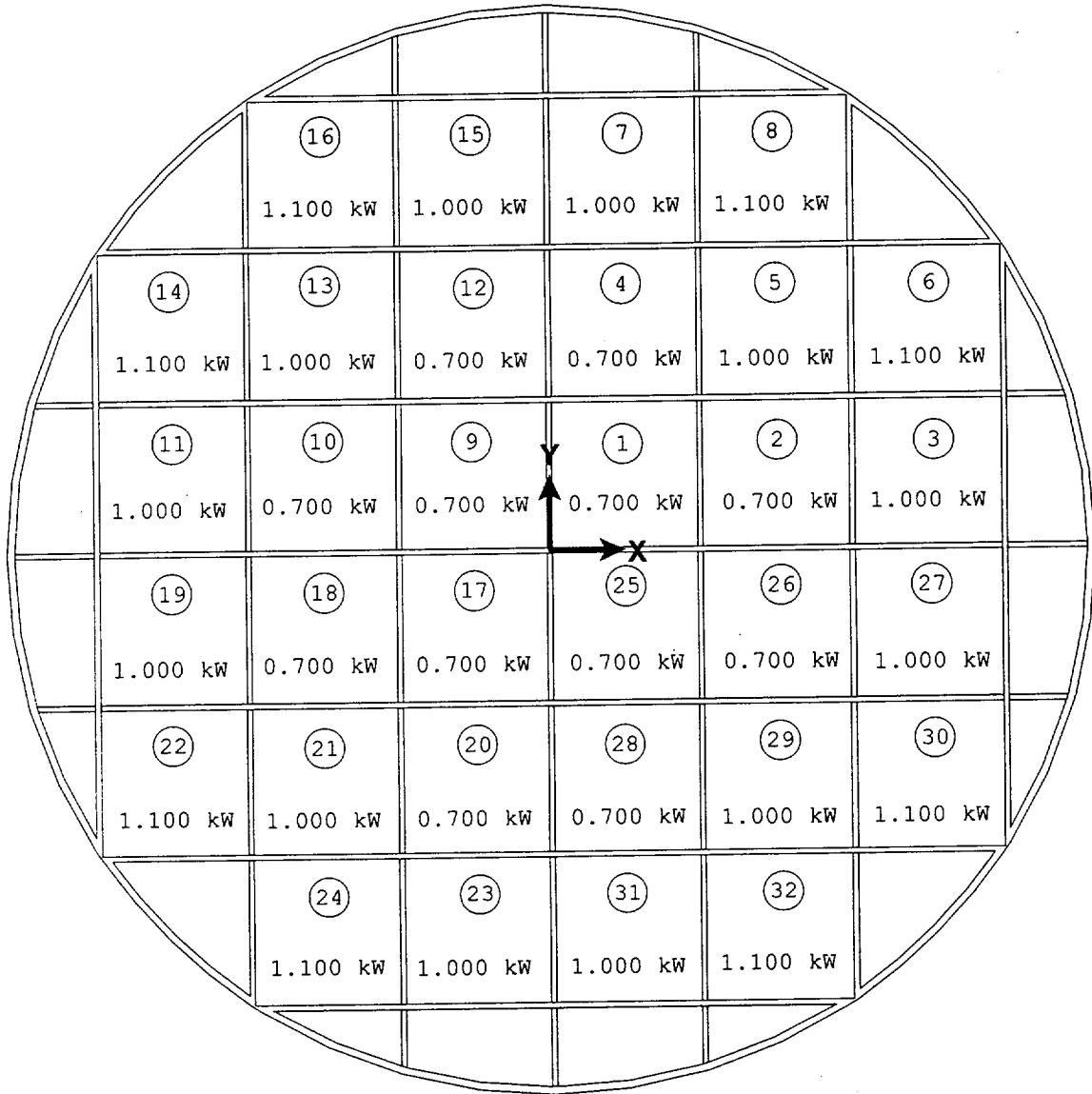


Figure 4.4.1.2.2-3 PWR Basket – Advanced Configuration – Design Heat Load (29.2 kW)
Preferential Loading Pattern



4.4.1.2.3 Three-Dimensional Advanced Transfer Cask and Canister Model

A three-dimensional finite element model is generated for the Advanced transfer cask with the Advanced canister for PWR fuel as shown in Figure 4.4.1.2.3-1. The model is used to evaluate the transfer operation for PWR fuel with the design heat load of 29.2 kW and heat load cases less than the design heat load. A quarter-section of the transfer cask, canister, fuel basket and fuel assemblies is modeled due to the symmetry of the components and thermal loads. The planes of symmetry are considered to be adiabatic. The finite element model is comprised of SOLID70 three-dimensional conduction elements, MATRIX50 radiation matrix elements, and SHELL57 three-dimensional conduction elements (which are used for the basket cooling shunts). The canister and its contents are modeled using the model and methodology described for the three-dimensional canister model in Section 4.4.1.2.2.

Transient thermal analyses are performed using the model to determine the thermal response of the transfer cask and its contents during the transfer operation.

The canister and its contents include the fuel assemblies, neutron absorber plates, basket plates, cooling inserts, cooling shunts, basket top and bottom assemblies, canister shell, canister lids and bottom plate, and canister media (water, vacuum, and helium). The effective thermal properties for the fuel assemblies are calculated in Section 4.4.1.2.5. The effective thermal properties for the fuel basket neutron absorber plates are calculated in Section 4.4.1.2.6. The effective thermal properties for the fuel basket cooling inserts are calculated in Section 4.4.1.2.7. The effective properties for these regions take into the different types of media (water, vacuum, and helium) in the canister.

The Advanced transfer cask in the three-dimensional model consists of the inner shell, lead (gamma shield), neutron shield (radial and lower), outer shell, and the air gap between the inner shell and the lead shield. Convection and radiation boundary conditions are considered at the side and top surfaces of the transfer cask and at the top of the canister. The natural convection film coefficient, h_c , applied to the model is:

$$h_c = 0.00132(\Delta T)^{1/3} \text{ Btu/hr-in}^2\text{-}^\circ\text{F}$$

where:

ΔT = temperature difference between the surface and the ambient.

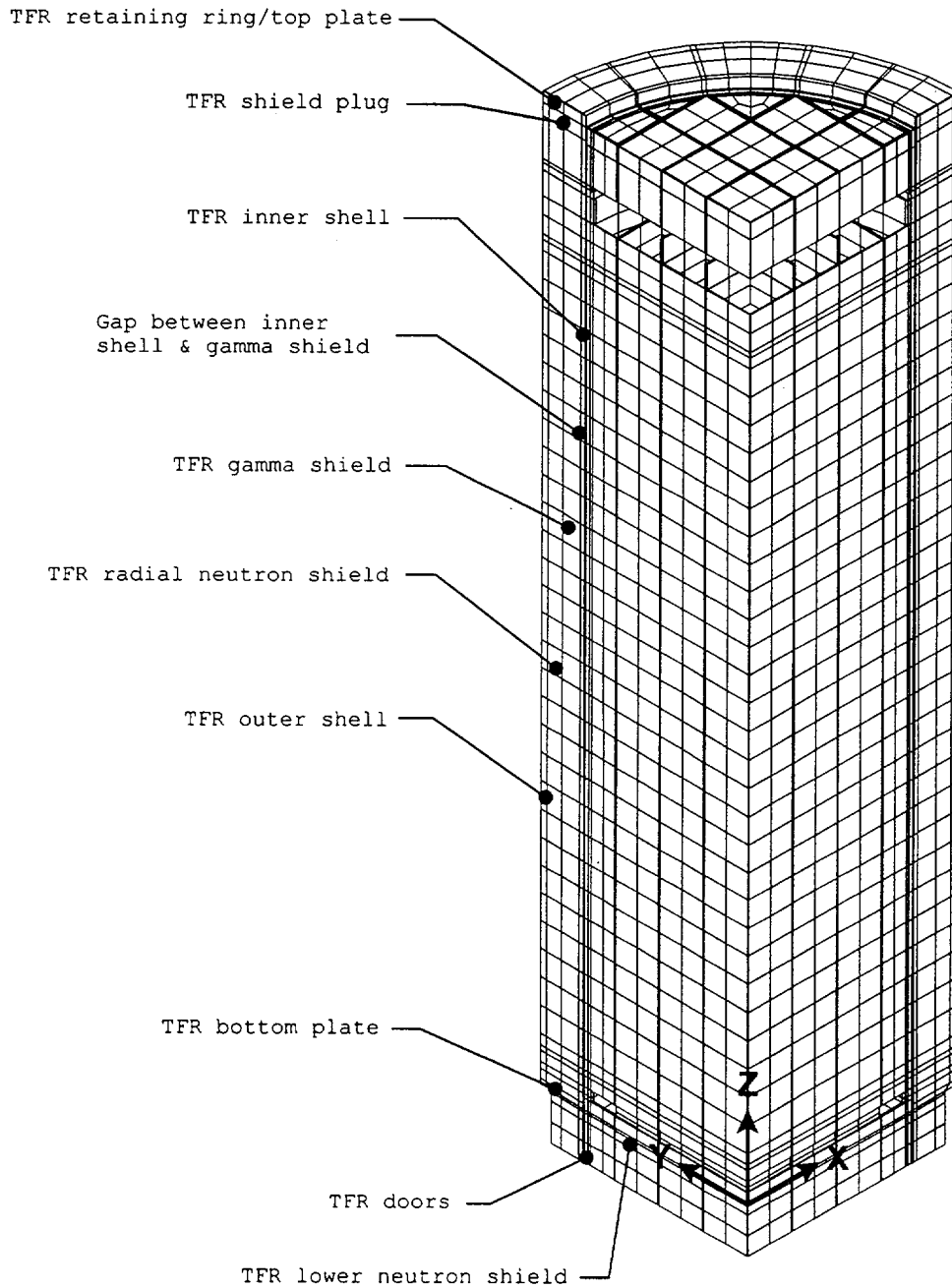
Two air gaps (radial) outside of the canister are considered: a gap of 0.345 inches between the canister and transfer cask inner shell and a gap of 0.03 inches (based on tolerance) between the transfer cask inner shell and lead gamma shield. Only conduction and radiation are considered across the gaps (no convection).

The ambient temperature is 76°F. For the transient analyses of the transfer operation, an initial uniform temperature of 100°F is considered in the model on the basis of the typical average water temperature in the spent fuel pool.

The transfer cask is provided in a Standard, Advanced or 100-ton configuration. The 100-ton transfer cask weighs less than the Standard or Advanced transfer casks and is designed to accommodate sites having a 100-ton cask handling crane weight limit. Canister handling, fuel loading and canister closing are operationally identical for all transfer cask configurations.

The thermal evaluation for the 100-ton transfer cask is bounded by the evaluation using the models presented in this section. The overall wall thickness for the 100-ton transfer cask is less than that for the Standard/Advanced configuration transfer casks. The water-neutron shield for the 100-ton transfer cask has better heat transfer capability (conduction and convection) than the NS-4-FR used for the Standard transfer cask. The 100-ton transfer cask may be handled in a horizontal orientation. Since there will be contact between basket, canister and transfer cask components when the cask is in the horizontal orientation, a more effective path for heat rejection results. The maximum temperatures for the fuel and basket components are expected to be lower compared with the condition when the transfer cask is in the vertical orientation.

Figure 4.4.1.2.3-1 Three-Dimensional Transfer Cask Canister Model for PWR Fuel –
Advanced Configuration



Note: The canister media and the
TFR media are not shown for
clarity.

4.4.1.2.4 Three-Dimensional Periodic Advanced Canister Internal Model

The three-dimensional periodic Advanced canister internal model is used to calculate the effective thermal properties of the canister internals in the active fuel region. These effective thermal properties are used in the two-dimensional airflow and concrete cask model (Section 4.4.1.2.1). The model is shown in Figure 4.4.1.2.4-1 and consists of a one-quarter symmetry section, the canister media, fuel assemblies, basket plates, neutron absorber plates, and cooling inserts. The fuel assemblies, neutron absorber plates, and cooling inserts are modeled as homogenous regions with the effective thermal properties calculated in Section 4.4.1.2.5, Section 4.4.1.2.6, and Section 4.4.1.2.7, respectively. The canister media is helium for this model.

Volumetric heat generation (Btu/hr-in³) is applied to the fuel region based on the design heat load of 29.2 kW, an active fuel length of 144 inches, and a peaking factor of 1.08 as shown in Figure 4.4.1.1.1-3. The design heat load of 29.2 kW is preferentially loaded into the 32 basket slots using the pattern shown in Figure 4.4.1.2.2-3.

The effective thermal conductivity (k_{eff}) of the fuel region in the radial direction is determined by considering the canister internals as a solid cylinder with heat generation. The temperature distribution in the cylinder may be expressed as [17]:

$$T - T_o = \frac{q''' R^2}{4k_{eff}} \left[1 - \left(\frac{r}{R} \right)^2 \right]$$

where:

T_o = the surface temperature of the cylinder
 T = temperature at radius "r" of the cylinder
 R = the outer radius of the cylinder
 r = radius

$$q''' = \text{the heat generation rate} = \frac{Q}{\pi R^2 H}$$

where: Q = total heat generated in the cylinder
 H = length of the cylinder

Considering the temperature at the center of the canister to be T_{\max} , the above equation can be simplified and used to compute the effective thermal conductivity (k_{eff}):

$$k_{\text{eff}} = \frac{Q}{4\pi H(T_{\max} - T_o)} = \frac{Q}{4\pi H\Delta T}$$

where:

Q = total heat generated by the fuel

H = length of the active fuel region

T_o = temperature at outer surface internals (inside surface of the canister)

$\Delta T = T_{\max} - T_o$

The value of ΔT is obtained from thermal analysis using the three-dimensional periodic canister internal model with the boundary temperature constrained to be T_o . The effective conductivity (k_{eff}) is then determined by using the above formula. Analysis is repeated by applying different boundary temperatures so that temperature-dependent conductivities can be determined.

The effective conductivity in the axial direction (the Z direction in Figure 4.4.1.2.4-1) is calculated by:

$$K_z = \sum A_i K_i / A_{\text{tot}}$$

where:

K_i = thermal conductivity of each region

A_i = area of each region

A_{tot} = total area of the model

The effective density and effective specific heat properties are calculated using volume and mass ratios, respectively. The effective thermal properties for the canister internal components are shown in Table 4.4.1.2.4-1.

Figure 4.4.1.2.4-1 Three-Dimensional Periodic Canister Internal Model – PWR –
Advanced Configuration

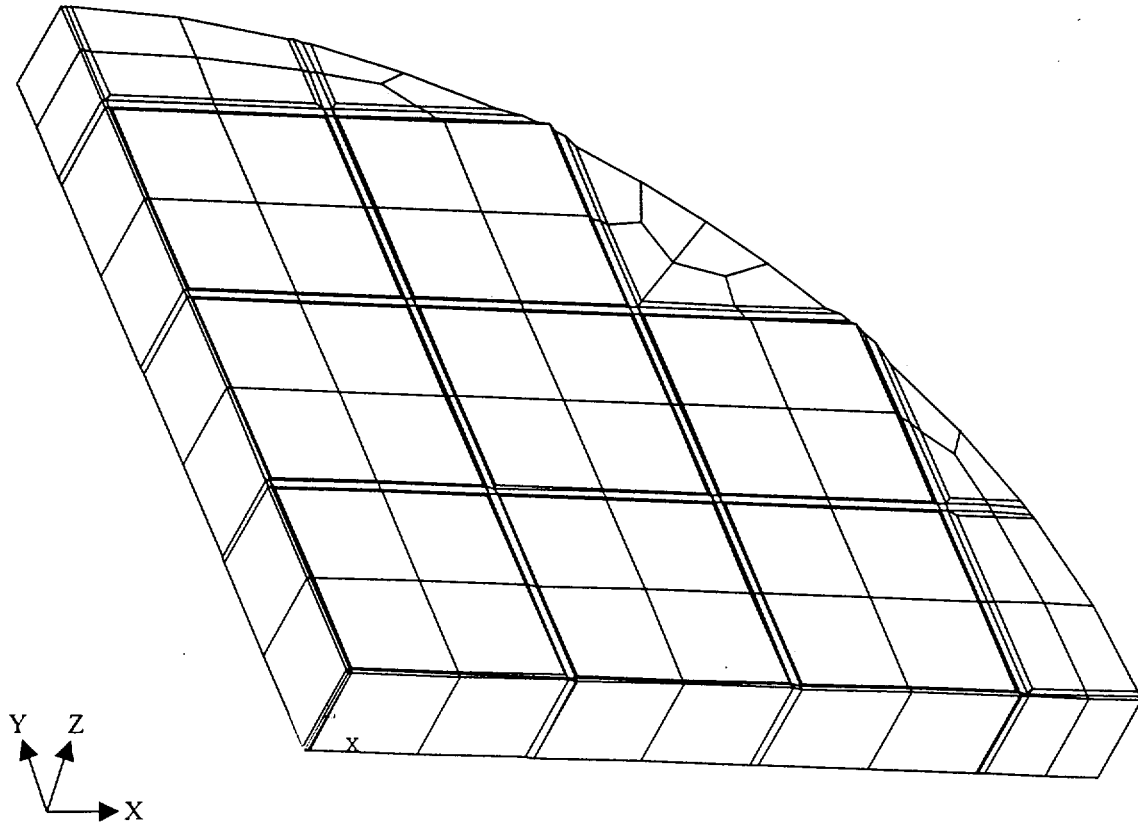


Table 4.4.1.2.4-1 Effective Thermal Conductivity for the Advanced Canister Internal Components

Conductivity (Btu/hr-in.-°F)	Temperature (°F)				
	101	212	431	651	761
Kr	0.129	0.135	0.149	0.163	0.171
Kz	0.580	0.577	0.557	0.540	0.536

Note: Kr is in the radial direction.
Kz is in the canister axial direction.

4.4.1.2.5 Two-Dimensional Fuel Model – Advanced Configuration

The effective conductivity of the fuel is determined by the two-dimensional finite element model of the fuel assembly. The effective conductivity is used in the three-dimensional canister model (Section 4.4.1.2.2), the three-dimensional transfer cask model (Section 4.4.1.2.3) and the three-dimensional periodic canister internal model (Section 4.4.1.2.4). A total of four models are required for the 14×14, 15×15, 16×16 and 17×17 PWR fuels. Because of similarity, only the figure for the PWR 14×14 model is shown in this Section (Figure 4.4.1.2.5-1).

The model includes the fuel pellets, cladding, media between fuel rods and helium at the gap between fuel pellet and cladding. Three types of media are considered: helium, water and a vacuum. Modes of heat transfer modeled include conduction and radiation between individual fuel rods for the steady-state condition. ANSYS PLANE55 conduction elements and MATRIX50 radiation elements are used to model conduction and radiation. The radiation surfaces (i.e., the surface of the fuel pins and the inner surface of the basket neutron absorber plates) are defined using LINK32 elements. Radiation at the gap between the pellet and the cladding is conservatively ignored.

The effective conductivity for the fuel is determined by using an equation defined in a Sandia National Laboratory Report [30]. The equation is used to determine the maximum temperature of a square cross-section of an isotropic homogeneous fuel with a uniform volumetric heat generation. At the boundary of the square cross-section, the temperature is constrained to be uniform. The expression for the temperature at the center of the fuel is given by:

$$T_c = T_e + 0.29468 (Qa^2 / K_{eff})$$

where: T_c = the temperature at the center of the fuel (°F)

T_e = the temperature applied to the exterior of the fuel (°F)

Q = volumetric heat generation rate (Btu/hr-in³)

a = half length of the square cross-section of the fuel (inch)

K_{eff} = effective thermal conductivity for the isotropic homogeneous fuel material (Btu/hr-in-°F)

Volumetric heat generation (Btu/hr-in³) based on the design heat load is applied to the pellets. The effective conductivity is determined based on the heat generated and the temperature difference from the center of the model to the edge of the model. Temperature-dependent effective properties are established by performing multiple analyses using different boundary temperatures. The effective conductivity in the axial direction of the fuel assembly is calculated on the basis of the material area ratio (see the approach used in Section 4.4.1.2.4). The effective density and effective specific heat properties are calculated using volume and mass ratios, respectively. The calculated effective thermal properties for the PWR 14 × 14 fuel assembly are shown in Table 4.4.1.2.5-1. The effective thermal properties for the PWR 14 × 14 fuel assembly are used in thermal models described in Sections 4.4.1.2.2 and 4.4.1.2.3, since this fuel size has the lower effective thermal conductivity values when compared to the 15 × 15, 16 × 16, and 17 × 17 fuel sizes.

Figure 4.4.1.2.5-1 Two-Dimensional PWR (14×14) Fuel Model – Advanced Configuration

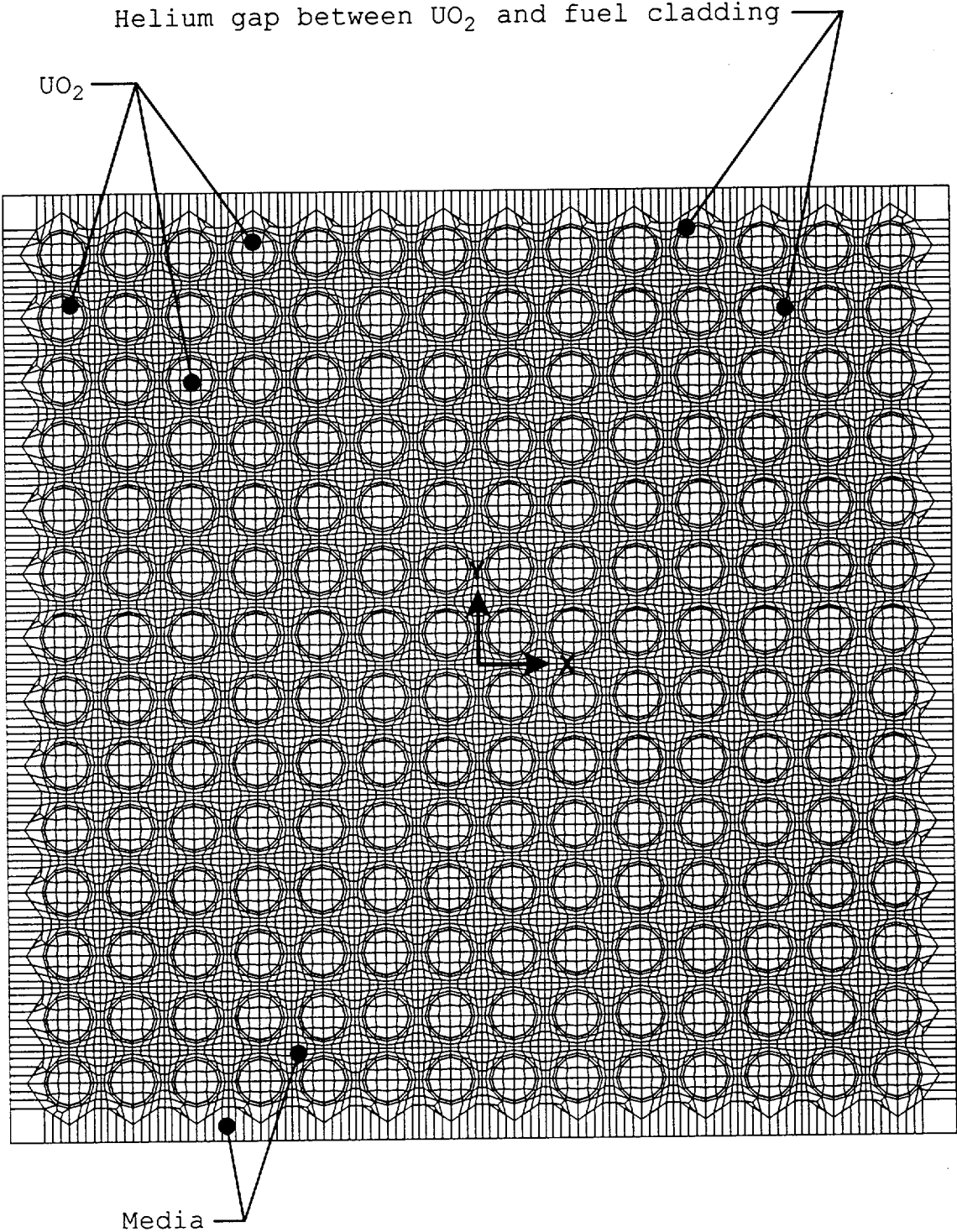


Table 4.4.1.2.5-1 Effective Thermal Conductivities for PWR 14 × 14 Fuel Assembly – Advanced Configuration

Media	Thermal Property	Temperature (°F)			
		218	412	609	810
Helium	Kxx (Btu/hr-in.-°F)	0.022	0.031	0.043	0.059
	Kyy (Btu/hr-in.-°F)	0.022	0.031	0.043	0.059
	Kzz (Btu/hr-in.-°F)	0.179	0.161	0.151	0.148
	Specific Heat (Btu/lbm-°F)	0.062	0.066	0.070	0.073
	Density (lbm/in ³)	0.151	0.151	0.151	0.151
Media	Thermal Property	Temperature (°F)			
		215	451	627	818
Vacuum	Kxx (Btu/hr-in.-°F)	0.005	0.015	0.025	0.041
	Kyy (Btu/hr-in.-°F)	0.005	0.015	0.025	0.041
	Kzz (Btu/hr-in.-°F)	0.174	0.152	0.144	0.141
	Specific Heat (Btu/lbm-°F)	0.062	0.067	0.070	0.074
	Density (lbm/in ³)	0.151	0.151	0.151	0.151
Media	Thermal Property	Temperature (°F)			
		-18	188		
Water	Kxx (Btu/hr-in.-°F)	0.050	0.055		
	Kyy (Btu/hr-in.-°F)	0.050	0.055		
	Kzz (Btu/hr-in.-°F)	0.199	0.195		
	Specific Heat (Btu/lbm-°F)	0.174	0.174		
	Density (lbm/in ³)	0.172	0.171		

Note: x, y, and z are in the coordinate system shown in Figure 4.4.1.2.5-1.

4.4.1.2.6 Two-Dimensional Fuel Basket Neutron Absorber Plate Model – Advanced Configuration

The two-dimensional fuel basket neutron absorber plate model is used to calculate the effective thermal properties of the region between the fuel assemblies and basket plates. This region is comprised of the neutron absorber plate and the gap between the neutron absorber plate and the basket plate. These effective thermal properties are used in the three-dimensional models (Sections 4.4.1.2.2, 4.4.1.2.3 and 4.4.1.2.4). The two-dimensional model is shown in Figure 4.4.1.2.6-1.

As shown in Figure 4.4.1.2.6-1, the neutron absorber plate model includes the gap between the neutron absorber plate and the fuel basket plate. Four conditions of media are considered in the gap: helium, vacuum and water. ANSYS PLANE55 conduction elements and LINK31 radiation elements are used to construct the model. The height of the model is defined as equal to the width of the model.

Heat flux is applied to the left side of the model, and the temperature at the right boundary of the model is constrained. The heat flux is determined based on the design heat load. The maximum steady-state temperature of the model (at the left boundary) and the temperature difference (ΔT) across the model are calculated by the ANSYS model. The effective conductivity (K_{xx}) is determined using the following formula:

$$q = K_{xx} (A/L) DT$$

or

$$K_{xx} = q L / (A DT)$$

where:

K_{xx} = effective conductivity (Btu/hr-in-°F) in X direction in Figure 4.4.1.2.6-1

q = heat rate (Btu/hr)

A = area (in²)

L = length (thickness) of model (in)

DT = temperature difference across the model (°F)

The temperature-dependent conductivity is determined by varying the temperature constraints at one boundary of the model and resolving for the heat rate (q) and temperature difference. The effective conductivity for the parallel path (the Y direction in Figure 4.4.1.2.6-1) is calculated by:

$$K_{yy} = \frac{\sum K_i t_i}{L}$$

where:

- K_i = thermal conductivity of each layer
- t_i = thickness of each layer
- L = total length (thickness) of the model

Similar to the effective thermal conductivity for the parallel path, the effective density and effective specific heat properties are calculated using volume and mass ratios, respectively. The effective thermal properties for the fuel basket neutron absorber plate are shown in Table 4.4.1.2.6-1.

Figure 4.4.1.2.6-1 Two-Dimensional Fuel Basket Neutron Absorber Plate Model – PWR Fuel – Advanced Configuration

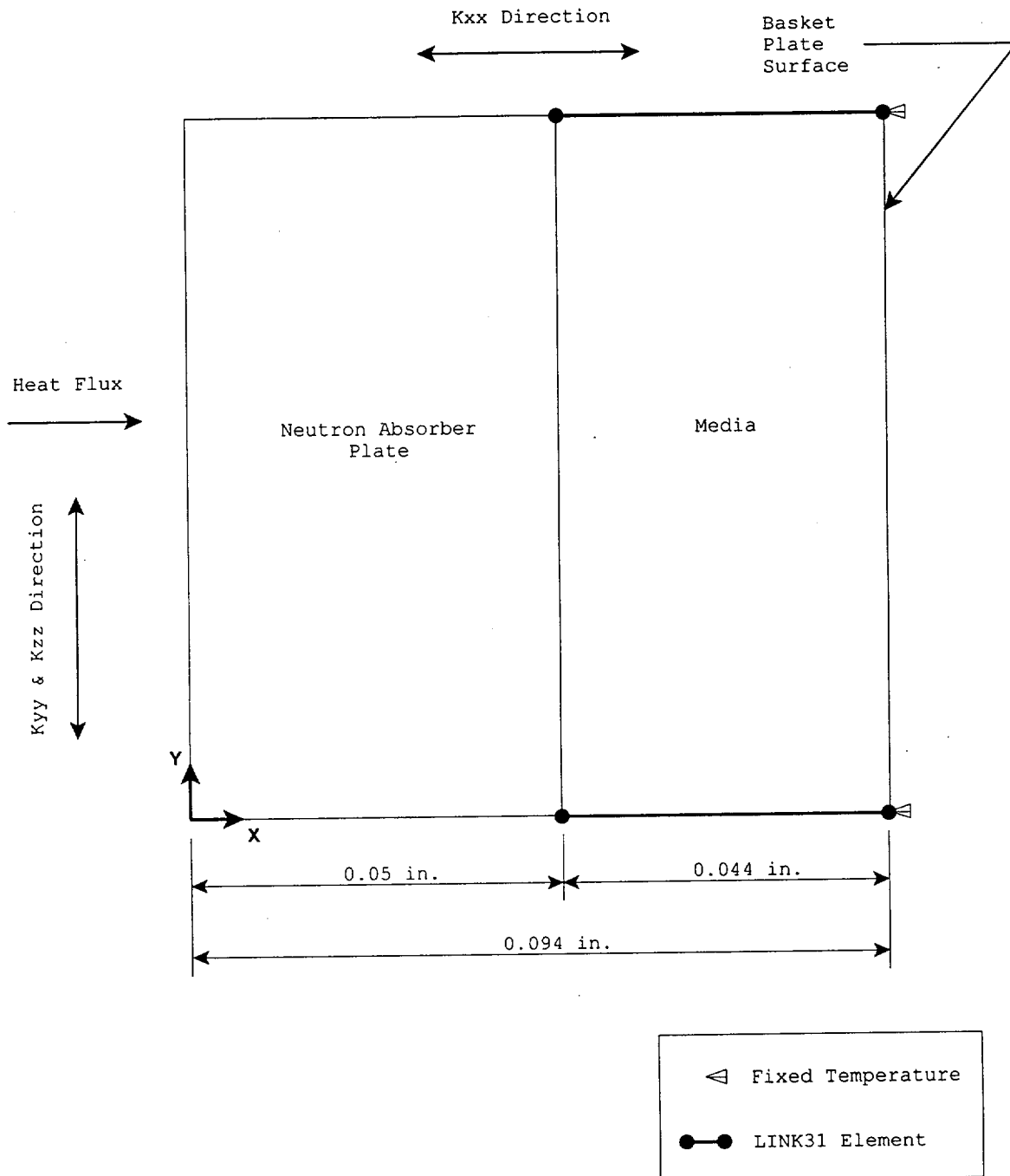


Table 4.4.1.2.6-1 Effective Thermal Properties for the Fuel Basket Neutron Absorber Plate Region –Advanced Configuration – PWR

Media	Thermal Property	Temperature (°F)			
		203	402	602	802
Helium	K _{xx} (Btu/hr-in.-°F)	0.018	0.021	0.024	0.026
	K _{yy} (Btu/hr-in.-°F)	2.334	2.412	2.447	2.447
	K _{zz} (Btu/hr-in.-°F)	2.334	2.412	2.447	2.447
	Specific Heat (Btu/lbm-°F)	0.239	0.275	0.290	0.290
	Density (lbm/in ³)	0.050	0.050	0.050	0.050
Media	Thermal Property	Temperature (°F)			
		235	402	646	828
Vacuum	K _{xx} (Btu/hr-in.-°F)	0.0002	0.0005	0.0011	0.0018
	K _{yy} (Btu/hr-in.-°F)	2.335	2.407	2.441	2.441
	K _{zz} (Btu/hr-in.-°F)	2.335	2.407	2.441	2.441
	Specific Heat (Btu/lbm-°F)	0.244	0.275	0.290	0.290
	Density (lbm/in ³)	0.050	0.050	0.050	0.050
Media	Thermal Property	Temperature (°F)			
		101		201	
Water	K _{xx} (Btu/hr-in.-°F)	0.064		0.070	
	K _{yy} (Btu/hr-in.-°F)	2.392		2.347	
	K _{zz} (Btu/hr-in.-°F)	2.392		2.347	
	Specific Heat (Btu/lbm-°F)	0.420		0.429	
	Density (lbm/in ³)	0.067		0.066	
	Density (lbm/in ³)	0.050	0.050	0.050	0.050

Note: K_{xx} is in the direction across the thickness of the neutron absorber plate and gap.
K_{yy} is in the direction parallel to the neutron absorber plate.
K_{zz} is in the canister axial direction.

4.4.1.2.7 Two-Dimensional Fuel Basket Cooling Insert Model

The two-dimensional fuel basket cooling insert model is used to calculate the effective thermal properties of the cooling inserts in the basket outer slots. This region is comprised of the cooling insert and the gap between the cooling insert and the basket plate. These effective thermal properties are used in the three-dimensional models (canister, periodic, and TFR). The two-dimensional model is shown in Figure 4.4.1.2.7-1.

As shown in Figure 4.4.1.2.7-1, the neutron absorber plate model includes the gap between the neutron absorber plate and the fuel basket plate. Additionally, a small section (0.001-inch thick) of the basket plate is modeled. Four conditions of media are considered in the gap: helium, vacuum, water, and steam. ANSYS PLANE55 conduction elements and LINK31 radiation elements are used to construct the model. The height of the model is defined as equal to the width of the model.

Heat flux is applied to the left side of the model, and the temperature at the right boundary of the model is constrained. The heat flux is determined based on the design heat load. The maximum steady-state temperature of the model (at the left boundary) and the temperature difference (ΔT) across the model are calculated by the ANSYS model. The effective conductivity (K_{xx}) is determined using the following formula:

$$q = K_{xx} (A/L) DT$$

or

$$K_{xx} = q L / (A DT)$$

where:

K_{xx} = effective conductivity (Btu/hr-in-°F) in X direction in Figure 4.4.1.2.7-1.

q = heat rate (Btu/hr)

A = area (in²)

L = length (thickness) of model (in)

DT = temperature difference across the model (°F)

The temperature-dependent conductivity is determined by varying the temperature constraints at one boundary of the model and resolving for the heat rate (q) and temperature difference. The effective conductivity for the parallel path (the Y direction in Figure 4.4.1.2.7-1) is calculated by:

$$K_{yy} = \frac{\sum K_i t_i}{L}$$

where:

K_i = thermal conductivity of each layer

t_i = thickness of each layer

L = total length (thickness) of the model

Similar to the effective thermal conductivity for the parallel path, the effective density and effective specific heat properties are calculated using volume and mass ratios, respectively. The effective thermal properties for the fuel basket cooling inserts are shown in Table 4.4.1.2.7-1.

Figure 4.4.1.2.7-1 Two-Dimensional Advanced PWR Basket Cooling Insert Model

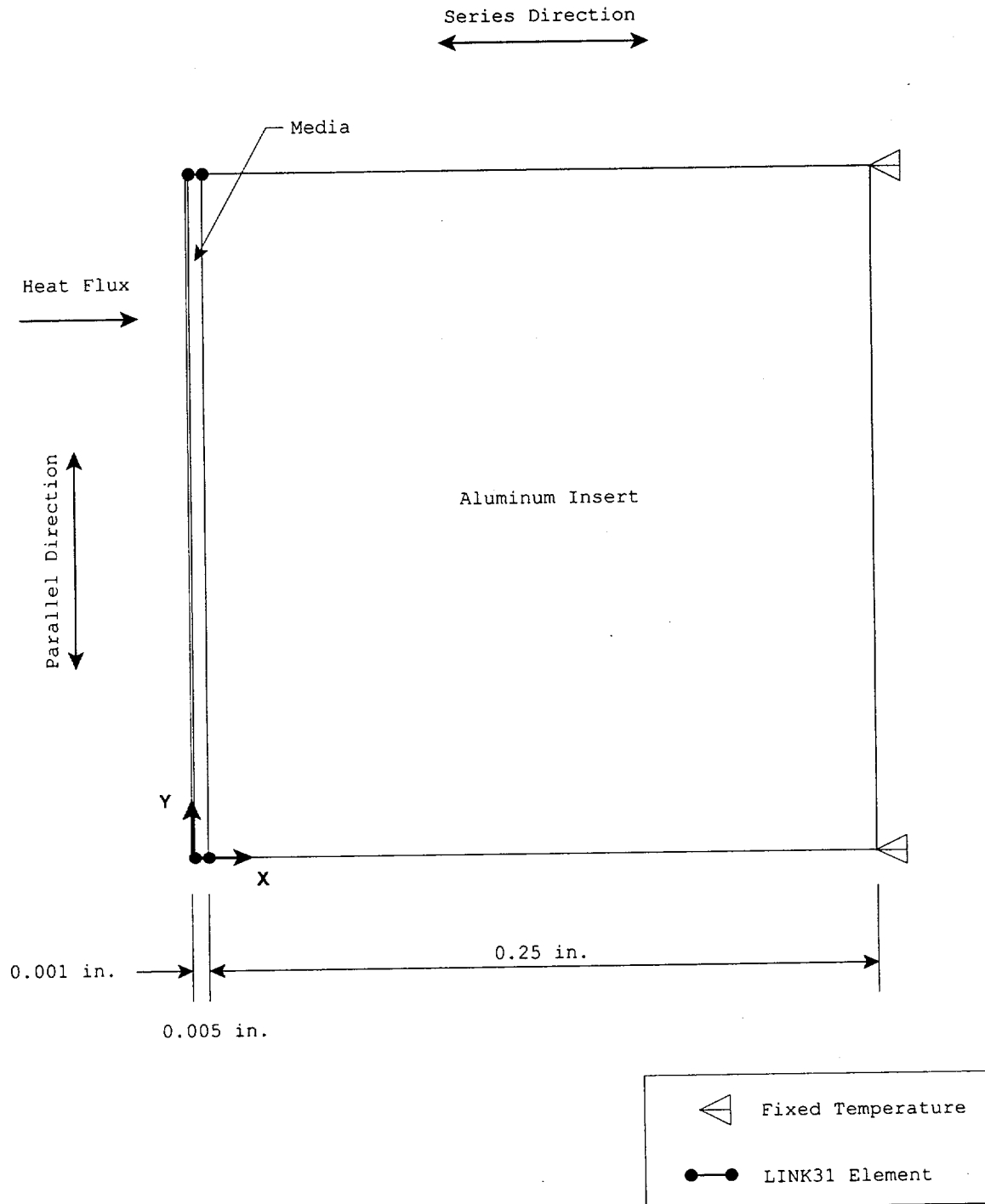


Table 4.4.1.2.7-1 Effective Thermal Properties for the Advanced PWR Basket Cooling Inserts Region

Media	Thermal Property	Temperature (°F)			
		200	400	500	700
Helium	Kxx (Btu/hr-in.-°F)	0.388	0.450	0.480	0.528
	Kyy (Btu/hr-in.-°F)	10.465	10.140	10.140	10.140
	Kzz (Btu/hr-in.-°F)	10.465	10.140	10.140	10.140
	Specific Heat (Btu/lbm-°F)	0.229	0.229	0.229	0.229
	Density (lbm/in ³)	0.097	0.097	0.097	0.097
Media	Thermal Property	Temperature (°F)			
		207	405	504	703
Vacuum	Kxx (Btu/hr-in.-°F)	0.001	0.002	0.003	0.004
	Kyy (Btu/hr-in.-°F)	10.453	10.140	10.140	10.140
	Kzz (Btu/hr-in.-°F)	10.453	10.140	10.140	10.140
	Specific Heat (Btu/lbm-°F)	0.229	0.229	0.229	0.229
	Density (lbm/in ³)	0.097	0.097	0.097	0.097
Media	Thermal Property	Temperature (°F)			
		100	200		
Water	Kxx (Btu/hr-in.-°F)	1.307	1.418		
	Kyy (Btu/hr-in.-°F)	10.734	10.466		
	Kzz (Btu/hr-in.-°F)	10.734	10.466		
	Specific Heat (Btu/lbm-°F)	0.234	0.234		
	Density (lbm/in ³)	0.098	0.097		
Media	Thermal Property	Temperature (°F)			
		200	400		
Steam	Kxx (Btu/hr-in.-°F)	0.060	0.084		
	Kyy (Btu/hr-in.-°F)	10.465	10.140		
	Kzz (Btu/hr-in.-°F)	10.465	10.140		
	Specific Heat (Btu/lbm-°F)	0.229	0.229		
	Density (lbm/in ³)	0.097	0.097		

Note: Kxx is in the direction across the thickness of the cooling insert plate and gap (series).
Kyy is in the direction parallel to the cooling insert plate (parallel).
Kzz is in the canister axial direction (parallel).

4.4.2 Test Model

The Universal Storage System is conservatively designed by analysis. Therefore, no physical model is employed for thermal analysis.

THIS PAGE INTENTIONALLY LEFT BLANK

4.4.3 Maximum Temperatures for PWR and BWR Fuel

4.4.3.1 Maximum Temperatures for the Standard Configuration

Temperature distribution and maximum component temperatures for the Universal Storage System Standard configuration under the normal conditions of storage and transfer are provided in this section. System components containing PWR and BWR fuels are addressed separately. Temperature distributions for the evaluated off-normal and accident conditions are presented in Sections 11.1 and 11.2.

Figure 4.4.3.1-1 shows the temperature distribution of the Standard Vertical Concrete Cask and the canister containing the PWR design basis fuel for the normal, long-term storage condition. The air flow pattern and air temperatures in the annulus between the PWR canister and the concrete cask liner for the normal condition of storage are shown in Figures 4.4.3.1-2 and 4.4.3.1-3, respectively. The temperature distribution in the concrete portion of the Standard concrete cask for the PWR assembly is shown in Figure 4.4.3.1-4. The temperature distribution for the BWR design basis fuel is similar to that of the PWR fuel and is, therefore, not presented. Table 4.4.3.1-1 shows the maximum component temperatures for the normal condition of storage for the PWR design basis fuel. The maximum component temperatures for the normal condition of storage for the BWR design basis fuel are shown in Table 4.4.3.1-2.

As shown in Figure 4.4.3.1-3, a high-temperature gradient exists near the wall of the canister and the liner of the concrete cask, while the air in the center of the annulus exhibits a much lower temperature gradient, indicating significant boundary layer features of the air flow. The temperatures at the concrete cask steel liner surface are higher than the air temperature, which indicates that salient radiation heat transfer occurs across the annulus. As shown in Figure 4.4.3.1-4, the local temperature in the concrete, directly affected by the radiation heat transfer across the annulus, can reach 186°F (less than the 300°F allowable temperature). The bulk temperature in the concrete, as determined using volume average of the temperatures in the concrete region, is 135°F, less than the allowable value of 150°F.

Under typical operations, the transient history of maximum component temperatures for the transfer conditions (Standard canister, inside the transfer cask, containing water for 17 hours, vacuum for 10 hours and helium for 16 hours for PWR fuel and for 24 hours for BWR fuel) is shown in Figures 4.4.3.1-5 and 4.4.3.1-6 for PWR and BWR fuels, respectively. The maximum

component temperatures for the transfer conditions (vacuum and helium conditions) are shown in Tables 4.4.3.1-3 and 4.4.3.1-4, for PWR and BWR fuels, respectively. The maximum calculated water temperature is 195°F and 204°F for PWR and BWR fuels, respectively, at the end of 17 hours based on an initial water temperature of 100°F. For the maximum temperatures shown in Tables 4.4.3.1-3 and 4.4.3.1-4 for the transfer conditions of vacuum and helium, the maximum basket temperatures (support disk and aluminum disk) are conservatively determined by using the maximum temperature in the canister content region of the two-dimensional axisymmetric transfer cask and canister models.

Maximum Temperatures at Reduced Total Heat Loads for the Standard Configuration

This section provides the evaluation of component temperatures for PWR fuel heat loads less than the design basis heat load of 23 kW. Transient thermal analyses are performed for heat loads of 20, 17.6, 14, 11 and 8 kW to establish the allowable time limits for the vacuum and helium conditions in the canister as described in the Technical Specifications (Chapter 12) for the Limiting Conditions of Operation (LCO), LCOs 3.1.1 and 3.1.4. These LCOs control the length of time that the loaded canister in the transfer cask can remain in a vacuum condition and the length of time the loaded canister can remain in the transfer cask after being filled with helium. The time limits ensure that the allowable temperatures of the limiting components – the heat transfer disks and the fuel cladding - are not exceeded. A steady state evaluation is also performed for heat loads of 14, 11 and 8 kW in the helium condition. If the steady state temperature calculated is less than the limiting component allowable temperature, then the allowable time duration in the helium condition is not limited.

The three-dimensional Standard transfer cask and canister model for the PWR fuel configuration, described in Section 4.4.1.1.8, is used for the transient and steady state thermal analysis for the reduced heat load cases. To obtain the bounding temperatures for all possible loading configurations, thermal analyses are performed for a total of fourteen (14) cases as tabulated below. The basket locations are shown in Figure 4.4.3.1-7. Since the maximum temperature for the limiting components (fuel cladding and heat transfer disk) always occurs at the central region of the basket, hotter fuels (maximum allowable heat load for 5-year cooled fuel: 0.958 kW = 23 kW/24) are specified at the central basket locations. The bounding cases for each heat load

condition are noted with an asterisk (*) in the tabulation which follows. Six cases (cases 3 through 8) are evaluated for the 17.6 kW heat load condition. The first four cases (cases 3 through 6) represent standard UMS system fuel loadings. The remaining two cases (cases 7 and 8) account for the preferential loading configuration for Maine Yankee site specific high burnup fuel (Section 4.5.1.2.2), with case 8 being the bounding case for the Maine Yankee high burnup fuel. Based on the analysis results of the 17.6 kW heat load cases, only two loading cases are required to establish the bounding condition for the 20, 14, 11 and 8 kW heat loads.

Canister Heat Load (kW)	Heat Load Case	Heat Load (kW) Evaluated in Each Basket Location (See Figure 4.4.3.1-7)					
		1	2	3	4	5	6
20	1	0.958	0.958	0.709	0.958	0.709	0.709
20*	2	0.958	0.958	0.958	0.958	0.958	0.210
17.6	3	0.958	0.958	0.509	0.958	0.509	0.509
17.6*	4	0.958	0.958	0.568	0.958	0.958	0.000
17.6	5	0.958	0.958	0.958	0.958	0.568	0.000
17.6	6	0.958	0.958	0.284	0.958	0.958	0.284
17.6	7	0.958	0.146	1.050	0.146	1.050	1.050
17.6	8	0.958	0.958	1.050	0.384	1.050	0.000
14	9	0.958	0.958	0.209	0.958	0.209	0.209
14*	10	0.958	0.958	0.000	0.958	0.626	0.000
11	11	0.958	0.896	0.000	0.896	0.000	0.000
11*	12	0.958	0.958	0.000	0.834	0.000	0.000
8	13	0.958	0.521	0.000	0.521	0.000	0.000
8*	14	0.958	0.958	0.000	0.084	0.000	0.000

The heat load (23 kW/24 Assemblies = 0.958 kW) at the four (4) central basket locations corresponds to the maximum allowable canister heat load for 5-year cooled fuel (Table 4.4.7.1-8). The non-uniform heat loads evaluated in this section bound the equivalent uniform heat loads, since they result in higher maximum temperatures of the fuel cladding and heat transfer disk.

Volumetric heat generation (Btu/hr-in³) is applied to the active fuel region in each fuel assembly location of the model using the axial power distribution for PWR fuel (Figure 4.4.1.1.1-3) in the axial direction.

The thermal analysis results for the closure and transfer of a loaded PWR fuel canister in the transfer cask for the reduced heat load cases are shown in Table 4.4.3.1-5. The temperatures shown are the maximum temperatures for the limiting components (fuel cladding and heat transfer disk). The maximum temperatures of the fuel cladding and the heat transfer disk are less

than the allowable temperatures (Table 4.1-3) of these components for the short-term conditions of vacuum drying and helium backfill. As shown in Table 4.4.3.1-5, there is no time limit for movement of the canister out of the transfer cask for the cases with a heat load less than 14 kW, after the canister is filled with helium. For heat loads equal to or less than 14 kW, the maximum fuel cladding/heat transfer disk temperatures for the steady state condition are well below the short term allowable temperatures of the fuel cladding and the heat transfer disk. Note that the maximum water temperature at the end of the "water period" is considered to be the volumetric average temperature of the calculated cladding temperatures in the active fuel region of the hottest fuel assembly. The results indicate that the volumetric average water temperature is below 212°F for all cases evaluated. This is consistent with the thermal model that only considers conduction in the fuel assembly region and between the disks. This approach does not include consideration of convection of the water or the energy absorbed by latent heat of vaporization.

The Technical Specifications specify the remedial actions, either in-pool or forced air cooling, required to ensure that the fuel cladding and basket component temperatures do not exceed their short-term allowable temperatures, if the time limits are not met. LCOs 3.1.1 and 3.1.4 incorporate the operating times for heat loads that are less than the design basis heat loads as evaluated in this section.

Using the same three-dimensional transfer cask/canister model, analysis is performed for the conditions of in-pool cooling followed by the vacuum drying and helium backfill operation (LCO 3.1.1). The condition at the end of the vacuum drying as shown in Table 4.4.3.1-5 is used as the initial condition of the analysis. The LCO 3.1.1 "Action" analysis results are shown in Table 4.4.3.1-6. The maximum temperatures for the fuel cladding and the heat transfer disk are below the short-term allowable temperatures.

The in-pool cooling followed by the helium backfill operation in LCO 3.1.4 is also evaluated. The condition at the end of the helium condition as shown in Table 4.4.3.1-5 is used as the initial condition. Based on the in-pool cooling analysis for LCO 3.1.1, the minimum temperature reduction due to in-pool cooling is 216°F (706-490) for the 20 kW heat load case. The evaluation for LCO 3.1.4 in-pool cooling conservatively considers a temperature reduction of 150°F for in-pool cooling and a heat up rate of 6°F/hour (helium condition) for an additional 16 hours and 20 hours for 20 kW and 17.6 kW heat load cases, respectively. The maximum fuel temperature and heat transfer disk temperatures at the end of the helium condition for the governing case of 17.6 kW are determined to be 668°F $((698-150)+(20\times 6))$ and 612°F $((642-150)+(20\times 6))$, respectively, which are well below the short-term allowable temperatures.

Figure 4.4.3.1-1 Temperature Distribution (°F) for the Normal Storage Condition:
PWR Fuel – Standard Configuration

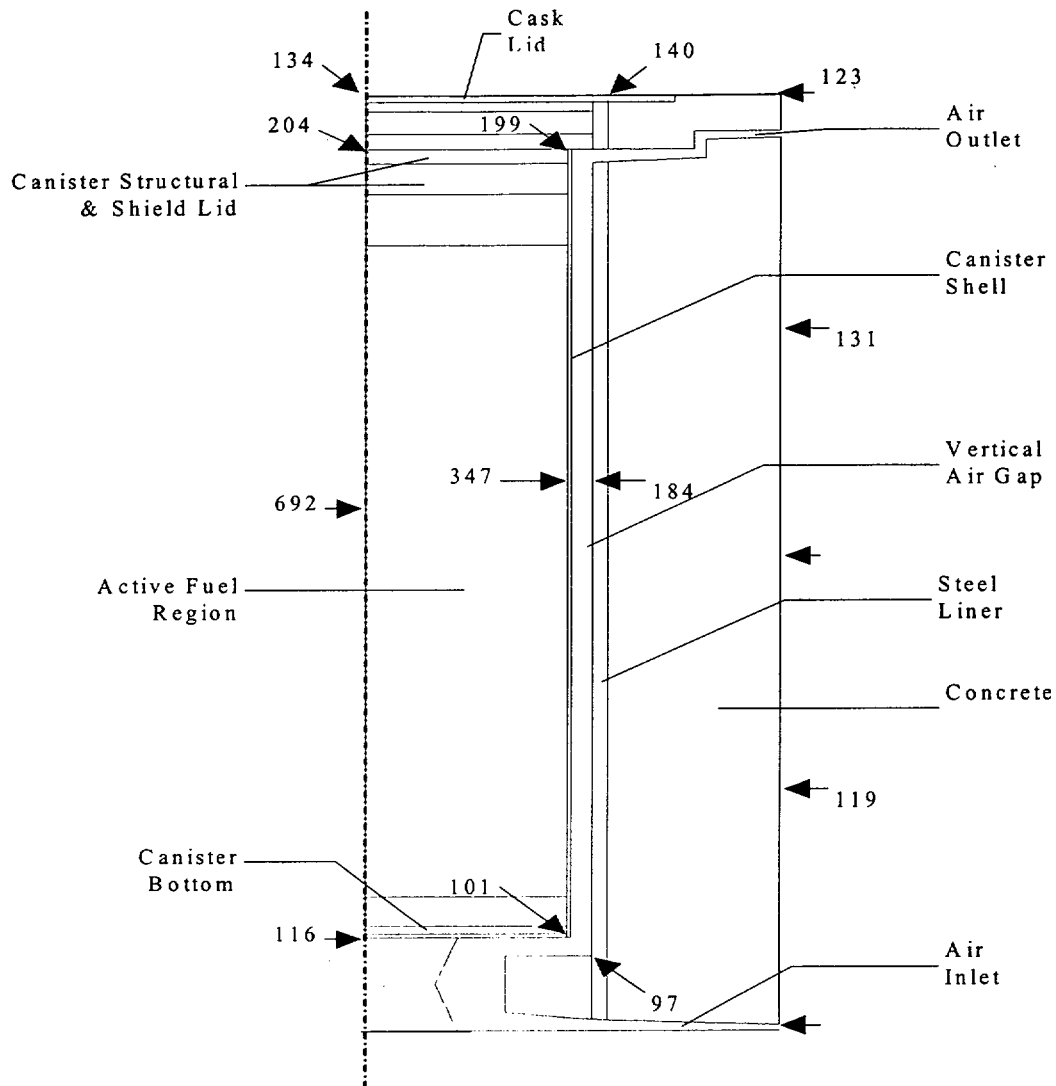


Figure 4.4.3.1-2 Air Flow Pattern in the Concrete Cask in the Normal Storage Condition:
PWR Fuel – Standard Configuration

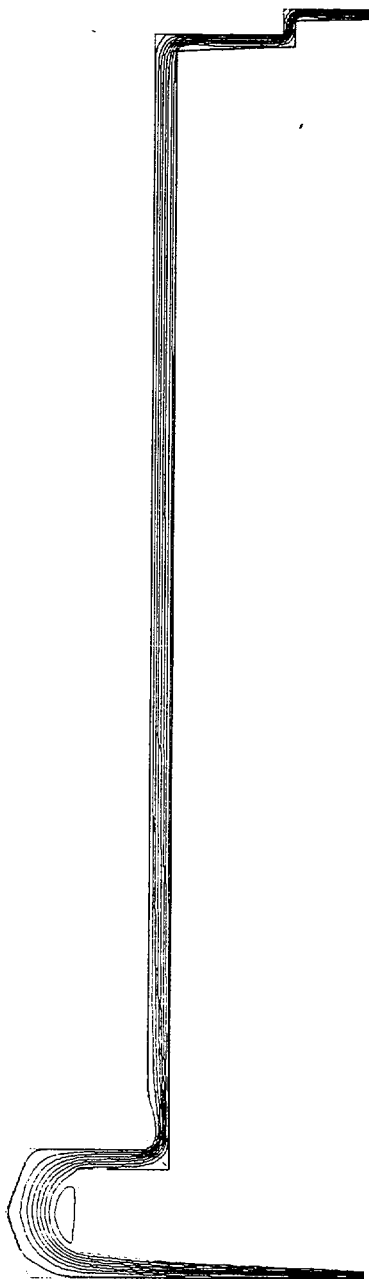


Figure 4.4.3.1-3 Air Temperature (°F) Distribution in the Concrete Cask During the Normal Storage Condition: PWR Fuel – Standard Configuration

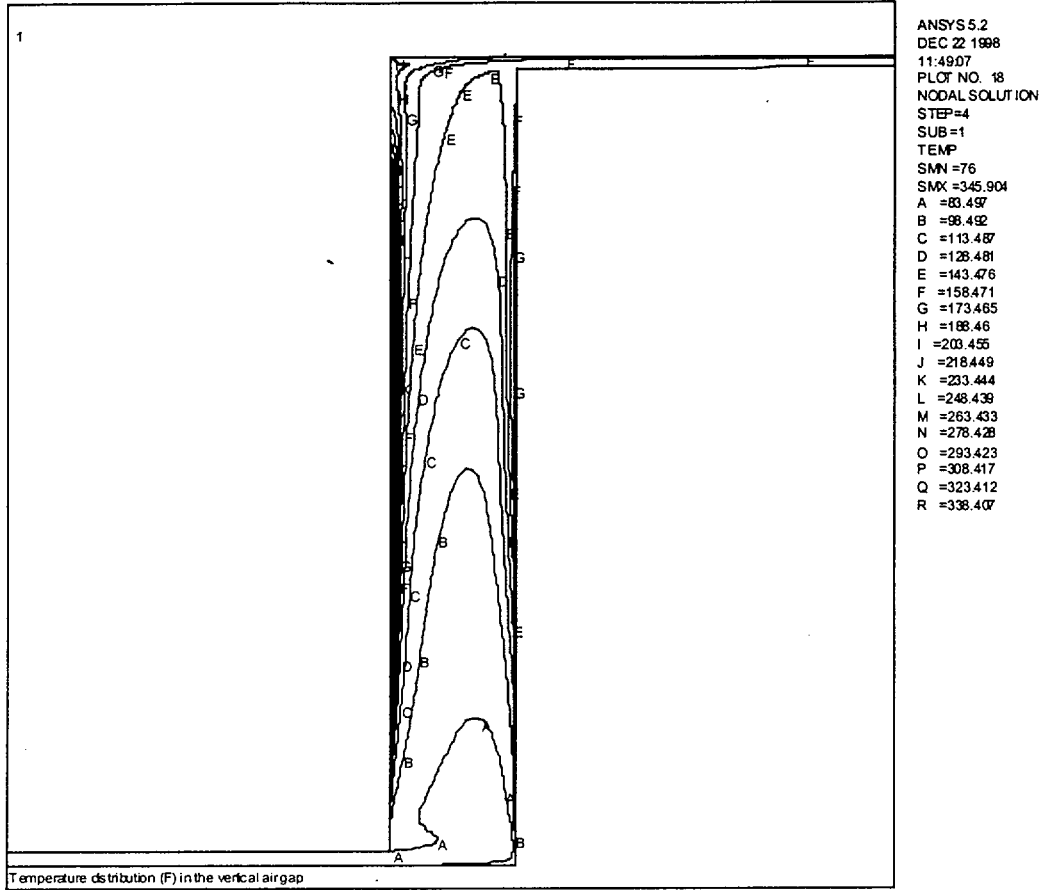


Figure 4.4.3.1-4 Concrete Temperature (°F) Distribution During the Normal Storage
Condition: PWR Fuel – Standard Configuration

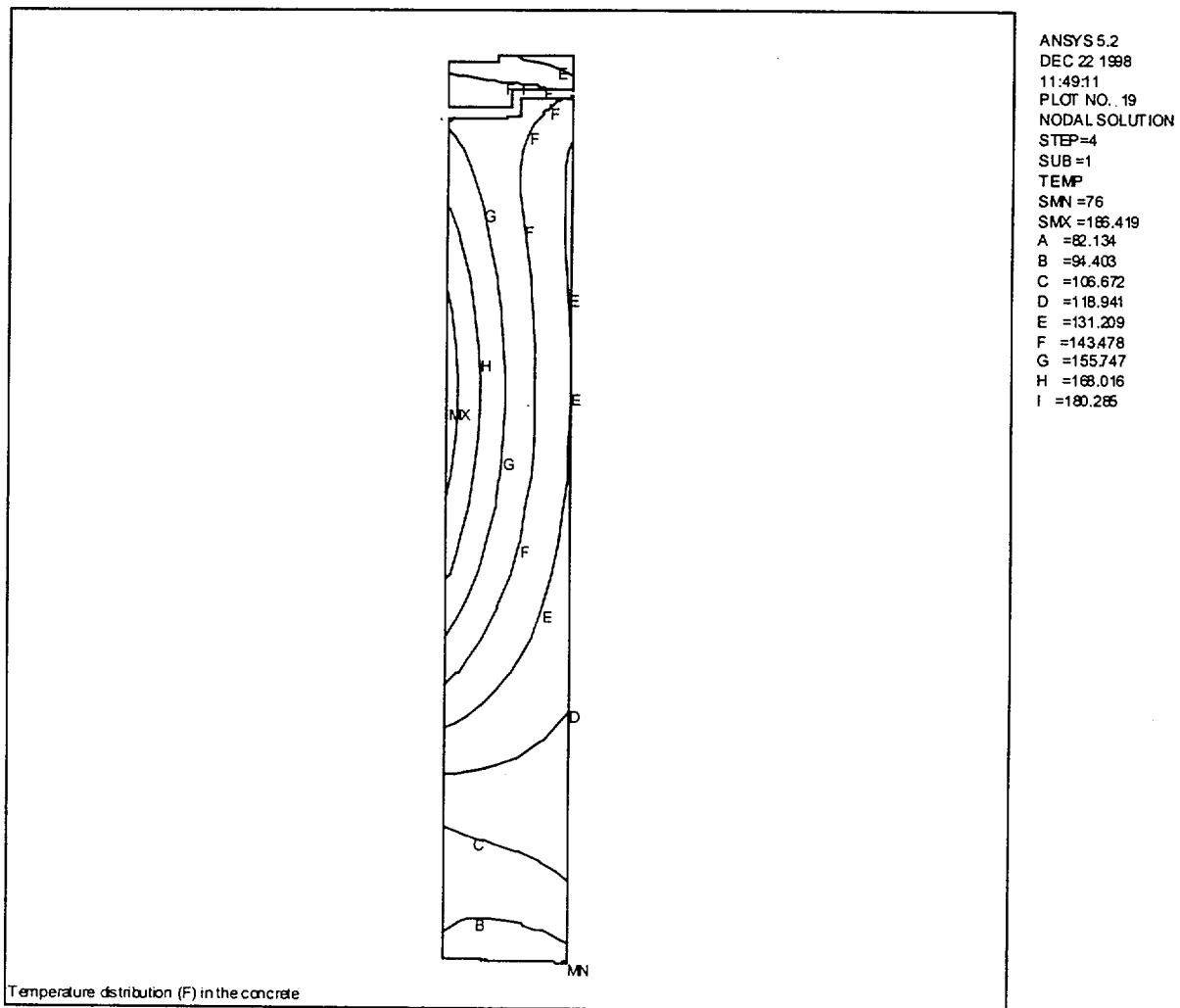
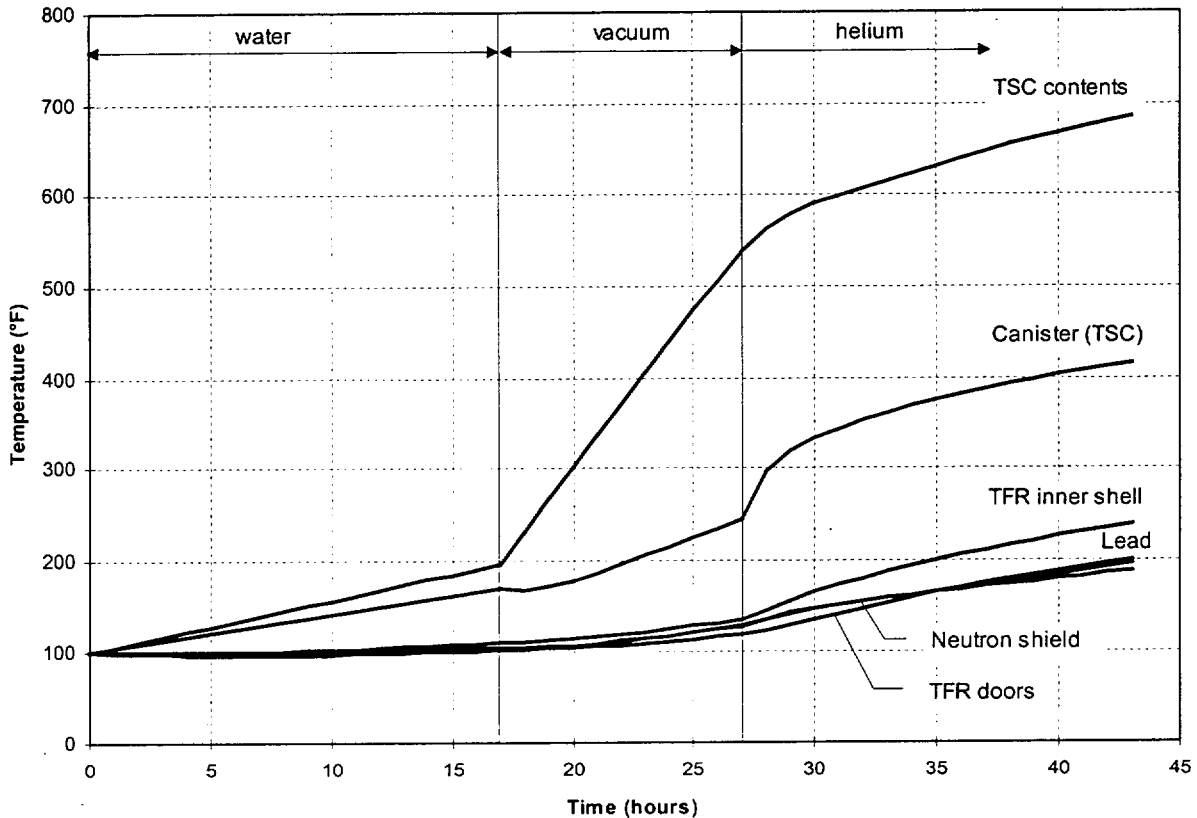


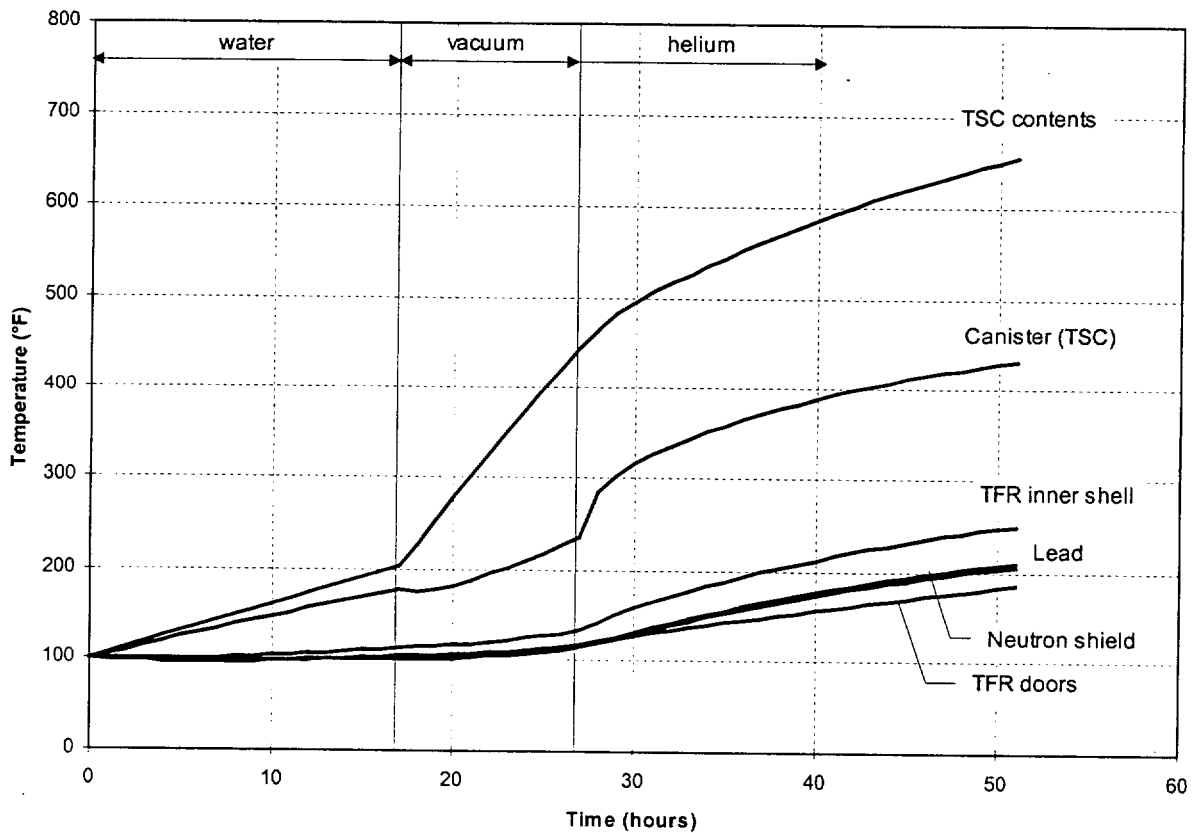
Figure 4.4.3.1-5 History of Maximum Component Temperature (°F) for Transfer Conditions for PWR Fuel with Design Basis 23 kW Uniformly Distributed Heat Load – Standard Configuration



Notes:

1. This graph corresponds to a canister containing water for 17 hours, vacuum for 10 hours and helium for 16 hours – normal operations, with a uniformly distributed decay heat load of 23 kW.
2. The temperature of “TSC contents” represents the maximum fuel cladding temperature. The maximum basket component (heat transfer disk and support disk) temperatures are conservatively assumed to be the same as the maximum fuel cladding temperature (see Table 4.4.3.1-3).

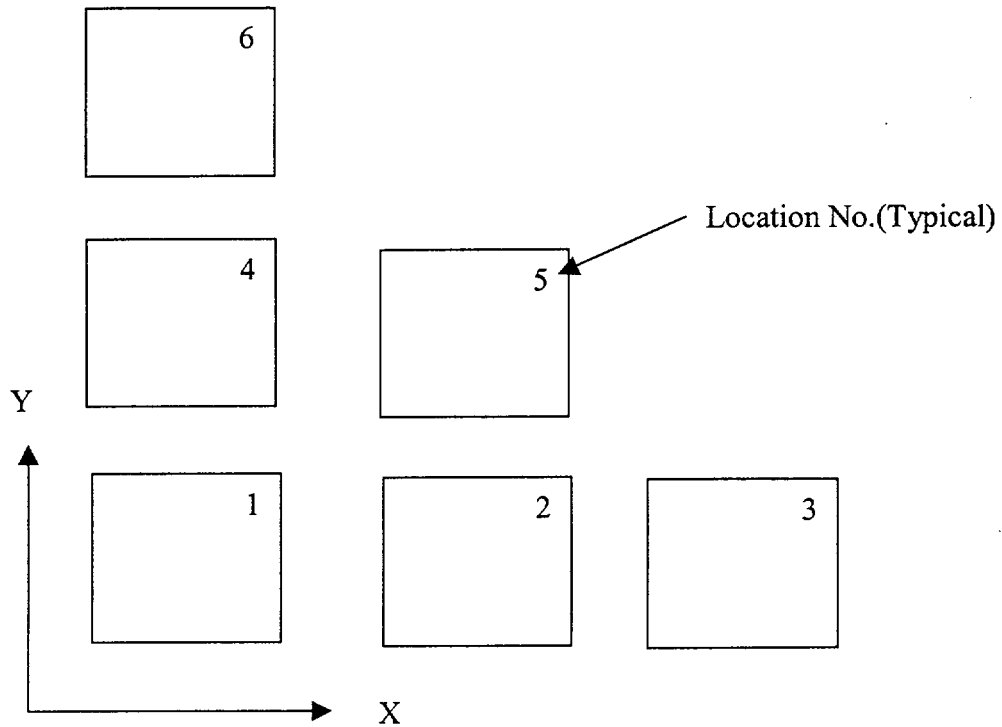
Figure 4.4.3.1-6 History of Maximum Component Temperature (°F) for Transfer Conditions for BWR Fuel with Design Basis 23 kW Uniformly Distributed Heat Load – Standard Configuration



Notes:

1. This graph corresponds to a canister containing water for 17 hours, vacuum for 10 hours and helium for 24 hours – normal operations, with a decay heat load of 23 kW.
2. The temperature of “TSC contents” represents the maximum fuel cladding temperature. The maximum basket component (heat transfer disk and support disk) temperatures are conservatively assumed to be the same as the maximum fuel cladding temperature (see Table 4.4.3.1-4).

Figure 4.4.3.1-7 Basket Location for the Thermal Analysis for Reduced Heat Load Cases – Standard Configuration



Basket locations correspond to the quarter symmetry model (Figure 4.4.1.1.8-1). X and Y axes are at the centerlines of the basket.

Table 4.4.3.1-1 Maximum Component Temperatures for the Normal Storage Condition – Standard Configuration – PWR

Component	Maximum Temperature (°F)	Allowable Temperatures (°F)
Fuel Cladding	670	716
Heat Transfer Disk	612	650
Support Disk	615	650
Top Weldment	419	800
Bottom Weldment	151	800
Canister Shell	351	800
Canister Structural Lid	212	800
Canister Shield Lid	202	800
Concrete	186 (local) 135 (bulk*)	300 (local) 150 (bulk)

* The volume average temperature of the concrete region is used as the bulk concrete temperature.

Table 4.4.3.1-2 Maximum Component Temperatures for the Normal Storage Condition – Standard Configuration – BWR

Component	Maximum Temperature (°F)	Allowable Temperatures (°F)
Fuel Cladding	651	716
Heat Transfer Disk	622	650
Support Disk	624	700
Top Weldment	360	800
Bottom Weldment	272	800
Canister Shell	376	800
Canister Structural Lid	212	800
Canister Shield Lid	202	800
Concrete	192 (local) 136 (bulk*)	300 (local) 150 (bulk)

*The volume average temperature of the concrete region is used as the bulk concrete temperature.

Table 4.4.3.1-3 Maximum Component Temperatures for the Transfer Condition – PWR Fuel with Design Basis 23 kW Uniformly Distributed Heat Load – Standard Configuration

Component	Maximum Temperature (°F)		Allowable Temperature (°F)
	Vacuum	Helium	
Fuel	538	686	1058
Lead	119	199	600
Neutron Shield	128	195	300
Heat Transfer Disk	538 ²	686 ²	700
Support Disk	538 ²	686 ²	800
Canister	244	416	800
Transfer Cask Shells	136	237	700

- 1 Maximum temperatures at the end of 10 hours vacuum condition and 16 hours helium condition, respectively (see Figure 4.4.3.1-5).
- 2 Conservatively, the maximum fuel cladding temperature is used.

Table 4.4.3.1-4 Maximum Component Temperatures for the Transfer Condition – BWR Fuel with Design Basis 23 kW Uniformly Distributed Heat Load – Standard Configuration

Component	Maximum Temperature (°F)		Allowable Temperature (°F)
	Vacuum ¹	Helium ¹	
Fuel	447	654	1,058
Lead	117	210	600
Neutron Shield	116	206	300
Heat Transfer Disk	447 ²	654 ²	700
Support Disk	447 ²	654 ²	700
Canister	235	432	800
Transfer Cask Shells	133	251	700

- 1 Maximum temperatures at the end of 10 hours vacuum condition and 24 hours helium condition, respectively (see Figure 4.4.3.1-6).
- 2 Conservatively, the maximum fuel cladding temperature is used.

Table 4.4.3.1-5 Maximum Limiting Component Temperatures in Transient Operations for the Reduced Heat Load Cases for PWR Fuel – Standard Configuration

Canister Total Heat Load (kW)	Water			Vacuum			Helium		
	Duration (hours)	Maximum Temperature (°F)		Duration (hours)	Maximum Temperature (°F)		Duration (hours)	Max. Temp./ Temp. at End of Duration (°F)	
		Fuel	Heat Transfer Disk		Fuel	Heat Transfer Disk		Fuel	Heat Transfer Disk
20	18	233	210	15	707	547	20	707/705 ¹	651/651 ¹
17.6	20	240	215	19	760	587	48	760/698 ¹	674/642 ¹
17.6 ³	20	233	210	19	761	575	48	761/683 ¹	658/625 ¹
14	22	242	216	23	776	577	No Limit ²	776/645 ²	676/583 ²
11	24	239	212	30	792	569	No Limit ²	792/586 ²	673/518 ²
8	26	226	198	34	758	489	No Limit ²	758/509 ²	602/431 ²

Notes:

1. Temperature at the end of helium duration.
2. Based on the steady state analysis performed for the 14 kW, 11 kW and 8 kW cases for the helium condition, the maximum calculated steady state fuel cladding temperatures are 645°F, 586°F and 509°F, respectively. The maximum calculated steady state heat transfer disk temperatures are 583°F, 518°F and 431°F, respectively. Since these temperatures are well below the allowable material temperatures, there is no time limit for the helium condition for these load cases.
3. Bounding case for the Maine Yankee Site Specific high burnup fuel.

Table 4.4.3.1-6 Maximum Limiting Component Temperatures in Transient Operations for the Reduced Heat Load Cases for PWR Fuel after In-Pool Cooling – Standard Configuration

Canister Total Heat Load (kW)	Helium (In-Pool)			Vacuum			Helium		
	Duration (hours)	Temperature at End of Duration in Pool (°F)		Duration (hours)	Maximum Temperature (°F)		Duration (hours)	Max. Temp./ Temp. at End of Duration (°F)	
		Fuel	Heat Transfer Disk		Fuel	Heat Transfer Disk		Fuel	Heat Transfer Disk
20	24	490	407	10	714	543	20	714/703 ¹	650/650 ¹
17.6	24	478	392	10	700	509	48	700/693 ¹	637/637 ¹
14	24	456	365	14	731	521	No Limit ²	731/645 ²	622/583 ²
11	24	431	337	14	706	465	No Limit ²	706/586 ²	577/518 ²
8	24	391	296	14	675	390	No Limit ²	675/509 ²	509/431 ²

Notes:

1. Temperature at the end of helium duration.
2. Based on the steady state analysis performed for the 14 kW, 11 kW and 8 kW cases for the helium condition, the maximum calculated steady state fuel cladding temperatures are 645°F, 586°F and 509°F, respectively. The maximum calculated steady state heat transfer disk temperatures are 583°F, 518°F and 431°F, respectively. Since these temperatures are well below the allowable material temperatures, there is no time limit for the helium condition for these load cases.

4.4.3.2 Maximum Temperatures for the Advanced Configuration

Temperature distribution and maximum component temperatures for the Advanced Configuration of the Universal Storage System under the normal conditions of storage and transfer conditions are provided in this section. Temperature distributions for the evaluated off-normal and accident conditions are presented in Sections 11.1 and 11.2.

Figure 4.4.3.2-1 shows the temperature distribution of the Advanced Vertical Concrete Cask and the canister containing the PWR design basis fuel for the normal, long-term storage condition. Contour plots of velocity magnitude in the air annulus are shown in Figures 4.4.3.2-2 and 4.4.3.2-3. A contour plot of temperature distribution in the Advanced Vertical Concrete Cask is shown in Figure 4.4.3.2-4. Table 4.4.3.2-1 shows the maximum component temperatures for the normal condition of storage for the PWR design basis fuel. The local maximum temperature in the concrete, directly affected by the radiation heat transfer across the annulus, does not reach the maximum allowable temperature of 300°F. The bulk temperature in the concrete, as determined using volume average of the temperatures in the concrete region, is 138°F, less than the allowable value of 150°F. The maximum temperatures for all components are well below their allowable temperatures.

Transfer Conditions

Using the three-dimensional transfer cask and canister model described in Section 4.4.1.2.3, the transient temperature distribution of the loaded transfer cask (containing PWR fuel in the Advanced configuration) is determined using ANSYS 5.5 for the design heat load of 29.2 kW (see Figure 4.4.1.2.2-3 for the preferential loading pattern for the design heat load) for a typical transfer operation. During the water stage of the transfer condition, the duration is established such that the water remains below the boiling temperature of water (212°F). During the vacuum and helium stages of the transfer condition, the durations are established such that all components remain below their allowable temperatures. The following transfer condition times are established for a typical transfer operation for the Advanced configuration design heat load of 29.2 kW:

1. 17 hours for the drain operation
2. 44 hours for the vacuum and drying operation
3. 30 hours for the helium condition which includes the helium backfill process and the period of time until the canister is placed into the vertical concrete cask for storage.

The temperature history for the design heat load of 29.2 kW is presented in Figure 4.4.3.2-5, and the maximum component temperatures for the vacuum and helium stages are presented in Table 4.4.3.2-2.

If the time limits of the LCO 3.1.1 for the vacuum drying process are not met, the Technical Specifications require that either in-pool or forced air cooling be initiated and maintained for a minimum of 24 hours (or 48 hours as required) to ensure that the fuel cladding and basket component temperatures do not exceed their short-term allowable temperatures.

Using the three-dimensional transfer cask and canister model described in Section 4.4.1.2.3, a transient thermal analysis is performed to simulate the 24-hour in-pool cooling procedure following the 44-hour vacuum and drying stage for normal transfer conditions. The maximum fuel cladding and basket component temperatures are calculated for the end of this 24-hour in-pool cooling period to determine the additional vacuum and drying duration allowed following this remedial action. During the in-pool cooling, the canister atmosphere is modeled as helium, and the surface temperatures of the canister shell and transfer cask are considered to be 100°F. At the end of the 24-hour in-pool cooling period, the maximum temperature of the fuel cladding is 584°F, and the maximum temperature of the basket plates is 559°F. A time limit for the vacuum and drying operation is then established by interpolating where these temperatures fall on the vacuum operations heat-up curve for normal transfer conditions. The established time limits for the transfer operation with in-pool cooling are presented in Table 4.4.3.2-3. The maximum component temperatures for this condition are presented in Table 4.4.3.2-4.

Using the three-dimensional transfer cask and canister model described in Section 4.4.1.2.3, a transient thermal analysis is performed to simulate the 48-hour forced air cooling procedure following the 44-hour vacuum and drying stage for normal transfer conditions. The maximum fuel cladding and basket component temperatures are calculated for the end of this 48-hour forced air cooling period to determine the additional vacuum and drying duration allowed following this remedial action. During the forced air cooling, the canister atmosphere is modeled as helium. During the 48-hour forced air cooling period, a convection boundary condition is applied to the vertical surfaces of the canister shell and the transfer cask inner shell using the following correlation for flow past a flat plate (Guyer):

$$h = \frac{Nu \times k}{L_c}$$

where:

$$\text{Nu (Average Nusselt Number)} = 0.664 \text{Re}^{0.5} \text{Pr}^{1/3}, \text{ for } \text{Pr} \geq 0.6, \text{Re} < 5 \times 10^5$$

$$\text{Nu} = 0.036(\text{Re}^{0.8} - 9200) \times \text{Pr}^{0.43} \left(\frac{\mu_{\infty}}{\mu_w} \right)^{0.25}, \text{ for } \text{Pr} > 0.6, 5 \times 10^5 < \text{Re} < 10^7$$

$$\text{Re (Reynolds Number)} = \frac{\rho V_c L_c}{\mu}$$

k = thermal conductivity of air evaluated at the film temperature

L_c = the characteristic length of the flat plate

Pr = the Prandtl number of air evaluated at the film temperature

μ_{∞} = the viscosity of air evaluated at the bulk temperature (75°F)

μ_w = the viscosity of air evaluated at the surface temperature

μ = the viscosity of air evaluated at the film temperature

ρ = the density of air evaluated at the film temperature

V_c = the velocity of the air flow (9.4 ft/sec based on 375 CFM).

At the end of the 48-hour forced air cooling period, the maximum temperature of the fuel cladding is 675°F, and the maximum temperature of the basket plates is 658°F. A time limit for the vacuum and drying operation is then established by interpolating where these temperatures fall on the vacuum curve for normal transfer conditions. The established time limits for the transfer operation with forced air cooling following vacuum drying are presented in Table 4.4.3.2-5. The maximum component temperatures for this condition are presented in Table 4.4.3.2-6.

Additionally, if the time limits of LCO 3.1.4 for the helium backfill process are not met (i.e., the helium backfill process is complete, but the canister cannot be loaded into the concrete cask within the specified time), the Technical Specifications require that either in-pool or forced air cooling be initiated and maintained for a minimum of 24 hours (or 48 hours as required) to ensure that the fuel cladding and basket component temperatures do not exceed their short-term allowable limits. Using the same methodology described for in-pool/forced air cooling following vacuum drying, the established time limits for the transfer operation with in-pool cooling following helium backfill are presented in Table 4.4.3.2-7. The maximum component temperatures for this condition are presented in Table 4.4.3.2-8. The established time limits for the transfer operation with forced air cooling following helium backfill and hold are presented in

Table 4.4.3.2-9. The maximum component temperatures for this condition are presented in Table 4.4.3.2-10.

Maximum Temperatures at Reduced Total Heat Loads for the Advanced Configuration

This section provides the evaluation of component temperatures for the Advanced transfer cask components for Advanced canister heat loads less than the design heat load of 29.2 kW. Transient and steady-state analyses are performed on the three-dimensional transfer cask and canister model described in Section 4.4.1.2.3 for canister heat loads totaling 27, 25, 22, 18, and 14 kW. The fuel assembly heat loads are grouped into four zones (A, B, C, and D—see Figure 4.4.3.2-6) with varying heat loads per preferential loading zone as shown in Table 4.4.3.2-11.

Using the methodology previously described for the design basis heat load case, the time limits for each stage of the normal transfer condition are established for the reduced heat loads. These established time limits are presented in Table 4.4.3.2-12. If the maximum component temperatures for steady-state conditions are below the allowable temperatures, the stage has no limit on duration. Additionally, the maximum temperatures of the fuel cladding and basket plates for the reduced heat loads for normal transfer conditions are presented in Table 4.4.3.2-13, with a comparison to the results for the design heat load case.

If the time limits of the LCO 3.1.8 for the vacuum drying process are not met, the Technical Specifications require that either in-pool or forced air cooling be initiated and maintained for a minimum of 24 hours (or 48 hours as required) to ensure that the fuel cladding and basket component temperatures do not exceed their short-term allowable temperatures.

The time limits for the vacuum drying and helium backfill stages following the in-pool cooling stage are established and presented in Table 4.4.3.2-14. The maximum temperatures of the fuel cladding and basket plates for this condition are shown in Table 4.4.3.2-15.

The time limits for the vacuum drying and helium backfill stages following the forced air cooling stage are established and presented in Table 4.4.3.2-16. The maximum temperatures of the fuel cladding and basket plates for this condition are shown in Table 4.4.3.2-17.

If the time limits of LCO 3.1.9 for the maximum time in transfer cask are not met, the Technical Specifications require that either in-pool or forced air cooling be initiated and maintained for a minimum of 48 hours to ensure that the fuel cladding and basket component temperatures do not exceed their short-term allowable temperatures. Using the same methodology described for in-

pool/forced air cooling following vacuum drying, the established time limits for the transfer operation with in-pool cooling following helium backfill are presented in Table 4.4.3.2-18. The maximum component temperatures for this condition are presented in Table 4.4.3.2-19. The established time limits for the transfer operation with forced air cooling following helium backfill and hold are presented in Table 4.4.3.2-20. The maximum component temperatures for this condition are presented in Table 4.4.3.2-21.

Figure 4.4.3.2-1 Temperature Distribution (°F) for the Normal Storage Condition: PWR Fuel for the Advanced Configuration

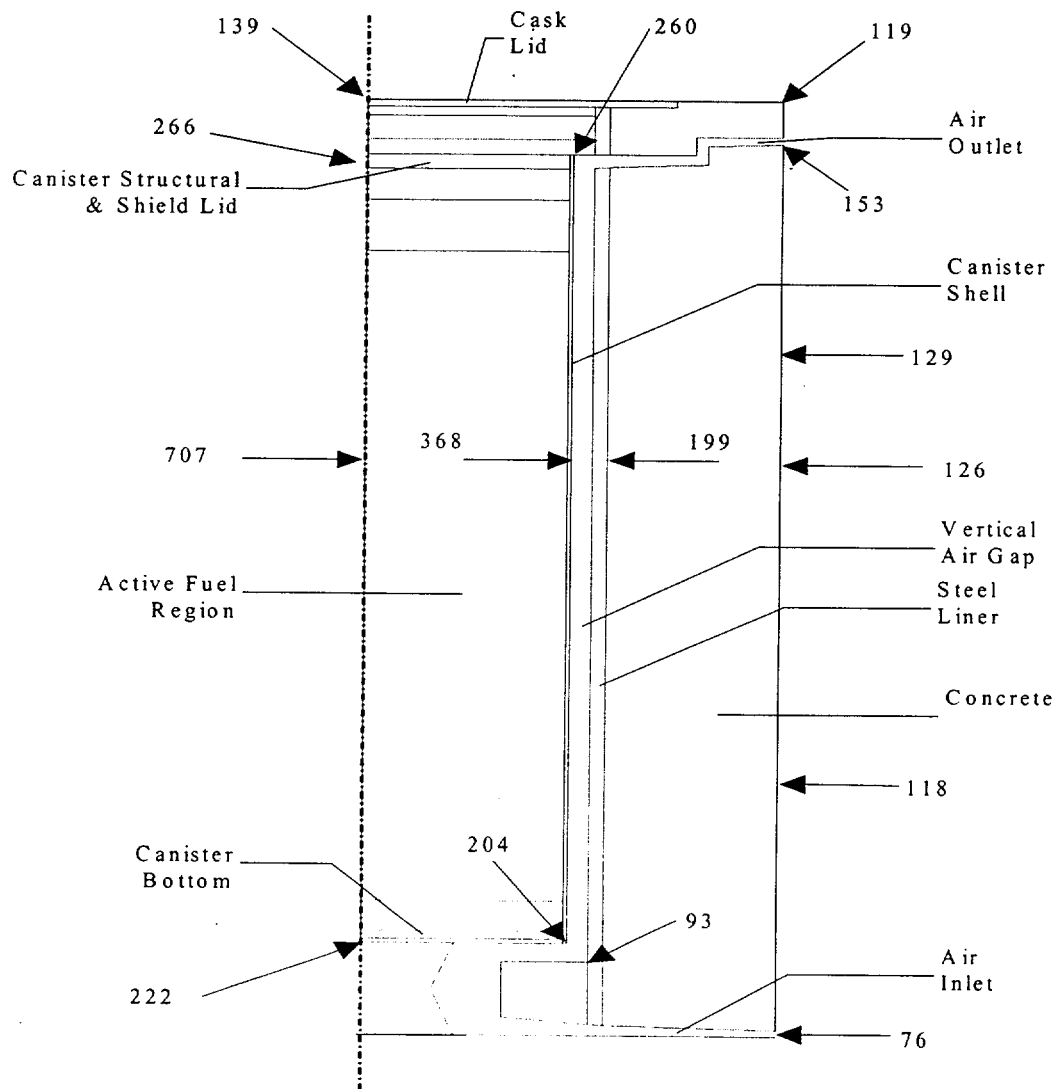


Figure 4.4.3.2-2 Contours of Velocity Magnitude (m/s) in the Lower Portion of the Model for the Normal Storage Condition (PWR Fuel) for the Advanced Configuration

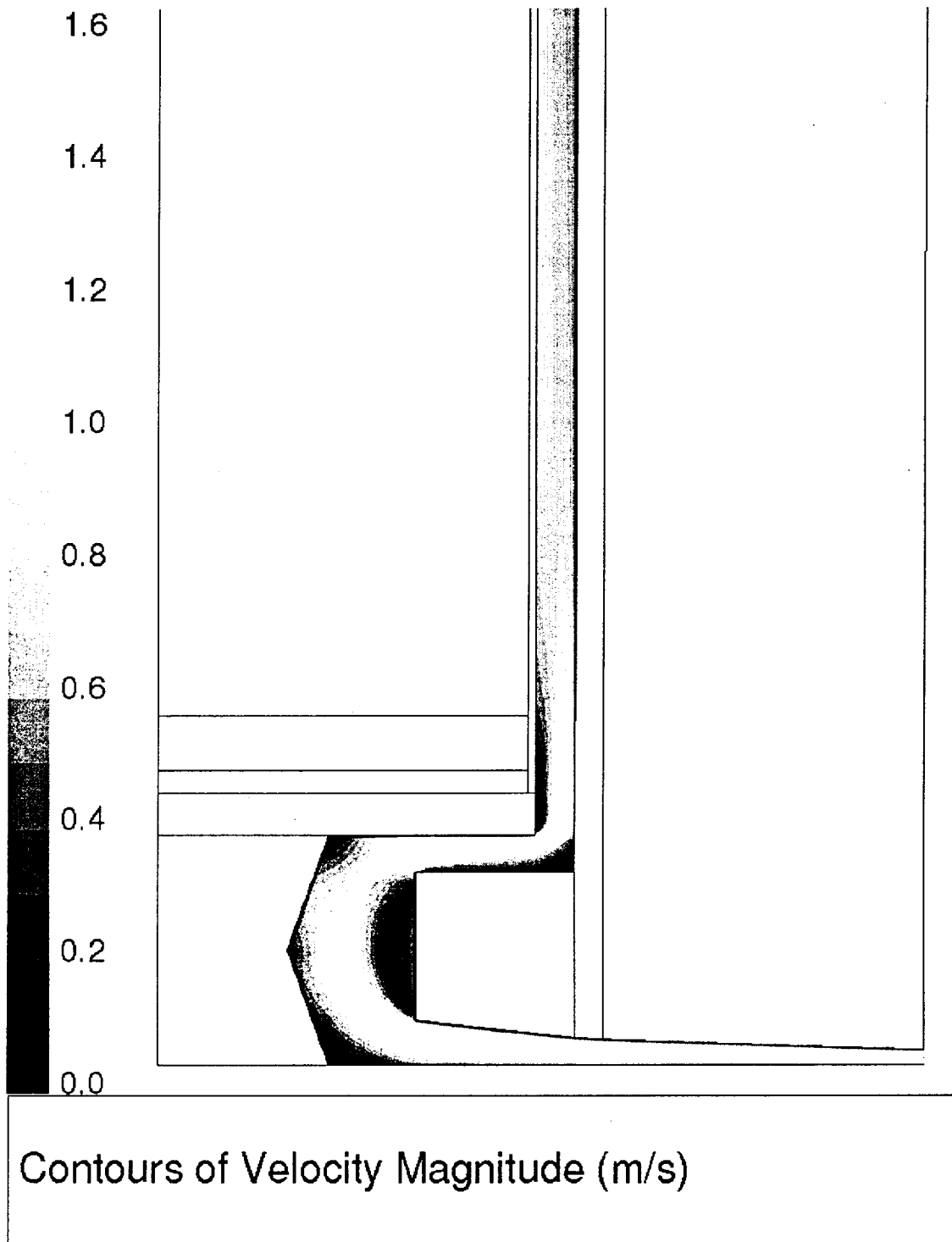


Figure 4.4.3.2-3 Contours of Velocity Magnitude (m/s) in the Upper Portion of the Model for the Normal Storage Condition (PWR Fuel) for the Advanced Configuration

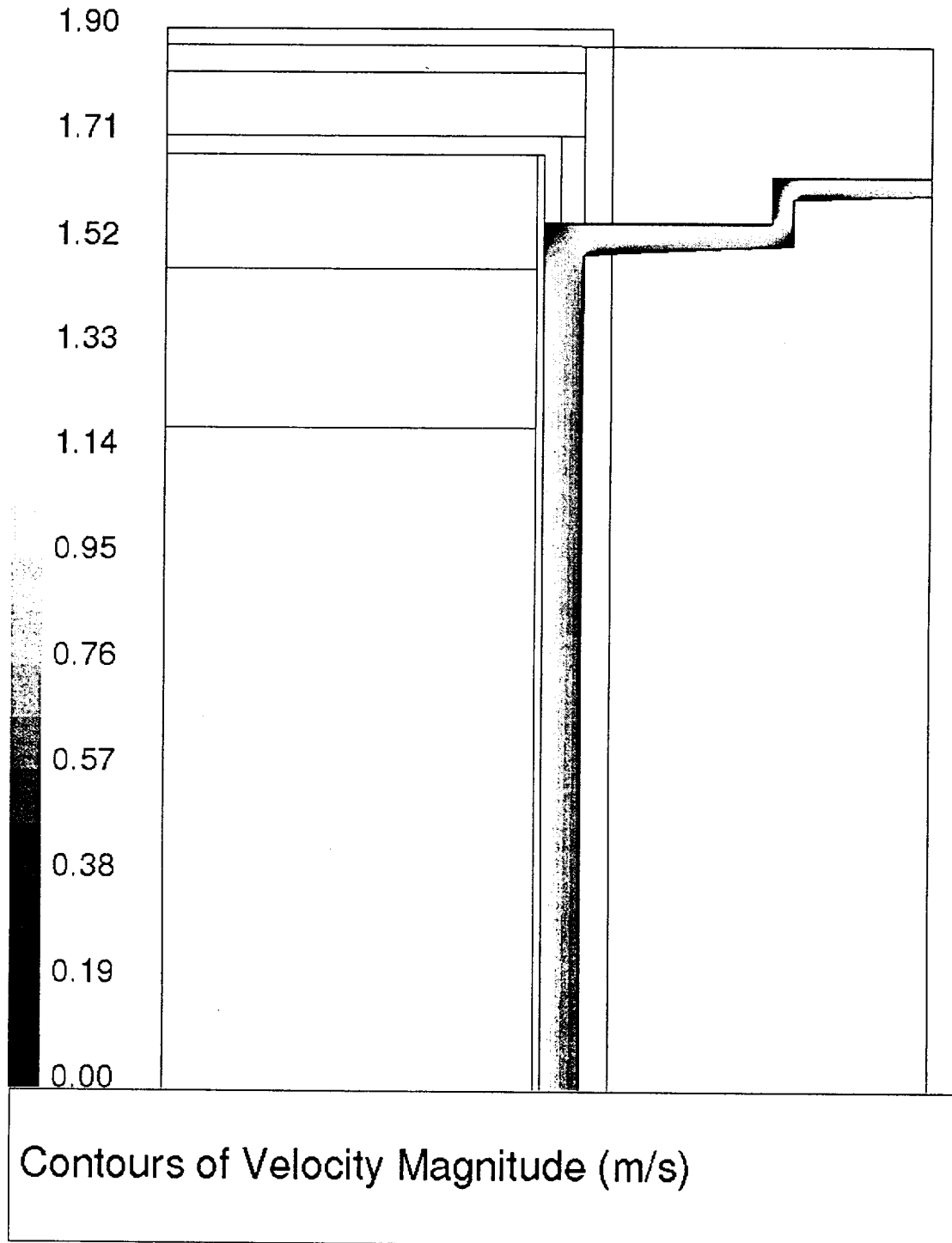


Figure 4.4.3.2-4 Temperature (°F) Distribution, in the Range of 76°F – 200°F, in the Concrete Cask During the Normal Storage Condition: PWR Fuel for the Advanced Configuration

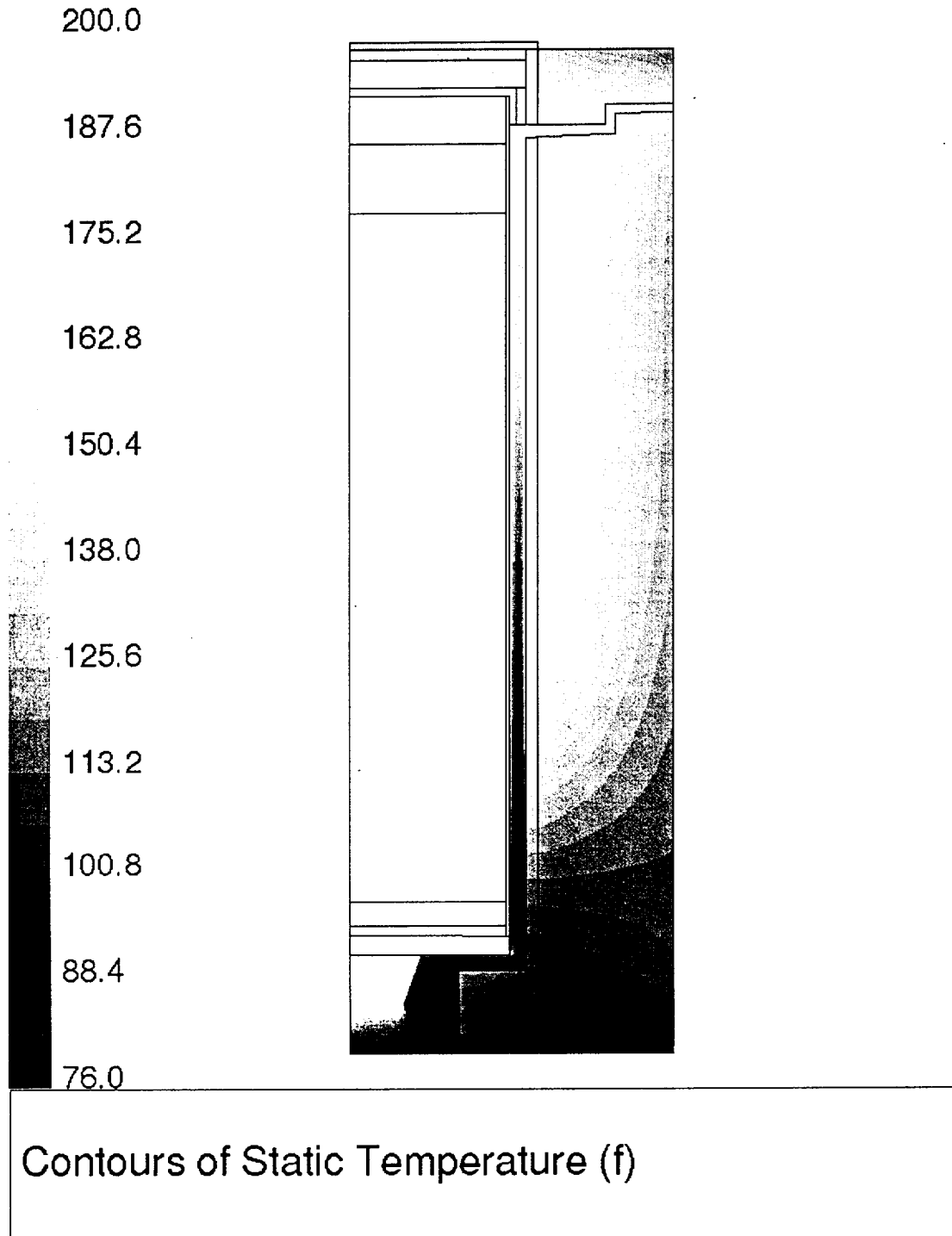


Figure 4.4.3.2-5 Component Temperature History for the Normal Condition with the Design Heat Load (29.2 kW) – PWR Fuel – Advanced Configuration

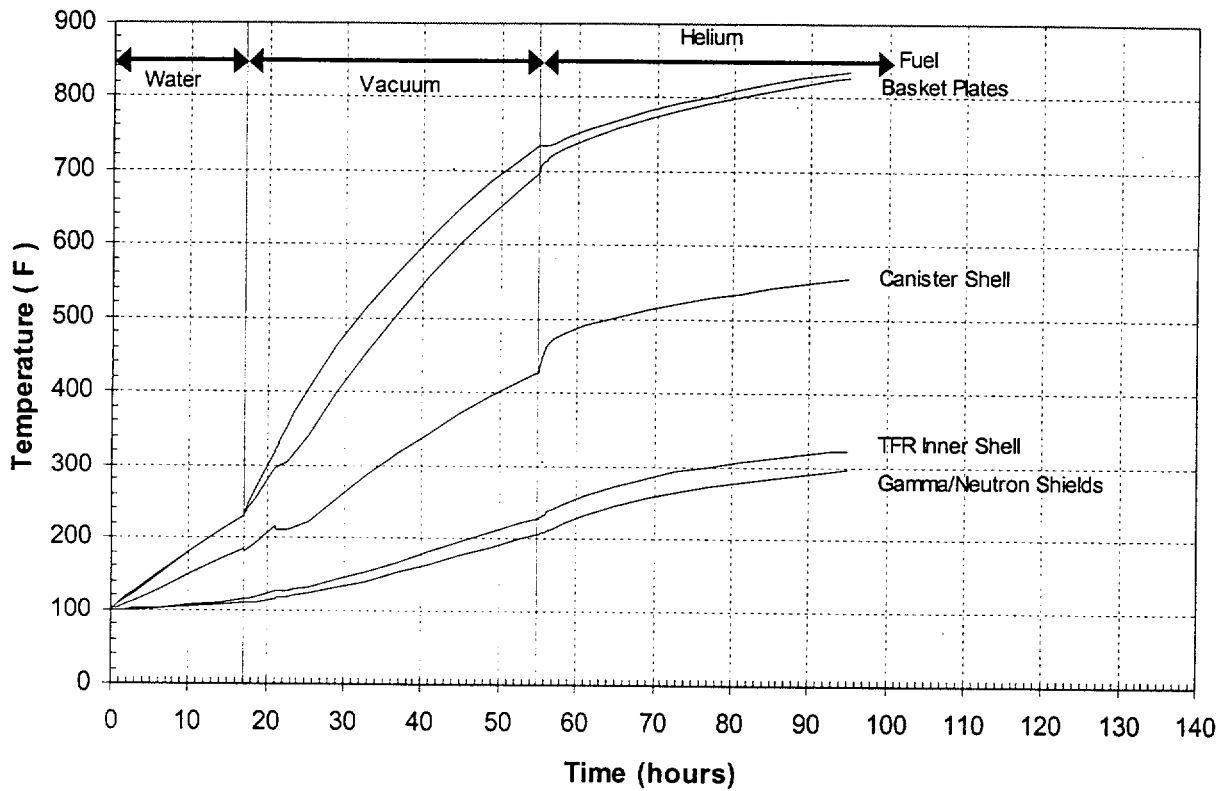


Figure 4.4.3.2-6 PWR Fuel Basket Preferential Loading Zones for Reduced Heat Loads During Transfer Conditions for the Advanced Configuration

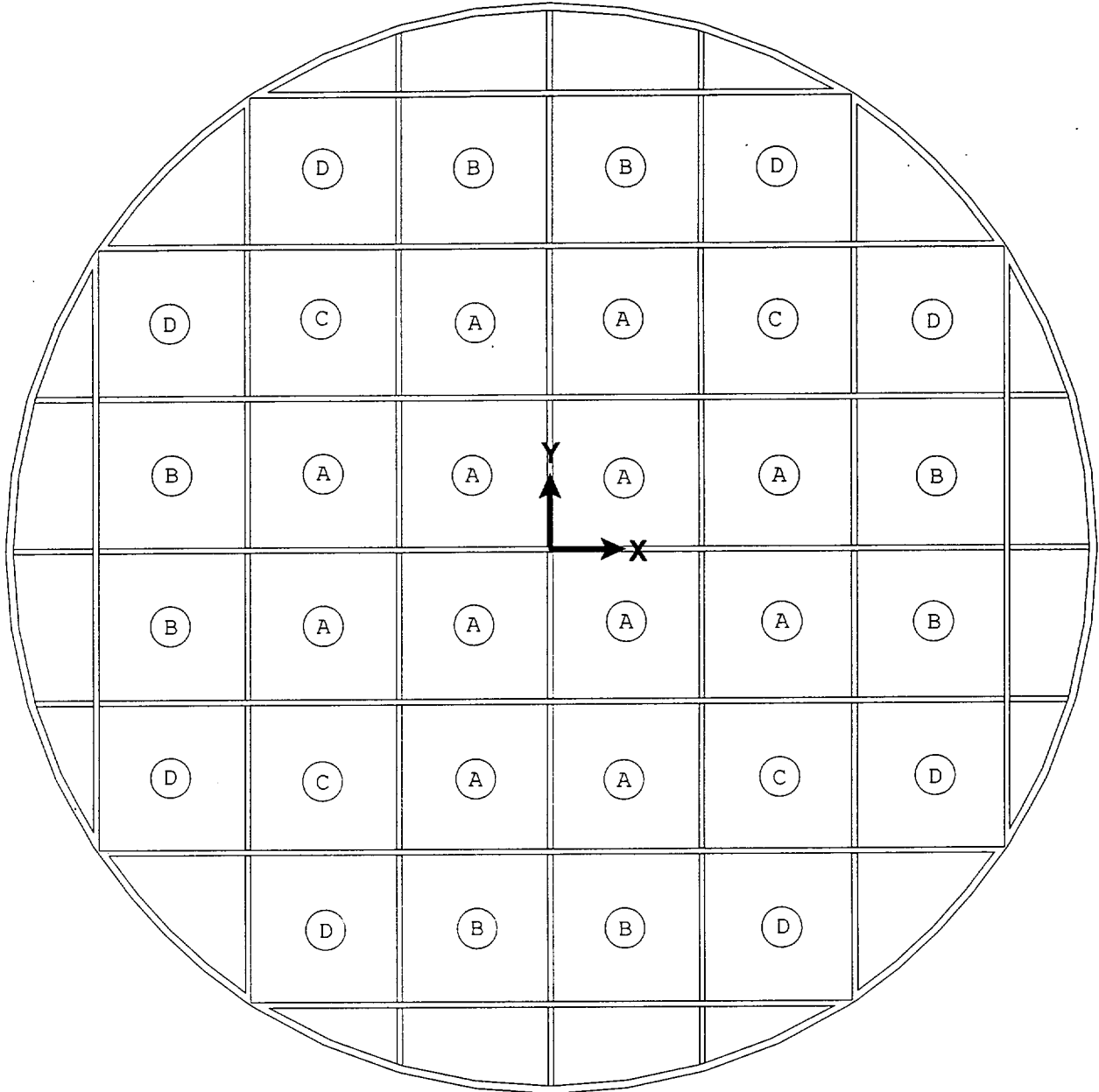


Table 4.4.3.2-1 Maximum Component Temperatures for the Normal Storage Condition – PWR – Advanced Configuration

Component	Maximum Temperature (°F)	Allowable Temperature (°F)
Fuel Cladding	707	734
Basket Plates	693	700
Neutron Absorber Plates	693	750
Basket Top Assembly	459	700
Basket Bottom Assembly	295	700
Canister Shell	368	800
Canister Structural Lid	268	800
Canister Shield Lid	272	800
Canister Bottom Plate	241	800
Concrete	199 (local) 138 (bulk*)	300 (local) 150 (bulk)

* The volume average temperature of the concrete region is used as the bulk concrete temperature.

Table 4.4.3.2-2 Maximum Component Temperatures for the Normal Transfer Condition with the Design Heat Load (29.2 kW) – PWR – Advanced Configuration

Component	Maximum Temperature (°F)		Allowable Temperature (°F)
	Vacuum	Helium	
Fuel Cladding	777	837	1,058
Basket Plates	741	827	850
Neutron Absorber Plates	755	828	900
Canister	452	553	800
Transfer Cask Shells	246	322	700
Transfer Cask Lead Gamma Shield	222	293	600
Transfer Cask Neutron Shield	220	290	300

Table 4.4.3.2-3 Time Limits for Transfer Operations with In-Pool Remedial Action – PWR – Advanced Configuration

Water	Time Limits (hours)			
	Vacuum	In-Pool (Helium)	Vacuum	Helium
17	44	24	15	30

Table 4.4.3.2-4 Maximum Component Temperatures for In-Pool Cooling Following the Vacuum and Drying Operations for the Design Heat Load of 29.2 kW – PWR – Advanced Configuration

Canister Heat Load (kW)	In-Pool (Helium)			Vacuum			Helium		
	Duration (hours)	Maximum Temperature (°F)		Duration (hours)	Maximum Temperature (°F)		Duration (hours)	Maximum Temperature (°F)	
		Fuel	Basket Plates		Fuel	Basket Plates		Fuel	Basket Plates
29.2	48	584	559	15	777	741	30	837	827

Table 4.4.3.2-5 Time Limits for Transfer Operations with Forced Air Cooling Remedial Action – PWR – Advanced Configuration

Time Limits (hours)				
Water	Vacuum	Forced Air (Helium)	Vacuum	Helium
17	44	24	14	30

Table 4.4.3.2-6 Maximum Component Temperatures for Forced Air Cooling Following the Vacuum and Drying Operations for the Design Heat Load of 29.2 kW – PWR – Advanced Configuration

Canister Heat Load (kW)	Forced Air (Helium)			Vacuum ¹			Helium ¹		
	Duration (hours)	Maximum Temperature (°F)		Duration (hours)	Maximum Temperature (°F)		Duration (hours)	Maximum Temperature (°F)	
		Fuel	Basket Plates		Fuel	Basket Plates		Fuel	Basket Plates
29.2	48 ²	675	658	14	777	741	30	837	827

- Notes: 1 Based on the temperatures for the vacuum & helium stages for normal transfer conditions.
 2 48-hour forced air cooling period with CFM.

Table 4.4.3.2-7 Time Limits for Transfer Operations with In-Pool Cooling Following Helium Backfill for the Design Heat Load of 29.2 kW – Advanced Configuration (PWR)

Time Limits (hours)				
Water	Vacuum	Helium	In-Pool (Helium)	Helium
17	44	30	24	30

Table 4.4.3.2-8 Maximum Component Temperatures for In-Pool Cooling Following Helium Backfill for the Design Heat Load of 29.2 kW – Advanced Configuration (PWR)

Canister Heat Load (kW)	In-Pool (Helium)			Helium ¹		
	Duration (hours)	Maximum Temperature (°F)		Duration (hours)	Maximum Temperature (°F)	
		Fuel	Basket Plates		Fuel	Basket Plates
29.2	24	597	573	30	837 ¹	827 ¹

Note: 1 Based on the temperatures for the helium stage for normal transfer conditions.

Table 4.4.3.2-9 Time Limits for Transfer Operations with Forced Air Cooling Following Helium Backfill for the Design Heat Load of 29.2 kW – Advanced Configuration (PWR)

Time Limits (hours)				
Water	Vacuum	Helium	Forced Air (Helium)	Helium
17	44	30	48 ¹	30

Note: 1 48-hour forced air cooling period with 500 CFM.

Table 4.4.3.2-10 Maximum Component Temperatures for Forced Air Cooling Following Helium Backfill for the Design Heat Load of 29.2 kW – Advanced Configuration (PWR)

Canister Heat Load (kW)	Forced Air (Helium)			Helium ¹		
	Duration (hours)	Maximum Temperature (°F)		Duration (hours)	Maximum Temperature (°F)	
		Fuel	Basket Plates		Fuel	Basket Plates
29.2	48 ²	688	672	30	837 ¹	827 ¹

Note: 1 Based on the temperatures for the helium stage for normal transfer conditions.
 2 48-hour forced air cooling period with 500 CFM.

Table 4.4.3.2-11 Reduced Heat Loads Preferential Loading Patterns – PWR – Advanced Configuration

Canister Total Heat Load (kW)	Heat Load in Each Basket Zone (kW)			
	A	B	C	D
27	0.700	1.000	1.000	0.830
25	0.700	1.000	1.000	0.580
22	0.700	1.000	1.000	0.200
18	0.700	0.700	1.000	0.000
14	0.700	0.350	0.700	0.000

Note: See Figure 4.4.3.2-6 for zone locations.

Table 4.4.3.2-12 Time Limits for Normal Transfer Conditions for Reduced Heat Loads – PWR – Advanced Configuration

Canister Heat Load (kW)	Time Limits (hours)		
	Water	Vacuum	Helium
27	17	46	50
25	18	74	No Limit
22	19	96	No Limit
18	21	No Limit	No Limit
14	23	No Limit	No Limit

Table 4.4.3.2-13 Time Limits for Normal Transfer Conditions for Reduced Heat Loads – PWR – Advanced Configuration

Canister Heat Load (kW)	Water			Vacuum			Helium		
	Duration (hours)	Maximum Temperature (°F)		Duration (hours)	Maximum Temperature (°F)		Duration (hours)	Max. Temp / Temp. at End (°F)	
		Fuel	Basket Plates		Fuel	Basket Plates		Fuel	Basket Plates
29.2 ²	17	231	230	44	777	741	40	837/837	827/827
27	17	229	225	50	789	751	50	829/829	820/820
25	18	234	230	74	853	819	No Limit	853/840 ¹	831/830 ¹
22	19	237	233	96	853	817	No Limit	853/754 ¹	827/780 ¹
18	21	241	237	No Limit	843 ¹	803 ¹	No Limit	718 ¹ /718 ¹	705 ¹ /705 ¹
14	23	240	235	No Limit	762 ¹	709 ¹	No Limit	636 ¹ /636 ¹	618 ¹ /618 ¹

Notes: 1 Steady-state value.
 2 Design heat load.

Table 4.4.3.2-14 Time Limits for Transfer Operations with In-Pool Cooling Remedial Action for Reduced Heat Loads – PWR – Advanced Configuration

Canister Heat Load (kW)	Time Limits (hours)				
	Water	Vacuum	In-Pool (Helium)	Vacuum	Helium
27	17	50	24	25	40
25	18	74	24	46	No Limit
22	21	96	24	68	No Limit

Table 4.4.3.2-15 Maximum Component Temperatures for In-Pool Cooling Following the Vacuum and Drying Operations – PWR – Advanced Configuration

Canister Heat Load (kW)	In-Pool (Helium)		Vacuum ²		Helium ²				
	Duration (hours)	Maximum Temperature (°F)		Duration (hours)	Maximum Temperature (°F)		Duration (hours)	Max. Temp / Temp. at End (°F)	
		Fuel	Basket Plates		Fuel	Basket Plates		Fuel	Basket Plates
27	24	579	553	25	789	751	40	829/829	820/820
25	24	586	560	46	853	819	No Limit	853/840 ¹	831/830 ¹
22	24	575	549	68	853	817	No Limit	853/754 ¹	827/780 ¹

- Notes: 1 Steady-state value.
2 Based on the temperatures for the vacuum & helium stages for normal transfer conditions.

Table 4.4.3.2-16 Time Limits for Transfer Operations with Forced Air Cooling Remedial Action for Reduced Heat Loads – PWR – Advanced Configuration

Canister Heat Load (kW)	Time Limits (hours)				
	Water	Vacuum	Forced Air (Helium)	Vacuum	Helium
27	17	50	48	20	40
25	18	74	24	22	No Limit
22	21	96	24	40	No Limit

Table 4.4.3.2-17 Maximum Component Temperatures for Forced Air Cooling Following the Vacuum and Drying Operations -- PWR – Advanced Configuration

Canister Heat Load (kW)	Forced Air (Helium)			Vacuum ²			Helium ²		
	Duration (hours)	Maximum Temperature (°F)		Duration (hours)	Maximum Temperature (°F)		Duration (hours)	Max. Temp / Temp. at End (°F)	
		Fuel	Basket Plates		Fuel	Basket Plates		Fuel	Basket Plates
27	48	656	639	20	789	751	40	829/829	820/820
25	24	752	739	22	853	819	No Limit	853/840 ¹	831/830 ¹
22	24	728	714	40	853	817	No Limit	853/754 ¹	827/780 ¹

- Notes: 1 Steady-state value.
2 Based on the temperatures for the vacuum & helium stages for normal transfer conditions.

Table 4.4.3.2-18 Time Limits for Transfer Operations with In-Pool Cooling Following Helium Backfill for Reduced Heat Loads — Advanced Configuration (PWR)

Canister Heat Load (kW)	Time Limits (hours)				
	Water	Vacuum	Helium	In-Pool (Helium)	Helium
27	17	50	40	24	40

Table 4.4.3.2-19 Maximum Component Temperatures for In-Pool Cooling Following Helium Backfill for Reduced Heat Loads—Advanced Configuration (PWR)

Canister Heat Load (kW)	In-Pool (Helium)			Helium ¹		
	Duration (hours)	Maximum Temperature (°F)		Duration (hours)	Maximum Temperature (°F)	
		Fuel	Basket Plates		Fuel	Basket Plates
27	24	589	563	40	829 ¹	820 ¹

Note: 1 Based on the temperatures for the helium stage for normal transfer conditions.

Table 4.4.3.2-20 Time Limits for Transfer Operations with Forced Air Cooling Following Helium Backfill for Reduced Heat Loads — Advanced Configuration (PWR)

Canister Heat Load (kW)	Time Limits (hours)				
	Water	Vacuum	Helium	Forced Air (Helium)	Helium
27	17	50	40	24	40

Table 4.4.3.2-21 Maximum Component Temperatures for Forced Air Cooling Following Helium Backfill for Reduced Heat Loads—Advanced Configuration (PWR)

Canister Heat Load (kW)	Forced Air (Helium)			Helium ¹		
	Duration (hours)	Maximum Temperature (°F)		Duration (hours)	Maximum Temperature (°F)	
		Fuel	Basket Plates		Fuel	Basket Plates
27	48 ²	668	651	40	829 ¹	820 ¹

- Note:
- 1 Based on the temperatures for the helium stage for normal transfer conditions.
 - 2 48-hour forced air cooling at 500 CFM.

4.4.4 Minimum Temperatures

The minimum temperatures of the Vertical Concrete Cask and components occur at -40°F with no heat load. The temperature distribution for this off-normal environmental condition is provided in Section 11.1. At this extreme condition, the component temperatures are above their minimum material limits.

THIS PAGE INTENTIONALLY LEFT BLANK

4.4.5 Maximum Internal Pressures

The maximum internal operating pressures for normal conditions of storage are calculated in Sections 4.4.5.1 and 4.4.5.2 for PWR and BWR fuel, respectively, in the Standard configuration and in Section 4.4.5.3 for PWR fuel in the Advanced configuration.

4.4.5.1 Maximum Internal Pressure for PWR Fuel in the Standard Canister

The internal pressure within a PWR fuel canister is a function of fuel type, fuel condition (failure fraction), burnup, canister class and the backfill gases in the canister cavity. Gases included in the canister pressure evaluation include fuel rod fission and backfill gases, canister backfill gases and burnable poison generated gases. Each of the fuel types is separately evaluated to arrive at a bounding canister pressure.

Fission gases include all fuel material generated gases including helium generated by long-term actinide decay. Based on detailed SAS2H calculations of the maximum fissile material mass in each canister class, the quantity of gas generated by the fuel rises as burnup and cool time is increased and enrichment is decreased. The maximum gas available for release is conservatively calculated based on the PWR inventory for the 60,000 MWD/MTU burnup cases at an enrichment of 1.9 wt. % ^{235}U and a cool time of 40 years. The calculated inventory is conservative since the maximum allowable burnup is 45,000 MWD/MTU for PWR fuel in the Standard configuration. Gases included are all krypton, iodine, and xenon isotopes in addition to helium and tritium (^3H). Molar quantities of gas for each of the maximum fissile mass assemblies are summarized in Table 4.4.5-1. For other fuel assemblies, fissile mass is scaled to obtain the quantity of fuel-generated gases.

Fuel rod backfill pressure varies significantly between the PWR fuel types. The maximum reported backfill pressure reported is for the Westinghouse 17×17 fuel assembly at 500 psig. All fuel assemblies are evaluated using the 500 psig backfill reported for the Westinghouse assembly, except B&W assemblies, which have a backfill pressure of 435 psig. Backfill quantities are based on the free volume between the pellet and the clad and the plenum volume. The fuel rod backfill gas is conservatively assumed to have an initial temperature of 68°F.

Burnable poison rod assemblies (BPRAs) placed within the canister may contribute additional gas quantities due to alpha-n reactions of fission generated neutrons with ^{10}B during in-core operation. ^{10}B forms a portion of the neutron poison population. Other neutron poisons, such as

gadolinium and erbium, do not produce a significant amount of helium nuclides (alpha particles). The principal BPRAs in use include the Westinghouse Pyrex (borosilicate glass) and WABA (wet annular burnable absorber) configurations, as well as B&W BPRAs and shim rods used in CE cores. The CE shim rods replace standard fuel rods to form a complete assembly array. The quantity of helium available for release from the BPRAs is directly related to the initial boron content of the rods and the release fraction of gas from the matrix material. Release from either of the low temperature, solid matrix materials, is likely to be limited but no release fractions were available in open literature. Consequently, a 100% release fraction is assumed based on a boron content of 0.0063 g/cm ¹⁰B per rod, from the maximum number of rods in an assembly. The maximum number of rods is 16 for Westinghouse 14×14 assemblies, 20 rods for Westinghouse and B&W 15×15 assemblies, and 24 rods for Westinghouse and B&W 17×17 assemblies. The length of the absorber is conservatively taken as the active fuel length. CE core shim rods are modeled at 0.0126 g/cm ¹⁰B for 16, 12, and 12 rods applied to CE manufactured 14×14, 15×15 and 16×16 assemblies, respectively.

The canister backfill gases are conservatively assumed to be at 250°F. The initial pressure of the canister backfill gas is 1 atm (0.0 psig). Free volume inside each PWR canister class is listed in Table 4.4.5-2. The free volumes do not include fuel assembly components since these vary for each assembly type and fuel insert. The free volume of the canister is obtained by subtracting the rod, guide tube and hardware volumes for the fuel assemblies and BPRAs. For the Westinghouse BPRAs, the Pyrex volume is employed since it displaces more volume than the WABA rods.

The total pressure for each of the Standard canister contents is found by calculating the releasable molar quantity of each gas (30% of the fission gas and 100% of the rod backfill adjusted for the 1% fuel failure fraction), and summing the quantities directly. The quantity of gas is used in the ideal gas equation, with the average gas temperature at normal operating conditions, to arrive at canister pressures. The normal condition average temperature of the gas within the canister is conservatively considered to be 420°F (500 K). This temperature bounds the calculated gas temperature (418°F) for normal conditions of storage using the three-dimensional canister model.

Each of the Standard PWR fuel types is individually evaluated for normal condition pressure. As shown in Table 4.4.5-3, the maximum pressure of 4.22 psig occurs for the B&W 17×17 assembly in the Class 2 canister.

4.4.5.2 Maximum Internal Pressure for BWR Fuel in the Standard Canister

BWR Standard canister maximum pressures are determined in the same manner as those for the PWR Standard canister cases described in Section 4.4.5.1. For the BWR analysis, the maximum normal condition rod backfill gas pressure is 132 psig and the pressurizing gases are limited to fission gases (including helium actinide decay gas), rod backfill gases, and canister backfill gas. The 132 psig backfill pressure is significantly higher than the 6 atmosphere (~90 psig) maximum pressure reported in open literature. BWR assemblies do not contain a component equivalent to the PWR BPRAs and therefore do not require ¹⁰B helium-generated gases to be added. Fissile gas inventories for the maximum fissile material assemblies in each of the three BWR lattice configurations (7×7, 8×8, and 9×9) are shown in Table 4.4.5-4. For other fuel assemblies, fissile mass is scaled to obtain the quantity of fuel-generated gases. Free volumes, without fuel components, in canister classes 4 and 5 are shown in Table 4.4.5-5. Maximum pressures for each canister class are listed in Table 4.4.5-6. The maximum calculated normal condition pressure of 3.98 psig is based on a GE 7×7 assembly, designed for a BWR/2-3 reactor, with gas inventories conservatively taken from a 60,000 MWD/MTU source term. This is conservative, since the maximum burnup in the Standard configuration is 45,000 MWD/MTU. The normal condition pressure for a Standard canister containing the GE 9×9 fuel assembly with 79 fuel rods is 3.90 psig.

4.4.5.3 Maximum Internal Pressure for PWR Fuel in the Advanced Canister

Advanced PWR canister maximum pressures are determined in the same manner as those documented for the Standard PWR canister cases. The design basis PWR fuel loading resulting in the maximum Advanced UMS normal condition internal pressure is a Class 1 canister loaded with Westinghouse 15×15 fuel assemblies (corresponding to the n15b3 assembly listed in Table 6.2.2-1). This assembly has the highest fuel rod backfill pressure (500 psig) and the smallest canister free volume, and takes credit for the insertion of 20 BPRA rods. The fission gas generation is analyzed conservatively at 60,000 MWD/MTU, as opposed to the maximum allowable burnup of 55,000 MWD/MTU.

The calculated volume occupied by the basket components was conservatively rounded up for this analysis, and both the calculated and analyzed values are reported in Table 4.4.5-7. The canister backfill gases are conservatively considered to be at 250°F. The initial backfill pressure is conservatively considered to be 2 atm. The normal condition average temperature of the gases within the PWR fuel is conservatively considered to be 500°F. This temperature bounds the

calculated gas temperature (465°F) for normal conditions of storage. Using the same methodology of the calculations for the internal pressure of the Standard PWR canister, the maximum internal pressure for the Advanced PWR canister for normal conditions of storage is 26.6 psig.

Table 4.4.5-1 UMS® PWR Per Assembly Fuel Generated Gas Inventory (Standard and Advanced)

Array	Assembly Type	MTU	Moles
14×14	WE Standard	0.4144	35.52
15×15	B&W Mark B	0.4807	41.32
16×16	CE (System 80)	0.4417	38.10
17×17	WE Standard	0.4671	40.18

Table 4.4.5-2 Standard PWR Canister Free Volume

Canister Class	1	2	3
Basket Volume (in ³)	69,800	74,494	77,459
Canister Height (inch)	175.05	184.15	191.75
Canister Free Volume without Fuel or Inserts (liter)	7,966	8,397	8,772

Table 4.4.5-3 Standard PWR Maximum Normal Condition Pressure by Canister Class

Canister Class	Fuel Type	Pressure (psig)
1	West. 17×17 Standard	4.20
2	B&W 17×17 Mark C	4.22
3	CE 16×16 ANO2	4.09

Table 4.4.5-4 Fuel Generated Gas Inventory for BWR Fuel in the Standard Canister

Array	Assembly Type	MTU	Moles
7×7	GE 7×7 (49 Rods)	0.1985	16.78
8×8	GE 8×8 (63 Rods)	0.1880	16.07
9×9	GE 9×9 (79 Rods)	0.1979	16.86

Table 4.4.5-5 Standard BWR Canister Free Volume (No Fuel or Inserts)

Canister Class	4	5
Basket Volume (in ³)	73,109	74,682
Canister Height (inch)	185.55	190.35
Canister Free Volume without Fuel or Inserts (liter)	8,497	8,739

Table 4.4.5-6 Standard BWR Maximum Normal Condition Pressure by Canister Class

Canister Class	Fuel Type	Pressure (psig)
4	GE 7×7 (49 rods)	3.98
5	GE 7×7 (49 rods)	3.97

Table 4.4.5-7 Advanced PWR Canister Free Volume (No Fuel or Inserts)

Canister Class	1	2	3
Basket Volume (in ³)	74,671	78,402	82,753
Basket Volume used (in ³)	75,500	79,000	83,500
Canister Height (inch)	175.30	184.40	192.00
Canister Free Volume without Fuel or Inserts (liter)	7,873	8,323	8,673

Table 4.4.5-8 Advanced PWR Maximum Normal Condition Pressure by Canister Class

Canister Class	Fuel Type	Pressure (psig)
1	West. 15×15 Standard (n15b3)	26.63
2	Hybrid 15×15 (208 rods) (n15e3) ¹	26.63
3	CE 16×16 (System 80) (n16b3)	26.40

1. B&W 15×15 with 0.428-inch pellet diameter and 0.023-inch clad thickness.

4.4.6 Maximum Thermal Stresses

The results of thermal stress calculations for normal conditions of storage are reported in Section 3.4.4.1 for PWR and BWR fuel in the Standard configuration and in Section 3.4.4.3 for PWR fuel in the Advanced configuration.

THIS PAGE INTENTIONALLY LEFT BLANK

4.4.7 Maximum Allowable Cladding Temperature and Canister Heat Load

4.4.7.1 Maximum Allowable Cladding Temperature and Canister Heat Load for the Standard Configuration

The maximum allowable cladding temperatures are calculated for PWR and BWR systems based on fuel assembly type, maximum burnup, and minimum initial cool time. Allowable heat loads are determined by relating cladding temperature to canister heat load.

Cladding stresses are calculated for a set of representative PWR and BWR assemblies at 40,000 MWD/MTU and 380°C. The limiting, highest stress assemblies, the Westinghouse 14×14 and GE 9×9 (150-inch fuel region), are then evaluated at various burnups to determine the maximum allowable fuel cladding temperature based on PNL-6364 criteria [33]. Maximum allowable cladding temperatures are calculated for burnups ranging from 35,000 MWD/MTU to 45,000 MWD/MTU. After applying a bias to the maximum allowable cladding temperatures, the maximum allowable heat load is calculated as a function of burnup and minimum initial cool time.

Based on PNL-6364, the cladding temperature limit is expressed as a function of initial dry storage temperature, initial cladding stress at the dry storage temperature, and initial storage time.

The initial cladding stress is a function of the rod internal pressure, temperature, diameter of the fuel rod, and fuel cladding thickness. The initial cladding stress (σ_{mhoop}) for a particular assembly is calculated as [33]:

$$\sigma_{mhoop} = \frac{(P)(D_{mid})}{2t} \times \alpha \times \frac{T_2}{T_1} \times \frac{69.684}{10,000}$$

where:

- σ_{mhoop} = dry storage cladding hoop stress, MPa
- P = internal gas pressure of the rod, psi
- T_1 = temperature at which P was determined, K
- t = cladding wall thickness, in.
- D_{mid} = cladding midwall diameter, in.
- α = a factor, 0.95 for PWR rods or 0.90 for BWR rods
- T_2 = allowable storage temperature for σ_{mhoop} , K

To account for cladding oxidation during in-core fuel assembly operation and storage of the fuel in the spent fuel pool, the nominal cladding thickness is reduced by 0.06 mm and 0.125 mm for PWR and BWR fuel rods respectively [34].

The pressure in the fuel assembly rods is produced by the combination of fill gas and fission gas.

For a given fuel assembly design, the fill gas quantity is fixed and does not vary with discharge burnup. Based on the initial pressure and temperature of the fill gas, the number of moles of gas are calculated using the ideal gas law:

$$PV = NRT$$

where:

- P = Pressure
- V = Volume (free volume inside fuel rod)
- N = Number of moles of gas
- R = Universal gas constant
- T = Temperature of the gas

The number of moles of fill gas are added to the fission gas quantity and converted to a cladding internal pressure at storage conditions.

The fission gas quantity pressurizing the fuel cladding is calculated on the basis of the burnup and a fission gas release fraction. While the amount of fission gas produced is a predictable quantity (directly correlated to the number of fissions required to produce the desired burnup), the release fraction of the gas from the pellet into the pellet-cladding void depends on fill gas pressure and reactor operating conditions.

The number of fissions (Z) is related to the burnup by:

$$Z = X \text{ Burnup} \frac{\text{MWd}}{\text{MTU}} \times 1.0 \times 10^6 \frac{\text{W}}{\text{MW}} \times 86,400 \frac{\text{sec}}{\text{d}} \times \frac{1 \text{ MeV}}{1.602 \times 10^{-13} \text{ J}} \times \frac{1 \text{ Fission}}{200 \text{ MeV}}$$

$$\times \frac{1 \text{ Mole}}{6.02 \times 10^{23} \text{ Atoms}} \times \text{Mass} \frac{\text{MTU}}{\text{Assembly}} \times \frac{\text{Assembly}}{\# \text{ Rods}}$$

Multiplying the number of fissions by 0.3125 (0.25×1.25) atoms/fission then derives the quantity of fission gas produced. Olander's "Fundamental Aspects of Nuclear Reactor Fuel Elements" [31] lists the number of gas atoms from a single fission as 0.25. Based on a detailed SAS2H isotope generated fission gas inventory, this fraction is increased by 25% to account for decay chains not included in Olander (particularly those leading to ^{136}Xe). By employing a conservative fission gas fraction rather than the SAS2H output itself, the allowable cladding temperature calculation is decoupled from source term calculations.

Based on Sandia report 90-2406, "A Method for Determining the Spent-Fuel Contribution to Transport Cask Containment Requirements" [30], gas release fractions from the fuel pellets are assumed to be 12% for PWR fuel rods and 25% for BWR fuel rods. Relying on a gas diffusion model (as applied to pre-pressurized light water reactor fuel rods), the Sandia report indicates a release fraction of approximately 1% for PWR rods and approximately 2% for BWR rods [Page I-62 of Ref. 30]. Experimental release fractions reach as high as 16% for PWR rods and 25% for BWR rods [Page I-64 and I-65 of Ref. 30]. The higher release fractions are associated with unpressurized fuel rods or those rods run at uncharacteristically high temperatures and linear heat generation rates. While these rods show higher release rates, they are not expected to produce higher "burned fuel" pressures, since the partial pressure of the fill gas is not present, thereby allowing a larger number of fission gas molecules to accumulate before reaching limiting cladding pressure. The 12% PWR fission gas release fraction excludes the unpressurized Maine Yankee rod data while including the 43,000 MWD/MTU Calvert Cliff data through a burnup of approximately 56,000 MWD/MTU. An additional analysis is performed comparing the 12% PWR and 25% BWR release fractions to the element specific release fractions in Reg. Guide 1.25 [Ref. 35]. The 12% PWR release fraction results in gas releases similar to those indicated by the Regulatory Guide, while the BWR 25% release fraction is twice the Regulatory Guide indicated gas release. Note that both the Sandia report and the Regulatory Guide release fractions are for punctured fuel rods where the release of the pressurizing gas allows additional gaseous isotopes to migrate from the fuel matrix. Using the 12% PWR and 25% BWR fuel rod release fractions, therefore, results in a conservative cladding pressurization assumption for the intact rod analysis.

Fuel rod free volume is calculated based on the fuel characteristics documented in Table 4.4.7.1-1 and Table 4.4.7.1-2 for PWR and BWR fuel assemblies, respectively. Not all assemblies requested for loading are included in the tables, since assemblies with significantly higher free volume or lower fuel mass are bound by the cladding stress evaluations presented. Section 4.4.5 contains a sample free volume calculation of a fuel rod. While the maximum

canister pressure calculation conservatively neglected the plenum spring volume, the spring volume is subtracted out of the plenum volume in the cladding maximum stress calculation to increase internal rod pressure.

Substituting the internal gas pressure resulting from the releasable gas inventories produced by 40,000 MWD/MTU burned fuel into the hoop stress equation at a temperature of 380°C results in the assembly-specific maximum cladding stresses shown in Table 4.4.7.1-1 and Table 4.4.7.1-2. The Westinghouse 14×14 and GE 9×9 (150-inch fuel region) are the limiting PWR and BWR assembly types at 113.9 and 70.5 MPa stress levels, respectively.

The stress levels in the limiting assemblies are then evaluated at burnups ranging from 35,000 MWD/MTU to 45,000 MWD/MTU and temperatures of 300°C and 400°C for PWR fuels and 300°C and 450°C for BWR fuel. The evaluation results are presented in Table 4.4.7.1-3. This data is overlaid on generic stress versus limiting temperature curves to arrive at cool time and burnup-specific maximum cladding allowable temperatures. The data, shown in Table 4.4.7.1-4, from which the generic curves are constructed, is taken from Table 3.1 of PNL-6189 [5].

The cladding temperature limit curves for the limiting PWR and BWR fuel assemblies are provided in Figure 4.4.7.1-1 and Figure 4.4.7.1-2. The intercept of each of the curves represents the maximum allowable cladding temperature at a given cool time and maximum assembly burnup. Fuel rod peak cladding stress level and the allowable cladding temperature are calculated using the assembly average burnup, even though some rods experience a higher burnup than the average. The average burnup is used since the quantity of fission gas formation and the fuel rod gas temperature are conservatively determined. As shown in Table 4.4.7.1-5, allowable cladding temperature varies only slightly over a wide range of burnup for a given required cooling time. Consequently, the variation in cladding stress with burnup is also small.

Thermal analysis was performed at three heat loads to determine the corresponding maximum fuel cladding temperature for both PWR and BWR fuel. The thermal models and methods, described in Section 4.4.1, used to determine the temperature of fuel cladding and system components for the design basis heat load are applied to determine the cladding temperature at reduced heat loads. The cladding temperatures versus heat load in Table 4.4.7.1-6 and Table 4.4.7.1-7 are the results of rounding the ANSYS calculated temperatures up to provide a conservative, bounding input for correlating allowable cladding temperature to allowable heat

load. The temperatures versus heat load curves are plotted in Figure 4.4.7.1-3. To provide adequate design margin, the maximum allowable cladding temperatures are reduced by a temperature bias, shown in Table 4.4.7.1-9, prior to their use in the calculation of maximum allowable canister heat load. Maximum allowable canister heat loads are calculated for initial cool times ranging from 5 to 15 years and burnups ranging from 35,000 MWD/MTU to 45,000 MWD/MTU. The results of the PWR and BWR analysis are presented in Table 4.4.7.1-8. Since these temperatures are based on the PWR and BWR assemblies having the highest cladding stress levels, the maximum heat loads can be applied to all Universal Storage System Standard configuration design basis contents.

Figure 4.4.7.1-1 PWR Fuel Dry Storage Temperature versus Cladding Stress – Standard Configuration

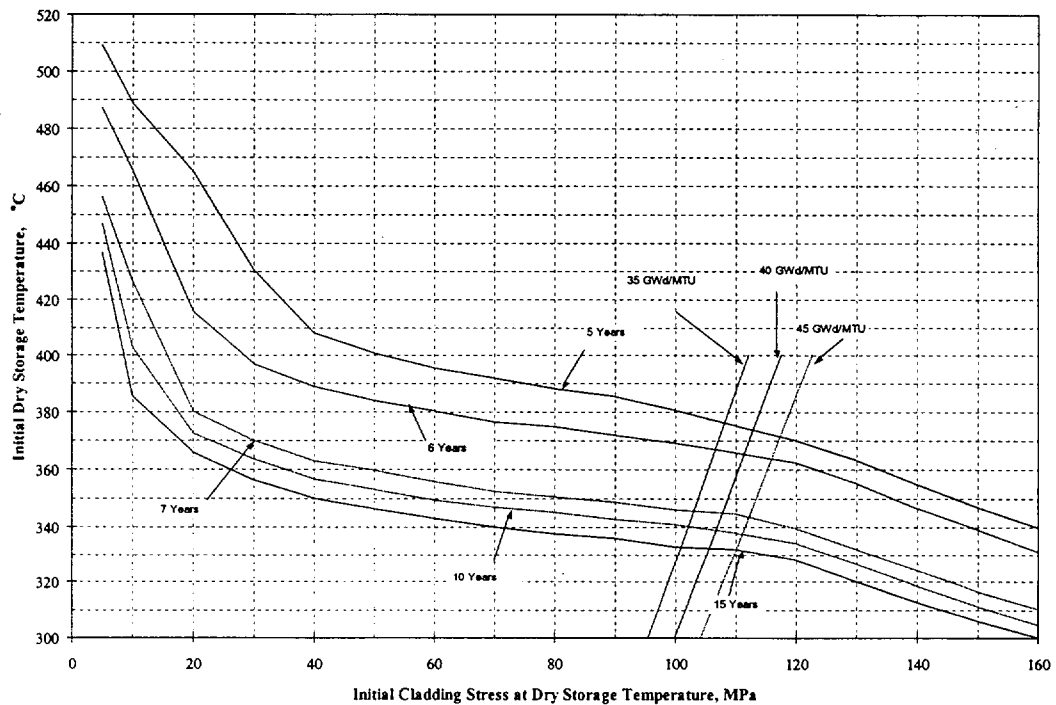


Figure 4.4.7.1-2 BWR Fuel Dry Storage Temperature versus Cladding Stress – Standard Configuration

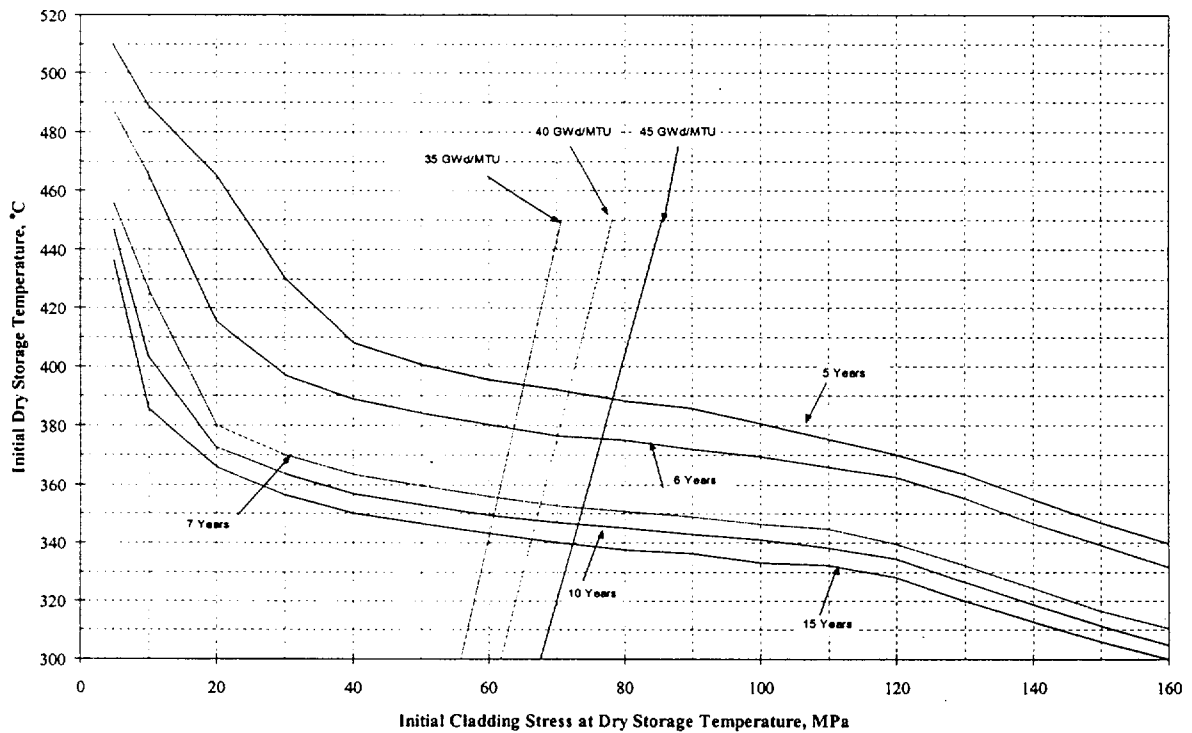


Figure 4.4.7.1-3 PWR and BWR Fuel Cladding Dry Storage Temperature versus Basket Heat Load – Standard Configuration

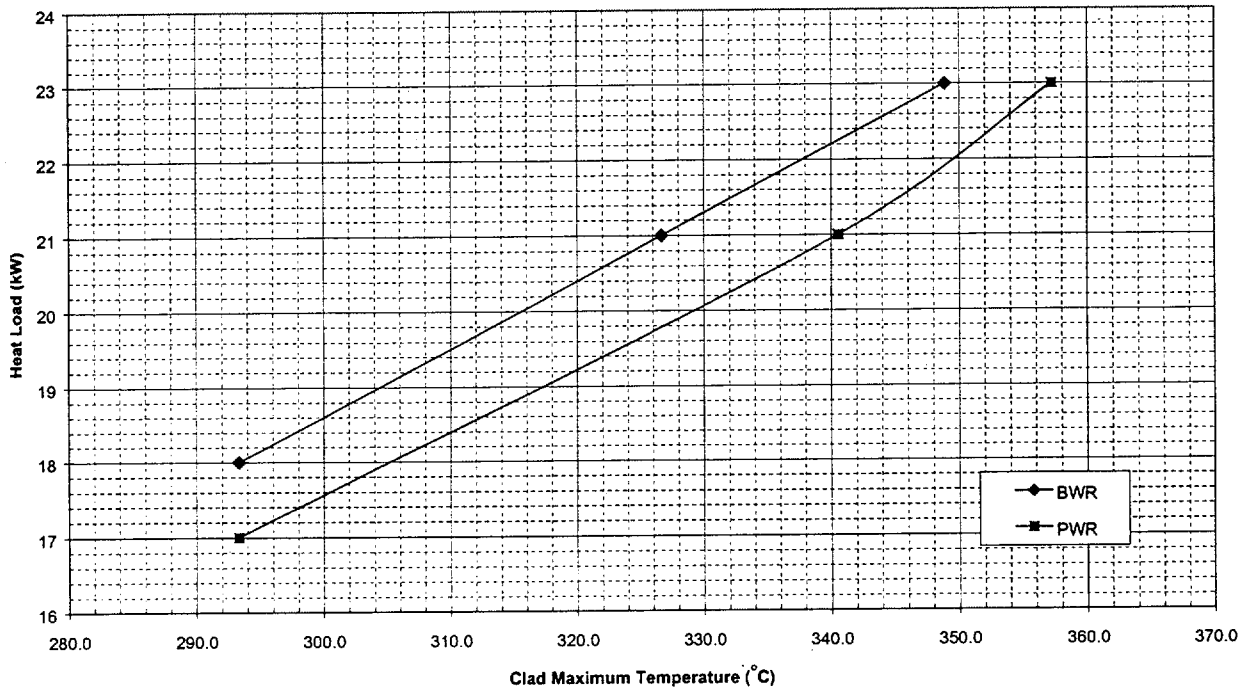


Table 4.4.7.1-1 PWR Cladding Stress Level Comparison Chart – Standard Configuration

Fuel Type	Units	B&W 15×15	B&W 17×17	CE 14×14	CE 16×16	WE 14×14	WE 15×15	WE 17×17
Rod OD	inch	0.43	0.379	0.44	0.382	0.422	0.422	0.374
Cladding Thickness	inch	0.0265	0.024	0.028	0.025	0.0225	0.0242	0.0225
Pellet OD	inch	0.3686	0.3232	0.3765	0.325	0.3674	0.3659	0.3225
Active Fuel Length	inch	144	143	137	150	145.2	144	144
Plenum Length	inch	7.755	8.318	8.528	9.927	5.790	7.386	6.260
Spring Weight	lb	0.042	0.026	0.1	0.1	0.07	0.044	0.037
Backfill Pressure	psig	435	435	500	500	500	500	500
Fuel Mass	MTU	0.4807	0.4658	0.4037	0.4417	0.4144	0.4646	0.4671
# of Fuel Rods		208	264	176	236	179	204	264
Free Volume	inch ³	1.427	1.198	1.252	1.052	1.217	1.300	0.882
Pressure (380°C)	psia	1525	1478	1739	1722	1762	1713	1795
Stress Level	MPa	83.1	78.9	91.2	88.5	113.9	101.7	102.1

Table 4.4.7.1-2 BWR Cladding Stress Level Comparison Chart – Standard Configuration

Fuel Type	Units	EX 7×7	EX 8×8	EX 9×9	GE 7×7	GE 8×8a	GE 8×8b	GE 9×9
Rod OD	inch	0.57	0.484	0.424	0.563	0.493	0.483	0.441
Cladding Thickness	inch	0.036	0.036	0.03	0.032	0.034	0.032	0.028
Pellet OD	inch	0.49	0.4045	0.3565	0.487	0.416	0.41	0.376
Active Fuel Length	inch	144	150	150	144	144	150	150
Plenum Length	inch	10.200	10.024	9.578	11.190	10.960	9.580	9.580
Spring Weight	lb	0.13	0.1	0.047	0.083	0.066	0.066	0.047
Backfill Pressure	psig	44.1	132.0	132.0	44.1	132.0	132.0	132.0
Fuel Mass	MTU	0.196	0.1793	0.1666	0.1977	0.1855	0.1847	0.1979
# of Fuel Rods		48	62	74	49	63	62	79
Free Volume	inch ³	2.426	1.708	1.469	3.236	2.181	1.970	1.758
Pressure (380°C)	psia	1264	1469	1359	971	1236	1345	1286
Stress Level	MPa	66.7	65.1	65.4	58.2	59.8	68.7	70.5

Table 4.4.7.1-3 Cladding Stress as a Function of Fuel Assembly Average Burnup and Temperature – Standard Configuration

Burnup	PWR Stress Level		BWR Stress Level	
	300°C	400°C	300°C	450°C
35,000 MWd/MTU	95.4 MPa	112.3 MPa	55.9 MPa	70.8 MPa
40,000 MWd/MTU	99.9 MPa	117.4 MPa	61.8 MPa	78.2 MPa
45,000 MWd/MTU	104.2 MPa	122.6 MPa	67.6 MPa	85.5 MPa

Table 4.4.7.1-4 Maximum Allowable Initial Storage Temperature (°C) As a Function of Initial Cladding Stress and Initial Cool Time – Standard Configuration

MPa	5 years	6 years	7 years	10 years	15 years
5	509.2	487.3	455.9	447	436.5
10	488.8	465.5	426.4	403	385.6
20	465.2	415.5	380.1	372.4	366
30	430.4	397	370.1	363.8	356.5
40	408.1	389	363.2	356.6	350
50	400.6	384	359.7	353.1	346.5
60	395.6	380.4	355.9	349.6	343.1
70	391.9	376.5	352.5	347	340
80	388.2	375	350.8	345.2	337.6
90	385.7	372	348.8	342.8	336.1
100	380.7	369.3	346.2	341	333.2
110	375.2	365.9	344.6	338	332.1
120	370	362.4	339.5	334.3	328.2
130	363.5	355.2	332.2	326.6	320
140	355	346.6	324.2	318.6	312.6
150	346.9	339.1	316.5	311.2	306
160	339.6	331.4	310.3	304.7	299.9

Table 4.4.7.1-5 Maximum Allowable Cladding Temperature for PWR and BWR Fuel Assemblies – Standard Configuration

Cool Time [years]	PWR Clad Temperature Limit [°C]			BWR Clad Temperature Limit [°C]		
	Burnup [MWD/MTU]			Burnup [MWD/MTU]		
	35,000	40,000	45,000	35,000	40,000	45,000
5	376	374	371	394	391	389
6	367	365	364	379	376	376
7	346	345	343	355	353	352
10	340	339	338	349	348	346
15	333	333	332	343	341	339

Table 4.4.7.1-6 Cladding Maximum Temperature as a Function of Basket Heat Load (PWR) – Standard Configuration

Fuel Clad		Heat Load
Temp (°F)	Temp (°C)	kW
560	293.3	17
645	340.6	21
675	357.2	23

Table 4.4.7.1-7 Cladding Maximum Temperature as a Function of Basket Heat Load (BWR) – Standard Configuration

Fuel Clad		Heat Load
Temp (°F)	Temp (°C)	kW
560	293.3	18
620	326.7	21
660	348.9	23

Table 4.4.7.1-8 Maximum Allowable Decay Heat for Standard Configuration PWR and BWR Universal Storage Systems

Cool Time ¹ [years]	PWR Burnup [MWD/MTU]			BWR Burnup [MWD/ MTU]		
	35,000	40,000	45,000	35,000	40,000	45,000
5	23 kW	23 kW	23 kW	23 kW	23 kW	23 kW
6	22.4 kW	22.1 kW	21.9 kW	23 kW	23 kW	23 kW
7	20.2 kW	20.1 kW	20 kW	22.1 kW	21.9 kW	21.8 kW
10	19.7 kW	19.6 kW	19.5 kW	21.6 kW	21.5 kW	21.4 kW
15	19.1 kW	19 kW	18.9 kW	21.1 kW	20.9 kW	20.7 kW

1. Based on temperature bias shown in Table 4.4.7.1-9.

Table 4.4.7.1-9 Temperature Bias Applied to Maximum Allowable Decay Heats

Cool Time [years]	PWR Clad Temperature Bias [°C] Burnup [MWD/MTU]			BWR Clad Temperature Bias [°C] Burnup [MWD/MTU]		
	35,000	40,000	45,000	35,000	40,000	45,000
5	-15	-15	-14	-18	-17	-18
6	-15	-15	-16	-18	-17	-19
7	-15	-15	-14	-16	-16	-17
10	-15	-15	-15	-16	-16	-15
15	-15	-16	-16	-15	-16	-16

4.4.7.2 Maximum Allowable Cladding Temperature and Canister Heat Load for the Advanced Configuration

The NAC High Burnup Topical Report 790-TR-001 provides the bases for determining the peak clad temperature (PCT) limit based on saturated cladding creep. The current NRC limit for total creep strain is 1%. The creep of the fuel cladding in dry storage is influenced by the PCT, its rate of change, and the fuel burnup. The fuel burnup determines:

- The assembly heat load as a function of cooling time
- The fission gas inventory in the fuel rod and thus, with the fuel rod geometry and helium inventory, defines the gas pressure, the driving force of creep
- The waterside oxide thickness on the cladding – this reduces the effective clad thickness and thus increases hoop stress and creep
- The amount of hydrogen in the cladding – this hardens the cladding and thus reduces creep
- The amount of irradiation damage to the cladding – this hardens the cladding and reduces creep.

The maximum allowable heat load for the Advanced configuration canister containing PWR fuel is 29.2 kW. Different canister loading configurations can be utilized that meet this canister heat load limit. However, only some of these will minimize the PCT in the canister. In this regard, an optimized three-zone loading pattern was established for PWR fuel, as shown in Figure 4.4.7.2-1, to conservatively limit the maximum calculated PCT to 375°C (707°F). This PCT is calculated using the thermal models described in Section 4.4.1.2.

By ensuring that the individual PWR assembly heat loads comply with this preferential loading pattern, the current NRC 1% limit on total creep strain will be met without placing undue restrictions on the placement of spent fuel bundles over a broad range of burnups or requiring a canister load specific creep analysis. Note that the NAC High Burnup Topical Report 790-TR-001 justifies the acceptance of a total creep strain of 2.5%.

Using the methodology developed in the NAC High Burnup Topical Report, the earlier CSFM-based PCT limit criterion is replaced with a canister zone based limit on the maximum allowed fuel assembly heat load. Table 4.4.7.2-1

The cooling times in this table are based on [REDACTED]
[REDACTED]
[REDACTED]
[REDACTED]

For specific PWR canister loading situations, the actual cooling times required to meet the assembly heat load limits by zone may be less than the values shown on Table 4.4.7.2-1. [REDACTED]
[REDACTED]
[REDACTED]
[REDACTED]

It should be noted that if the heat load or the burnup of a spent fuel assembly in the cask is outside the applicability range given in Table 4.4.7.2-1, [REDACTED]
[REDACTED]
[REDACTED]

The following sections will:

- Demonstrate that the PCT in dry storage becomes bounding when all spent fuel assemblies in dry storage are at the highest allowed burnup level (55 GWD/MTU)
- Describe how the bounding PCT for the three-zone PWR loading pattern are obtained
- Demonstrate that for the bounding PCT the 1% creep limit can be met within the 15 GWD/MTU to 55 GWD/MTU target burnup range of all PWR fuel
- Determine the PCT margin to the conservative creep limit of 1%
- Establish a conservative PCT limit based on the above PCT margin.

4.4.7.2.1 Bounding PCT History at the Highest Allowed Burnup

The PCT in the canister decreases as a function of dry storage time. For a given burnup and internal rod pressure level, the maximum initial PCT and its rate of change determine the total accumulated creep strain. The rate at which the PCT decreases in dry storage is determined by the decaying heat load of each spent fuel assembly. The reduction in the assembly heat load is controlled by isotopic decay. [REDACTED]
[REDACTED]

[REDACTED]

The higher the assembly burnup [REDACTED]
[REDACTED] This is shown in Figure 4.4.7.2-2 [REDACTED],
and demonstrated in Table 4.4.7.2-2 for the three canister zone heat load limits. The rate of heat
load reduction shown in Table 4.4.7.2-2 [REDACTED]
[REDACTED]
[REDACTED]
[REDACTED]

[REDACTED]
[REDACTED]
[REDACTED]
[REDACTED]
[REDACTED]
[REDACTED]
[REDACTED]

4.4.7.2.2 Bounding PCT History for the Three-Zone Loading Pattern

Based on the bounding decay heat curve for the limiting [REDACTED] fuel at 55 GWD/MTU
burnup, as shown in Figure 4.4.7.2-2, a total of 11 cases for different PWR canister heat loads as
a function of time in storage are established and shown on the following table.

The analysis in this section uses the methodology of 790-TR-001, maintains the fundamental conservatisms, [REDACTED]

4.4.7.2.3.1 Burnup Dependent Input Parameters for Dry Storage Creep Analysis

End-of Life (EOL) Pressure/Temperature State

Following the methodology of 790-TR-001, the end of life (EOL) fuel rod pressure and gas temperature was evaluated as a function of burnup. As shown in the Topical Report, the rod pressure was determined for fuel rods [REDACTED]

[REDACTED]

[REDACTED]

[REDACTED]

Fuel Rod Gas Temperature Decay Curve

The methodology for generating the temperature decay curve of the gas inside the spent fuel rod is described in Topical Report 790-TR-001. The gas temperature curve used for this evaluation is shown in Figure 4.4.7.2-3 [REDACTED]

[REDACTED]

Initial Gas Volume

As discussed in 790-TR-001,

[REDACTED]

Maximum Measured Oxide Thickness versus Burnup

In 790-TR-001, a maximum oxide thickness of 100 μm (4 mils) was used.

[REDACTED]

The DSCREEP methodology is conservative,

[REDACTED]

[REDACTED]

[REDACTED]

[REDACTED]

Data from Figure 2-3 from 790-TR-001 shows [REDACTED]

[REDACTED]

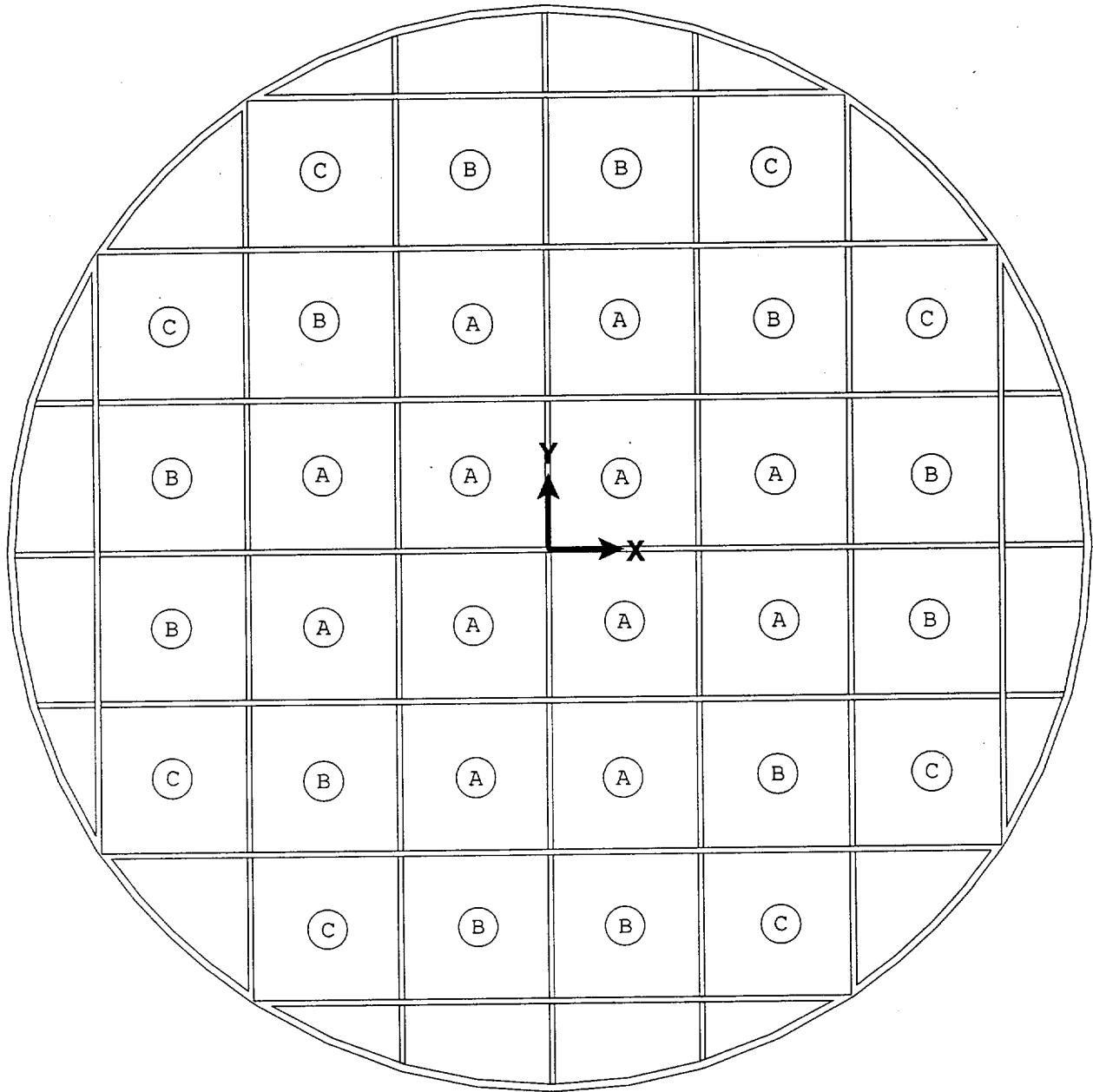
[REDACTED]

[REDACTED]

[REDACTED]

[REDACTED] Therefore, it is conservative to establish a PCT limit of 390°C for the PWR fuel based on the methodology of 790-TR-001.

Figure 4.4.7.2-1 Maximum Allowable Assembly Heat Load by PWR Canister Zone – Advanced Configuration



	Zone A	Zone B	Zone C
Maximum Allowed Heat Load	0.7 kW	1.0 kW	1.1 kW

Figure 4.4.7.2-2

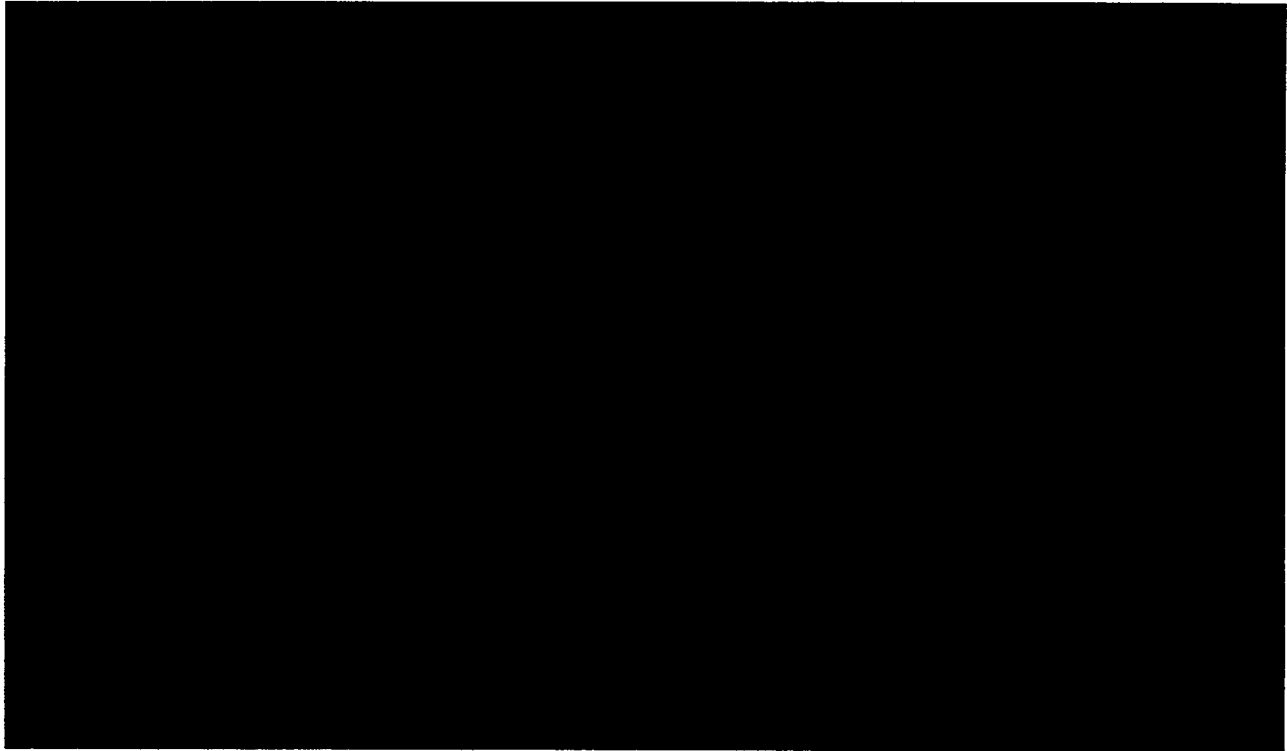


Figure 4.4.7.2-3

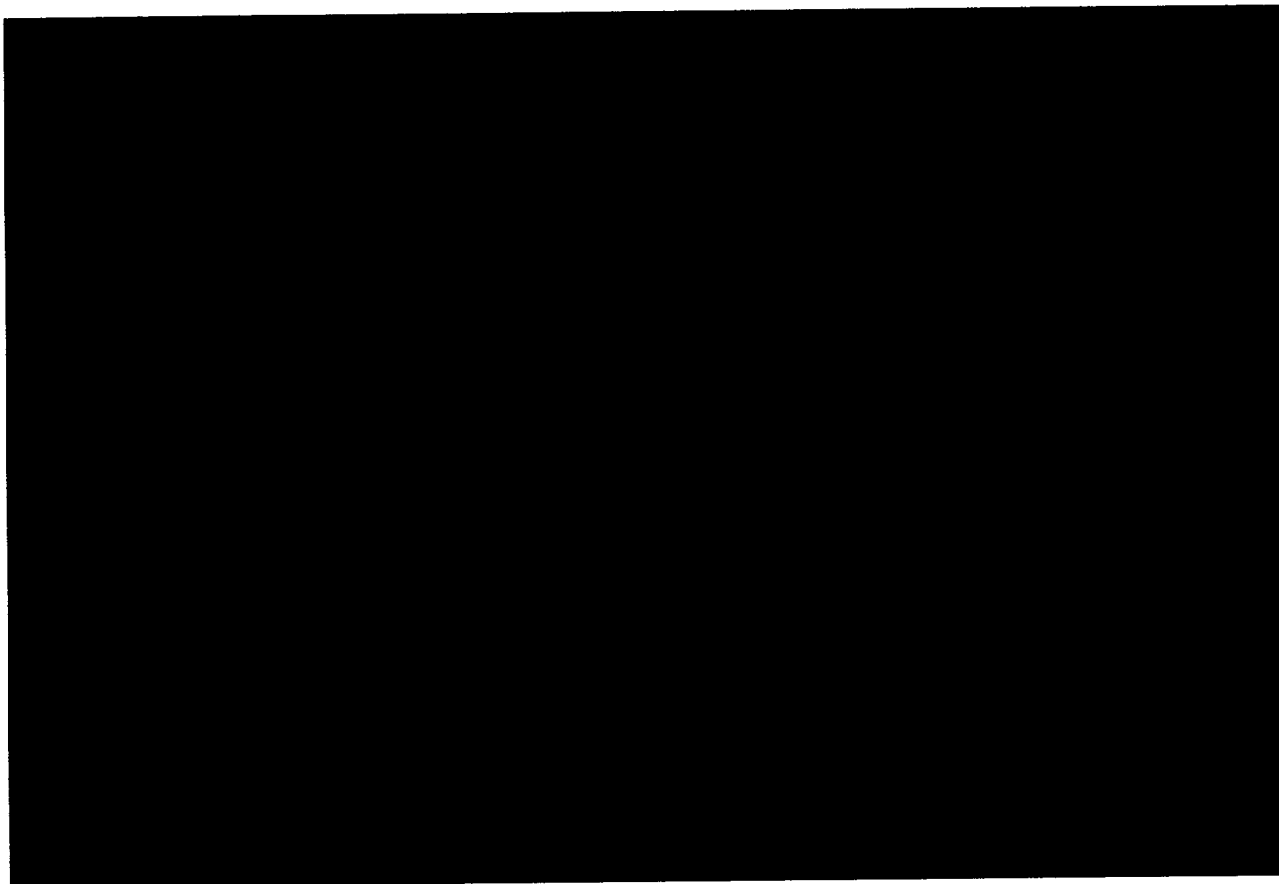


Figure 4.4.7.2-4

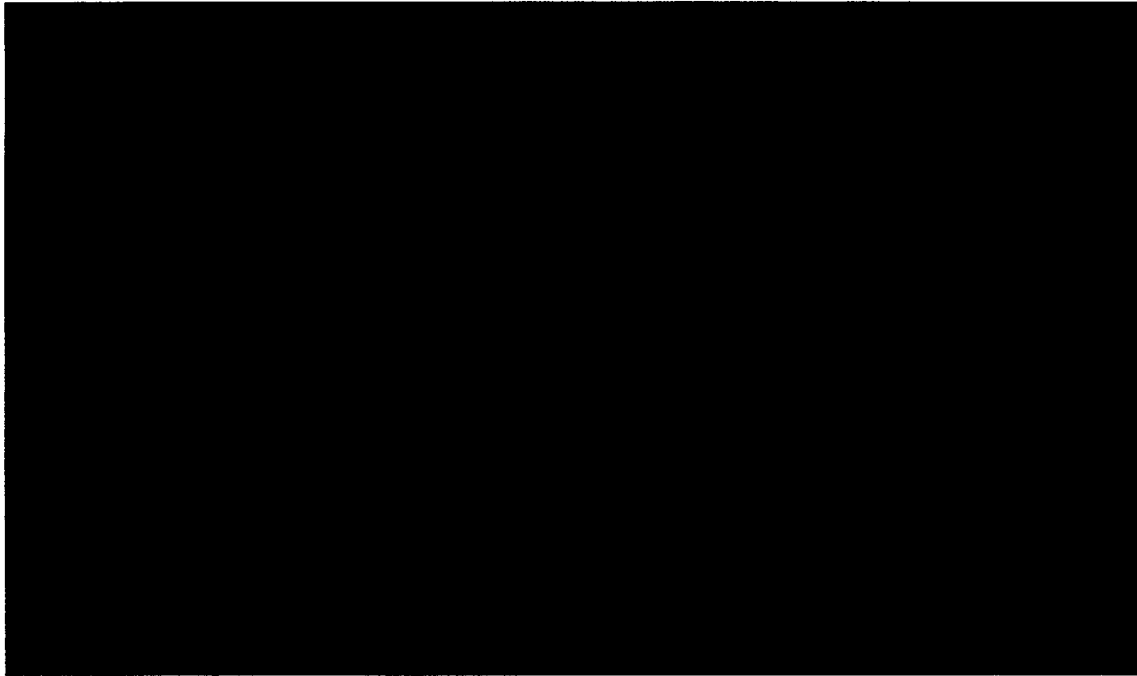


Figure 4.4.7.2-5

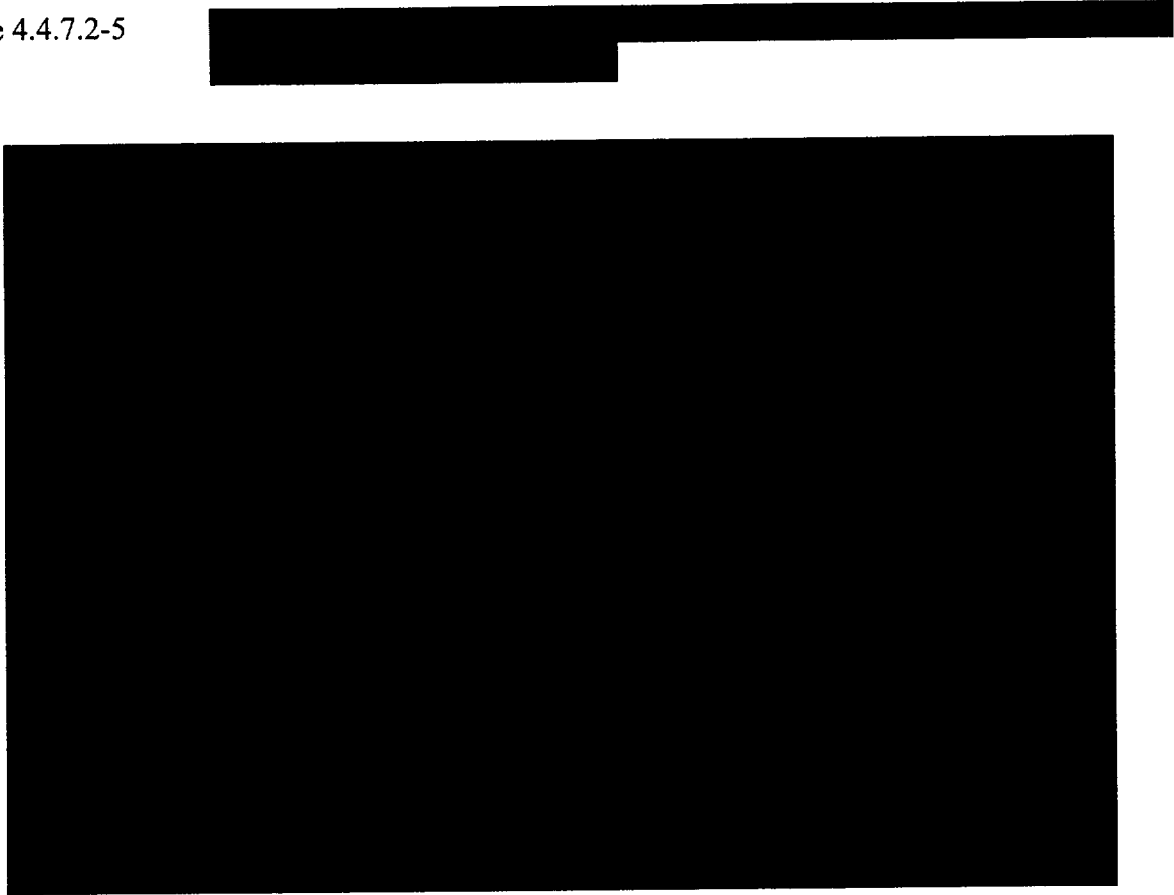


Figure 4.4.7.2-6

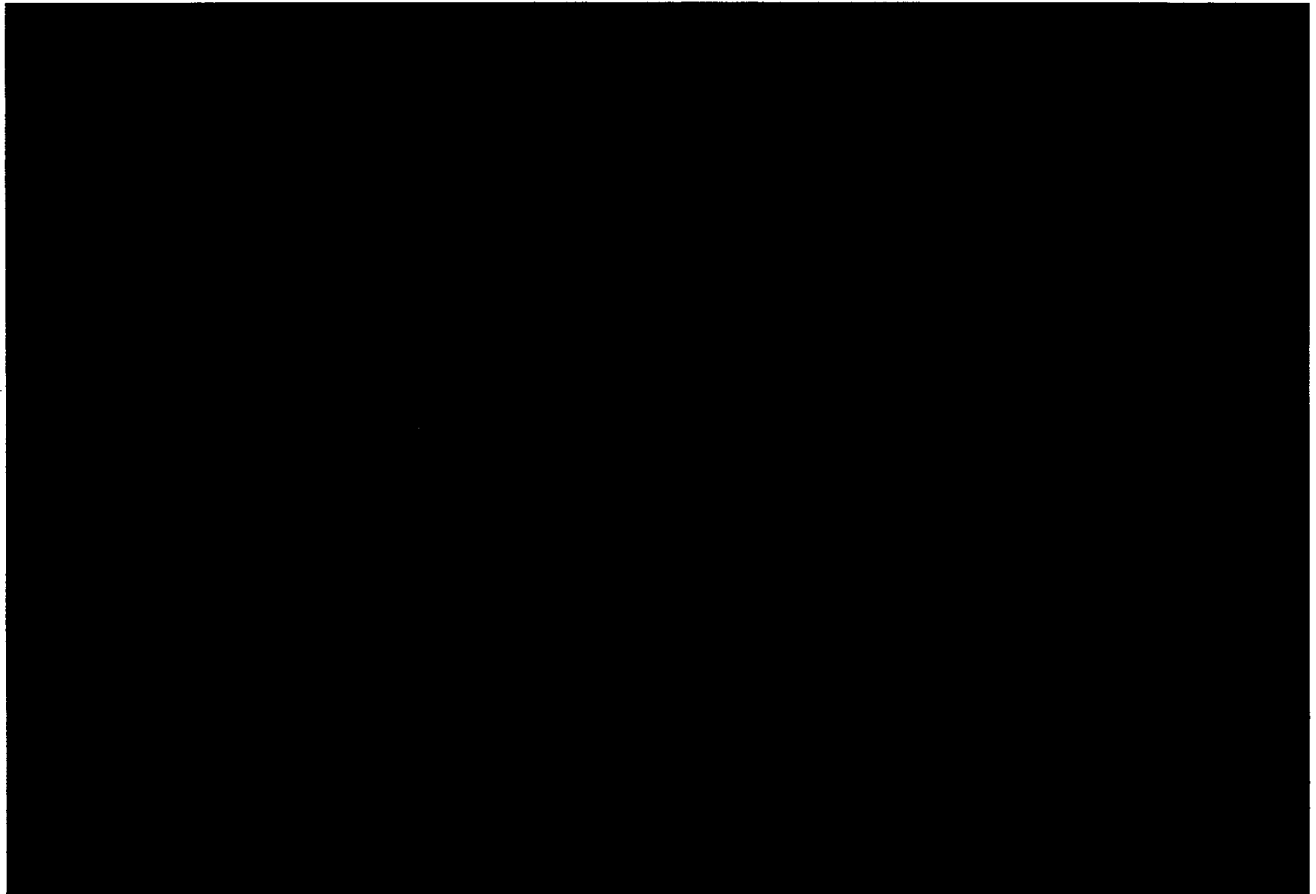


Figure 4.4.7.2-7

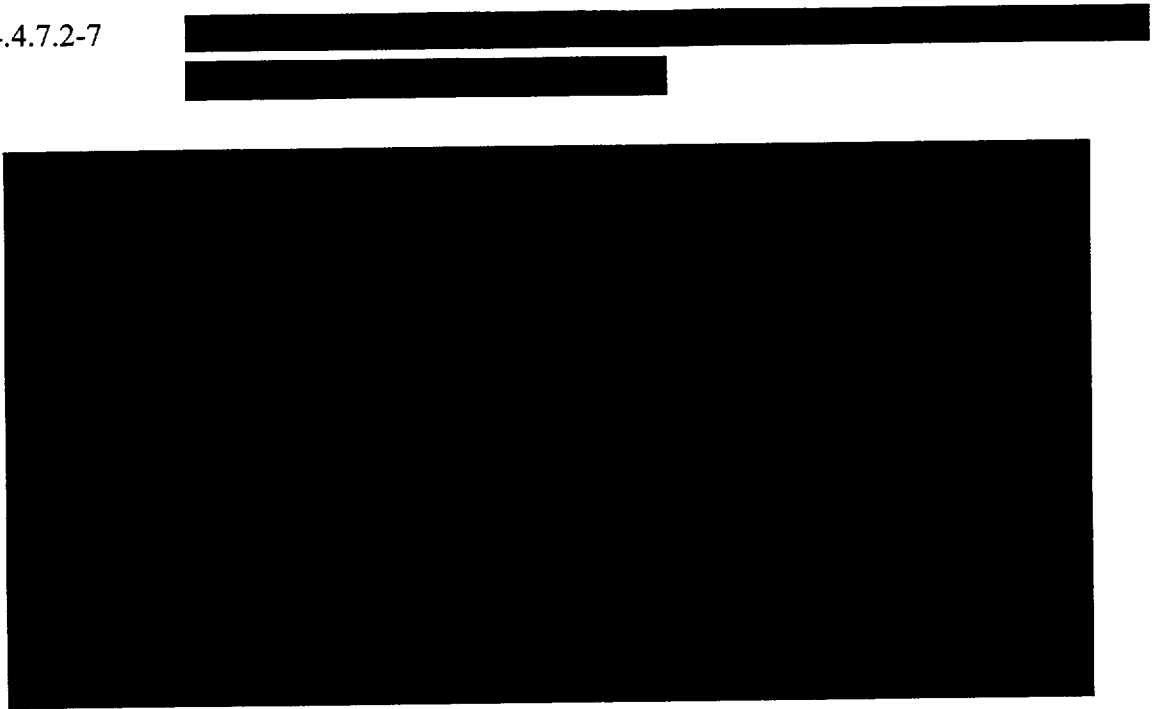


Table 4.4.7.2-1

[Redacted text block]

[Redacted]	[Redacted]	[Redacted]	[Redacted]
[Redacted]	[Redacted]	[Redacted]	[Redacted]
[Redacted]	[Redacted]	[Redacted]	[Redacted]
[Redacted]	[Redacted]	[Redacted]	[Redacted]
[Redacted]	[Redacted]	[Redacted]	[Redacted]
[Redacted]	[Redacted]	[Redacted]	[Redacted]
[Redacted]	[Redacted]	[Redacted]	[Redacted]
[Redacted]	[Redacted]	[Redacted]	[Redacted]
[Redacted]	[Redacted]	[Redacted]	[Redacted]

Table 4.4.7.2-2

[Redacted text block]

[Redacted]	[Redacted]	[Redacted]	[Redacted]
[Redacted]	[Redacted]	[Redacted]	[Redacted]
[Redacted]	[Redacted]	[Redacted]	[Redacted]
[Redacted]	[Redacted]	[Redacted]	[Redacted]
[Redacted]	[Redacted]	[Redacted]	[Redacted]
[Redacted]	[Redacted]	[Redacted]	[Redacted]
[Redacted]	[Redacted]	[Redacted]	[Redacted]
[Redacted]	[Redacted]	[Redacted]	[Redacted]

Table 4.4.7.2-3

[Redacted]

[Redacted]	[Redacted]	[Redacted]	[Redacted]
[Redacted]	[Redacted]	[Redacted]	[Redacted]
[Redacted]	[Redacted]	[Redacted]	[Redacted]
[Redacted]	[Redacted]	[Redacted]	[Redacted]
[Redacted]	[Redacted]	[Redacted]	[Redacted]
[Redacted]	[Redacted]	[Redacted]	[Redacted]
[Redacted]	[Redacted]	[Redacted]	[Redacted]
[Redacted]	[Redacted]	[Redacted]	[Redacted]
[Redacted]	[Redacted]	[Redacted]	[Redacted]

Table 4.4.7.2-4

[Redacted]

[Redacted]	[Redacted]	[Redacted]	[Redacted]
[Redacted]	[Redacted]	[Redacted]	[Redacted]
[Redacted]	[Redacted]	[Redacted]	[Redacted]
[Redacted]	[Redacted]	[Redacted]	[Redacted]
[Redacted]	[Redacted]	[Redacted]	[Redacted]
[Redacted]	[Redacted]	[Redacted]	[Redacted]
[Redacted]	[Redacted]	[Redacted]	[Redacted]
[Redacted]	[Redacted]	[Redacted]	[Redacted]
[Redacted]	[Redacted]	[Redacted]	[Redacted]

Table 4.4.7.2-5

[Redacted]

[Redacted]	[Redacted]	[Redacted]	[Redacted]
[Redacted]	[Redacted]	[Redacted]	[Redacted]
[Redacted]	[Redacted]	[Redacted]	[Redacted]
[Redacted]	[Redacted]	[Redacted]	[Redacted]
[Redacted]	[Redacted]	[Redacted]	[Redacted]
[Redacted]	[Redacted]	[Redacted]	[Redacted]
[Redacted]	[Redacted]	[Redacted]	[Redacted]
[Redacted]	[Redacted]	[Redacted]	[Redacted]
[Redacted]	[Redacted]	[Redacted]	[Redacted]

THIS PAGE INTENTIONALLY LEFT BLANK

4.4.8 Evaluation of System Performance for Normal Conditions of Storage

Results of thermal analysis of the Universal Storage System containing PWR or BWR fuel under normal conditions of storage are summarized in Section 4.4.3.1 for the Standard configuration and Section 4.4.3.2 for the Advanced configuration. The maximum PWR and BWR fuel rod cladding temperatures are below the allowable temperatures; temperatures of safety-related components during storage and transfer operations under normal conditions are maintained within their safe operating ranges; and thermally induced stresses in combination with pressure and mechanical load stresses are shown in the structural analysis of Chapter 3.0 to be less than the allowable stresses. Therefore, the Universal Storage System performance meets the requirements for the safe storage of design basis fuel under the normal operating conditions specified in 10 CFR 72.

THIS PAGE INTENTIONALLY LEFT BLANK

4.5 Thermal Evaluation for Site Specific Spent Fuel

This section presents the thermal evaluation of fuel assemblies or configurations, which are unique to specific reactor sites or which differ from the UMS[®] Storage System design basis fuel. These site specific configurations result from conditions that occurred during reactor operations, participation in research and development programs, and from testing programs intended to improve reactor operations. Site specific fuel includes fuel assemblies that are uniquely designed to accommodate reactor physics, such as axial fuel blanket and variable enrichment assemblies, and fuel that is classified as damaged. Damaged fuel includes fuel rods with cladding that exhibit defects greater than pinhole leaks or hairline cracks.

Site specific fuel assembly configurations are either shown to be bounded by the analysis of the standard design basis fuel assembly configuration of the same type (PWR or BWR), or are shown to be acceptable contents by specific evaluation.

4.5.1 Maine Yankee Site Specific Spent Fuel

Maine Yankee site specific fuel is stored in the Standard configuration of the Universal Storage System. The standard spent fuel assembly for the Maine Yankee site is the Combustion Engineering (CE) 14×14 fuel assembly. Fuel of the same design has also been supplied by Westinghouse and by Exxon. The standard 14×14 fuel assembly is included in the population of the design basis PWR fuel assemblies for the UMS[®] Storage System (See Table 2.1.1-1). The maximum decay heat for the standard Maine Yankee fuel is the design basis heat load for the PWR fuels (23 kW total, or 0.958 kW per assembly). This heat load is bounded by the thermal evaluations in Section 4.4 for the normal conditions of storage, Section 4.4.3.1 for less than design basis heat loads and Chapter 11 for off-normal and accident conditions.

Some Maine Yankee site specific fuel has a burnup greater than 45,000 MWD/MTU, but less than 50,000 MWD/MTU. This fuel is evaluated in Section 4.5.1.2. As shown in that section, loading of fuel assemblies in this burnup range is subject to preferential loading in designated basket positions in the Transportable Storage Canister and certain fuel assemblies in this burnup range must be loaded in a Maine Yankee fuel can.

The site specific fuels included in this evaluation are:

1. Consolidated fuel rod lattices consisting of a 17 × 17 lattice fabricated with 17 × 17 grids, 4 stainless steel support rods and stainless steel end fittings. One of these

- lattices contains 283 fuel rods and 2 rod position vacancies. The other contains 172 fuel rods, with the remaining rod position locations either empty or containing stainless steel dummy rods.
2. Standard fuel assemblies with a Control Element Assembly (CEA) inserted in each one.
 3. Standard fuel assemblies that have been modified by removing damaged fuel rods and replacing them with stainless steel dummy rods, solid zirconium rods, or 1.95 wt % enriched fuel rods.
 4. Standard fuel assemblies that have had the burnable poison rods removed and replaced with hollow Zircaloy tubes.
 5. Standard fuel assemblies with in-core instrument thimbles stored in the center guide tube.
 6. Standard fuel assemblies that are designed with variable enrichment (radial) and axial blankets.
 7. Standard fuel assemblies that have some fuel rods removed.
 8. Standard fuel assemblies that have damaged fuel rods.
 9. Standard fuel assemblies that have some type of damage or physical alteration to the cage (fuel rods are not damaged).
 10. Two (2) rod holders, designated CF1 and CA3. CF1 is a lattice having approximately the same dimensions as a standard fuel assembly. It is a 9×9 array of tubes, some of which contain damaged fuel rods. CA3 is a previously used fuel assembly lattice that has had all of the rods removed, and in which damaged fuel rods have been inserted.
 11. Standard fuel assemblies that have damaged fuel rods stored in their guide tubes.
 12. Standard fuel assemblies with inserted startup sources and other non-fuel items.

The Maine Yankee site specific fuels are also described in Section 1.3.2.1.

The thermal evaluations of these site specific fuels are provided in Section 4.5.1.1. Section 4.5.1.2 presents the evaluation of Maine Yankee fuel inventory that is not bounded by the evaluation performed in Section 4.4.7. This fuel may have higher burnup than the design basis fuel, have a higher decay heat on a per assembly basis, have a burnup/cool time condition that is outside of the cladding temperature evaluation presented in Section 4.4.7, or be subject to all of these differences.

4.5.1.1 Thermal Evaluation for Maine Yankee Site Specific Spent Fuel

The maximum heat load per assembly for site specific fuel considered in this section is limited to the design basis heat load (0.958 kW). The evaluation of fuel configurations having a greater heat load is presented in Section 4.5.1.2.

4.5.1.1.1 Consolidated Fuel

There are two (2) consolidated fuel lattices. One lattice contains 283 fuel rods and the other contains 172 fuel rods. Conservatively, only one consolidated fuel lattice is loaded in any Transportable Storage Canister.

The maximum decay heat of the consolidated fuel lattice having 283 fuel rods is 0.279 kW. This heat load is bounded by the design basis PWR fuel assembly, since it is less than one-third of the design basis heat load.

The second consolidated fuel lattice has 172 fuel rods with 76 stainless steel dummy rods at the outer periphery of the lattice. Due to the existence of the stainless steel rods, the effective thermal conductivities of this assembly may be slightly lower than those of the standard CE 14×14 fuel assembly. While the stainless steel rods provide better conductance in the axial direction, the radiation heat transfer is less effective at the surface of stainless steel rods, as compared to the standard fuel rods. The radiation is a function of surface emissivity and the emissivity for stainless steel (0.36) is less than one-half of that for Zircaloy (0.75). A parametric study is performed to demonstrate that the thermal performance of the UMS PWR basket loading configuration consisting of 23 standard CE 14×14 fuel assemblies and the consolidated fuel lattice with stainless rods is bounded by that of the configuration consisting of 24 standard CE 14×14 fuel assemblies. Two finite element models are used in the study: a two-dimensional fuel assembly model and a three-dimensional periodic canister internal model.

The two-dimensional model is used to determine the effective thermal conductivities of the consolidated fuel lattice with stainless steel rods. Considering the symmetry of the consolidated fuel, the finite element model represents a one-quarter section as shown in Figure 4.5.1.1-1. The methodology used in Section 4.4.1.1.5 for the two-dimensional fuel model for PWR fuel is employed in this model. The model includes the fuel pellets, cladding, helium between the fuel rods, and helium occupying the gap between the fuel pellets and cladding. In addition, the

rods at the two outer layers are modeled as solid stainless steel rods to represent the configuration of this consolidated fuel lattice. Modes of heat transfer modeled include conduction and radiation between individual rods for steady-state condition. ANSYS PLANE55 conduction elements and LINK31 radiation elements are used in the model. Radiation elements are defined between rods and from rods to the boundary of the model. The effective conductivity for the fuel is determined using the procedure described in Section 4.4.1.1.5.

The three-dimensional periodic canister internal model consists of a periodic section of the canister internals. The model contains one support disk with two heat transfer disks (half thickness) on its top and bottom, the fuel assemblies, the fuel tubes and the helium in the canister, as shown in Figure 4.5.1.1-2. The purpose of this model is to compare the maximum fuel cladding temperatures of the following cases:

- 1) Base Case: All 24 positions loaded with standard CE 14×14 fuel assemblies.
- 2) Case 2: 23 positions with standard fuel, with one consolidated fuel lattice in position 2.
- 3) Case 3: 23 positions with standard fuel, with one consolidated fuel lattice in position 3.
- 4) Case 4: 23 positions with standard fuel, with one consolidated fuel lattice in position 4.
- 5) Case 5: 23 positions with standard fuel, with one consolidated fuel lattice in position 5.

Positions 2, 3, 4, and 5 are shown in Figure 4.5.1.1-3. Based on symmetry, these locations represent all of the possible locations for consolidated fuel in the basket.

The fuel assemblies and fuel tubes are represented by homogeneous regions with effective thermal conductivities. The effective conductivities for the consolidated fuel are determined by the two-dimensional fuel assembly model discussed above. The effective conductivities for the CE 14×14 fuel assemblies are established based on the model described in Section 4.4.1.1.5. Effective properties for the fuel tubes are determined by the two-dimensional fuel tube model in Section 4.4.1.1.6. Volumetric heat generation corresponding to the design basis heat load of 0.958 kW per assembly is applied to the CE 14×14 fuel regions in the model. Similarly, a heat generation rate corresponding to 0.279 kW is applied to the consolidated fuel assembly region. The heat conduction in the axial direction is conservatively ignored by assuming that the top and

bottom surfaces of the model are adiabatic. A constant temperature of 400°F is applied to the outer surface of the model as boundary conditions. Note that the maximum canister temperature is 351°F for PWR configurations for the normal condition of storage (Table 4.1-4). Steady state thermal analysis is performed for all five cases and the calculated maximum fuel cladding temperatures in the model are:

	Base Case	Case 2	Case 3	Case 4	Case 5
Maximum Fuel Cladding Temperature (°F)	755	733	738	740	740

As shown, the maximum temperatures for Cases 2 through 5 are less than those of the Base Case. It is concluded that the thermal performance of the configuration consisting of 23 standard CE 14×14 fuel assemblies and one consolidated fuel lattice is bounded by that of the configuration consisting of 24 standard CE 14×14 fuel assemblies. This study shows that a consolidated fuel lattice can be located in any basket position. However, as shown in Table 12B2-6 in Chapter 12, the consolidated fuel assembly must be loaded in a corner position of the fuel basket (e.g., Position 5 shown in Figure 4.5.1.1-3).

4.5.1.1.2 Standard CE 14 × 14 Fuel Assemblies with Control Element Assemblies

A Control Element Assembly (CEA) consists of five solid B₄C rods encapsulated in stainless steel tubes. The B₄C material has a conductivity of 1.375 BTU/hr-in-°F. With the CEA inserted into the guide tubes of the CE 14×14 fuel assembly, the effective conductivity in the axial direction of the fuel assembly is increased because solid material replaces helium in the guide tubes. The change in the effective conductivity in the transverse direction of the fuel assembly is negligible since the CEA is inside of the guide tubes. Note that the total heat load, including the small amount of extra heat generated by the CEA, remains below the design basis heat load. Therefore, the thermal performance of the fuel assemblies with CEAs inserted is bounded by that of the standard fuel assemblies.

4.5.1.1.3 Modified Standard Fuel Assemblies

These assemblies include those standard fuel assemblies that have been modified by removing damaged fuel rods and replacing them with stainless steel dummy rods, solid zirconium rods or 1.95 wt % enriched fuel rods.

The maximum number of fuel rods replaced by stainless steel rods is six (6) per assembly, which is about 3% of the total number of fuel rods in each assembly (176). The conductivity of the stainless steel is similar to that of Zircaloy and better than that of the UO_2 . The resultant increase in effective conductivity of the modified fuel assembly in the axial direction offsets the decrease in the effective conductivity in the transverse direction (due to slight reduction of radiation heat transfer at the surface of the stainless steel rods). The maximum number of fuel rods replaced by solid Zirconium rods is five (5) per assembly. Since the solid Zirconium rod has a higher conductivity than the fuel rod (UO_2 with Zircaloy clad), the effective conductivity of the repaired fuel assembly is increased. The thermal properties for the enriched fuel rod remain the same as for standard fuel rods, so there is no change in effective conductivity of the fuel assembly results from the use of fuel rods enriched to 1.95 wt % ^{235}U . These rods replace other fuel rods in the assembly after the first or second burnup cycles were completed. Therefore, these replacement fuel rods have been burned a minimum of one cycle less than the remainder of the assembly, producing a proportionally lower per rod heat load. The heat load (on a per rod basis) of the fuel rods in a standard assembly, bounds the heat load of the 1.95 wt % ^{235}U enriched fuel rods. Consequently, the loading of modified fuel assemblies is bounded by the thermal evaluation of the standard fuel assembly.

4.5.1.1.4 Use of Hollow Zircaloy Tubes

Certain standard fuel assemblies have had the burnable poison rods removed. These rods were replaced with hollow Zircaloy tubes.

There are 16 locations where burnable poison rods were removed and hollow Zircaloy tubes were installed in their place. Since the maximum heat load for these assemblies is 0.552 kW per assembly (less than two-thirds of the design basis heat load) and the number of hollow Zircaloy rods is only about one-tenth (16/176) of the total number of the fuel rods, the thermal performance of these fuel assemblies is bounded by that of the standard fuel assemblies.

4.5.1.1.5 Standard Fuel with In-core Instrument Thimbles

Certain fuel assemblies have in-core instrument thimbles stored within the center guide tube of each fuel assembly. Storing an in-core instrument thimble assembly in the center guide tube of a fuel assembly will slightly increase the axial conductance of the fuel assembly (helium replaced by solid material). Therefore, there is no negative impact on the thermal performance of the fuel

assembly with this configuration. The thermal performance of these fuel assemblies is bounded by that of the standard fuel assemblies.

4.5.1.1.6 Standard Fuel Assemblies with Variable Enrichment and Axial Blankets

The Maine Yankee variably enriched fuel assemblies are limited to two batches of fuel, which have a maximum burnup less than 30,000 MWD/MTU. The variably enriched rods in the fuel assemblies have enrichments greater than 3.4 wt % ^{235}U , except that the axial blankets on one batch are enriched to 2.6 wt % ^{235}U . As shown in Table 12B2-8, fuel at burnups less than or equal to 30,000 MWD/MTU with any enrichment greater than, or equal to, 1.9 wt % ^{235}U may be loaded with 5 years cool time.

The thermal conductivities of the fuel assemblies with variable enrichment (radial) and axial blankets are considered to be essentially the same as those of the standard fuel assemblies. Since the heat load per assembly is limited to the design basis heat load, there is no effect on the thermal performance of the system due to this loading configuration.

4.5.1.1.7 Standard Fuel Assemblies with Removed Fuel Rods

Except for assembly number EF0046, the maximum number of missing fuel rods from a standard fuel assembly is 14, or 8% (14/176) of the total number of rods in one fuel assembly. The maximum heat load for any one of these fuel assemblies is conservatively determined to be 0.63 kW. This heat load is 34% less than the design basis heat load of 0.958 kW. Fuel assembly EF0046 was used in the consolidated fuel demonstration program and has only 69 rods remaining in its lattice. This fuel assembly has a heat load of 70 watts, or 7% of the design basis heat load of 0.958 kW. Therefore, the thermal performance of fuel assemblies with removed fuel rods is bounded by that of the standard fuel assemblies.

4.5.1.1.8 Fuel Assemblies with Damaged Fuel Rods

Damaged fuel assemblies are standard fuel assemblies with fuel rods with known or suspected cladding defects greater than hairline cracks or pinhole leaks. Fuel, classified as damaged, will be placed in a Maine Yankee fuel can. The primary function of the fuel can is to confine fuel material within the can and to facilitate handling and retrievability. The Maine Yankee fuel can is shown in Drawings 412-501 and 412-502. The placement of the loaded fuel cans is restricted

by the operating procedures and/or Technical Specifications to loading into the four fuel tube positions at the periphery of the fuel basket as shown in Figure 12B2-1. The heat load for each damaged fuel assembly is limited to the design basis heat load 0.958 kW (23 kW/24).

A steady-state thermal analysis is performed using the three-dimensional canister model described in Section 4.4.1.1.2 simulating 100% failure of the fuel rods, fuel cladding, and guide tubes of the damaged fuel held in the Maine Yankee fuel can. The canister is assumed to contain twenty (20) design basis PWR fuel assemblies and damaged fuel assemblies in fuel cans in each of the four corner positions.

Two debris compaction levels are considered for the 100% failure condition: (Case 1) 100% compaction of the fuel rod, fuel cladding, and guide tube debris resulting in a 52-inch debris level in the bottom of each fuel can, and (Case 2) 50% compaction of the fuel rod, fuel cladding, and guide tube debris resulting in a 104-inch debris level in the bottom of each fuel can. The entire heat generation rate for a single fuel assembly (i.e., 0.958 kW) is concentrated in the debris region with the remainder of the active fuel region having no heat generation rate applied. To ensure the analysis is bounding, the debris region is located at the lower part of the active fuel region in lieu of the bottom of the fuel can. This location is closer to the center of the basket where the maximum fuel cladding temperature occurs. The effective thermal conductivities for the design basis PWR fuel assembly (Section 4.4.1.1.5) are used for the debris region. This is conservative since the debris (100% failed rods) is expected to have higher density (better conduction) and more surface area (better radiation) than an intact fuel assembly. In addition, the thermal conductivity of helium is used for the remainder of the active fuel length. Boundary conditions corresponding to the normal condition of storage are used at the outer surface of the canister model (see Section 4.4.1.1.2). A steady-state thermal analysis is performed. The results of the thermal analyses performed for 100% fuel rod, fuel cladding, and guide tube failure are:

Description	Maximum Temperature (°F)			
	Fuel Cladding	Damaged Fuel	Support Disk	Heat Transfer Disk
Case 1 (100% Compaction)	654	672	598	594
Case 2 (50% Compaction)	674	594	620	616
Design Basis PWR Fuel	670	N/A	615	612
Allowable	716	N/A	650	650

As demonstrated, the extreme case of 100% fuel rod, fuel cladding, and guide tube failure with 50% compaction of the debris results in temperatures that are less than 1% higher than those calculated for the design basis PWR fuel. The maximum temperatures for the fuel cladding, damaged fuel assembly, support disks, and heat transfer disks remain within the allowable temperature range for both 100% failure cases. Additionally, the temperatures used in the structural analyses of the fuel basket envelop those calculated for both 100% failure cases.

Additionally, the above analysis has been repeated to consider a maximum heat load of 1.05 kW/assembly (maximum heat load for the 50,000 MWD/MTU fuel, see Section 4.5.1.2.1) in the Maine Yankee fuel cans. To maintain the 23 kW total heat load per canister, the model considers a heat load of 1.05 kW/assembly in the four (4) Maine Yankee fuel cans and 0.94 kW/assembly in the rest of the twenty (20) basket locations. The analysis results indicate that the maximum temperatures for the fuel cladding and basket components are slightly lower than those for the case with a heat load of 0.958 kW in the damaged fuel can, as presented above. The maximum fuel cladding temperature is 650°F (< 654°F) and 672°F (< 674°F) for 100% and 50% compaction ratio cases, respectively. Therefore, the case with 1.05 kW/assembly in the Maine Yankee fuel can is bounded by the case with 0.958 kW/assembly in the fuel cans.

4.5.1.1.9 Standard Fuel Assemblies with Damaged Lattice

Certain standard fuel assemblies may have damage or physical alteration to the lattice or cage that holds the fuel rods, but not exhibit damage to the fuel rods. Fuel assemblies with lattice damage are evaluated in Section 11.2.16. The structural analysis demonstrates that these assemblies retain their configuration in the design basis accident events and loading conditions.

The effective thermal conductivity for the fuel assembly used in the thermal analyses in Section 4.4 is determined by the two-dimensional fuel model (Section 4.4.1.1.5). The model conservatively ignores the conductance of the steel cage of the fuel assembly. Therefore, damage or physical alteration to the cage has no effect on the thermal conductivity of the fuel assembly used in the thermal models. The thermal performance of these fuel assemblies is bounded by that of the standard fuel assemblies.

4.5.1.1.10 Damaged Fuel Rod Holders

The Maine Yankee site specific fuel inventory includes two (2) damaged fuel rod holders designated CF1 and CA3. CF1 is a 9×9 array of tubes having roughly the same dimensions as a fuel assembly. Some of the tubes hold damaged fuel rods. CA3 is a previously used fuel assembly cage (i.e., a fuel assembly with all of the fuel rods removed), into which damaged fuel rods have been inserted.

Similar to the fuel assemblies that have damaged fuel rods, the damaged fuel rod holders will be placed in Maine Yankee fuel cans and their location in the basket is restricted to one of the four corner fuel tube positions of the basket. The decay heat generated by the fuel in each of these rod holders is less than one-fourth of the design basis heat load of 0.958 kW. Therefore, the thermal performance of the damaged fuel rod holders is bounded by that of the standard fuel assemblies.

4.5.1.1.11 Assemblies with Damaged Fuel Rods Inserted in Guide Tubes

Similar to fuel assemblies that have damaged fuel rods, fuel assemblies that have up to two damaged fuel rods or poison rods stored in each guide tube are placed in Maine Yankee fuel cans and their loading positions are restricted to the four corner fuel tubes in the basket. The rods inserted in the guide tubes can not be from a different fuel assembly (i.e., any rod in a guide tube originally occupied a rod position in the same fuel assembly). Storing fuel rods in the guide tubes of a fuel assembly slightly increases the axial conductance of the fuel assembly (helium replaced by solid material). The design basis heat load bounds the heat load for these assemblies. Therefore, the thermal performance of fuel assemblies with rods inserted in the guide tubes is bounded by that of the standard fuel assemblies.

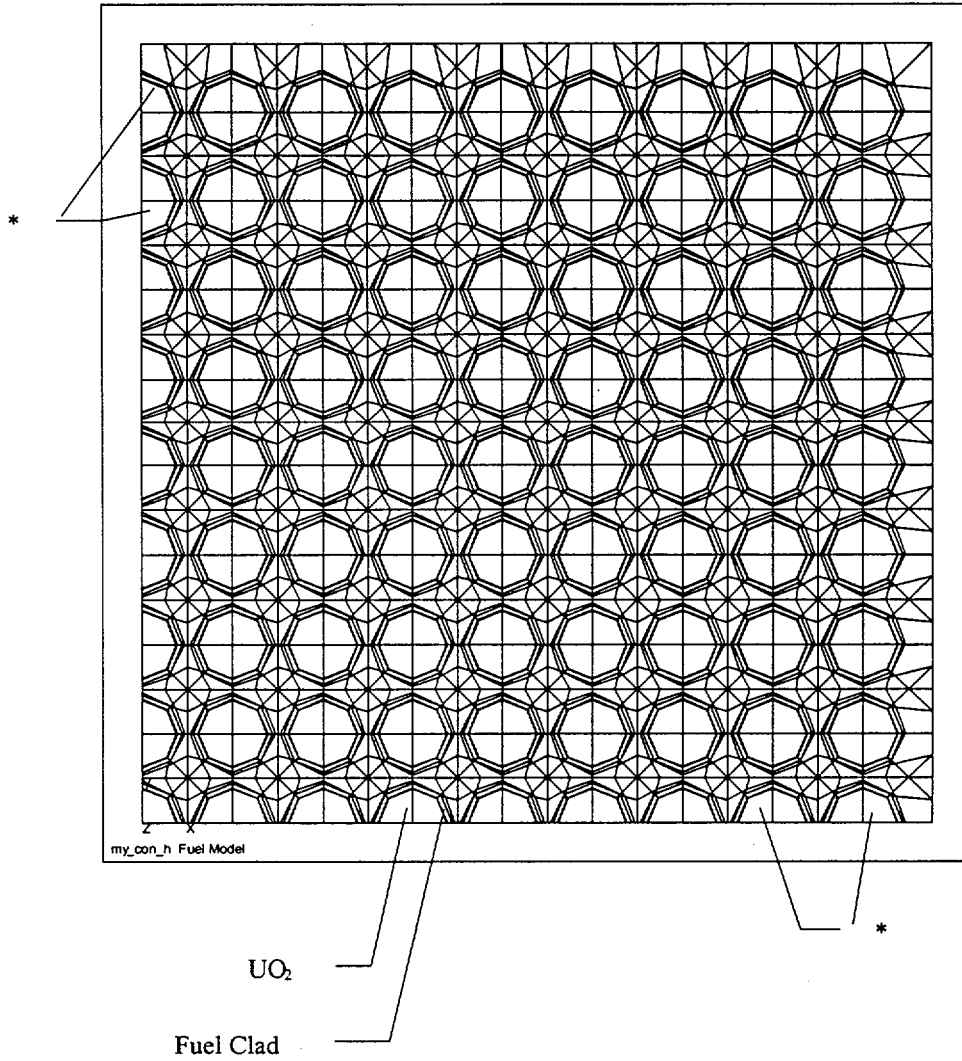
4.5.1.1.12 Standard Fuel Assemblies with Inserted Startup Sources and Other Non-Fuel Items

Five Control Element Assembly (CEA) fingertips and a 24-inch ICI segment may be placed into the guide tubes of a fuel assembly. In addition, four irradiated start-up neutron sources and one unirradiated source, having a combined total heat load of 15.4 watts, will be loaded into separate fuel assemblies. With the CEA fingertips and the neutron sources inserted into the guide tubes of the fuel assemblies, the effective conductivity in the axial direction of the fuel assembly is increased because solid material replaces helium in the guide tubes. The change in the effective

conductivity in the transverse direction of the fuel assembly is negligible, since the non-fuel items are inside of the guide tubes. In addition, the fuel assemblies that hold these non-fuel items are restricted to basket corner loading locations, which have an insignificant effect on the maximum fuel cladding and basket component temperatures at the center of the basket.

Note that the total heat load of the fuel assembly, including the small amount of extra heat generated by the CEA fingertips, ICI 24-inch segment, and the neutron sources, remains below the design basis heat load. Therefore, the thermal performance of the fuel assemblies with these non-fuel items inserted is bounded by that of the standard fuel assemblies.

Figure 4.5.1.1-1 Quarter Symmetry Model for Maine Yankee Consolidated Fuel



* Two outer layers (rows) of rods are modeled as stainless steel

Figure 4.5.1.1-2 Maine Yankee Three-Dimensional Periodic Canister Internal Model

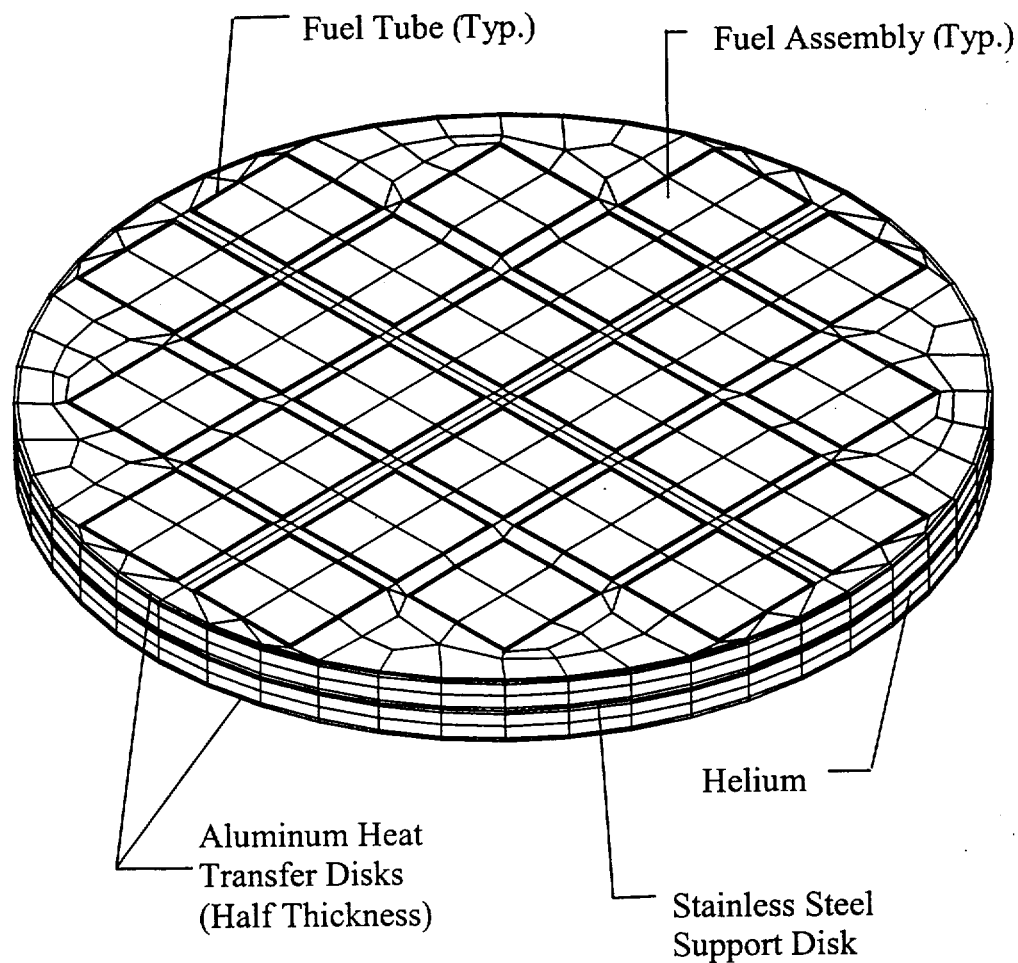


Figure 4.5.1.1-3 Evaluated Locations for the Maine Yankee Consolidated Fuel Lattice in the PWR Fuel Basket

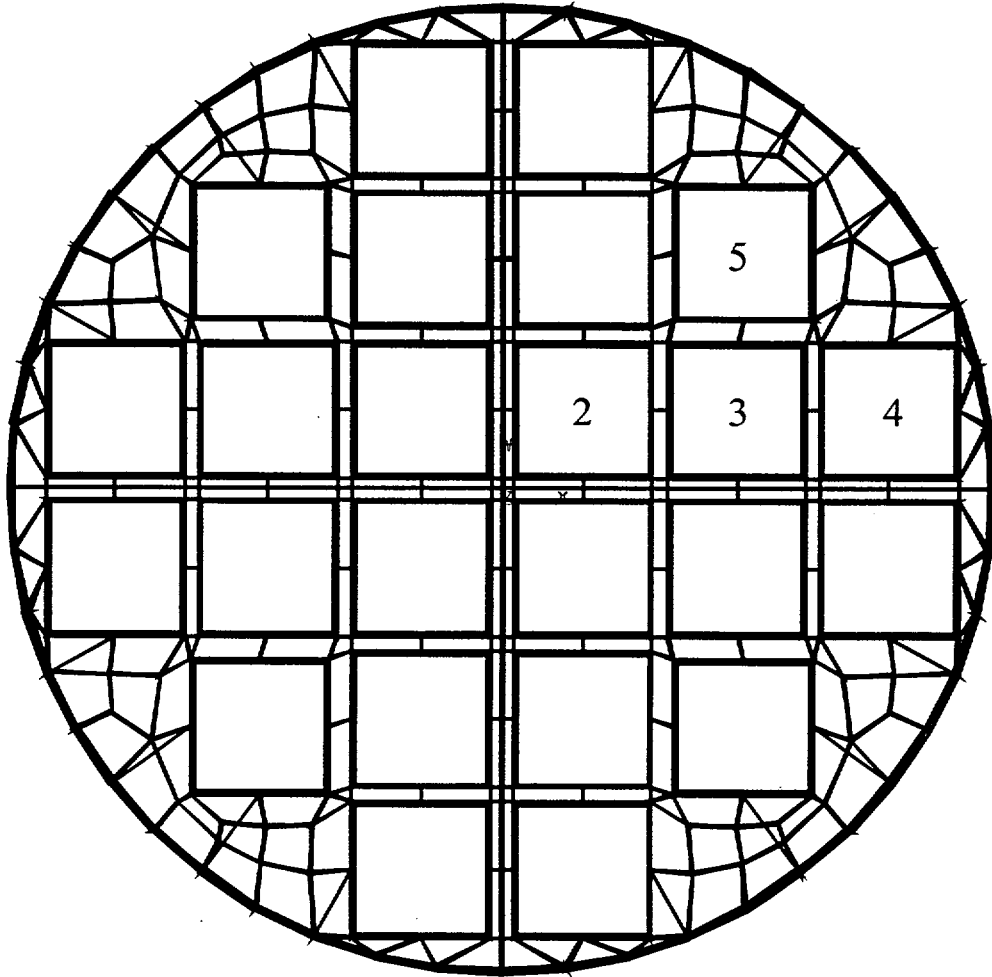
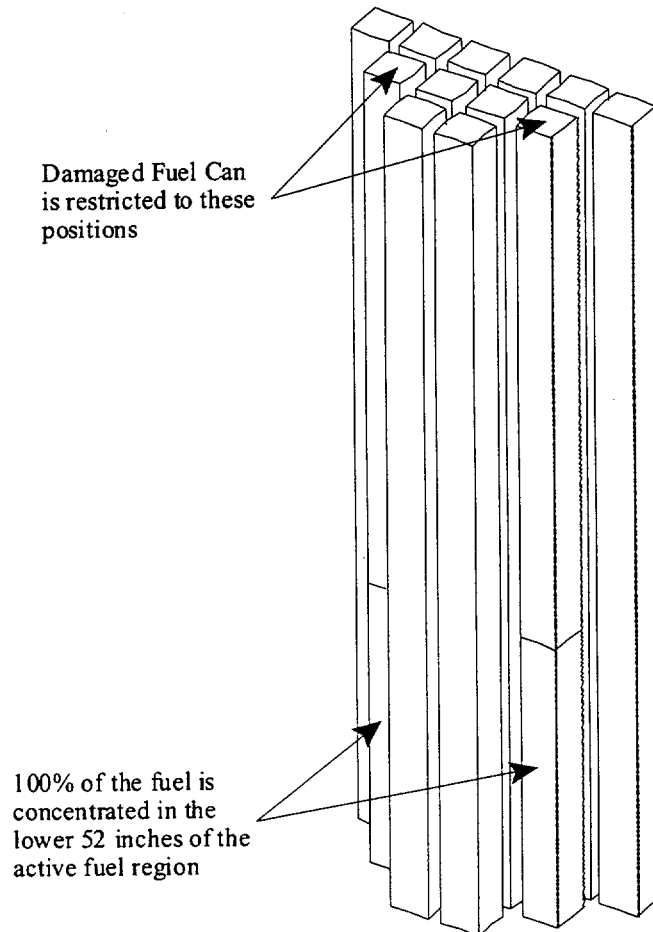
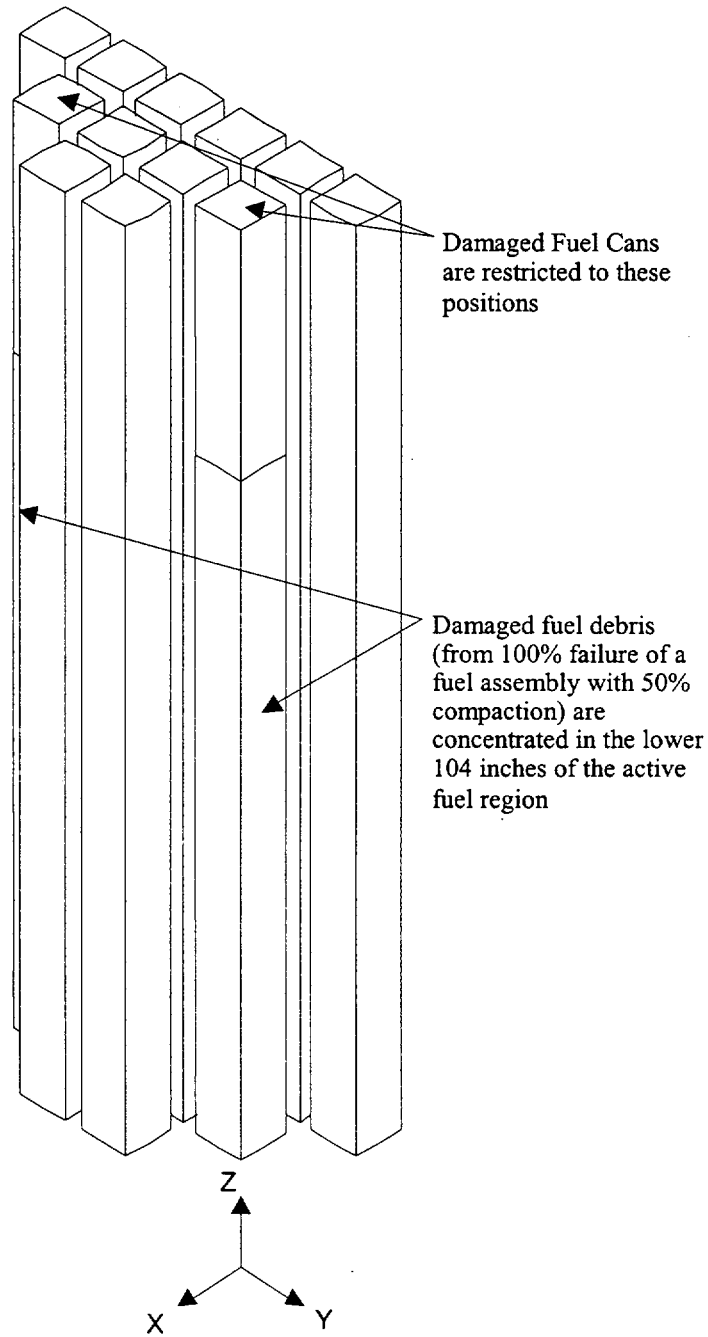


Figure 4.5.1.1-4 Active Fuel Region in the Three-Dimensional Canister Model



Note: Finite element mesh not shown for clarity.

Figure 4.5.1.1-5 Fuel Debris and Damaged Fuel Regions in the Three-Dimensional Canister Model



4.5.1.2 Maximum Allowable Heat Loads for Maine Yankee Site Specific Spent Fuel

This section includes evaluations for the Maine Yankee fuel inventory that is not bounded by the evaluation performed in Section 4.4.7. This fuel may have higher burnup than the design basis fuel, have a higher decay heat on a per assembly basis, have a burnup/cool time condition that is outside of the cladding temperature evaluation presented in Section 4.4.7, or be subject to all of these differences.

Maximum allowable clad temperatures and decay heats are evaluated for:

1. Fuel with burnup in excess of 45,000 MWD/MTU (maximum 50,000 MWD/MTU),
2. Preferential loading patterns with hotter fuel on the periphery of the basket, and
3. Preferential loading with fuel exceeding design basis heat load (0.958 kW) per assembly on the basket periphery.

As shown in Section 4.4.7, the standard CE 14×14 fuel assembly has a significantly lower cladding stress level than the equivalent burnup Westinghouse 14×14 assembly. It is, therefore, conservative to apply the characteristics of the design basis assembly to the CE 14×14 Maine Yankee fuel assemblies (Note that the Westinghouse 14×14 assembly evaluated in Section 4.4.7 is the fuel assembly used in Westinghouse reactors, but it is not the Westinghouse 14×14 assembly built for use in the CE reactors, such as the Maine Yankee reactor).

The maximum allowable decay heat, listed either on a per canister or per assembly basis, is combined with dose rate limits in Chapter 5 to establish cool time limits as a function of burnup and initial enrichment. Cool time limits are shown in Tables 5.6.1-10 for Maine Yankee fuel assemblies without installed control components, and in Table 5.6.1-12 for fuel assemblies with installed control components.

High burnup fuel (45,000 – 50,000 MWD/MTU) may be loaded as intact fuel provided that no more than 1% of the fuel rods in the assembly have a peak cladding oxide thickness greater than 80 microns, and no more than 3% of the fuel rods in the assembly have a peak oxide layer thickness greater than 70 microns. The high burnup fuel must be loaded as failed fuel (i.e., in a Maine Yankee fuel can), if these criteria are not met, or if the cladding oxide layer is detached or spalled from the cladding. Since the transportable storage canister is tested to be leak tight, no additional confinement analysis is required for the high burnup fuel.

4.5.1.2.1 Maximum Allowable Temperature and Decay Heat for 50,000 MWD/MTU Fuel

To evaluate higher burnup fuel, cladding oxidation layer thickness and fission gas release fractions are established. Maine Yankee reports that for high burnup fuel rods (i.e., rod peak burnup up to 55,000 MWD/MTU), ABB/Combustion Engineering Incorporated imposes a cladding oxide layer thickness of 120 microns as an operational limit and reports that the maximum gas release fraction (fuel pellet to rod plenum in intact fuel rods) is less than 3% [36]. Therefore, the allowable cladding temperature calculations employ a cladding oxide layer thickness of 0.012 cm (120 microns). This is conservative with respect to the 80 micron cladding oxide layer thickness considered for high burnup fuel that is loaded as intact fuel. A 12% release fraction, established for standard PWR fuel burned up to 45,000 MWD/MTU, is conservatively applied to higher burnup PWR fuel.

Using the evaluation method presented in Section 4.4.7 and a cladding oxidation layer thickness of 0.012 cm, the cladding stress levels for the 50,000 MWD/MTU burnup PWR assembly (maximum stress) are determined and listed in Table 4.5.1.2-1. The data is plotted against the generic allowable temperature curves in Figure 4.5.1.2-2. Included in Figure 4.5.1.2-2 are the 35,000 MWD/MTU to 45,000 MWD/MTU limit lines developed in Section 4.4.7. The intercept of the 50,000 MWD/MTU results in the limiting cladding temperatures shown in Table 4.5.1.2-2, which considers the 1% creep strain limit. The resulting maximum allowable heat load per canister for fuel assemblies with burnup of 50,000 MWD/MTU is listed in Table 4.5.1.2-3.

4.5.1.2.2 Preferential Loading with Hotter Fuel on the Periphery of the Basket

The design basis heat load for the UMS thermal analysis is 23 kW uniformly distributed throughout the basket (0.958 kW per assembly). This heat load applies to the basket structural components at any initial fuel loading time. Further reduction in heat load is required for the Maine Yankee fuel assemblies that fall outside the bounds of the requirement of maximum heat load as shown in Tables 4.4.7.1-8 and 4.5.1.2-3. These assemblies include:

1. Fuel assemblies (with specific burnup and cool time) that may exceed the maximum allowable decay heat dictated by their cladding temperature allowable (exceeding the limits as shown in Tables 4.4.7.1-8 and 4.5.1.2-3), if loaded uniformly (all 24 fuel assemblies with the same burnup and cool time, i.e., the same decay heat).
2. Fuel assemblies that are expected to exceed the design basis heat load of 0.958 kW per assembly (maximum heat per assembly less than 1.05 kW).

To ensure that these fuel assemblies do not exceed their allowable cladding temperatures, a loading pattern is considered that places higher heat load assemblies at the periphery of the basket (Positions "A" in Figure 4.5.1.2-1) and compensates by placing lower heat load assemblies in the basket interior positions (Positions "B" in Figure 4.5.1.2-1). There are 12 interior basket locations and 12 peripheral basket locations in the UMS PWR basket design. The maximum total basket heat loads indicated in Tables 4.4.7.1-8 and 4.5.1.2-3 are maintained for these peripheral loading scenarios.

Two preferential loading scenarios are evaluated. The first approach limits any assembly to the 0.958 kW design basis heat load limit (23 kW divided by 24 assemblies), while the second approach increases the per assembly heat load limit to 1.05 kW for assemblies in the basket peripheral locations. The split approach allows maximum flexibility at fuel loading.

In order to load the preferential pattern, the fuel cladding maximum temperature must be maintained below the allowable temperatures for peripheral and interior assemblies. The requirement of maximum total heat load per basket, as shown in Tables 4.4.7.1-8 and 4.5.1.2-3, must also be met.

4.5.1.2.2.1 Peripheral Assemblies Limited to a Decay Heat Load of 0.958 kW per Assembly

With a basket heat load of 23 kW, uniformly loaded, the maximum cladding temperature of a peripheral assembly location was determined to be 566°F (297°C) based on the thermal analysis using the three-dimensional canister model as presented in Section 4.4.1.1.2. While any basket location is restricted to a heat load of 0.958 kW, any non-uniform loading with a total basket heat load less than 23 kW will result in a peripheral assembly cladding temperature less than 297°C. This temperature is well below the lowest maximum allowable clad temperature of 313°C indicated in Table 4.5.1.2-2 (which was already reduced from the actual allowable of 322°C). Fuel assemblies at a maximum heat load of 0.958 kW may, therefore, be loaded into the peripheral basket location at any cool time, provided interior assemblies meet the restrictions outlined below.

Decay Heat Limit on Fuel Assemblies Loaded into Basket Interior Positions

Interior fuel assembly decay heat loads must be reduced from those in a uniform loading configuration, see Table 4.4.7.1-8 and Table 4.5.1.2-3, to allow loading of the higher heat load assemblies in the peripheral locations. A parametric study is performed using the

three-dimensional periodic model as described in Section 4.5.1.1 (Figure 4.5.1.1-2) to demonstrate that placing a higher heat load in the peripheral locations does not result in heating of the fuel assemblies in the interior locations beyond that found in the uniform heat loading case. The side surface of the model is assumed to have a uniform temperature of 350°F.

Two cases are considered (total heat load per cask = 20 kW for both cases):

1. Uniform loading: Heat load = 0.833 (20/24) kW per assembly for all 24 assemblies
2. Non-uniform loading:
Heat load = 0.958 (23/24) kW per assembly for 12 Peripheral assemblies
Heat load = 0.708 (17/24) kW per assembly for 12 Interior assemblies

The analysis results (maximum temperatures) are:

	<u>Case 1</u>	<u>Case 2</u>
	<u>Uniform Loading (°F)</u>	<u>Non-Uniform Loading (°F)</u>
Fuel (Location 1)	675	648
Fuel (Locations 2 & 4)	632	611
Fuel (Location 5)	577	588
Fuel (Locations 3 & 6)	563	576
Basket	611	592

Locations are shown in Figure 4.5.1.2-1.

The maximum fuel cladding temperature for Case 2 (non-uniform loading pattern) is well below that for Case 1 (uniform loading pattern). The comparison shows that placing hotter fuel in the peripheral locations of the basket and cooler fuel in the interior locations (while maintaining the same total heat load per basket) reduces the maximum fuel cladding temperature (which occurs in the interior assembly), as well as the maximum basket temperature.

Because the basket interior temperatures decrease for non-uniform loading, it is conservative to determine the maximum allowable heat load for the interior assemblies based on the values (total allowed heat load) shown in Tables 4.4.7.1-8 and 4.5.1.2-3, and the heat load for the fuel assemblies in 12 peripheral locations (12 × 0.958 kW). For example, the 10-year cooled, 45,000 MWD/MTU fuel in a uniform loading pattern, is restricted to a basket average heat load of 19.5 kW per Table 4.4.7.1-8. Placing 12 fuel assemblies at 23/24 (0.958) kW into the basket

periphery requires the interior assemblies to be reduced to 0.667 kW per assembly to retain the 19.5 kW basket total heat load. Table 4.5.1.2-4 contains the matrix of maximum allowable heat loads per assembly as a function of burnup and cool time for interior assemblies for the configuration with the peripheral assemblies having a maximum heat load of 0.958 kW per assembly.

4.5.1.2.2.2 Peripheral Assemblies Limited to a Decay Heat Load of 1.05 kW per Assembly

The Maine Yankee fuel inventory includes fuel assemblies that will exceed the initial per assembly heat load of 0.958 kW at a loading prior to August 2002. To enable loading of these assemblies into the storage cask, higher peripheral heat load is evaluated. The maximum heat load for peripheral assemblies is set at 1.05 kW.

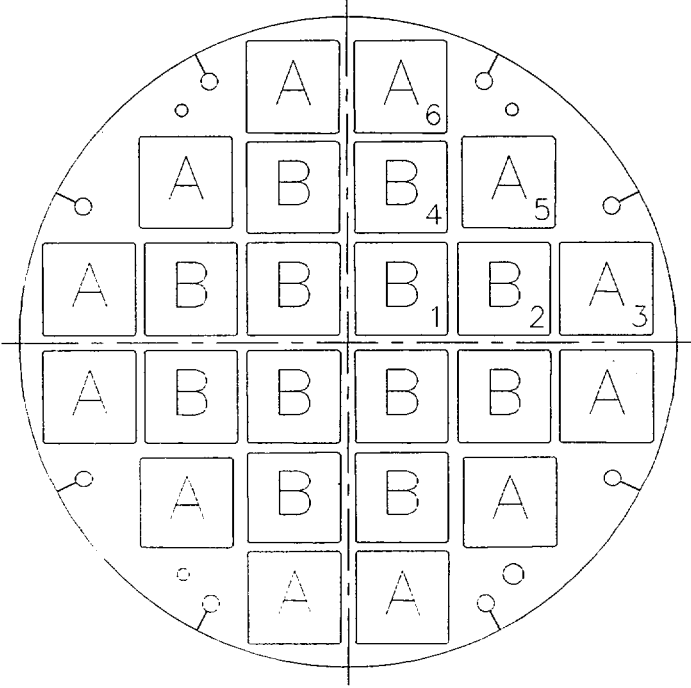
The maximum basket heat load for this configuration is restricted to 23 kW. Given the higher than design basis heat load in peripheral basket locations, an evaluation is performed to assure that maximum cladding allowable temperatures are not exceeded.

Based on the parametric study (uniform versus non-uniform analysis) of the 20 kW basket, a 15% redistribution of heat load resulted in a maximum increase of 13°F (576-563=13) in a peripheral basket location. Changing the basket peripheral location heat load from 0.958 kW maximum to 1.05 kW is a less than 10% redistribution for the 23 kW maximum basket heat load. The highest temperature of a peripheral basket location may, therefore, be estimated by adding 13°F to 566°F (maximum temperature in peripheral assemblies for the 23 kW basket). The 579°F (304°C) is less than the lowest maximum allowable cladding temperature of 313°C indicated in Table 4.5.1.2-2 (which was already reduced from the actual allowable of 322°C). Fuel assemblies at a maximum heat load of 1.05 kW may, therefore, be loaded into the peripheral basket location at any cool time, provided interior assemblies meet the restrictions outlined below.

Decay Heat Limit on Fuel Assemblies Loaded into Basket Interior Positions

Basket interior assemblies heat load limits are based on the same method used for the configuration with 0.958 kW assemblies in peripheral locations, with the exception that each peripheral fuel assembly is assigned a maximum decay heat of 1.05 kW. The higher peripheral heat load in turn will reduce the allowable heat load in the interior locations. Table 4.5.1.2-5 contains the maximum allowable decay heats for basket interior fuel assemblies with an assembly heat load of 1.05 kW for peripheral locations.

Figure 4.5.1.2-1 Canister Basket Preferential Loading Plan



“A” indicates peripheral locations.
“B” indicates interior locations.
Numbered locations indicate positions where maximum fuel temperatures are presented.

Figure 4.5.1.2-2 Maximum Allowable Cladding Temperature at Initial Storage versus Cladding Stress (50,000 MWD/MTU)

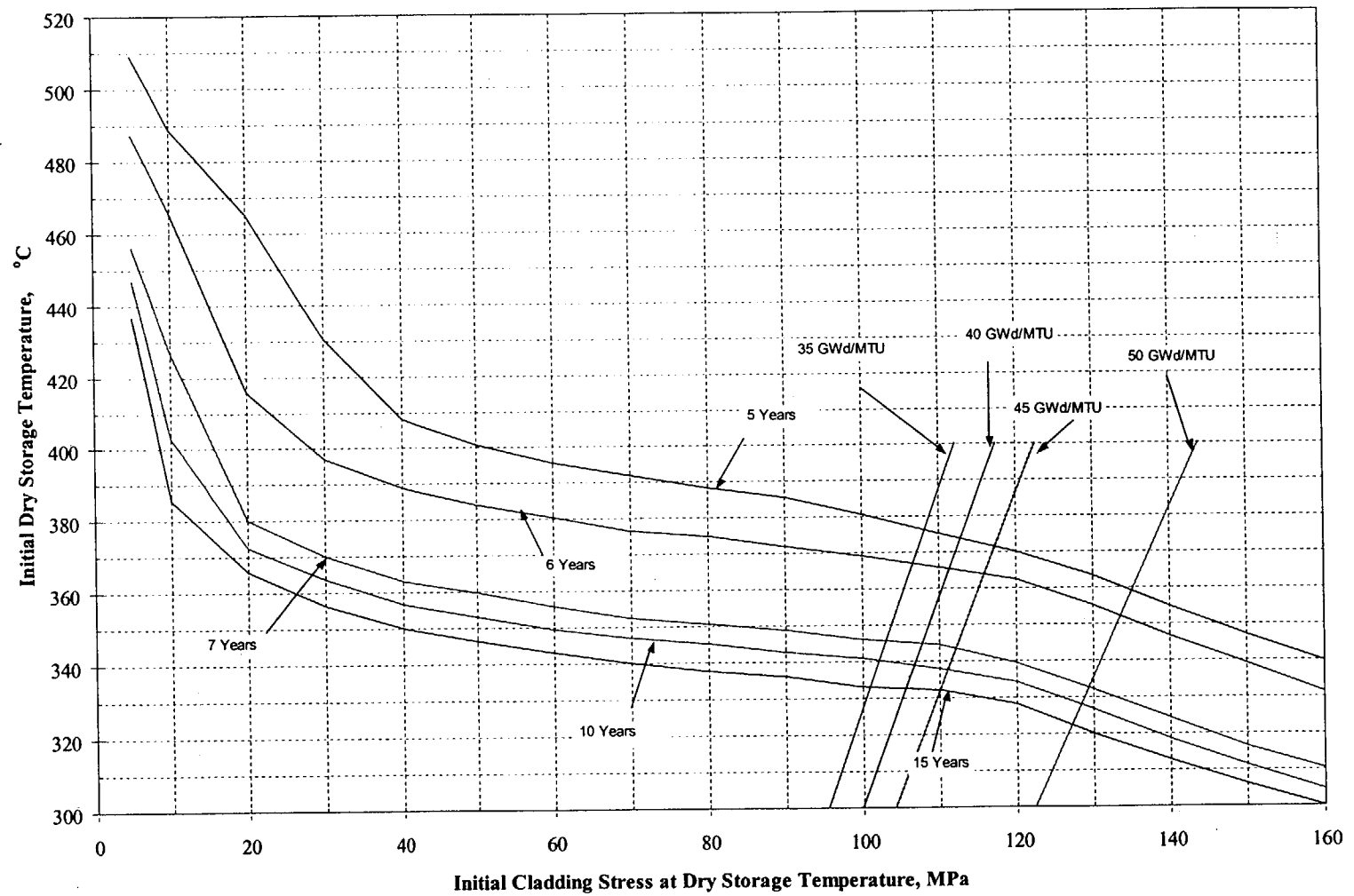


Table 4.5.1.2-1 Cladding Stress for 50,000 MWD/MTU Burnup Fuel – Standard Configuration

Clad Maximum Temperature	300°C	400°C
Stress (MPa)	122.3	143.9

Table 4.5.1.2-2 Maximum Allowable Cladding Temperature for 50,000 MWD/MTU Burnup Fuel – Standard Configuration

Cool Time	Maximum Allowable Cladding Temperature	Bias-Adjusted Cladding Temperature
5 yr	359°C	350°C
6 yr	352°C	342°C
7 yr	333°C	323°C
10 yr	328°C	318°C
15 yr	322°C	313°C

Table 4.5.1.2-3 Maximum Allowable Canister Heat Load for 50,000 MWD/MTU Burnup Fuel – Standard Configuration

Cool Time	Maximum Allowable Heat Load
5 yr	22.1 kW
6 yr	21.2 kW
7 yr	19.5 kW
10 yr	19.1 kW
15 yr	18.7 kW

Table 4.5.1.2-4 Heat Load for Interior Assemblies for the Configuration with 0.958 kW Assemblies in Peripheral Locations

Heat Load Limit (kW)¹				
Interior Assembly	Burnup (MWD/MTU)			
	35,000	40,000	45,000	50,000
Cool Time (years)	---	---	---	---
5	0.958	0.958	0.958	0.883
6	0.908	0.883	0.867	0.808
7	0.725	0.717	0.708	0.667
10	0.683	0.675	0.667	0.633
15	0.633	0.625	0.617	0.600

1. Decay heat per assembly, based on twelve (12) 0.958 kW assemblies in peripheral locations.

Table 4.5.1.2-5 Heat Load Limit for Interior Assemblies for the Configuration with 1.05 kW Assemblies in Peripheral Locations

Heat Load Limit (kW)¹				
Interior Assembly	Burnup (MWD/MTU)			
	35,000	40,000	45,000	50,000
Cool Time (years)	---	---	---	---
5	0.867	0.867	0.867	0.792
6	0.817	0.792	0.775	0.717
7	0.633	0.625	0.617	0.575
10	0.592	0.583	0.575	0.542
15	0.542	0.533	0.525	0.508

1. Decay heat per assembly, based on twelve (12) 1.05 kW assemblies in peripheral locations.

THIS PAGE INTENTIONALLY LEFT BLANK

4.6 References

1. Code of Federal Regulations, "Licensing Requirements for the Independent Storage of Spent Nuclear Fuel and High Level Radioactive Waste," Part 72, Title 10, January 1996.
2. PNL-4835, Johnson, A.B., and Gilbert, E.R., "Technical Basis for Storage of Zircaloy-Clad Fuel in Inert Gases," 1985.
3. PNL-4555, "Results of Simulated Abnormal Heating Events for Full-Length Nuclear Fuel Rods," Gwenther, R.J., Pacific Northwest Laboratories, 1983.
4. ACI-349-85, American Concrete Institute, "Code Requirement for Nuclear Safety Related Concrete Structures and Commentary."
5. PNL-6189, Levy, et al., Pacific Northwest Laboratory, "Recommended Temperature Limits for Dry Storage of Spent Light-Water Zircalloy Clad Fuel Rods in Inert Gas," May 1987.
6. ANSYS Revision 5.2, Computer Program, ANSYS, Inc., Houston, PA.
7. MIL-HDBK-5G, Military Handbook, "Metallic Materials and Elements for Aerospace Vehicle Structures," U.S. Department of Defense, November 1994.
8. Genden Engineering Services & Construction Company, NS-4-FR Fire Resistant Neutron and/or Gamma Shielding Material - Product Technical Data.
9. Baumeister T. and Mark, L.S., Standard Handbook for Mechanical Engineers, 7th Edition, New York, McGraw-Hill Book Co., 1967.
10. The American Society of Mechanical Engineers, "ASME Boiler and Pressure Vessel Code," 1995.
11. ARMCO Product Data Bulletin No. S-22, "17-4PH, Precipitation Hardening Stainless Steel," ARMCO, Inc., 1988.

12. The American Society of Mechanical Engineers, "ASME Boiler and Pressure Vessel Code, Code Cases - Boilers and Pressure Vessels," Code Case N-71-17, 1996.
13. The American Society of Mechanical Engineers, "ASME Boiler and Pressure Vessel Code, Section II, Part D - Properties," 1995.
14. Hanford Engineering Development Laboratory, "Nuclear Systems Materials Handbook," Volume 1, Design Data, Westinghouse Hanford Company, TID26666.
15. Bucholz, J.A., "Scoping Design Analyses for Optimized Shipping Casks Containing 1, 2-, 3-, 5-, 7-, or 10-Year-Old Spent Fuel, Oak Ridge National Library," ORNL/CSD/TM-149, 1983.
16. Ross R. B., "Metallic Specification Handbook," 4th Edition, London, Chapman and Hall, 1992.
17. Kreith, F., and Bohn, M. S., "Principles of Heat Transfer," 5th Edition, West Publishing Company, 1993.
18. Edwards, "TRUMP, A Computer Program for Transient and Steady State Temperature Distributions in Multidimensional Systems," Lawrence Radiation Laboratory, Livermore, Rept, UCLR-14754, Rev. 1, May 1968.
19. Kreith, F., "Principles of Heat Transfer," 3rd Edition, New York, Intext Educational Publishers.
20. Vargaftik, Natan B., et al., "Handbook of Thermal Conductivity of Liquids and Gases," CRC Press, October 1993.
21. Chapman, A.J., "Heat Transfer," 4th Edition, MacMillan Publishing Company, New York, 1987.

22. Hagrman, D.L., Reymann, G.A., "Matpro-Version 11 A Handbook of Material Properties for Use in the Analysis of Light Water Reactor Rod Behavior," Idaho Falls, ID, EG&G Idaho, Inc., 1979.
23. Rust, J.H., "Nuclear Power Plant Engineering," Atlanta, GA, S.W., Holland Company, 1979.
24. AAR BORAL Sheet Manufacturers Data, Sheet Product Performance Report 624, Brooks & Perkins Advanced Structures Company, 1983.
25. AAR Standard Specification Sheet for BORAL™ Composite Sheet, Brooks & Perkins Advances Structures Company, BRJREVO-940107.
26. Fintel, M., "Handbook of Concrete Engineering," 2nd Edition, Van Nostrand Reinhold Co., New York.
27. ASTM C150-95a, American Society for Testing and Materials, "Standard Specification for Portland Cement."
28. Siegel, R., and Howell, J. R., "Thermal Radiation Heat Transfer," 3rd Edition, Hemisphere Publishing Co., 1992.
29. Incropera, E. P., and DeWitt, D. P., "Fundamentals of Heat and Mass Transfer," 4th Edition, 1996.
30. SAND90-2406, Sanders, T.L., et al., "A Method for Determining the Spent-Fuel Contribution to Transport Cask Containment Requirements," TTC-1019, UC-820, November 1992.
31. Olander, D. R., "Fundamental Aspects of Nuclear Reactors Fuel Elements," Technical Information Center (U. S. Department of Energy), 1985.
32. Kreith, F., "Principles of Heat Transfer," 2nd Edition, 1965.

33. PNL-6364, "Control of Degradation of Spent LWR Fuel During Dry Storage in an Inert Atmosphere," Pacific Northwest Laboratory, Richland, Washington, October 1987.
34. PNL-4835, "Technical Basis for Storage of Zircaloy-Cladding Spent Fuel in Inert Gas," September 1983.
35. Regulatory Guide 1.25, "Assumptions Used for Evaluating the Potential Radiological Consequences of a Fuel Handling Accident in the Fuel Handling and Storage Facility for Boiling and Pressurized Water Reactors (Safety Guide 25)," March 1972.
36. Pati, S.R., Garde, A. M., Clink, L.J., "Contribution of Pellet Rim Porosity to Low-Temperature Fission Gas Release at Extended Burnups," American Nuclear Society Topical Meeting on LWR Fuel Performance, April 17-20, 1988, Williamsburg, VA.
37. NET 152-03, "METAMIC Qualification Program for Nuclear Fuel Storage Applications – Final Test Results," Revision 0, Northeast Technology Corporation, September 2001.
38. The American Society of Mechanical Engineers, "ASME Boiler and Pressure Vessel Code, Section II, Part D - Properties," Conductivity: Table TCD, Page 612. Specific Heat: Table NF-2, Page 619, 1995
39. NAC Topical Report 790-TR-001, Rev. 0, "Requirements for Dry Storage of High Burnup Fuel", an NAC Topical Report prepared for NRC by I. Frankl, L. Goldstein and J. Harbottle of Stoller Nuclear Fuel, a Unit of NAC International (July 2001).
40. ANSYS Revision 5.5, Computer Program, ANSYS, Inc., Houston, PA.
41. Fluent, Revision 5.5, CFD Program, Fluent, Inc., Lebanon, NH.
42. Gambit CFD Preprocessor, Version 1.3, Fluent, Inc., Lebanon, NH.
43. NUREG-1536, Standard Review Plan for Dry Cask Storage Systems, U.S. Nuclear Regulatory Commission, 1997.

44. The American Society of Mechanical Engineers, "ASME Boiler and Pressure Vessel Codes, Code Cases – Boiler and Pressure Vessels," Code Case N-650, 2001.
45. Rohsenow, W. M. and Hartnett, J. P., Handbook of Heat Transfer, 1973.

THIS PAGE INTENTIONALLY LEFT BLANK